UNIVERSITY OF CALIFORNIA SAN DIEGO

Identifying astrocyte-secreted protein factors linked to altered neuronal development in neurodevelopmental disorders

A dissertation submitted in partial satisfaction
of the requirements for the Doctor of Philosophy

in

Neurosciences with a Specialization in Anthropogeny

by

Alison Leigh McKenzie Caldwell

Committee in charge:

Professor Nicola Allen, Chair
Professor Shelley Halpain, Co-Chair
Professor Hollis Cline
Professor Joseph Gleeson
Professor Yimin Zou

2019

The Dissertation of Alison Leigh McKenzie Caldwell is approved, and it is acceptable in quality and form for publication on microfilm and electronically:

_____

_____

_____

_____
Co-Chair

_____
Chair

University of California, San Diego

2019

DEDICATION

I would like to dedicate this work to my grandfather, Arno A. Schubert, who is the reason I became a scientist. His love for me and his joy in my curiosity ensured that I always knew I could do anything I set my mind to, and his appreciation for good food, fast motorcycles, and jazz music ensured that he was way cooler than I'll ever be.

EPIGRAPH

The Cosmos are also within us; we are made of star stuff. We are a way for the Cosmos to know itself.

Carl Sagan, Cosmos: A Personal Voyage, PBS, 1980

Astrocytes: they do stuff!

Matt Boisvert, at most MNL-A meetings, circa 2017

TABLE OF CONTENTS

LIST OF SUPPLEMENTAL FILES

Supplemental Table 1_Caldwell_ASD_MassSpec_NSAF.xlsx

Supplemental Table 2_Caldwell_ASD_RNAseq-FPKM.xlsx

Supplemental Table 3_Caldwell_ASD_ProteinChange.xlsx

Supplemental Table 4_Caldwell_ASD_mRNA_Change.xlsx

Supplemental Table 5_Caldwell_ASD_Protein_mRNA_Overlap.xlsx

Supplemental Table 6_Caldwell_AllASD_Protein_Overlap.xlsx

Supplemental Table 7_Caldwell_AllASD_mRNA_Overlap.xlsx

LIST OF FIGURES

LIST OF TABLES

ACKNOWLEDGEMENTS

I am most grateful to Dr. Nicola Allen for her support and mentorship during my graduate school career. From the start of my rotation in the lab, she made me feel wanted, appreciated, and skilled. I am grateful to her for her help developing an exciting, interesting project that I have loved working on, and for supporting me as a scientist, a writer, and a person.

I would also like to acknowledge the mentorship and support of the members of the Allen Lab. I thank Isabella Farhy-Tselnicker, Elena Blanco-Suaréz, and Matt Boisvert for their advice, feedback, and patient training. I'm grateful to Audrey Miglietta for her hard work and her optimism. Laura Sancho-Fernandez was instrumental in developing and executing the final experiments for this project, and I am thankful for her time and expertise. I would also like to thank the core facility staff at the Salk Institute for their help with troubleshooting and executing experiments every step of the way; in particular, Jolene Diedrich's expertise in mass spectrometry made our unbiased screening possible, and this project could not have happened without her.

I would never have gotten to graduate school without the unconditional support and love of my family, and I would never have gotten through it without the friends I've made along the way. Finally, I would like to thank my husband, Micah Caldwell, for being so willing to pack his bags and move across the country with me just two weeks after our wedding, and for calmly holding my hand while I've been on this roller coaster of a journey.

I am grateful to my funding source, the Dennis Weatherstone Pre-Doctoral Fellowship from the Autism Speaks Foundation, for their support of my final year of graduate school.

Chapters 1 and 3, in parts, are reprints of the material as it appears in Blanco-Suaréz E*, Caldwell ALM*, and Allen NJ, Role of astrocyte–synapse interactions in CNS disorders. Journal of Physiology. 2017 Mar 15;595(6):1903-1916. The dissertation author was the co-first author of this review and was the primary author of the portions used in this dissertation.

Chapters 2, 3, 4, 5 and 6 are, in part, in preparation for submission for publication. The dissertation author will be the first author of this publication, with Dr. Jolene Diedrich as second author and Dr. Nicola Allen as the senior author and principle investigator.

VITA

2011	Bachelor of Science in Brain and Cognitive Sciences Massachusetts Institute of Technology
2019	Doctor of Philosophy in Neurosciences with a Specialization in Anthropogeny University of California San Diego
2019	Bigelow Science Communication Fellow University of California San Diego Health Sciences

PUBLICATIONS

Caldwell, A.L.M., Deidrich, J. and Allen, N.J. (2019) “Altered protein secretion from astrocytes from multiple neurodevelopmental disorders inhibits neuronal development”. In preparation.

Zainabadi K., Liu C.J., **Caldwell A.L.M.,** Guarente L. (2017). “SIRT1 is a positive regulator of in vivo bone mass and a therapeutic target for osteoporosis”. PLOS ONE 12(9): e0185236

Blanco-Suárez, E.*, **Caldwell, A.L.M.***, and Allen, N.J. (2016). Role of astrocyte-synapse interactions in CNS disorders. Journal of Physiology, 2017 Mar 15;595(6):1903-1916. doi: 10.1113/JP270988. Epub 2016 Aug 8. **Contributed equally*

ABSTRACT OF THE DISSERTATION

Identifying astrocyte-secreted protein factors linked to
altered neuronal development in neurodevelopmental disorders

by

Alison Leigh McKenzie Caldwell

Doctor of Philosophy in Neurosciences with a Specialization in Anthropogeny

University of California San Diego, 2019

Professor Nicola Allen, Chair
Professor Shelley Halpain, Co-chair

Astrocytes secrete proteins that are critical for normal neuronal development, but while work has identified some important proteins in this process, little is known about the protein secretion of astrocytes at time points when they are most actively involved in supporting neuronal outgrowth and synapse formation. This dissertation seeks to elucidate the protein secretion profile of murine astrocytes at postnatal day 7, using a newly developed immunopanning technique to prospectively isolate astrocytes. These astrocytes are maintained in vitro in minimal media in order to examine their secreted proteins to identify key mediators of neuronal development. By comparing the protein secretion profiles of wild-type astrocytes to those of astrocytes isolated from mouse models of genetic neurodevelopmental disorders

associated with autism, this work also seeks to identify alterations in protein secretion in disordered astrocytes that play a role in the pathology of autism.

Using mass spectrometry, I identified over 1200 proteins secreted by astrocytes in vitro and nearly 100 proteins that show differential secretion patterns in wild-type astrocytes compared to three different genetic neurodevelopmental disorders (Rett Syndrome, Fragile X Syndrome, and Down Syndrome). Furthermore, I identified two proteins that show dramatically increased secretion in astrocytes from all three disorders compared to wild-type: insulin-like growth factor binding protein 2 (IGFBP2) and bone morphogenetic protein 6 (BMP6), implicated in the pathology of Rett Syndrome and Fragile X Syndrome, respectively. Wild-type astrocyte conditioned media (ACM) is capable of supporting neuronal outgrowth compared to a minimal media while disordered ACM results in outgrowth deficits. Addition of IGFBP2 to wild-type ACM leads to outgrowth deficits in vitro, which can be blocked with the application of an IGFBP2-neutralizing antibody. Addition of IGFBP2-neutralizing antibody can rescue deficits induced by Rett Syndrome but not Fragile X Syndrome ACM. Conversely, BMP6 treatment of wild-type astrocytes generates ACM that is similarly incapable of supporting neuronal outgrowth, and blocking BMP activity in Fragile X astrocytes with the application of noggin protein can rescue the aforementioned outgrowth deficits. Thus I have identified astrocyte-secreted proteins that may prove to be critical for neuronal development, and provide targets for therapeutic treatments of these genetic neurodevelopmental disorders.

Chapter 1: Introduction

Formatting note: every chapter in this dissertation has its own, self-contained introduction and discussion. The introduction and conclusion chapters are intended to broadly frame and contextualize the dissertation. All methods are confined to a single methods chapter at the end of the dissertation.

An overview of neuronal pathfinding and synaptogenesis

The human brain is comprised of roughly 100 billion electrically excitable neurons, and nearly as many non-neuronal brain cells, collectively known as glia, or “brain glue”. With such a vast number of players, the formation of proper circuitry in the brain is a delicate and complex process, requiring careful coordination of signaling between the many different cells populating the brain. What are the signals being produced by the different cell types in the brain, and what role do those signals play in genetic neurodevelopmental disorders associated with functional changes in neuronal circuitry? In this dissertation, I will describe a new approach to identifying signals from non-neuronal brain cells that play important roles in neuronal growth.

Axonal pathfinding

Before they can exchange signals, neurons must first find the appropriate partner. During development, neurons begin to find their targets by extending an axon, and concurrently develop their own dendrites to receive information from other neurons. Axons grow toward their targets by means of the axonal growth cone, which is exquisitely sensitive to local environmental cues. A number of critical axonal guidance molecules found in both the extracellular matrix (ECM) and on adjacent cell surfaces have been identified, which may have attractive effects (as in the case of laminin and nerve growth factor) or inhibitory effects (such as Slits or Semaphorins) or differential effects depending on the nature of their expression and receptor interactions (netrins, ephrins, sonic hedgehog) (Alberts et al., 2002; Cavalcante et al., 2002; Kuhn et al., 1995; Peng et al., 2018; Rünker et al., 2008; Serafini et al., 1996; Sofroniew et al., 2001; Yokoyama et al., 2001). Furthermore, various brain cells produce neurotrophic factors to support the survival of young neurons; many newborn neurons receive trophic support from surrounding cells and will apoptose when they do not receive enough of these factors (Squire et al., 2014). Those that do survive are thus properly positioned to form active synaptic connections with their targets.

Neuronal synaptogenesis

Synapses are specialized structures between the presynaptic terminal of one neuron and the postsynaptic terminal of another neuron that enable the chemical communication between neurons, allowing neurons to pass on the electrical signals that control and coordinate the entire body and mind. At the functional synapse, neurotransmitters are released from the presynaptic terminal of the axon into the synaptic cleft, and bind to receptors on the postsynaptic terminal on the dendrite to activate them and pass on the signal (Waites et al., 2005).

Synaptogenesis is the process by which neurons establish connections with the correct targets. Synaptogenesis and morphological modification of synapses are controlled by diverse factors, none of which can induce development of a fully mature synapse on their own. Neurons produce intrinsic factors that contribute to the development of the synapse, such as neurexin (at the presynapse) and neuroligin (at the postsynapse), which bind with each other across the synaptic cleft to induce receptor clustering and the recruitment of scaffolding proteins (Craig and Kang, 2010), and brain derived neurotrophic factor (BDNF), which enhances synaptic vesicle docking and protein production (Suzuki et al., 2007). Other factors are secreted by surrounding cells and are required for the formation and development of mature synapses.

Glutamatergic neurotransmission

A large number of neurotransmitters and their associated receptors have been identified, such as γ-aminobutyric acid (GABA), dopamine (DA), norepinephrine (NE), and serotonin (5-HT). In the scope of this discussion, I will focus on glutamatergic synapses, in which glutamate is the primary neurotransmitter. The two primary glutamate receptors on the postsynaptic terminal are α-amino-3-hydroxy-5-methyl-4-isoxazolepropionic acid receptors (AMPARs) and N-methyl-D-aspartate receptor (NMDARs). AMPARs are ionotropic transmembrane receptors that require glutamate binding for activation and are responsible for much of the fast excitatory neurotransmission in the central nervous system (CNS) (Shepherd and Huganir, 2007). NMDARs are likewise ionotropic receptors but unlike AMPARs, require binding of both glutamate and a co-

agonist (D-serine or glycine) before the channel will open for the exchange of Na^+, K^+, and Ca^{2+} ions.

Glutamate receptors play critical roles in the development and plasticity of most excitatory synapses (Dongen, 2009). A number of disorders associated with synaptic function have implicated alterations in NMDAR and AMPAR expression, trafficking, and signaling in the pathology of the disease. Glutamate signaling at the synapse can have other, secondary effects in addition to ion exchange and excitatory signaling. Metabotropic glutamate receptors (mGluRs) are G-protein-coupled receptors expressed in both neurons and glial cells. mGluRs are involved in cytoskeleton regulation, scaffolding functions and synaptic plasticity. Defects in mGluRs are linked to several pathological conditions which involve loss of memory due to altered synaptic plasticity and synaptic strength fluctuations (Mukherjee and Manahan-Vaughan, 2013). In addition, glutamate clearance and recycling at the synapse can have dramatic effects on synapse function. Glutamate is cleared from the synaptic cleft by uptake transporters on nearby astrocytes, where it is enzymatically transformed to glutamine. The glutamine is then recycled to neurons to synthesize glutamate to maintain synaptic transmission (Danbolt, 2001). Excessive glutamate release at the synapse and/or deficits in glutamate clearance can lead to excitotoxicity at the synapse and has been linked to a number of psychiatric conditions associated with synaptic dysfunction (Jia et al., 2015).

Dendritic spines and synaptic plasticity

Spines are actin-rich structures that protrude from the dendritic shaft and contain the post-synaptic machinery, including postsynaptic AMPA and NMDA receptors, mGluRs, and numerous scaffolding proteins that are responsible for the clustering, trafficking and surface expression of these receptors (Kasai et al., 2010; Verpelli et al., 2012). Spine size and morphology correlate with synaptic strength and determine the efficiency of synaptic transmission. For example, the larger mushroom spines are considered to be relatively stable and contain functional synapses,

while thin filopodia-type spines are considered immature or unstable (Yoshihara et al., 2009). Spines are plastic structures (Hotulainen and Hoogenraad, 2010; Shirao and González-Billault, 2013), and are rapidly formed and eliminated in the developing brain. In the mature adult brain, spine elimination decreases and a higher percentage of spines are stable (Alvarez and Sabatini, 2007). It has been proposed that loss of synapse and spine stability at later life stages may trigger neurodegenerative disorders where memory, learning and cognition are compromised (Kasai et al., 2010; Koleske, 2013).

Synaptic plasticity is the process by which synaptic strength is modulated over time in response to changes in synaptic activity. It is the cellular phenomenon underlying learning and memory in the brain. Long-term potentiation (LTP) is the long-lasting strengthening of a synaptic connection in response to repeated activation, while long-term depression (LTD) has the opposite effect (Malenka and Bear, 2004). Activation of neurons through NDMA receptors plays an important role in most forms of LTP, as glutamate binding to the NMDAR opens the channel and allows intracellular Ca2+ concentrations to rise, which in turn activate protein kinases that phosphorylate AMPARs (improving the conduction of cations) and recruit additional receptors to the postsynaptic membrane (Lüscher and Malenka, 2012). This results in enhanced postsynaptic excitation in responses to a given presynaptic stimulus and thus, a stronger synaptic connection. Alterations to NMDAR and AMPAR expression and trafficking may therefore have significant impacts on synaptic plasticity.

Astrocytes in the mammalian brain

Neurons only comprise about half of the cells in the mammalian brain (von Bartheld et al., 2016). The remaining half of the brain is made up of a group of cells collectively called neuroglia, a Greek word that literally translates to “brain glue”. While glia were identified and catalogued by early neuroscientists such as Rudolf Virchow and Santiago Ramón y Cajal, for many decades it

was assumed that these cells acted as no more than connective tissue or scaffolding for neurons, and little attention was paid to their morphology and function (Somjen, 1988). Since the 1980s, however, researchers have begun to appreciate the critical roles these cells play in the brain throughout the lifetime.

Neuroglia subtypes in the central nervous system (CNS) include microglia (often considered the brain's immune cells) and oligodendrocytes (which myelinate axons and act as insulation for neuronal electrical signals). In the mammalian brain, however, astrocytes are one of the most abundant cells, making up about 40% of all glial cells (Allen and Lyons, 2018; von Bartheld et al., 2016). Neurons and glia arise from the same pool of neuroepithelial cells, which in the cortex first differentiate into radial glia cells to generate neurons before differentiating into astrocytes once neurogenesis has mostly completed (Reemst et al., 2016). These newborn astrocytes then divide, expand, and begin to develop elaborate processes concurrently with neuronal axonal and dendritic outgrowth and spine and synapse formation (Farhy-Tselnicker and Allen, 2018). Astrocytes are star-shaped cells with numerous functions (Figure 1.1). These morphologically and functionally diverse cells tile the brain, connecting to one another via gap junctions, extending endfeet to contact the blood vessels of the brain, and wrapping fine processes around neuronal synapses (Barres, 2008). In this way, astrocytes are poised to support neurons in the adult brain.

Astrocytes maintain homeostasis and provide metabolic support for neurons

Positioned between neurons and blood vessels, astrocytes act as messengers, shuttling nutrients such as glucose and oxygen from the blood vessels directly to the neurons (Molofsky et al. 2013). Astrocytes can also store glycogen and release lactate in response to glutamate uptake (Stobart and Anderson, 2013). This provides neurons with the metabolic support required for their function and enables the coordination of neuronal function and blood flow (Molofsky et al. 2013). Unlike neurons, astrocytes are not electrically excitable, and instead use alterations in the

intracellular concentration of calcium as a means of signaling (Perea et al., 2009). Astrocytes respond to neuronal activity, such as the release of glutamate, via transient elevation of calcium concentrations (Bazargani and Attwell, 2016). This allows astrocytes to release gliotransmitters (such as ATP, adenosine and D-serine) that act to regulate synaptic transmission and plasticity (Figure 1.1) (Allen, 2014).

At the majority of excitatory synapses in the CNS, fine astrocytic processes, together with the pre and postsynaptic terminals, form the tripartite synapse. During neurotransmission, neurons release transmitters into the synaptic cleft. Synaptic transmission is regulated by astrocyte transporters that clear glutamate from the synaptic cleft, and astrocytes can recycle glutamate by converting it to glutamine and releasing it back to neurons (Allen and Barres, 2009). The main transporters expressed in astrocytes that are responsible for glutamate clearance from the synaptic cleft are GLAST and GLT1 (Perego et al., 2002). Neurons also release potassium (K+) during neuronal signaling. Astrocytes can modulate neuronal networks by buffering extracellular K+ after its release, removing excess potassium and preventing its accumulation, which if not removed can lead to inappropriate neuronal depolarization and epileptic activity (Gabriel et al., 2004; Walz, 2000).

Astrocytes support neuronal survival and outgrowth

In addition to their roles in the adult brain, it is now known that neurons require astrocytes to grow and develop normally. In vitro studies have demonstrated that neurons grown in isolation have decreased survival, stunted neurite outgrowth and defects in synapse formation, whereas the presence of astrocytes or astrocyte secreted proteins (ACM) is sufficient to reverse these deficits and promote neuronal development (Banker, 1980; Pfrieger and Barres, 1997; Ullian et al., 2001).

Astrocytes have since been found to produce proteins critical for neuronal survival and outgrowth, including glial-derived neurotrophic factor (GDNF) and ciliary neurotrophic factor

(CNTF) (Chen et al., 2010), brain derived neurotrophic factor (BDNF) (Dougherty et al., 2000), and insulin-like growth factor 1 (IGF1) (Labandeira-Garcia et al., 2017; Recio-Pinto et al., 1986). Astrocytes also secrete proteins that influence neuronal guidance. During brain development, astrocytes express laminin and fibronectin, two extracellular matrix (ECM) proteins important for axon elongation and pathfinding (Liesi and Silver, 1988; Tonge et al., 2012), while conversely, a particular subset of astrocytes in the ventral spinal cord express semaphorin-3a (SEMA3a), a protein involved in repulsion of the axonal growth cone (Molofsky et al., 2014). Some regional populations of astrocytes expressing extracellular matrix proteins such as tenascin, chondroitin sulfate proteoglycan (CSPG), and heparan sulfate proteoglycan (HSPG) can restrict neurite outgrowth, contributing to the refinement of neuronal circuit formation (Cavalcante et al., 2002; Powell et al., 1997). Directional, coordinated astrocytic calcium waves triggered by neuronal activity can attract axonal growth cones in vitro (Hung and Colicos, 2008). Additionally, perisynaptic astrocyte processes and axonal growth cones express ephrins and their receptors, an interaction that plays a role in a wide variety of function including cell proliferation and migration, repulsion of the growth cone, and neurite extension and branching (Cahoy et al., 2008; Carmona et al., n.d.; Ethell et al., 2001; Filosa et al., 2009; Murai and Pasquale, 2011). These studies provide insight into the roles of astrocytes in supporting neuronal outgrowth and process elaboration, but many questions remain about the effects of astrocyte secreted proteins during this process.

A role for astrocytes in neuronal synapse formation and function

Synapse formation and stabilization are processes mediated by numerous factors, including proteins released by astrocytes that directly influence synaptogenesis (Figure 1.2). These factors include thrombospondin, hevin, cholesterol, glypicans, SPARC, transforming growth factor-β (TGFβ), tumor necrosis factor-α (TNFα), Wnt, activity-dependent neurotrophic factor (ADNF), and chondroitin sulfate proteoglycans (CSPGs) (Allen et al., 2012; Beattie et al.,

2002; Bialas and Stevens, 2013; Blondel et al., 2000; Christopherson et al., 2005; Jones et al., 2011; Kerr et al., 2014; Kucukdereli et al., 2011; Mauch et al., 2001; Pyka et al., 2011). Exposure of neurons to astrocyte secreted factors is enough to promote synaptogenesis, as evidenced by the fact that contact between astrocytes and neurons is not necessary to see the synaptogenic effect of astrocytes (Christopherson et al., 2005; Pfrieger and Barres, 1997; Ullian et al., 2001). Thrombospondin and hevin are capable of inducing the formation of structurally mature synapses, but they lack functionality (Christopherson et al., 2005; Kucukdereli et al., 2011). Thrombospondin interacts with α2δ1 and neuroligin at synaptic sites to induce synapse formation. Other astrocytic-secreted factors are responsible for inducing functional synaptic transmission, such as glypican 4 (GPC4) and chordin-like 1 (CHRDL1). GPC4 is a heparan sulfate proteoglycan that recruits GluA1-containing AMPARs to the surface of dendrites, inducing synapse formation and synaptic activity (Allen et al., 2012). Conversely, CHRDL1 mediates the transition from immature, plastic synapses to mature, stable synapses by recruiting calcium-impermeable GluA2-containing AMPARs to the synapse (Blanco-Suarez et al., 2018). ADNF from astrocytes increases synaptic NMDA glutamate receptors (Blondel et al., 2000). Not all factors identified have synaptogenic functions. For instance, astrocytes produce and release secreted protein acidic and rich in cysteine (SPARC), an anti-synaptogenic factor that blocks synapse formation and decreases AMPAR levels at synapses (Kucukdereli et al., 2011).

Neuronal defects in genetic neurodevelopmental disorders

Autism Spectrum Disorder (ASD) is a sporadic and variable disorder that occurs in an estimated 1% of children globally. Around 10-20% of ASD patients have a known genetic mutation to which the condition can be attributed, and that number may rise to as high as 30-40% as detection technology improves (Beaudet, 2007; Iossifov et al., 2014). ASD and multiple other neurodevelopmental disorders (NDs) give rise to similar cellular defects in the developing brain,

including altered dendritic arbor growth and defects in neuronal synapse formation and function. For example, Rett's syndrome (RTT) is a genetic disorder caused by mutations to methyl-CpG binding protein 2 (MECP2) on the X-chromosome (Amir et al., 1999). It presents as a progressive, severe neurological disorder, affecting predominantly females (Hagberg et al., 1983). Children develop normally for 6-18 months before experiencing a regression of motor and language skills and the loss of purposeful hand movements. As regression continues, many symptoms of autism arise, including hand stereotypies, intellectual disabilities, and respiratory irregularities (Neul et al., 2010). MECP2 is an important regulator of synaptogenesis and synaptic pruning (Calfa et al., 2011). RTT pathology is associated with abnormalities in dendritic morphology, including reductions in dendritic complexity and decreased spine density (Xu et al., 2014).

Like RTT, Fragile X Syndrome (FXS) is an X-linked genetic disorder. The disease is caused by a failure to express Fragile X mental retardation protein (FMRP) due to an expansion in the CGG trinucleotide repeat in the Fragile X mental retardation 1 (FMR1) gene (Yudkin et al., 2014). FXS is associated with an autism-like phenotype in many individuals with the disorder, including hand stereotypies, intellectual disability, and social anxiety (McDuffie et al., 2015). FXS has been linked to defects in synaptic development and plasticity (Berry-Kravis, 2014). Post-mortem analysis of neocortical morphology has found that Fragile X patients have long, thin, and immature-appearing dendritic spines (Hinton et al., 1991; Rudelli et al., 1985), a morphology also seen in FMR1 knock-out (KO) mice (Irwin et al., 2000; Nimchinsky et al., 2001). FMRP is highly expressed in the brain (Feng et al., 1997; Pacey and Doering, 2007), and is essential for spine maturation.

Abnormalities in dendritic spine morphology are characteristic of Down's Syndrome (DS) (Marin-Padilla, 1976; Suetsugu and Mehraein, 1980; Takashima et al., 1989). DS is the most common genetic cause of intellectual disability (Presson et al., 2013; Ross and Olsen, 2014) and is due to trisomy of chromosome 21. Neurons in DS brains have reduced numbers of spines, and

these spines frequently show a long, tortuous morphology (Benavides-Piccione et al., 2004), which has been linked to the development of Alzheimer's Disease in adults with DS (Ferrer and Gullotta, 1990). A study on induced pluripotent stem cells (stem cells derived from human fibroblasts, iPSCs) derived from monozygotic twins, where one twin had DS while the other did not, demonstrated that DS lineage cells show increased astroglial and oligodendrocyte cell populations, along with decreased neurogenesis. Neuronal cells derived from DS iPSCs show deficits in dendritic development and reduced expression of both pre and postsynaptic proteins, including postsynaptic density protein 95 (PSD95) and SYNAPSIN (Hibaoui et al., 2014).

A role for astrocytes in the pathology of genetic neurodevelopmental disorders

With an abundance of roles in the brain and their involvement in many key processes, astrocytes are poised to have dramatic impact on neuronal function. It is clear that these cells are important for normal neuronal development. As discussed, astrocyte proteins are critical for neuronal survival, growth, and synapse formation. In the case of genetic neurodevelopmental disorders associated with neuronal defects, astrocyte dysfunction may play a role in the pathology of the disorders.

Astrocytes in Rett Syndrome

Studies have implicated astrocyte dysfunction in disorders associated with ASD. Studies in mouse lines and cells derived from patient-obtained induced pluripotent stem cells (iPSCs) have demonstrated that RTT astrocytes fail to support the development of wild-type neurons in vitro, while conditioned media from wild-type astrocytes rescues dendritic defects in RTT neurons (Ballas et al., 2009; Freitas et al., 2012; Williams et al., 2014). Additional examination revealed that the addition of insulin-like growth factor-1 (IGF1) or GPE (a peptide containing the first 3 amino acids of IGF1) to RTT human iPSC astrocyte and neuron co-cultures was sufficient to significantly improve the outgrowth of neurons in vitro (Williams et al., 2014). It is particularly

interesting that this effect is seen with the application of conditioned media (the solution the astrocytes have been grown in), as it indicates that contact between astrocytes and neurons is not required to induce deficits in neuronal outgrowth or to rescue them. Systemic delivery of MECP2 protein rescues some of the behavioral phenotype in mice (Garg et al., 2013), and importantly, rescuing MECP2 expression selectively in astrocytes attenuates disease outcomes in vivo (Lioy et al., 2011). Additionally, treatment with IGF1 significantly improves dendritic and synaptic deficits as well as breathing abnormalities in MECP2 knock out mice in vivo (Tropea et al., 2009). MECP2-null astrocytes show enrichment for a number of genes associated with LTD, including corticotropin-releasing hormone (CRH), PPP2R2B encoding protein phosphatase 2, and GRIA1 encoding glutamate receptor (Yasui et al., 2013), which may influence the efficacy of active synapses in RTT.

Astrocytic regulation of glutamate at the synapse is an important component of synaptic maintenance and plasticity. Additional research has demonstrated that MECP2 plays a role in glutamate clearance by astrocytes through regulation of the glutamate transporters EAAT1 and EAAT2 and glutamine synthetase. MECP2-null astrocytes demonstrate impaired downregulation of EAAT1/2 expression and higher levels of glutamine synthetase protein following exposure to glutamate in vitro, and these changes may lead to deficits in glutamate clearance at the synapse and thus, synaptic dysfunction (Okabe et al., 2012). Other work in mice has found that MECP2-deficient medullary astrocytes have impaired CO_2 sensitivity, which may contribute to the respiratory irregularities seen in patients with this disorder. Restoration of MECP2 to these astrocytes leads to normal respiratory patterns (Turovsky et al., 2015). These studies indicate that impaired interactions between astrocytes and neurons in RTT are part of the pathology of the disease, and further work is required to understand how that interaction affects the disease phenotype and outcomes.

Astrocytes in Fragile X Syndrome

Co-culture studies have demonstrated roles for astrocytes in FXS. Wild-type hippocampal neurons grown in culture with astrocytes from an FXS mouse show abnormal dendritic morphology and impaired synaptic protein clustering at 7 days in vitro (DIV), but not 21 DIV (Jacobs et al., 2010; Jacobs and Doering, 2010), indicating a delay in normal neuronal development. In contrast, FXS neurons that are grown on wild-type astrocytes develop normally. Alterations in AMPARs have been noted in FXS. The FMRP-regulated proteins STEP and Arc are associated with endocytosis of AMPARs (Berry-Kravis, 2014). Impairments in AMPAR subunit GluA1 delivery to the synapse, connected to changes in Ras-phosphoinositide 3-kinase (PI3K)-protein kinase B (PKB) signaling, have been noted in FMR1 KO mice, resulting in impaired LTP (Hu et al., 2008). Additional work has demonstrated that FMRP directly promotes GluA1 membrane delivery, while its paralog FXR2P acts to increase GluA1 mRNA stability (Guo et al., 2015). Astrocytes can regulate synaptic recruitment of AMPARs via secretion of GPC4 (Allen et al., 2012), but it is not yet known whether alterations in GPC4 play a role in FXS.

Glutamate clearance dysfunction may also play a role in the pathology of FXS. In FMR1 KO mice, reduced GLT1 expression leads to a reduction in glutamate reuptake by astrocytes (Higashimori et al., 2013). In addition, mGluR5 has been shown to play a role in FXS. In the absence of FMRP, excessive mGluR signaling has been linked to abnormal dendritic spine morphology and maturation (Berry-Kravis, 2014) and alterations in LTD. This hypothesis is supported by work demonstrating that chronic pharmacological inhibition of mGluR5 rescues the abnormal dendritic spine phenotype and leads to significant recovery from cognitive deficits associated with FXS in mice (Michalon et al., 2012). Conversely, there is evidence that FMRP-dependent downregulation of mGluR5 in astrocytes underlies the reduced GLT1 expression and the reduction in glutamate reuptake, contributing to abnormal neuronal excitability in FXS mice (Higashimori et al., 2013). Further research has found that there is a reduction in astrocyte presence at hippocampal CA1 synapses in *Fmr1* KO mice, in addition to immature synaptic

densities (Jawaid et al., 2018). The research has thus far been promising and future work on the role of astrocytes in the morphological deficits in FXS may provide better insight into potential treatments.

Astrocytes in Down Syndrome

Astrocytes have been implicated in the pathology of Down Syndrome through co-culture studies, identifying thrombospondin-1 (TSP-) as a critical secreted astrocytic factor; decreased TSP1 release by DS astrocytes leads to alterations in spine density and morphology in DS (Garcia et al., 2010). In addition, hippocampal neurons grown on top of TSP1 KO astrocytes exhibit a dramatic increase in filopodia-like spines, much like the pathology described in DS, and the addition of TSP1 to neuronal cultures grown in DS astrocyte conditioned media can reverse the reduced synapse number seen in culture (Garcia et al., 2010). While TSP1 KO mice show dendritic spine abnormalities and behavioral deficit similar to those seen in DS (Torres et al., 2018), it remains unknown whether or not application of TSP1 might rescue the DS spine pathology in vivo. Further research on DS astroglial cells derived from iPSCs has found that these cells exhibit increased levels of S100β, GFAP, and reactive oxygen species (ROS), indicating that they are in a reactive state. Medium collected from these cells does not support normal neurite outgrowth or synapse formation, resulting in abnormal dendritic and spine morphology. This phenotype was partially rescued through the application of minocycline (Chen et al. 2014), indicating promise for therapeutic treatment. DS astrocytes also demonstrate deficits in amyloid precursor protein (APP) metabolism and secretion, associated with mitochondrial dysfunction (Busciglio et al., 2002), which may contribute to the comorbidity of DS and Alzheimer's disease (Takashima et al., 1989). Increased deposition of APP during development in DS brains may result in inflammatory responses that hinder normal dendritic growth and development (Benavides-Piccione et al., 2004). Further research into the connection between APP deposition, inflammation, and dendritic alterations may reveal a role for astrocytes in this pathology.

Astrocytes: A new hope for therapeutic targets in ASD

The overlapping neuronal phenotypes and their connection to astrocytes suggest there may be common alterations in the molecular mechanisms of neuronal development across multiple NDs that can be targeted therapeutically. However, while a number of astrocyte-secreted proteins have been identified as being important for normal neuronal development, there are still many questions to be answered. In particular, the popular method for the isolation of rodent astrocytes makes it difficult to determine if these cells represent an accurate picture of astrocyte behavior in vivo. Since it is difficult to study secreted proteins in vivo, the development of new and more advanced methods to isolate various brain cell types in vitro is critical to better understand their individual roles in the brain, and in the case of this dissertation, to get a clear understanding of the secretome of astrocytes.

Several changes in astrocyte-secreted proteins have been determined to play a role in some of these disorders individually, which will be discussed in chapter 3. To date, however, there has not been an in-depth examination of the secretome of wild-type or ND astrocytes at a time point when astrocytes are involved in the process of neuronal development, dendritic outgrowth, and synapse formation. This thesis sets out to investigate: 1) What does the normal, wild-type astrocyte secretome look like? 2) How does astrocyte protein secretion change in genetic neurodevelopmental disorders? 3) Are there common changes in protein secretion and gene expression in RTT, FXS and DS? This dissertation seeks to answer these questions by taking an unbiased approach to study astrocyte secreted proteins in a new model of astrocytes in vitro, using an updated protocol to isolate astrocytes at a physiologically relevant time point under serum-free culture conditions. This approach generates astrocytes that more closely resemble astrocytes in vivo when compared to traditional methods for culturing astrocytes. This provides an opportunity to conduct deep analysis of astrocyte secreted proteins via mass spectrometry,

while conducting concurrent RNA sequencing analysis of gene expression in the same samples. With this technique, I have isolated astrocytes from WT, RTT, FXS, and DS mouse brains at postnatal day 7 (P7), cultured them, and identified over 1200 unique proteins secreted by astrocytes in vitro. This research has generated a database of proteins secreted by astrocytes and their gene expression profiles across these three disorders as well as in WT healthy brains, to allow for a better understanding of the roles astrocytes play in the brain during normal development and in neurodevelopmental disorders.

Acknowledgements

This chapter is, in part, a reprint of the material as it appears in Blanco-Suaréz E*, Caldwell ALM*, and Allen NJ, Role of astrocyte–synapse interactions in CNS disorders. Journal of Physiology. 2017 Mar 15;595(6):1903-1916. The dissertation author was the co-first author of this review and was the primary author of the portions used in this chapter.

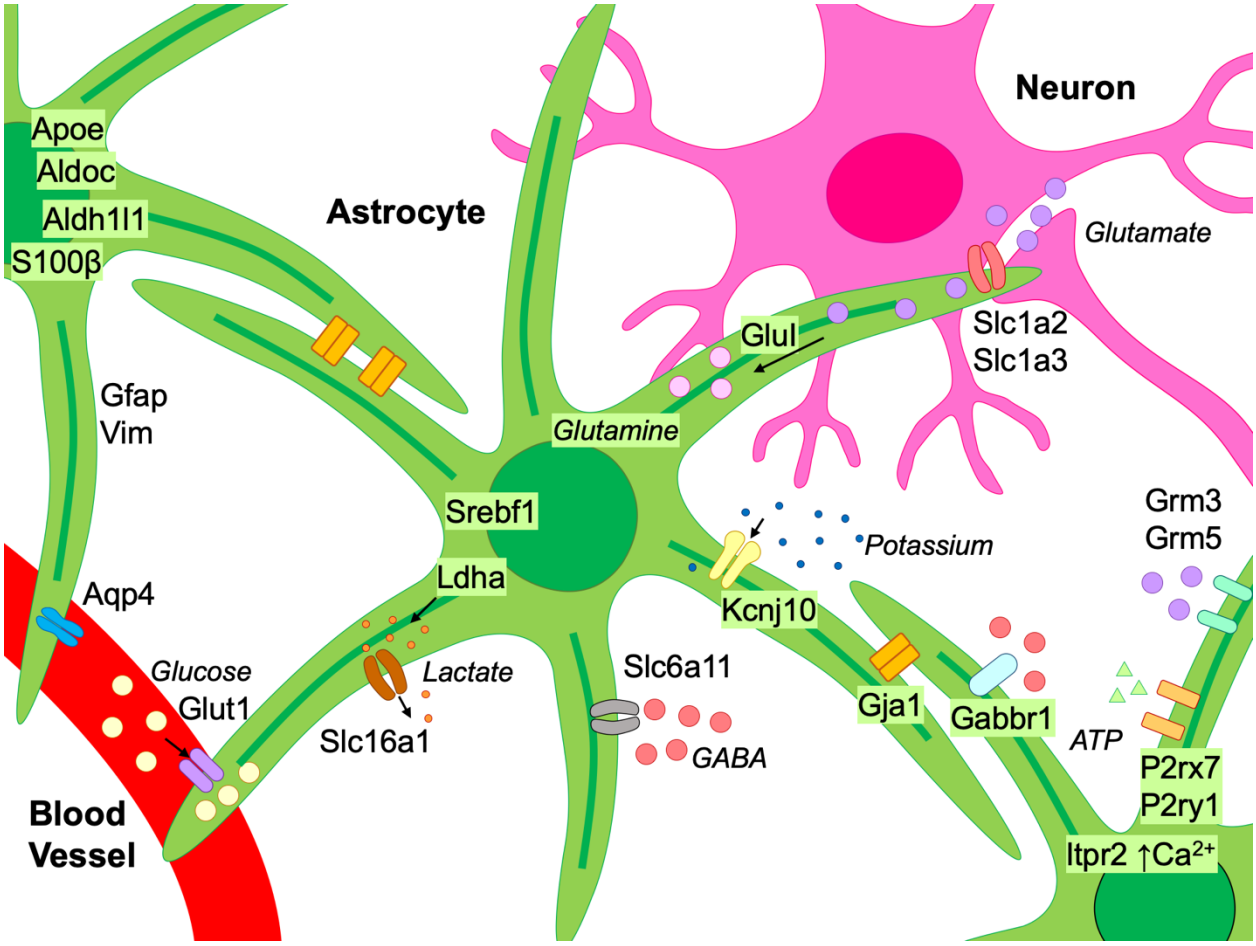

Figure 1.1: Astrocytes perform critical functional roles in the brain. Astrocytes (green) express cell-specific markers that determine their cellular identity (top left astrocyte), contact blood vessels and neuronal synapses to engage in metabolism and homeostatic functions (center astrocyte), and bind and respond to neurotransmitters released by neurons (lower right astrocyte).

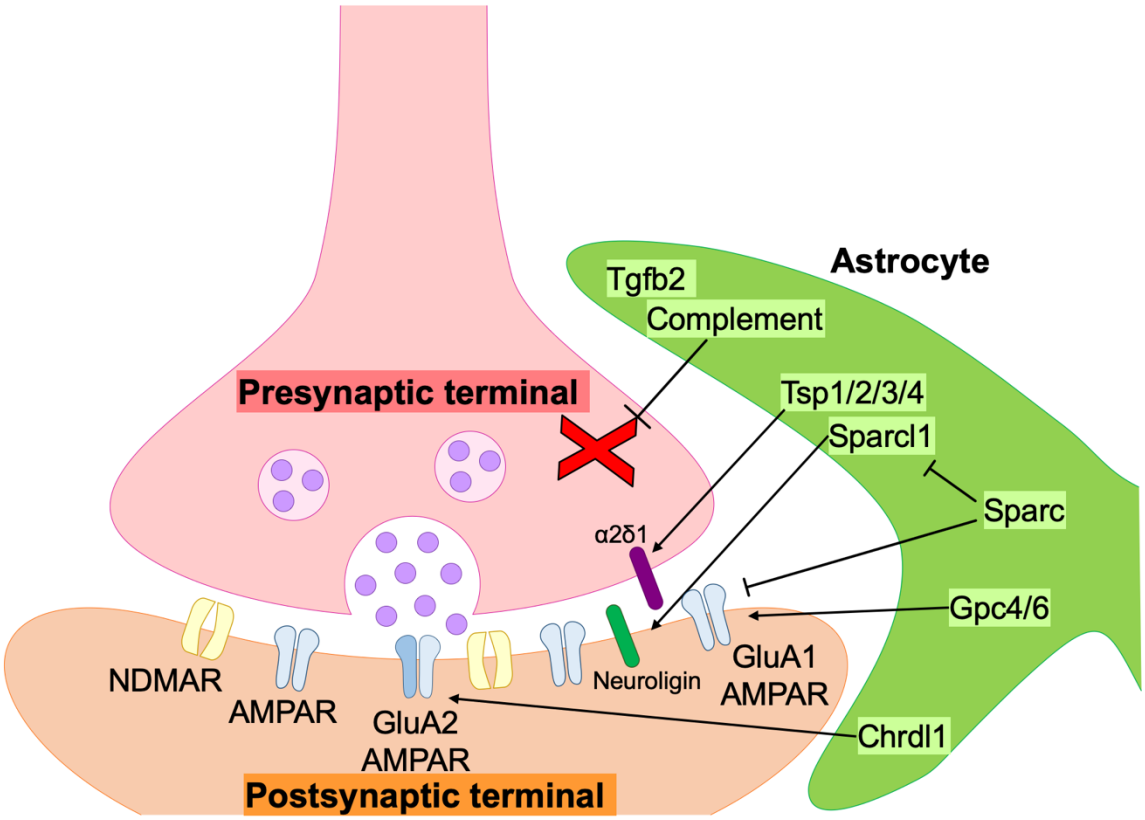

Figure 1.2: Astrocytes secrete factors important for synapse formation at the tripartite synapse. Astrocytes induce synapse formation by secreting factors such as thrombospondins 1 and 2 (TSP/2) and SPARCL1 (also called hevin), which bind to α2δ1 and neuroligin to induce structural synapse formation, and GPC4/6, which recruits GluA1-containing AMPA receptors to the synapse. Astrocytes can also block synapse formation and modulate synapse maturation and plasticity through the secretion of factors like TGFβ, which regulates synaptic pruning, SPARC, which prevents synapse formation and decreases the level of AMPARs at synapses, and chordin-like 1 (CHRDL1), which increases the presence of GluA2-containing AMPARs.

References

Alberts, B., Johnson, A., Lewis, J., Raff, M., Roberts, K., Walter, P., 2002. Molecular biology of the cell. Garland Science.

Allen, N.J., 2014. Astrocyte Regulation of Synaptic Behavior. Annu. Rev. Cell Dev. Biol. 30, 439–463. https://doi.org/10.1146/annurev-cellbio-100913-013053

Allen, N.J., Barres, B. a, 2009. Neuroscience: Glia - more than just brain glue. Nature 457, 675–677. https://doi.org/10.1038/457675a

Allen, N.J., Bennett, M.L., Foo, L.C., Wang, G.X., Chakraborty, C., Smith, S.J., Barres, B. a., 2012. Astrocyte glypicans 4 and 6 promote formation of excitatory synapses via GluA1 AMPA receptors. Nature 486, 410–414. https://doi.org/10.1038/nature11059

Allen, N.J., Lyons, D.A., 2018. Glia as architects of central nervous system formation and function. Science (80-.). 362, 181–185. https://doi.org/10.1126/science.aat0473

Alvarez, V.A., Sabatini, B.L., 2007. Anatomical and Physiological Plasticity of Dendritic Spines. Annu. Rev. Neurosci. 30, 79–97. https://doi.org/10.1146/annurev.neuro.30.051606.094222

Amir, R.E., Van den Veyver, I.B., Wan, M., Tran, C.Q., Francke, U., Zoghbi, H.Y., 1999. Rett syndrome is caused by mutations in X-linked MECP2, encoding methyl-CpG-binding protein 2. Nat. Genet. 23, 185–8. https://doi.org/10.1038/13810

Ballas, N., Lioy, D.T., Grunseich, C., Mandel, G., 2009. Non-cell autonomous influence of MeCP2-deficient glia on neuronal dendritic morphology. Nat. Neurosci. 12, 311–7. https://doi.org/10.1038/nn.2275

Banker, G.A., 1980. Trophic interactions between astroglial cells and hippocampal neurons in culture. Science (80-.). 209, 809–810. https://doi.org/10.1126/science.7403847

Barres, B. a., 2008. The Mystery and Magic of Glia: A Perspective on Their Roles in Health and Disease. Neuron 60, 430–440. https://doi.org/10.1016/j.neuron.2008.10.013

Bazargani, N., Attwell, D., 2016. Astrocyte calcium signaling: the third wave. Nat. Neurosci. 19, 182–189. https://doi.org/10.1038/nn.4201

Beattie, E.C., Stellwagen, D., Morishita, W., Bresnahan, J.C., Ha, B.K., Von Zastrow, M., Beattie, M.S., Malenka, R.C., 2002. Control of Synaptic Strength by Glial TNFalpha. Science (80-.). 295, 2282–2285. https://doi.org/10.1126/science.1067859

Beaudet, A.L., 2007. Autism: highly heritable but not inherited. Nat. Med. 13, 534–536. https://doi.org/10.1038/nm0507-534

Benavides-Piccione, R., Ballesteros-Yáñez, I., Martínez De Lagrán, M., Elston, G., Estivill, X., Fillat, C., Defelipe, J., Dierssen, M., 2004. On dendrites in Down syndrome and DS murine models: A spiny way to learn. Prog. Neurobiol. 74, 111–126. https://doi.org/10.1016/j.pneurobio.2004.08.001

Berry-Kravis, E., 2014. Mechanism-based treatments in neurodevelopmental disorders: Fragile X syndrome. Pediatr. Neurol. 50, 297–302. https://doi.org/10.1016/j.pediatrneurol.2013.12.001

Bialas, A.R., Stevens, B., 2013. TGF-β signaling regulates neuronal C1q expression and developmental synaptic refinement. Nat. Neurosci. 16, 1773–1782. https://doi.org/10.1038/nn.3560

Blanco-Suarez, E., Liu, T.F., Kopelevich, A., Allen, N.J., 2018. Astrocyte-Secreted Chordin-like 1 Drives Synapse Maturation and Limits Plasticity by Increasing Synaptic GluA2 AMPA Receptors. Neuron 1–17. https://doi.org/10.1016/j.neuron.2018.09.043

Blondel, O., Collin, C., McCarran, W.J., Zhu, S., Zamostiano, R., Gozes, I., Brenneman, D.E., McKay, R.D., 2000. A glia-derived signal regulating neuronal differentiation. J. Neurosci. 20, 8012–20. https://doi.org/10.1523/JNEUROSCI.20-21-08012.2000

Busciglio, J., Pelsman, A., Wong, C., Pigino, G., Yuan, M., Mori, H., Yankner, B. a., 2002. Altered metabolism of the amyloid β precursor protein is associated with mitochondrial dysfunction in Down's syndrome. Neuron 33, 677–688. https://doi.org/10.1016/S0896-6273(02)00604-9

Cahoy, J.D., Emery, B., Kaushal, A., Foo, L.C., Zamanian, J.L., Christopherson, K.S., Xing, Y., Lubischer, J.L., Krieg, P. a, Krupenko, S. a, Thompson, W.J., Barres, B. a, 2008. A transcriptome database for astrocytes, neurons, and oligodendrocytes: a new resource for understanding brain development and function. J. Neurosci. 28, 264–278. https://doi.org/10.1523/JNEUROSCI.4178-07.2008

Calfa, G., Percy, A.K., Pozzo-Miller, L., 2011. Experimental models of Rett syndrome based on Mecp2 dysfunction. Exp. Biol. Med. (Maywood). 236, 3–19. https://doi.org/10.1258/ebm.2010.010261

Carmona, M.A., Murai, K.K., Wang, L., Roberts, A.J., Pasquale, E.B., Pawson, A.J., n.d. Glial Ephrin-A3 Regulates Hippocampal Dendritic Spine Morphology and Glutamate Transport. Proc. Natl. Acad. Sci. U. S. A. https://doi.org/10.2307/40484169

Cavalcante, L.A., Garcia-Abreu, J., Neto, V.M., Silva, L.C., Weissmüller, G., 2002. Modulators of axonal growth and guidance at the brain midline with special reference to glial heparan sulfate proteoglycans. An. Acad. Bras. Cienc. 74, 691–716. https://doi.org/10.1590/S0001-37652002000400010

Chen, C., Jiang, P., Xue, H., Peterson, S.E., Tran, H.T., McCann, A.E., Parast, M.M., Li, S., Pleasure, D.E., Laurent, L.C., Loring, J.F., Liu, Y., Deng, W., 2014. Role of astroglia in Down's syndrome revealed by patient-derived human-induced pluripotent stem cells. Nat. Commun. 5, 4430. https://doi.org/10.1038/ncomms5430

Chen, E.Y., Fox, D., Kordower, J.H., 2010. Neurotrophic factor therapy: GDNF and CNTF. Encycl. Neurosci. 1085–1092. https://doi.org/10.1016/B978-008045046-9.00015-2

Christopherson, K.S., Ullian, E.M., Stokes, C.C. a, Mullowney, C.E., Hell, J.W., Agah, A., Lawler, J., Mosher, D.F., Bornstein, P., Barres, B. a., 2005. Thrombospondins are astrocyte-secreted proteins that promote CNS synaptogenesis. Cell 120, 421–433. https://doi.org/10.1016/j.cell.2004.12.020

Craig, A.M., Kang, Y., 2010. Neurexin-Neuroglian signalling in synapse development. Brain Res. 17, 1–16. https://doi.org/10.1016/j.conb.2007.01.011.Neurexin

Danbolt, N.C., 2001. Glutamate uptake. Prog. Neurobiol. 65, 1–105. https://doi.org/10.1016/S0301-0082(00)00067-8

Dongen, A.M. Van, 2009. Biology of the NMDA Receptor, Biology of the NMDA Receptor. CRC Press/Taylor & Francis.

Dougherty, K.D., Dreyfus, C.F., Black, I.B., 2000. Brain-derived neurotrophic factor in astrocytes, oligodendrocytes, and microglia/macrophages after spinal cord injury. Neurobiol. Dis. 7, 574–85. https://doi.org/10.1006/nbdi.2000.0318

Ethell, I.M., Irie, F., Kalo, M.S., Couchman, J.R., Pasquale, E.B., Yamaguchi, Y., 2001. EphB/syndecan-2 signaling in dendritic spine morphogenesis. Neuron 31, 1001–13. https://doi.org/10.1016/S0896-6273(01)00440-8

Farhy-Tselnicker, I., Allen, N.J., 2018. Astrocytes, neurons, synapses: a tripartite view on cortical circuit development. Neural Dev. 13, 7. https://doi.org/10.1186/s13064-018-0104-y

Feng, Y., Gutekunst, C. a, Eberhart, D.E., Yi, H., Warren, S.T., Hersch, S.M., 1997. Fragile X mental retardation protein: nucleocytoplasmic shuttling and association with somatodendritic ribosomes. J. Neurosci. 17, 1539–1547.

Ferrer, I., Gullotta, F., 1990. Down's syndrome and Alzheimer's disease: dendritic spine counts in the hippocampus. Acta Neuropathol. 79, 680–5.

Filosa, A., Paixão, S., Honsek, S.D., Carmona, M.A., Becker, L., Feddersen, B., Gaitanos, L., Rudhard, Y., Schoepfer, R., Klopstock, T., Kullander, K., Rose, C.R., Pasquale, E.B., Klein, R., 2009. Neuron-glia communication via EphA4/ephrin-A3 modulates LTP through glial glutamate transport. Nat. Neurosci. 12, 1285–1292. https://doi.org/10.1038/nn.2394

Freitas, B.C.G., Trujillo, C. a., Carromeu, C., Yusupova, M., Herai, R.H., Muotri, A.R., 2012. Stem cells and modeling of autism spectrum disorders. Exp. Neurol. 260, 33–43. https://doi.org/10.1016/j.expneurol.2012.09.017

Gabriel, S., Njunting, M., Pomper, J.K., Merschhemke, M., Sanabria, E.R.G., Eilers, A., Kivi, A., Zeller, M., Meencke, H.-J., Cavalheiro, E.A., Heinemann, U., Lehmann, T.-N., 2004. Stimulus and Potassium-Induced Epileptiform Activity in the Human Dentate Gyrus from Patients with and without Hippocampal Sclerosis. J. Neurosci. 24, 10416–10430. https://doi.org/10.1523/JNEUROSCI.2074-04.2004

Garcia, O., Torres, M., Helguera, P., Coskun, P., Busciglio, J., 2010. A role for thrombospondin-1 deficits in astrocyte-mediated spine and synaptic pathology in down's syndrome. PLoS One 5. https://doi.org/10.1371/journal.pone.0014200

Garg, S.K., Lioy, D.T., Cheval, H., McGann, J.C., Bissonnette, J.M., Murtha, M.J., Foust, K.D., Kaspar, B.K., Bird, A., Mandel, G., 2013. Systemic delivery of MeCP2 rescues behavioral and cellular deficits in female mouse models of Rett syndrome. J. Neurosci. 33, 13612–20. https://doi.org/10.1523/JNEUROSCI.1854-13.2013

Guo, W., Polich, E.D., Su, J., Gao, Y., Christopher, D.M., Allan, A.M., Wang, M., Wang, F., Wang, G., Zhao, X., 2015. Fragile X Proteins FMRP and FXR2P Control Synaptic GluA1 Expression and Neuronal Maturation via Distinct Mechanisms. Cell Rep. 11, 1651–1666. https://doi.org/10.1016/j.celrep.2015.05.013

Hagberg, B., Aicardi, J., Dias, K., Ramos, O., 1983. A progressive syndrome of autism, dementia, ataxia, and loss of purposeful hand use in girls: Rett's syndrome: report of 35 cases. Ann. Neurol. 14, 471–9. https://doi.org/10.1002/ana.410140412

Hibaoui, Y., Grad, I., Letourneau, A., Sailani, M.R., Dahoun, S., Federico, a, Gimelli, S., Guipponi, M., Franc, M., 2014. Modelling and rescuing neurodevelopmental defect of Down syndrome using induced pluripotent stem cells from monozygotic twins discordant for trisomy 21 6, 259–277.

Higashimori, H., Morel, L., Huth, J., Lindemann, L., Dulla, C., Taylor, A., Freeman, M., Yang, Y.,

2013. Astroglial FMRP-dependent translational down-regulation of mGluR5 underlies glutamate transporter GLT1 dysregulation in the fragile X mouse. Hum. Mol. Genet. 22, 2041–54. https://doi.org/10.1093/hmg/ddt055

Hinton, V.J., Brown, W.T., Wisniewski, K., Rudelli, R.D., 1991. Analysis of neocortex in three males with the fragile X syndrome. Am. J. Med. Genet. 41, 289–294. https://doi.org/10.1002/ajmg.1320410306

Hotulainen, P., Hoogenraad, C.C., 2010. Actin in dendritic spines: connecting dynamics to function. J. Cell Biol. 189, 619–29. https://doi.org/10.1083/jcb.201003008

Hu, H., Qin, Y., Bochorishvili, G., Zhu, Y., van Aelst, L., Zhu, J.J., 2008. Ras signaling mechanisms underlying impaired GluR1-dependent plasticity associated with fragile X syndrome. J. Neurosci. 28, 7847–7862. https://doi.org/10.1523/JNEUROSCI.1496-08.2008

Hung, J., Colicos, M.A., 2008. Astrocytic Ca2+ Waves Guide CNS Growth Cones to Remote Regions of Neuronal Activity. PLoS One 3, e3692. https://doi.org/10.1371/journal.pone.0003692

Iossifov, I., O'Roak, B.J., Sanders, S.J., Ronemus, M., Krumm, N., Levy, D., Stessman, H.A., Witherspoon, K.T., Vives, L., Patterson, K.E., Smith, J.D., Paeper, B., Nickerson, D.A., Dea, J., Dong, S., Gonzalez, L.E., Mandell, J.D., Mane, S.M., Murtha, M.T., Sullivan, C.A., Walker, M.F., Waqar, Z., Wei, L., Willsey, A.J., Yamrom, B., Lee, Y., Grabowska, E., Dalkic, E., Wang, Z., Marks, S., Andrews, P., Leotta, A., Kendall, J., Hakker, I., Rosenbaum, J., Ma, B., Rodgers, L., Troge, J., Narzisi, G., Yoon, S., Schatz, M.C., Ye, K., McCombie, W.R., Shendure, J., Eichler, E.E., State, M.W., Wigler, M., 2014. The contribution of de novo coding mutations to autism spectrum disorder. Nature 515, 216–21. https://doi.org/10.1038/nature13908

Irwin, S.A., Galvez, R., Greenough, W.T., 2000. Dendritic Spine Structural Anomalies in Fragile-X Mental Retardation Syndrome. Cereb. Cortex 10, 1038–1044. https://doi.org/10.1093/cercor/10.10.1038

Jacobs, S., Doering, L.C., 2010. Astrocytes prevent abnormal neuronal development in the fragile x mouse. J. Neurosci. 30, 4508–14. https://doi.org/10.1523/JNEUROSCI.5027-09.2010

Jacobs, S., Nathwani, M., Doering, L.C., 2010. Fragile X astrocytes induce developmental delays in dendrite maturation and synaptic protein expression. BMC Neurosci. 11, 132. https://doi.org/10.1186/1471-2202-11-132

Jawaid, S., Grahame, I, Kidd, J., Wang, J., Swetlik, C., Dutta, R., Trapp, B.D., Kidd, G.J., Wang,

J., Swetlik, C., Dutta, R., Trapp, B.D., 2018. Alterations in CA1 hippocampal synapses in a mouse model of fragile X syndrome. Glia 66, 789–800. https://doi.org/10.1002/glia.23284

Jia, M., Njapo, S.A.N., Rastogi, V., Hedna, V.S., 2015. Taming Glutamate Excitotoxicity: Strategic Pathway Modulation for Neuroprotection. CNS Drugs 29, 153–162. https://doi.org/10.1007/s40263-015-0225-3

Jones, E. V, Bernardinelli, Y., Tse, Y.C., Chierzi, S., Wong, T.P., Murai, K.K., 2011. Astrocytes control glutamate receptor levels at developing synapses through SPARC-beta-integrin interactions. J. Neurosci. 31, 4154–65. https://doi.org/10.1523/JNEUROSCI.4757-10.2011

Kasai, H., Fukuda, M., Watanabe, S., Hayashi-Takagi, A., Noguchi, J., 2010. Structural dynamics of dendritic spines in memory and cognition. Trends Neurosci. 33, 121–9. https://doi.org/10.1016/j.tins.2010.01.001

Kerr, K.S., Fuentes-Medel, Y., Brewer, C., Barria, R., Ashley, J., Abruzzi, K.C., Sheehan, A., Tasdemir-Yilmaz, O.E., Freeman, M.R., Budnik, V., 2014. Glial wingless/Wnt regulates glutamate receptor clustering and synaptic physiology at the Drosophila neuromuscular junction. J. Neurosci. 34, 2910–20. https://doi.org/10.1523/JNEUROSCI.3714-13.2014

Koleske, A.J., 2013. Molecular mechanisms of dendrite stability. Nat. Rev. Neurosci. 14, 536–550. https://doi.org/10.1038/nrn3486

Kucukdereli, H., Allen, N.J., Lee, A.T., Feng, A., Ozlu, M.I., Conatser, L.M., Chakraborty, C., Workman, G., Weaver, M., Sage, E.H., Barres, B.A., Eroglu, C., 2011. Control of excitatory CNS synaptogenesis by astrocyte-secreted proteins Hevin and SPARC. Proc. Natl. Acad. Sci. U. S. A. 108, E440-9. https://doi.org/10.1073/pnas.1104977108

Kuhn, T.B., Schmidt, M.F., Kater, S.B., 1995. Laminin and fibronectin guideposts signal sustained but opposite effects to passing growth cones. Neuron 14, 275–85. https://doi.org/10.1016/0896-6273(95)90285-6

Labandeira-Garcia, J.L., Costa-Besada, M.A., Labandeira, C.M., Villar-Cheda, B., Rodríguez-Perez, A.I., 2017. Insulin-Like Growth Factor-1 and Neuroinflammation. Front. Aging Neurosci. 9, 365. https://doi.org/10.3389/fnagi.2017.00365

Liesi, P., Silver, J., 1988. Is astrocyte laminin involved in axon guidance in the mammalian CNS? Dev. Biol. 130, 774–785. https://doi.org/10.1016/0012-1606(88)90366-1

Lioy, D.T., Garg, S.K., Monaghan, C.E., Raber, J., Foust, K.D., Kaspar, B.K., Hirrlinger, P.G., Kirchhoff, F., Bissonnette, J.M., Ballas, N., Mandel, G., 2011. A role for glia in the

progression of Rett's syndrome. Nature 475, 497–500. https://doi.org/10.1038/nature10214

Lüscher, C., Malenka, R.C., 2012. NMDA receptor-dependent long-term potentiation and long-term depression (LTP/LTD). Cold Spring Harb. Perspect. Biol. 4. https://doi.org/10.1101/cshperspect.a005710

Malenka, R.C., Bear, M.F., 2004. LTP and LTD: an embarrassment of riches. Neuron 44, 5–21. https://doi.org/10.1016/j.neuron.2004.09.012

Marin-Padilla, M., 1976. Pyramidal cell abnormalities in the motor cortex of a child with Down's syndrome. A Golgi study. J. Comp. Neurol. 167, 63–81. https://doi.org/10.1002/cne.901670105

Mauch, D.H., Nägler, K., Schumacher, S., Göritz, C., Müller, E.C., Otto, A., Pfrieger, F.W., Malenka, R.C., 2001. CNS synaptogenesis promoted by glia-derived cholesterol. Science 294, 1354–7. https://doi.org/10.1126/science.294.5545.1354

McDuffie, A., Thurman, A.J., Hagerman, R.J., Abbeduto, L., 2015. Symptoms of Autism in Males with Fragile X Syndrome: A Comparison to Nonsyndromic ASD Using Current ADI-R Scores. J. Autism Dev. Disord. 45, 1–13. https://doi.org/10.1007/s10803-013-2013-6

Michalon, A., Sidorov, M., Ballard, T.M., Ozmen, L., Spooren, W., Wettstein, J.G., Jaeschke, G., Bear, M.F., Lindemann, L., 2012. Chronic pharmacological mGlu5 inhibition corrects fragile X in adult mice. Neuron 74, 49–56. https://doi.org/10.1016/j.neuron.2012.03.009

Molofsky, A.V., Hochstim, C., Deneen, B., Rowitch, D., 2013. Mechanisms of Astrocyte Development. Patterning Cell Type Specif. Dev. CNS PNS 723–742. https://doi.org/10.1016/B978-0-12-397265-1.00080-0

Molofsky, A. V, Kelley, K.W., Tsai, H.-H., Redmond, S.A., Chang, S.M., Madireddy, L., Chan, J.R., Baranzini, S.E., Ullian, E.M., Rowitch, D.H., 2014. Astrocyte-encoded positional cues maintain sensorimotor circuit integrity. Nature 509, 189–94. https://doi.org/10.1038/nature13161

Mukherjee, S., Manahan-Vaughan, D., 2013. Role of metabotropic glutamate receptors in persistent forms of hippocampal plasticity and learning. Neuropharmacology 66, 65–81. https://doi.org/10.1016/J.NEUROPHARM.2012.06.005

Murai, K.K., Pasquale, E.B., 2011. Eph receptors and ephrins in neuron-astrocyte communication at synapses. Glia 59, 1567–1578. https://doi.org/10.1002/glia.21226

Neul, J.L., Kaufmann, W.E., Glaze, D.G., Christodoulou, J., Clarke, A.J., Bahi-Buisson, N., Leonard, H., Bailey, M.E.S., Schanen, N.C., Zappella, M., Renieri, A., Huppke, P., Percy, A.K., 2010. Rett syndrome: revised diagnostic criteria and nomenclature. Ann. Neurol. 68, 944–50. https://doi.org/10.1002/ana.22124

Nimchinsky, E. a, Oberlander, a M., Svoboda, K., 2001. Abnormal development of dendritic spines in FMR1 knock-out mice. J. Neurosci. 21, 5139–5146. https://doi.org/21/14/5139 [pii]

Okabe, Y., Takahashi, T., Mitsumasu, C., Kosai, K., Tanaka, E., Matsuishi, T., 2012. Alterations of gene expression and glutamate clearance in astrocytes derived from an MeCP2-null mouse model of Rett syndrome. PLoS One 7, e35354. https://doi.org/10.1371/journal.pone.0035354

Pacey, L.K.K., Doering, L.C., 2007. Developmental expression of FMRP in the astrocyte lineage: Implications for fragile X syndrome. Glia 55, 1601–1609. https://doi.org/10.1002/glia.20573

Peng, J., Fabre, P.J., Dolique, T., Swikert, S.M., Kermasson, L., Shimogori, T., Charron, F., 2018. Sonic Hedgehog Is a Remotely Produced Cue that Controls Axon Guidance Trans-axonally at a Midline Choice Point. Neuron 97, 326-340.e4. https://doi.org/10.1016/j.neuron.2017.12.028

Perea, G., Navarrete, M., Araque, A., 2009. Tripartite synapses: astrocytes process and control synaptic information. Trends Neurosci. 32, 421–31. https://doi.org/10.1016/j.tins.2009.05.001

Perego, C., Vanoni, C., Bossi, M., Massari, S., Basudev, H., Longhi, R., Pietrini, G., 2002. The GLT-1 and GLAST Glutamate Transporters Are Expressed on Morphologically Distinct Astrocytes and Regulated by Neuronal Activity in Primary Hippocampal Cocultures. J. Neurochem. 75, 1076–1084. https://doi.org/10.1046/j.1471-4159.2000.0751076.x

Pfrieger, F.W., Barres, B. a, 1997. Synaptic efficacy enhanced by glial cells in vitro. Science 277, 1684–1687. https://doi.org/10.1126/science.277.5332.1684

Powell, E.M., Meiners, S., DiProspero, N.A., Geller, H.M., 1997. Mechanisms of astrocyte-directed neurite guidance. Cell Tissue Res. 290, 385–393. https://doi.org/10.1007/s004410050945

Presson, A.P., Partyka, G., Jensen, K.M., Devine, O.J., Rasmussen, S.A., McCabe, L.L., McCabe, E.R.B., 2013. Current estimate of Down Syndrome population prevalence in the United States. J. Pediatr. 163, 1163–8. https://doi.org/10.1016/j.jpeds.2013.06.013

Pyka, M., Wetzel, C., Aguado, A., Geissler, M., Hatt, H., Faissner, A., 2011. Chondroitin sulfate proteoglycans regulate astrocyte-dependent synaptogenesis and modulate synaptic activity in primary embryonic hippocampal neurons. Eur. J. Neurosci. 33, 2187–2202. https://doi.org/10.1111/j.1460-9568.2011.07690.x

Recio-Pinto, E., Rechler, M., Ishii, D., 1986. Effects of insulin, insulin-like growth factor-II, and nerve growth factor on neurite formation and survival in cultured sympathetic and sensory neurons. J. Neurosci. 6, 1211–1219. https://doi.org/10.1523/jneurosci.06-05-01211.1986

Reemst, K., Noctor, S.C., Lucassen, P.J., Hol, E.M., 2016. The Indispensable Roles of Microglia and Astrocytes during Brain Development. Front. Hum. Neurosci. 10, 1–28. https://doi.org/10.3389/fnhum.2016.00566

Ross, W.T., Olsen, M., 2014. Care of the Adult Patient with Down Syndrome. South. Med. J. 107, 715–721. https://doi.org/10.14423/SMJ.0000000000000193

Rudelli, R.D., Brown, W.T., Wisniewski, K., Jenkins, E.C., Laure-Kamionowska, M., Connell, F., Wisniewski, H.M., 1985. Adult fragile X syndrome. Clinico-neuropathologic findings. Acta Neuropathol. 67, 289–95.

Rünker, A.E., Little, G.E., Suto, F., Fujisawa, H., Mitchell, K.J., 2008. Semaphorin-6A controls guidance of corticospinal tract axons at multiple choice points. Neural Dev. 3, 34. https://doi.org/10.1186/1749-8104-3-34

Serafini, T., Colamarino, S.A., Leonardo, E.D., Wang, H., Beddington, R., Skarnes, W.C., Tessier-Lavigne, M., 1996. Netrin-1 is required for commissural axon guidance in the developing vertebrate nervous system. Cell 87, 1001–14. https://doi.org/10.1016/s0092-8674(00)81795-x

Shepherd, J.D., Huganir, R.L., 2007. The Cell Biology of Synaptic Plasticity: AMPA Receptor Trafficking. Annu. Rev. Cell Dev. Biol. 23, 613–643. https://doi.org/10.1146/annurev.cellbio.23.090506.123516

Shirao, T., González-Billault, C., 2013. Actin filaments and microtubules in dendritic spines. J. Neurochem. 126, 155–164. https://doi.org/10.1111/jnc.12313

Sofroniew, M. V, Howe, C.L., Mobley, W.C., 2001. Nerve Growth Factor Signaling, Neuroprotection, and Neural Repair. Annu. Rev. Neurosci. 24, 1217–1281. https://doi.org/10.1146/annurev.neuro.24.1.1217

Somjen, G.G., 1988. Nervenkitt: Notes on the history of the concept of neuroglia. Glia 1, 2–9. https://doi.org/10.1002/glia.440010103

Squire, L.R., Berg, D.R., Bloom, F.E., du Lac, S., Ghosh, A., Spitzer, N.C., 2014. Fundamental Neuroscience. Elsevier.

Stobart, J.L., Anderson, C.M., 2013. Multifunctional role of astrocytes as gatekeepers of neuronal energy supply. Front. Cell. Neurosci. 7, 38. https://doi.org/10.3389/fncel.2013.00038

Suetsugu, M., Mehraein, P., 1980. Spine distribution along the apical dendrites of the pyramidal neurons in Down's syndrome. A quantitative Golgi study. Acta Neuropathol. 50, 207–10.

Suzuki, S., Kiyosue, K., Hazama, S., Ogura, A., Kashihara, M., Hara, T., Koshimizu, H., Kojima, M., 2007. Brain-Derived Neurotrophic Factor Regulates Cholesterol Metabolism for Synapse Development. J. Neurosci. 27, 6417–6427. https://doi.org/10.1523/jneurosci.0690-07.2007

Takashima, S., Ieshima, a, Nakamura, H., Becker, L.E., 1989. Dendrites, dementia and the Down syndrome. Brain Dev. 11, 131–133. https://doi.org/10.1016/S0387-7604(89)80082-8

Tonge, D.A., de Burgh, H.T., Docherty, R., Humphries, M.J., Craig, S.E., Pizzey, J., 2012. Fibronectin supports neurite outgrowth and axonal regeneration of adult brain neurons in vitro. Brain Res. 1453, 8–16. https://doi.org/10.1016/J.BRAINRES.2012.03.024

Torres, M.D., Garcia, O., Tang, C., Busciglio, J., 2018. Dendritic spine pathology and thrombospondin-1 deficits in Down syndrome. Free Radic. Biol. Med. 114, 10–14. https://doi.org/10.1016/j.freeradbiomed.2017.09.025

Tropea, D., Giacometti, E., Wilson, N.R., Beard, C., McCurry, C., Fu, D.D., Flannery, R., Jaenisch, R., Sur, M., Holm, I.A., Khatwa, U., Kapur, K., Alexander, M.E., Finnegan, D.M., Cantwell, N.G., Walco, A.C., Rappaport, L., Gregas, M., Fichorova, R.N., Shannon, M.W., Sur, M., Kaufmann, W.E., 2009. Partial reversal of Rett Syndrome-like symptoms in MeCP2 mutant mice. Proc. Natl. Acad. Sci. U. S. A. 106, 2029–2034. https://doi.org/10.1073/pnas.0812394106

Turovsky, E., Karagiannis, A., Abdala, A.P., Gourine, A. V, 2015. Impaired CO2 sensitivity of astrocytes in a mouse model of Rett syndrome. J. Physiol. 593, 3159–3168. https://doi.org/10.1113/JP270369

Ullian, E.M., Sapperstein, S.K., Christopherson, K.S., Barres, B. a, 2001. Control of synapse number by glia. Science 291, 657–661. https://doi.org/10.1126/science.291.5504.657

Verpelli, C., Schmeisser, M.J., Sala, C., Boeckers, T.M., 2012. Scaffold Proteins at the Postsynaptic Density, in: Advances in Experimental Medicine and Biology. pp. 29–61.

https://doi.org/10.1007/978-3-7091-0932-8_2

von Bartheld, C.S., Bahney, J., Herculano-Houzel, S., 2016. The search for true numbers of neurons and glial cells in the human brain: A review of 150 years of cell counting. J. Comp. Neurol. 524, 3865–3895. https://doi.org/10.1002/cne.24040

Waites, C.L., Craig, A.M., Garner, C.C., 2005. MECHANISMS OF VERTEBRATE SYNAPTOGENESIS. Annu. Rev. Neurosci. 28, 251–274. https://doi.org/10.1146/annurev.neuro.27.070203.144336

Walz, W., 2000. Role of astrocytes in the clearance of excess extracellular potassium. Neurochem. Int. 36, 291–300. https://doi.org/10.1016/S0197-0186(99)00137-0

Williams, E.C., Zhong, X., Mohamed, A., Li, R., Liu, Y., Dong, Q., Ananiev, G.E., Choongmok, J.C., Lin, B.R., Lu, J., Chiao, C., Cherney, R., Li, H., Zhang, S.-C.C., Chang, Q., Mok, J.C.C., Lin, B.R., Lu, J., Chiao, C., Cherney, R., Li, H., Zhang, S.-C.C., Chang, Q., 2014. Mutant astrocytes differentiated from Rett syndrome patients-specific iPSCs have adverse effects on wildtype neurons. Hum. Mol. Genet. 23, 2968–2980. https://doi.org/10.1093/hmg/ddu008

Xu, X., Miller, E.C., Pozzo-Miller, L., 2014. Dendritic spine dysgenesis in Rett syndrome. Front. Neuroanat. 8, 97. https://doi.org/10.3389/fnana.2014.00097

Yasui, D.H., Xu, H., Dunaway, K.W., LaSalle, J.M., Jin, L.-W., Maezawa, I., 2013. MeCP2 modulates gene expression pathways in astrocytes. Mol. Autism 4, 3. https://doi.org/10.1186/2040-2392-4-3

Yokoyama, N., Romero, M.I., Cowan, C.A., Galvan, P., Helmbacher, F., Charnay, P., Parada, L.F., Henkemeyer, M., 2001. Forward signaling mediated by ephrin-B3 prevents contralateral corticospinal axons from recrossing the spinal cord midline. Neuron 29, 85–97.

Yoshihara, Y., De Roo, M., Muller, D., 2009. Dendritic spine formation and stabilization. Curr. Opin. Neurobiol. 19, 146–153. https://doi.org/10.1016/j.conb.2009.05.013

Yudkin, D., Hayward, B.E., Aladjem, M.I., Kumari, D., Usdin, K., 2014. Chromosome fragility and the abnormal replication of the FMR1 locus in fragile X syndrome. Hum. Mol. Genet. 23, 2940–2952. https://doi.org/10.1093/hmg/ddu006

Chapter 2: Development of a novel protocol for the isolation of neonatal murine cortical astrocytes and neurons

Formatting note: every chapter in this dissertation has its own, self-contained introduction and discussion. The introduction and conclusion chapters are intended to broadly frame and contextualize the dissertation. All methods are confined to a single methods chapter at the end of the dissertation.

Introduction

Astrocytes play critical roles in normal neuronal growth and development, and in particular, the proteins they secrete are known to be important for synapse formation and plasticity (Blanco-Suárez, Caldwell, & Allen, 2016; Bosworth & Allen, 2017; Farhy-Tselnicker & Allen, 2018). However, due to methodological limitations, it has thus far been challenging to accurately survey the astrocyte secretome, even in animal models. Secreted proteins are challenging to study in vivo. In the context of the whole brain, it is difficult to quantify individual protein levels, and nearly impossible to determine which cells are producing which proteins. Thus it is necessary to isolate individual cells types in vitro to better understand their protein secretion patterns.

For several decades, researchers have used a popular and highly effective method for the isolation of rodent astrocytes, dubbed the MD method for its developers, Ken McCarthy and Jean DeVellis. The MD method of astrocyte isolation involves isolating the cerebral cortices from rat or mouse pups at postnatal day 0-2 (P0-2) and digesting the tissue in a papain solution before dissociating the tissue with a serological pipette and plating the single cell suspension in poly-D-lysine (PDL)-coated flasks with a serum-containing growth medium. At P0-2, the neurons are not viable under these conditions, and rapidly die in culture; the remaining glial cells form layers, with astroglia on the bottom, firmly attached to the flask surface. After several days, unwanted oligodendrocytes and floating microglia are removed by vigorous shaking to dislodge the top layers of cells, leaving the astroglia still attached to the flask (De Vellis and Cole, 2012; McCarthy and De Vellis, 1980). These isolated astroglial cells grow readily in culture in a serum-containing medium, and resemble astrocytes in several ways, but ultimately do not accurately recapitulate the morphology and behavior of astrocytes in vivo and appear to be more like astrocyte-precursor cells (Cahoy et al., 2008). There are a number of concerns regarding MD astrocytes and their utility in understanding astrocyte function, including 1) these cells have a flat, irregular morphology, compared to the bushy, process-bearing morphology of astrocytes in vivo; 2) MD

astrocytes continue to divide long after isolation, while in vivo astrocytes show limited division (Foo et al., 2011); 3) their gene expression profiles are more similar to those of astrocyte precursor cells than in vivo astrocytes (Cahoy et al., 2008); 4) isolating astrocytes at P0-2 means that the cells are not isolated during the time when they are involved in neuronal outgrowth and synapse formation (Farhy-Tselnicker and Allen, 2018), raising questions about whether or not these cells can accurately recapitulate the behavior of astrocytes at this critical time point; and 5) the presence of serum in the culture results in nonphysiological conditions, as serum is an undefined solution of proteins that are generally unlikely to cross the blood-brain barrier and may have a large impact on astrocyte properties in vitro (Foo et al., 2011).

These concerns create the necessity for a better method for the prospective isolation of astrocytes at a more physiologically relevant time point if we are to understand their roles in neuronal development. The innovative immunopanning approach pioneered by the Barres lab represents such an opportunity. Immunopanning involves the dissociation of neural tissue into a single cell suspension before passing that cell suspension over sequential Petri dishes coated with antibodies against cell-specific surface proteins to deplete unwanted cell types before a final, positive panning dish, where the desired cells are bound to the surface and unwanted cells are discarded. These viable isolated cells can then be collected and cultured for further analysis. In 2013, Lynette Foo published a protocol for the purification of rat astrocytes via immunopanning (Foo 2013) and demonstrated the viability of this technique for generating highly-enriched astrocyte cultures in serum-free medium from the rat brain at time points from P1 up until P18, that more closely resemble in vivo astrocytes when compared to MD astrocytes (Foo et al., 2011). However, while the Barres lab saw success in isolating rat astrocytes with this approach, it was not optimized for use in mice.

This presented a barrier in our research, as rat models of most genetic disorders are not readily available. In order to profile the proteins secreted by astrocytes under healthy, wild-type

(WT) conditions and in multiple genetic neurodevelopmental disorders (NDs), it was necessary to work with mice. Research has developed a new antibody targeting an astrocyte cell surface protein, astrocyte cell surface antigen-2 (ACSA2), now known to be ATPase Na+/K+ Transporting Subunit Beta 2 (ATP1b2), that may be utilized to isolate murine astrocytes across all developmental stages (Batiuk et al., 2017; G. Kantzer et al., 2017). This protein shows highly overlapping expression with the astrocyte marker GLAST, does not label non-astroglial cells, and is not papain-sensitive, making it a prime candidate for use with the immunopanning technique.

We have thus adapted the Foo et. al. astrocyte isolation protocol for use with an anti-ACSA2 antibody for the prospective isolation of mouse astrocytes at P7, when astrocytes are known to be involved in neuronal outgrowth and synapse formation (Figure 2.1A). Astrocytes isolated by immunopanning using this antibody show high expression of astrocyte markers by both qPCR/gene expression analysis and by immunocytochemical staining. The absence of serum in the media also enables us to identify the proteins secreted by astrocytes at this time point by conditioning the astrocytes in minimal protein-free media and collecting the media for an unbiased mass spectrometry analysis. This has allowed us to profile the proteins secreted by WT, Rett Syndrome (RTT), Fragile X Syndrome (FXS), and Down Syndrome (DS) astrocytes isolated from mouse models. This has, in turn, allowed us to compare the protein secretion profiles of WT and neurodevelopmental disordered (ND) astrocytes to identify changes that may play a role in the pathology of the NDs.

Beyond examining the protein secretome of WT and ND astrocytes in vitro, we also needed a system by which we could test any candidate proteins identified by the screen for effects on neuronal development. It was necessary to identify a means by which we could culture central nervous system (CNS) neurons under minimal media conditions to observe the effects of astrocyte-conditioned media (ACM) on neuronal growth. Many past studies on the role of astrocytes in neuronal development have involved mixed culture systems, wherein retinal

ganglion cells (RGCs) isolated from the retinas of neonatal rats are cultured with astrocyte-conditioned media or astrocyte inserts produced from cortical cell suspensions (Winzeler and Wang, 2013). This work has demonstrated important roles for astrocytes in supporting neuronal development and survival (Allen et al., 2012; Blanco-Suarez et al., 2018; Christopherson et al., 2005; Pfrieger and Barres, 1997; Ullian et al., 2001), but does not accurately recapitulate the full complexity of the interactions between neurons and astrocyte proteins in vivo. Additionally, the many studies that serve as the foundation for this dissertation used a multitude of mixed culture approaches; techniques ranged from growing rat hippocampal neurons on human fetal astrocytes (Garcia et al., 2010), to embryonic mouse hippocampal neurons grown with mouse cortical MD astrocyte feeder layers (Jacobs and Doering, 2010), to early postnatal mouse hippocampal neurons grown in rat cortical MD astrocyte-conditioned media (ACM) (Ballas et al., 2009), to human induced pluripotent stem cell (iPSC) mixed cultures (Chen et al., 2014). In no case had any one approach been used to consistently demonstrate the effects of astrocyte secreted proteins on the neurons they normally interact with in all three NDs.

Astrocyte heterogeneity is increasingly appreciated within the astrocyte biology community. Several studies have demonstrated that there are a wide variety of astrocyte subtypes, and that their gene expression varies across brain region, as well as across the life time (Bayraktar et al., 2014; Boisvert et al., 2018; Molofsky et al., 2014; Zhang and Barres, 2010). There is an increasing awareness, therefore, of the importance of recapitulating not only the relevant animal age using in vitro systems, but also the correct brain region. For the purposes of this research, we decided to adapt both the astrocyte immunopanning protocol (Foo 2013) and an existing cortical neuron immunopanning protocol (Steinmetz et al., 2006) to produce age-matched cortical neuron cultures. The approach is similar to the astrocyte immunopanning isolation, but instead of a prospective isolation for astrocytes, cortical neurons are selectively isolated using an antibody for neural cell adhesion molecule L1 (NCAM-L1). This method

produces viable neuronal cultures that survive in minimal media and show a 2-3 fold increase in neurite outgrowth in the presence of WT ACM (Figure 2.2). This has allowed us to study the effects of ACM from WT and ND astrocytes on age-matched cortical neurons to give deeper insight into the roles of astrocyte-secreted proteins on neuronal outgrowth in vitro.

Results and Discussion

Development of an immunopanned mouse astrocyte in vitro cell culture model.

To study astrocytes from the developing mouse cortex we used immunopanning to isolate the cells, modifying the procedure developed for rat astrocytes (Foo, 2013; Foo et al., 2011). The full protocol for the isolation of astrocytes can be found in Appendix 1, on page 188. Briefly, the cerebral cortices from P7 mice were isolated and the meninges removed before the tissue was digested with papain and manually triturated with a serological pipette to produce a single cell suspension. Cells were allowed to rest in solution at 34°C for at least 45 minutes to allow cell surface antigens to return to the surface for proper antibody binding. The cell suspension was then passed over antibody-coated plates to deplete irrelevant cell types. To obtain the most pure astrocyte cultures possible, we selected antibodies against most other cell types in the brain: Lectin to deplete endothelial cells, CD11b to deplete microglia, CD45 to deplete macrophages, and two separate plates of O4 for the depletion of oligodendrocyte precursor cells (OPCs). Positive selection of astrocytes was performed using an antibody against astrocyte cell surface protein 2 (ACSA2; against ATP1b2) (Figure 2.1A) (Batiuk et al., 2017; G. Kantzer et al., 2017). The remaining unbound cells (primarily neurons) were poured off and astrocytes were removed from this panning dish using trypsin, then resuspended in a minimal media.

Our approach included several additional changes compared to the Foo protocol for mouse astrocytes (Figure 2.1A). Firstly, we replaced a dish containing secondary antibody only, designed to deplete unwanted microglia and macrophages, with a plate containing lectin, to

capture microglia, macrophages, and endothelial cells. We next added a plate coated with CD11b antibody, to further deplete microglia, and an additional O4-coated plate to further deplete OPCs. Additionally, due to the nature of the genetic mutations causing RTT and FXS, we encountered difficulties achieving more than 3-4 animals of the appropriate genotype in any given mouse litter. Thus we further adapted the protocol for use with smaller Petri dishes and antibody volumes, allowing us to isolate the astrocytes from 2-4 brains at a time. This approach yielded approximately 1.2-1.5 million astrocytes per isolation, or roughly 300,000-400,000 astrocytes per mouse.

Isolated astrocytes were grown on poly-d-lysine (PDL)-coated glass coverslips in 24 well plates at a density of 40K-80K per well for immunocytochemical analysis, and in PDL-coated 6-well plastic tissue culture plates at 270K-350K to generate ACM. Cells were maintained in a 50:50 Neurobasal:DMEM serum-free media with the addition of the growth factor HB-EGF (heparin binding epidermal growth factor) to support cell survival, with the absence of serum essential to prevent the induction of genes associated with reactive astrocytes (Foo et al., 2011). These cells grew readily in culture, achieving confluence in 5-7 days.

We performed immunostaining quantification of the astrocyte cultures to determine astrocyte purity, and found that many cells express known astrocyte markers glial fibrillary acidic protein (GFAP) and aquaporin 4 (AQP4), while neurons and microglia are almost never detected, and OPCs are rarely detected (Figure 2.1D). However, this approach was challenging, as only around 35% of the cells expressed GFAP protein, while around 45% express Aqp4 (Figure 2.1E). This is likely due to variability of astrocyte expression of these proteins, rather than a problem with the isolation system; in images, it was clear that some cells expressed AQP4 and GFAP at much higher levels than others (Figure 2.1D). As GFAP protein expression is considered a marker of reactivity in astrocytes in vivo, and is induced by serum exposure in vitro, we took it as a promising sign that the astrocytes did not express high levels of GFAP. Further immunostaining

cultures for cell-specific markers showed the majority of cells are positive for the astrocyte marker GLAST (SLC1a3) (Figure 2.1B).

For a more accurate determination of astrocyte cell culture purity, we turned to a quantitative PCR approach. We designed qPCR primer pairs against genes that have been identified as cell-specific markers, including *Gfap* (astrocytes), *Syt1* (neurons), *Mog* (oligodendrocytes), *Cspg4* (OPCs), *Cd68* (microglia), and *Fgfr4* (fibroblasts). qRT-PCR analysis of astrocyte mRNA determined that immunopanned astrocytes are highly enriched for astrocyte markers and depleted for other cell type markers (Figure 2.1C). These results demonstrate that the immunopanning approach utilizing the ACSA2 antibody is a viable method for the isolation and culture of astrocytes. With this approach, we have successfully isolated and cultured astrocytes from WT and ND mouse models.

Generation of astrocyte conditioned media (ACM) for proteomics analysis and neuronal outgrowth assays.

To examine the protein secretome from WT and ND astrocytes, it was necessary to grow the cells in a very minimal media, containing no additional protein except for a small amount of the growth factor HB-EGF to support astrocyte survival, thus ensuring that the only protein present in the ACM would be proteins secreted by the astrocytes. This media was then collected and examined by mass spectrometry (see chapter 7, page 162). Additionally, ACM protein was also used for neuronal outgrowth assays in vitro, to study the effects of WT and ND astrocyte secreted proteins on neurite growth. Astrocytes were cultured after isolation for 5 to 7 days until confluent, then switched to a protein-free conditioning media for 5 days (50% phenol red-free neurobasal, 50% phenol red-free DMEM, pyruvate, glutamine, N-acetyl cysteine, penicillin, streptomycin, carrier-free HB-EGF). Astrocyte conditioned media (ACM) was concentrated 30-fold using a 3kDa cut-off centrifugal concentrator, to deplete small molecules and enrich for secreted proteins over

3kDa in size, giving a final protein yield of approximately 15μg in roughly 200 μl of ACM from 3 wells of a 6-well plate. Our initial mass spectrometry experiments determined that the presence of bovine serum albumin (BSA) in HB-EGF produced in the presence of BSA was sufficient to contribute to a high proportion of peptide spectra detected, necessitating the need to use carrier-free growth factors to enable detection of a high number of secreted proteins. This approach was used to analyze a large sample set of ACM (n=6 each for WT, RTT, FXS, and DS) for mass spectrometry analysis and whole cell lysate RNA (n=6 each for WT, RTT, and FXS; n=4 for DS) for RNASeq analysis (see chapter 3).

These results highlight the potential of this approach for generating consistent, matched ACM samples for deep quantitative examination of protein secretion in astrocytes from WT and disordered mice at P7, an important timepoint in the development and growth of neurons and in the formation of neuronal spines and synapses. This will allow for better study of the effects of astrocyte proteins on these processes. Furthermore, it demonstrates the importance of culturing astrocytes under completely serum free conditions to accurately detect astrocyte secreted proteins in vitro, as the presence of serum even as a stabilizing carrier protein for supportive factors is sufficient to dominate the peptides counted by mass spectrometry and may mask many low abundance proteins in an ACM sample. Thus the immunopanning approach represents an importance advancement in the study of astrocyte secreted proteins. One such application of this approach will be discussed in chapters 3-5 of this dissertation, as we describe the results of mass spectrometry analysis of astrocyte secreted proteins and the identification of protein factors that inhibit neuronal outgrowth.

Development of an immunopanned cortical neuron assay.

Previous studies demonstrated that WT neurons cultured with WT ACM or astrocytes show enhanced neurite outgrowth compared to neurons grown alone, whereas RTT, FXS and

DS astrocytes induce stunted outgrowth in WT neurons (Chen et al., 2014; Jacobs and Doering, 2010; Williams et al., 2014). However, this had not been studied using age-matched cortical neurons and cortical astrocytes in vitro, nor with cells isolated via immunopanning. To determine if ACM from immunopanned astrocytes has the same effects on neurite outgrowth as MD astrocyte ACM, we developed an immunopanning protocol to isolate age and region matched neurons from the P7 mouse cerebral cortex, using an antibody against the neuronal protein neuronal cell adhesion molecule L1 (NCAM-L1) (Figure 2.2A) (Steinmetz et al., 2006). Cortical neurons were plated in serum free medium (alone condition), or with ACM (3 µg/ml) added at the time of plating. To assess neurite outgrowth neurons were cultured for 48 hours and stained for MAP2 (dendrites) and Tau (axons) (Figure 2.2B,C), a time period used in previous studies to investigate effects of ND astrocytes on neurite development (Maezawa et al., 2009; Williams et al., 2014). At this early timepoint the longest processes are Tau positive, while the shorter processes are MAP2 positive (Fig 2.2C). We analyzed a number of parameters including total neurite outgrowth (axon + dendrite), longest neurite, and number of branches (Fig 2.2F). WT cortical neurons grown in isolation show minimal neurite outgrowth, and addition of WT ACM significantly increases total neurite outgrowth by 2 to 3-fold. ACM from astrocytes isolated from mice with null mutations in MECP2, a model of Rett's syndrome (RTT ACM), does not significantly increase neurite outgrowth compared to neurons alone (Figure 2.2D-F). We saw no significant changes in the number of processes or number of branches per process. These data demonstrate that immunopanned astrocytes from WT mice are able to support neurite outgrowth, whereas those from models of ND e.g. RTT cannot, and validate the cortical neuron outgrowth assay as a system to monitor functional differences between ND and WT astrocytes.

With these results, we determined that immunopanning is an appropriate method for the isolation of cortical neurons in vitro, and an assay by which we can test WT and ND ACM in vitro, and to examine the effects of candidate proteins identified by a proteomics analysis.

Immunopanning produces cortical astrocytes and neurons from age-matched postnatal mice, generating cultures that are more likely to recapitulate the interactions of these cells in the corresponding in vivo brain. This assay thus resolves some of the concerns surrounding astrocyte heterogeneity in the brain and further age-matches cortical neurons to cortical astrocytes at the relevant developmental timepoint, resulting in an assay that will be helpful for future studies on the roles of astrocytes in neuronal development. This approach also yields a consistent method by which to isolate neurons and astrocytes in vitro, to better compare the effects of ND and WT ACM on neurons and to further examine the similarities and differences between each ND and WT ACM, which will be discussed in chapter 3. This approach is used to assess the effects of ND and WT ACM, as well as individual protein factors identified as potential outgrowth inhibitory factors, and will be discussed in chapters 4 and 5 of this dissertation.

Acknowledgements

This chapter is, in part, in preparation for submission for publication. The dissertation author will be the first author of this publication, with Dr. Jolene Diedrich as second author and Dr. Nicola Allen as the senior author and principle investigator.

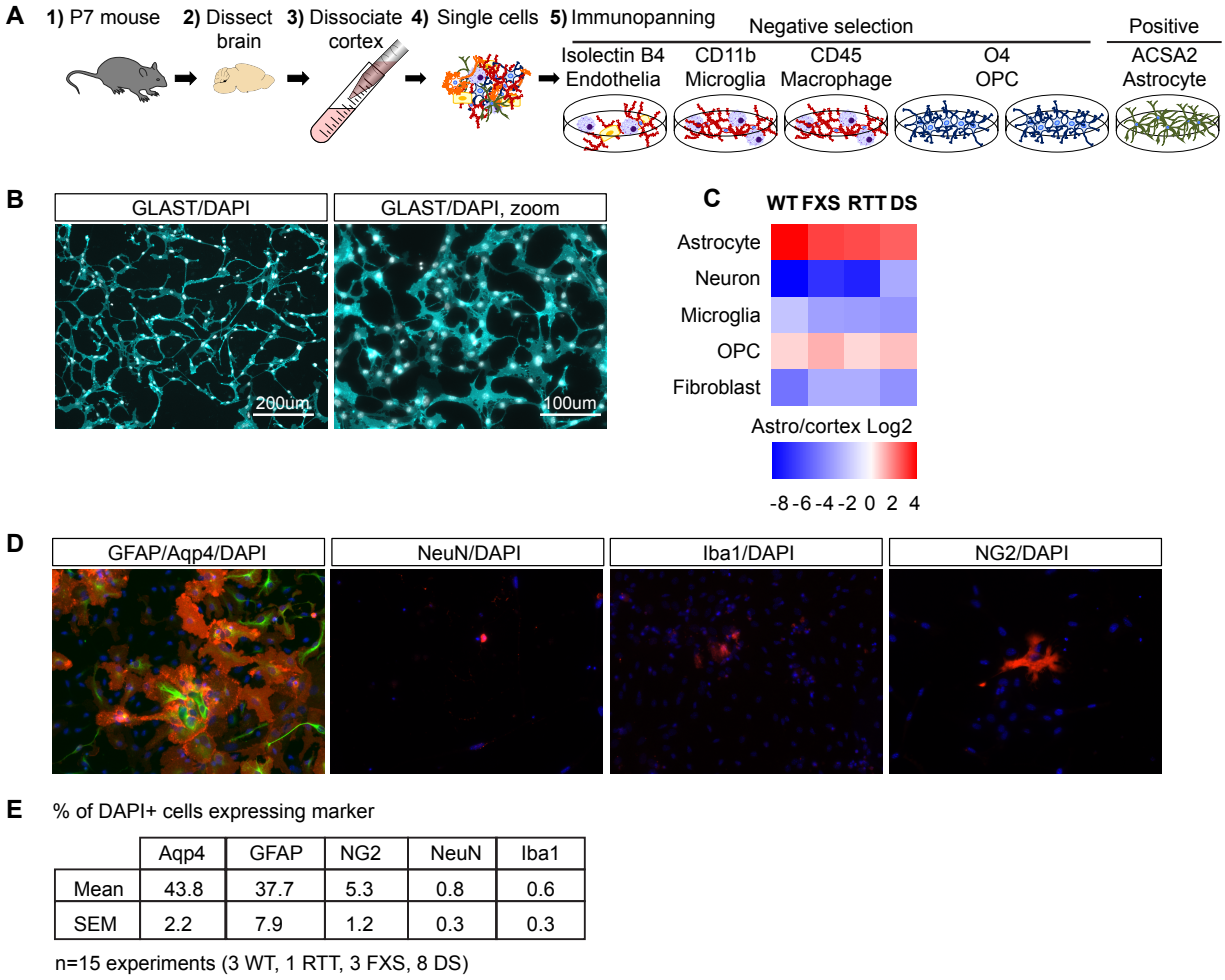

E % of DAPI+ cells expressing marker

	Aqp4	GFAP	NG2	NeuN	Iba1
Mean	43.8	37.7	5.3	0.8	0.6
SEM	2.2	7.9	1.2	0.3	0.3

n=15 experiments (3 WT, 1 RTT, 3 FXS, 8 DS)

Figure 2.1: Development and validation of mouse astrocyte immunopanning procedure. A. Schematic of the procedure: P7 mouse cortex is digested with papain to produce a single cell suspension, which undergoes a series of negative selection steps to deplete unwanted cells (endothelia, microglia, oligodendrocytes), followed by positive selection for astrocytes using an antibody against ACSA2. Neurons remain in the single cell suspension at the end of the procedure. **B.** Immunostaining IP-astrocyte cultures for the astrocyte marker GLAST (Slc1a3) demonstrates the majority of cells express this protein. **C.** qRT-PCR for cell-type markers from mRNA collected from IP astrocytes compared to P7 mouse cortex demonstrates enrichment for astrocytes (Gfap), a depletion of neurons (Syt1), microglia (Cd68), fibroblasts (Fgfr4), and a decrease in oligodendrocyte precursor cells (OPCs; Cspg4) in WT and ND IP astrocyte cultures. Averaged from N=6 cultures per genotype. **D,E.** Immunostaining IP-astrocyte cultures for cell type markers reveals that the majority of cells express astrocyte-associated proteins Gfap and Aqp4, while rarely expressing NeuN (neuronal marker), Iba1 (microglial marker) or NG2 (oligodendrocyte precursor cell marker). Images are representative. For quantification, n=15 total astrocyte cultures (3WT, 1 RTT, 3 FXS, 8 DS), with at least 3 ROIs analyzed per coverslip, 1 coverslip per assay per cell marker. No differences were observed between ND and WT expression of cell markers.

Figure 2.2: WT ACM supports WT neurite outgrowth, whereas RTT ACM does not. **A.** Schematic of the immunopanning procedure to isolate cortical neurons: P7 mouse cortex is digested with papain to produce a single cell suspension, which undergoes a series of negative selection steps to deplete unwanted cells (endothelia, microglia), followed by positive selection for neurons using an antibody against NCAM-L1. All other cells remain in the single cell suspension at the end of the procedure. **B-F.** Culturing WT cortical neurons for 48 hours with WT astrocyte conditioned media (ACM) increases neurite outgrowth, whereas RTT ACM does not. **B.** Example images of neurons in each condition, as analyzed by the MetaMorph software Neurite Outgrowth module. **C.** Example images from B, prior to processing and analysis. Neurons immunostained with MAP2 (dendrites, green) and tau (axon, red). **D,E.** Quantification of total neurite outgrowth (dendrite + axon) for each condition. Example experiment shown, experiment repeated 3 times with same result. **F.** Examination of other measures of neurite outgrowth (mean process length, maximum process length, etc.) reveal that there is an overall difference in outgrowth but not in process number or number of process branches. Bar graph represents mean ± s.e.m. Number inside bar = number of neurons analyzed. Statistics by one-way ANOVA, p values marked above each condition compared to neurons alone.

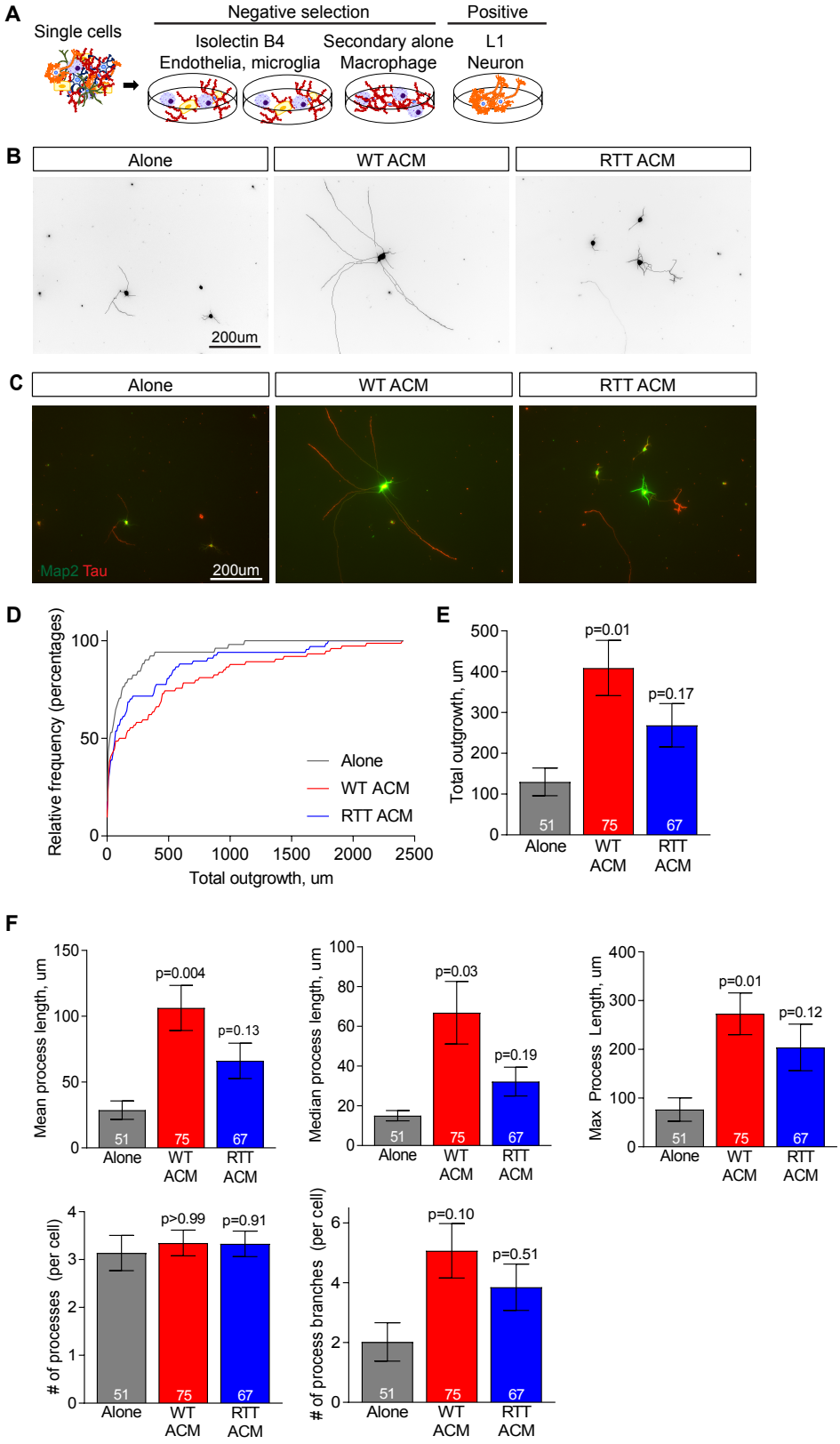
A
Single cells
Negative selection
Isolectin B4
Endothelia, microglia
Secondary alone
Macrophage
Positive
L1
Neuron
B
Alone
WT ACM
RTT ACM
200um
C
Alone
WT ACM
RTT ACM
Map2 Tau
200um
D
Relative frequency (percentages)
Total outgrowth, um
Alone
WT ACM
RTT ACM
E
Total outgrowth, um
p=0.01
p=0.17
51
75
67
Alone
WT ACM
RTT ACM
F
Mean process length, um
p=0.004
p=0.13
Median process length, um
p=0.03
p=0.19
Max Process Length, um
p=0.01
p=0.12
# of processes (per cell)
p>0.99
p=0.91
# of process branches (per cell)
p=0.10
p=0.51

References:

Allen, N.J., Bennett, M.L., Foo, L.C., Wang, G.X., Chakraborty, C., Smith, S.J., Barres, B. a., 2012. Astrocyte glypicans 4 and 6 promote formation of excitatory synapses via GluA1 AMPA receptors. Nature 486, 410–414. https://doi.org/10.1038/nature11059

Ballas, N., Lioy, D.T., Grunseich, C., Mandel, G., 2009. Non-cell autonomous influence of MeCP2-deficient glia on neuronal dendritic morphology. Nat. Neurosci. 12, 311–7. https://doi.org/10.1038/nn.2275

Batiuk, M.Y., de Vin, F., Duqué, S.I., Li, C., Saito, T., Saido, T., Fiers, M., Belgard, T.G., Holt, M.G., 2017. An Immunoaffinity-Based Method for Isolating Ultrapure Adult Astrocytes Based on ATP1B2 Targetting by the ACSA-2 Antibody. J. Biol. Chem. 292, jbc.M116.765313. https://doi.org/10.1074/jbc.M116.765313

Bayraktar, O.A., Fuentealba, L.C., Alvarez-Buylla, A., Rowitch, D.H., 2014. Astrocyte development and heterogeneity. Cold Spring Harb. Perspect. Biol. 7, a020362. https://doi.org/10.1101/cshperspect.a020362

Blanco-suárez, E., Caldwell, A.L.M., Allen, N.J., 2016. Role of astrocyte-synapse interactions in CNS disorders. J. Physiol. 00, 1–14. https://doi.org/10.1113/JP270988.This

Blanco-Suarez, E., Liu, T.F., Kopelevich, A., Allen, N.J., 2018. Astrocyte-Secreted Chordin-like 1 Drives Synapse Maturation and Limits Plasticity by Increasing Synaptic GluA2 AMPA Receptors. Neuron 1–17. https://doi.org/10.1016/j.neuron.2018.09.043

Boisvert, M.M., Erikson, G.A., Shokhirev, M.N., Allen, N.J., 2018. The Aging Astrocyte Transcriptome from Multiple Regions of the Mouse Brain. Cell Rep. 22, 269–285. https://doi.org/10.1016/j.celrep.2017.12.039

Bosworth, A.P., Allen, N.J., 2017. The diverse actions of astrocytes during synaptic development. Curr. Opin. Neurobiol. 47, 38–43. https://doi.org/10.1016/j.conb.2017.08.017

Cahoy, J.D., Emery, B., Kaushal, A., Foo, L.C., Zamanian, J.L., Christopherson, K.S., Xing, Y., Lubischer, J.L., Krieg, P. a, Krupenko, S. a, Thompson, W.J., Barres, B. a, 2008. A transcriptome database for astrocytes, neurons, and oligodendrocytes: a new resource for understanding brain development and function. J. Neurosci. 28, 264–278. https://doi.org/10.1523/JNEUROSCI.4178-07.2008

Chen, C., Jiang, P., Xue, H., Peterson, S.E., Tran, H.T., McCann, A.E., Parast, M.M., Li, S., Pleasure, D.E., Laurent, L.C., Loring, J.F., Liu, Y., Deng, W., 2014. Role of astroglia in Down's syndrome revealed by patient-derived human-induced pluripotent stem cells. Nat. Commun. 5, 4430. https://doi.org/10.1038/ncomms5430

Christopherson, K.S., Ullian, E.M., Stokes, C.C. a, Mullowney, C.E., Hell, J.W., Agah, A., Lawler, J., Mosher, D.F., Bornstein, P., Barres, B. a., 2005. Thrombospondins are astrocyte-secreted proteins that promote CNS synaptogenesis. Cell 120, 421–433. https://doi.org/10.1016/j.cell.2004.12.020

De Vellis, J., Cole, R., 2012. Preparation of Mixed Glial Cultures from Postnatal Rat Brain. pp. 49–59. https://doi.org/10.1007/978-1-61779-452-0

Farhy-Tselnicker, I., Allen, N.J., 2018. Astrocytes, neurons, synapses: a tripartite view on cortical circuit development. Neural Dev. 13, 7. https://doi.org/10.1186/s13064-018-0104-y

Foo, L.C., 2013. Purification of rat and mouse astrocytes by immunopanning. Cold Spring Harb. Protoc. 8, 421–432. https://doi.org/10.1101/pdb.prot074211

Foo, L.C., Allen, N.J., Bushong, E.A., Ventura, P.B., Chung, W.S., Zhou, L., Cahoy, J.D., Daneman, R., Zong, H., Ellisman, M.H., Barres, B.A., 2011. Development of a method for the purification and culture of rodent astrocytes. Neuron 71, 799–811. https://doi.org/10.1016/j.neuron.2011.07.022

G. Kantzer, C., Boutin, C., Herzig, I.D., Wittwer, C., Reiß, S., Tiveron, M.C., Drewes, J., Rockel, T.D., Ohlig, S., Ninkovic, J., Cremer, H., Pennartz, S., Jungblut, M., Bosio, A., 2017. Anti-ACSA-2 defines a novel monoclonal antibody for prospective isolation of living neonatal and adult astrocytes. Glia 990–1004. https://doi.org/10.1002/glia.23140

Garcia, O., Torres, M., Helguera, P., Coskun, P., Busciglio, J., 2010. A role for thrombospondin-1 deficits in astrocyte-mediated spine and synaptic pathology in down's syndrome. PLoS One 5. https://doi.org/10.1371/journal.pone.0014200

Jacobs, S., Doering, L.C., 2010. Astrocytes prevent abnormal neuronal development in the fragile x mouse. J. Neurosci. 30, 4508–14. https://doi.org/10.1523/JNEUROSCI.5027-09.2010

Maezawa, I., Swanberg, S., Harvey, D., LaSalle, J.M., Jin, L.-W., 2009. Rett syndrome astrocytes are abnormal and spread MeCP2 deficiency through gap junctions. J. Neurosci. 29, 5051–61. https://doi.org/10.1523/JNEUROSCI.0324-09.2009

McCarthy, K.D., De Vellis, J., 1980. PREPARATION OF SEPARATE ASTROGLIAL AND OLIGODENDROGLIAL CELL CULTURES FROM RAT CEREBRAL TISSUE A novel method has been developed for the preparation of nearly pure separate cultures of astrocytes and oligodendrocytes . The method is based on (a) the abs. J. Cell Biol. 85, 890–902.

Molofsky, A. V, Kelley, K.W., Tsai, H.-H., Redmond, S.A., Chang, S.M., Madireddy, L., Chan,

J.R., Baranzini, S.E., Ullian, E.M., Rowitch, D.H., 2014. Astrocyte-encoded positional cues maintain sensorimotor circuit integrity. Nature 509, 189–94. https://doi.org/10.1038/nature13161

Pfrieger, F.W., Barres, B. a, 1997. Synaptic efficacy enhanced by glial cells in vitro. Science 277, 1684–1687. https://doi.org/10.1126/science.277.5332.1684

Steinmetz, C.C., Buard, I., Claudepierre, T., Nägler, K., Pfrieger, F.W., 2006. Regional variations in the glial influence on synapse development in the mouse CNS. J. Physiol. 577, 249–61. https://doi.org/10.1113/jphysiol.2006.117358

Ullian, E.M., Sapperstein, S.K., Christopherson, K.S., Barres, B. a, 2001. Control of synapse number by glia. Science 291, 657–661. https://doi.org/10.1126/science.291.5504.657

Williams, E.C., Zhong, X., Mohamed, A., Li, R., Liu, Y., Dong, Q., Ananiev, G.E., Choongmok, J.C., Lin, B.R., Lu, J., Chiao, C., Cherney, R., Li, H., Zhang, S.-C.C., Chang, Q., Mok, J.C.C., Lin, B.R., Lu, J., Chiao, C., Cherney, R., Li, H., Zhang, S.-C.C., Chang, Q., 2014. Mutant astrocytes differentiated from Rett syndrome patients-specific iPSCs have adverse effects on wildtype neurons. Hum. Mol. Genet. 23, 2968–2980. https://doi.org/10.1093/hmg/ddu008

Winzeler, A., Wang, J.T., 2013. Purification and Culture of Retinal Ganglion Cells from Rodents. Cold Spring Harb. Protoc. 8, 643–652. https://doi.org/10.1101/pdb.prot074906

Zhang, Y., Barres, B. a, 2010. Astrocyte heterogeneity: an underappreciated topic in neurobiology. Curr. Opin. Neurobiol. 20, 588–94. https://doi.org/10.1016/j.conb.2010.06.005

Chapter 3: In-depth profiling of the protein secretion and gene expression profiles of wild-type and neurodevelopmental disordered astrocytes in vitro

Formatting note: every chapter in this dissertation has its own, self-contained introduction and discussion. The introduction and conclusion chapters are intended to broadly frame and contextualize the dissertation. All methods are confined to a single methods chapter at the end of the dissertation.

Introduction

The study of secreted proteins presents a challenge. There are no methods to quantitatively examine protein secretion in vivo, while in vitro approaches must include the caveat that isolated primary cell cultures cannot fully recapitulate the conditions of a living brain. Thus while a number of astrocyte-secreted proteins important for normal brain development and synapse formation have been identified, there are many questions still to be answered about the functional impact of astrocyte-secreted proteins during development in both wild-type (WT) and neurodevelopmental disordered (ND) brains.

A number of studies have attempted to profile the protein secretion of astrocytes in vitro. Short-term (24 hour) conditioning of astrocytes isolated at P0-P1 using the traditional method (McCarthy and De Vellis, 1980) identified 187 unique astrocyte-secreted proteins using a shotgun proteomics and bioinformatics approach; proteins identified included SPARC, Complement C3, insulin-like growth factor binding protein 5 (IGFBP5), insulin-like growth factor binding protein 2 (IGFBP2), apolipoprotein E (APOE), SPARC-like protein 1 (SPARCL1), and Carboxypeptidase E (CPE) (Dowell et al., 2009), most of which are also expressed at high levels in astrocytes by gene expression analysis (Zhang, Trautmann, Artelt, Burnet, & Schluesener, 2006). A similar study showed significant overlap in the secreted proteins detected, including SPARCL1 and CPE (Keene et al., 2009). Further research identified 516 proteins in astrocytes, 92 of which demonstrated significantly enriched levels in astrocyte conditioned media (ACM) compared to cell lysates, including APOE and SPARC (Greco et al., 2010).

It is important to note, however, that these studies faced certain limitations; in all cases, astrocytes were initially grown in serum-containing media, which has been found to profoundly alter the gene expression profiles of astrocytes in vitro and induces a reactive morphology (Cahoy et al., 2008; Foo et al., 2011). Furthermore, these studies were done using immature astrocytes isolated at P0-P1, making the results of limited use for identifying astrocyte proteins that might be

linked to neuronal outgrowth and synapse formation, which occur at later stages. Finally, these studies focused primarily on the secretome of WT astrocytes or WT astrocytes treated with individual protein factors; none attempted to identify functional changes between WT and ND astrocytes.

As discussed, astrocytes have been implicated in the pathology of a number of genetic neurodevelopmental disorders associated with autism. Research on the proteomics of ASD has generally been focused on the identification of biomarkers using noninvasive approaches, and little is known about protein alterations in glia. Proteomics analysis on post-mortem ASD brains across a wide age range and in both genders found an increased expression of glial markers such as GFAP (in the cerebellum), and myelin basic protein (MBP) and myelin-oligodendrocyte glycoprotein (MOG) (in the frontal cortex), while seeing a decrease in synaptic release associated proteins such as synapsin-2 (SYN2), and synaptotagmin-1 (SYT1) compared to controls (Broek et al., 2014), which may indicate changes in the number of glia and synaptic connectivity in ASD brains. Analysis of ASD patient plasma and serum has found alterations in proteins associated with the inflammatory response and with lipid metabolism compared to controls, such as increased levels of alpha-2-macroglobulin (A2M) and apolipoprotein E (APOE, in female patients) and lower levels of apolipoprotein J (APOJ) (Cortelazzo et al., 2016; Guest and Martins-de-Souza, 2017; Steeb et al., 2014). Other work has found changes in the levels of amyloid precursor protein (APP) and bone morphogenetic proteins (BMPs), proteins implicated in synapse formation and maintenance in ASD (Guest and Martins-de-Souza, 2017; Steeb et al., 2014).

There has been some research focused on protein changes in specific NDs associated with ASD. For example, proteomics analysis of neurons and synaptosomes in FXS mice showed increased levels of APP, while proteomic analysis of fibroblasts from DS patients saw upregulation in proteins such as APP and growth-arrest-specific gene 6 (GAS6) (Liu et al., 2017), which has been found to protect against apoptosis in neurons and oligodendrocytes (Shankar et

al., 2003; Yagami et al., 2002). Research on induced pluripotent stem cells from RTT patients and their fathers found alterations in the ratio of neurons to astrocytes during differentiation indicating a skew toward the expression of neuronal markers, which may bias overall proteomics data (Kim et al., 2019). Mass spectrometry analysis of the cortex of adult RTT mice showed a decrease in the expression of APOJ, corresponding to the results seen in human ASD patients (Cortelazzo et al., 2016; Pacheco et al., 2017). However, none of these studies have focused specifically on the roles of glial cells in the pathology of ASD or in genetic disorders associated with the condition, and the study of secreted proteins in plasma and serum has focused on the identification of biomarkers as opposed to therapeutic targets for the condition.

Some work has been done using other in vitro models to study astrocyte protein secretion in NDs; in particular, Krencik et. al. used induced pluripotent stem cells (iPSCs) from human patients with Costello syndrome as well as WT controls to generate astroglial cells for the study of alterations in the astrocyte secretome. Costello Syndrome, caused by a mutation in the Harvey rat sarcoma viral oncogene homolog (HRAS), is a genetic disorder that leads to alterations in the Ras/MAPK signaling pathway and has been associated with ASD (Garg et al., 2017; Schwartz et al., 2017; Young et al., 2018). Krencik et. al. found that astroglial cells differentiated from iPSCs derived from Costello Syndrome patient fibroblasts show accelerated maturation compared to wild-type counterparts, and demonstrate a dramatic increase in cell area. Transcriptional and proteomics analysis found that these cells overproduce extracellular matrix remodeling factors and proteoglycans (including CSPGs, HSPGs, SPARC, TSP1, and GPC6) (Krencik et al., 2015), indicating that there may be hyperactivation of astrocyte-to-neuron signaling in this disorder. However, this work did not explore the protein secretion profiles of other NDs associated with autism, nor did it utilize a serum-free model.

Here, we have focused our study on three NDs in particular: Rett Syndrome (RTT), Fragile X Syndrome (FXS), and Down Syndrome (DS). All three conditions present with similar neuronal

defects, including changes in dendritic arborization and altered dendritic spine and synapse formation. Previous research has been conducted on astrocytes from individual NDs to identify candidate factors that contribute to altered neuronal development. These studies showed that astrocytes from patients with DS have decreased expression of synaptogenic proteins thrombospondin and glypican (Chen et al., 2014; Garcia et al., 2010; Torres et al., 2018) and mouse FXS astrocytes release excess neurotrophin 3 (NT3) which inhibits dendrite growth, as well as decreased levels of synaptogenic thrombospondins and hevin (Blanco-Suárez, Caldwell, & Allen, 2016; Cheng, Lau, & Doering, 2016; Wallingford, Scott, Rodrigues, & Doering, 2017; Yang et al., 2012).

These studies of individual NDs and the limited proteomics studies of ASD provide compelling evidence that alterations in astrocyte function and protein secretion contribute to aberrant neuronal development, and raise the possibility that there may be alterations shared across multiple disorders that represent new therapeutic targets for sporadic ASD. We therefore set out to identify what the alterations in protein secretion are from astrocytes from multiple mouse models of NDs (FXS, RTT, DS) compared to WT, and determine which of these alterations functionally impact neuronal development. As there are currently no methods to identify alterations in protein secretion from specific cell types in vivo, as described in chapter 2, we developed an in vitro approach using immunopanning to prospectively isolate astrocytes from the postnatal day 7 (P7) mouse cortex of WT and ND mouse models and maintained the astrocytes in serum free media (Foo et al., 2011). We selected P7 as it is an active time of neurite outgrowth and synapse formation in the developing cortex, making this a relevant timepoint to identify alterations between astrocytes from WT and NDs (Farhy-Tselnicker and Allen, 2018).

Using this approach we identified for the first time the quantitative protein secretion profile of WT astrocytes from the developing brain, identifying ~1200 proteins present at more than 0.01% of total protein. We further determined how astrocytes from 3 models of ND differ in protein

secretion from WT, identifying unique changes for each disorder, as well as 88 proteins that are significantly increased in secretion across all NDs. Interestingly, although gene expression was altered between WT and ND astrocytes, there was little overlap in protein secretion and gene expression changes, highlighting the importance of a proteomics approach when studying secreted proteins. This work has generated a database of astrocyte-secreted proteins and gene expression profiles from WT and ND astrocytes that can be used to inform future studies on the roles of astrocytes in neuronal development and the functional impact of genetic disorders on astrocyte function. This unbiased approach allowed us to identify new candidate proteins and pathways that may present therapeutic targets for ASD.

Results

Identification of protein secretion and gene expression profile of immunopanned astrocytes.

The cortical neuron outgrowth experiments described in chapter 2 demonstrate that ACM from RTT astrocytes does not support neurite outgrowth (Figure 2.2B-F), meaning that a difference in the composition of proteins secreted from the astrocytes is likely responsible. To analyze what the differences are we compared protein secretion and gene expression from astrocytes from 3 mouse models of NDs to strain matched WT control: 1) RTT, *Mecp2* KO (Jax 003890), male KO mice; 2) FXS, *Fmr1* KO (Jax 003025), male and female KO mice; 3) DS, Down syndrome transgenic (Jax 005252), male and female mice with one copy of the duplicated chromosome; 4) WT control C57Bl6J (Jax 000664), male and female mice. We chose to use KO rather than heterozygous mice to make astrocyte cultures for RTT and FXS, as heterozygous cultures would be a mixture of WT and KO cells due to the gene of interest being present on the X chromosome and random inactivation of the X chromosome occurring.

For mass spectrometry analysis of protein secretion, ACM from 6 separate cultures per genotype was analyzed, giving a total of 24 samples. For each sample 5µg of ACM was analyzed in triplicate using a Thermo Orbitrap Fusion Tribrid Mass Spectrometer (technical replicates, 15µg total protein analyzed). Peptide spectra were assigned to proteins, and the number of spectra per protein normalized to the total number of spectra in the run, to give a quantitative readout represented as % of total protein in ACM (Supplemental Table 1). To focus on proteins that are robustly detected we filtered for proteins that were present as at least 0.01% of total protein in at least one of the genotypes. This identified 1236 unique proteins in WT ACM. Patternlab software was used to determine if proteins were present at significantly different levels between ACM from WT and each ND, with significance set at $p<0.05$, abundance >0.01%, fold change between WT and ND ≥1.5. For RNA sequencing analysis of gene expression, 6 separate cultures of WT, FXS and RTT, along with 4 separate cultures of DS were analyzed, giving a total of 22 samples (Supplemental Table 2). For WT astrocytes, 12451 genes are present at FPKM>1. Significance for differential expression was defined as adjusted $p<0.05$, calculated with EdgeR using Benjamini-Hochberg's procedure for multiple comparisons, along with expression FPKM>1 and fold change between ND and WT >1.5, comparing each ND and WT.

Analysis of immunopanned astrocyte properties.

We first asked if immunopanned astrocytes resemble in vivo astrocytes at P7 by analyzing expression levels of genes commonly associated with astrocyte function (Figure 3.1A,B). This included astrocyte markers *Gfap*, *Aqp4* and *Aldh1l1*, all of which are expressed at high levels by immunopanned astrocytes. Of note, there are no significant differences in marker gene expression between WT and ND astrocytes, except the calcium binding protein *S100β* which is significantly more highly expressed by DS astrocytes than WT. We next examined ion channels and transporters commonly associated with astrocyte function, including the potassium channel

Kir4.1 (Kcnj10), the glutamate uptake transporters *Glt1* (Slc1a2) and *Glast* (Slc1a3), and metabolic enzymes including *Ldha* (lactate dehydrogenase) and *Srebf1* (lipid synthesis). These are all expressed at high levels by immunopanned astrocytes, with similar levels detected across genotypes for most genes, except *Glt1* which is decreased in FXS and the GABA uptake transporter *Slc6a11* which is decreased in both FXS and DS. The decreased expression of *Glt1* in FXS astrocytes reproduces a finding previously reported for astrocytes in vivo in FXS KO mice, validating the immunopanning model for studying astrocyte properties in vitro (Higashimori et al., 2016, 2013). We further asked if expression of neurotransmitter receptors was altered between astrocytes from ND and WT, and determined that the metabotropic glutamate receptors *Grm3* and *Grm5*, as well as the metabotropic GABA receptor *Gabbr1* are downregulated in FXS astrocytes, while *Grm5* is decreased in DS. As with *Glt1*, the decrease in *Grm5* has previously been reported in FXS astrocytes in vivo (Higashimori et al., 2013).

As a next approach to validate the immunopanning model, we determined the top 15 most abundant proteins (out of 1236) secreted by and top 15 genes (out of 12451) most highly expressed by WT immunopanned astrocytes (Figure 3.1B,C). Both lists include well known astrocyte-secreted proteins such as DBI (diazepam binding inhibitor), APOE (apolipoprotein E, a component of astrocyte lipid particles) and SPARC (an inhibitor of synapse formation and function) (Allen and Eroglu, 2017; Christian and Huguenard, 2013). At the gene expression level there were few significant differences between WT and each ND in the top 15, with just an upregulation in *Mt1* and *Mt2* (metallothionein family members, zinc binding proteins) in DS astrocytes. There were more differences in protein secretion detected, of note a significant increase in IGFBP2 (a secreted binding protein for insulin-like growth factors 1 and 2 (IGF1/IGF2), CPE (carboxypeptidase E, a component of the secretory pathway) and APOE, from all 3 ND astrocytes compared to WT.

Synapse regulating factors in immunopanned astrocytes.

Having determined that immunopanned astrocytes express many of the same genes as developing astrocytes in vivo, we next asked if they produce known astrocyte-secreted synapse regulating proteins (Figure 3.1E-I). Synaptogenic proteins are present at varying abundances in WT ACM, for example SPARCL1/hevin (induces silent synapse formation) is the most abundant at 0.26%, glypican 4 (GPC4, induces immature GluA1 AMPAR-containing synapses) is at 0.11%, and thrombospondin 2 (TSP2, induces silent synapse formation) is the least abundant at 0.002% (Figure 3.1F) (Allen et al., 2012; Christopherson et al., 2005; Kucukdereli et al., 2011). This demonstrates that the abundance of a protein in ACM is not necessarily indicative of its functional effect. When comparing protein levels between WT and each ND, this identified a significant increase in chordin like 1 (CHRDL1, induces synapse maturation via recruitment of GluA2 AMPARs, (Blanco-Suarez et al., 2018)) in DS ACM, an increase in GPC4 and GPC6 in RTT and DS ACM, and an increase in SPARCL1 in RTT ACM, providing additional evidence that alterations in astrocyte secreted synaptogenic factors may be involved in these disorders. When looking at gene expression, only *Chrdl1* was also significantly altered at the mRNA level (Figure 3.1G). Conversely *Tsp2* mRNA was significantly decreased in FXS astrocytes, with no alteration in protein secretion (although the levels of protein are very low, making it challenging to detect a difference). As summarized in the introduction, previous studies of astrocytes from DS and FXS prepared from the P0-2 cortex and cultured in serum had detected decreased levels of synaptogenic genes including glypicans, thrombospondins and SPARCL1, a result not reproduced here, perhaps reflecting the difference in age of isolation or culture condition of the cells.

When looking at proteins implicated in developmental synapse elimination a similar pattern was seen, with more differences detected in secreted protein level than in gene expression (Figure 3.1H,I). For example, an increase in the extracellular portion of the membrane

protein MEGF10 (involved in phagocytosis of synapses) was detected in ACM from all NDs, with no corresponding change in mRNA level (Chung et al., 2013). TGFβ2 (transforming growth factor beta 2), which regulates expression of components of the complement cascade involved in synapse elimination, is also upregulated at the protein level across disorders with no change in mRNA (Bialas and Stevens, 2013). SPARC (a negative regulator of synapse formation) is highly abundant in WT ACM, present at 1.97%, and is further upregulated in DS to 3.58%, with no change in gene expression. Interestingly, two components of the complement cascade that are expressed by astrocytes show opposite changes in DS at both the protein and mRNA level, with C3 being increased and C4b decreased (Sekar et al., 2016; Stevens et al., 2007).

ND immunopanned astrocytes are not more reactive than WT astrocytes.

A hypothesis for why astrocytes in NDs have a negative impact on neuronal development is that they are in a reactive state and produce damaging inflammatory mediators (Russo et al., 2018; Yuskaitis et al., 2010), and some proteomics research has implicated increased expression of inflammatory factors in ASD (Guest and Martins-de-Souza, 2017). We compared the fold-change in gene expression between each ND and WT for a panel of reactive astrocyte genes recently described (Liddelow et al., 2017). No consistent upregulation of reactive genes was detected (Figure 3.1J). While this does not rule out that astrocytes are reactive in NDs in vivo, this culture system allows dissociation of reactive changes from other alterations to astrocyte function. These results indicate that IP astrocytes are a physiologically relevant in vitro model to examine protein secretion and gene expression differences of astrocytes in NDs.

Identification of altered protein secretion and gene expression between astrocytes from WT and individual NDs.

Having determined that immunopanned astrocytes are a good model to identify astrocyte protein secretion and gene expression, we next asked how astrocytes from each individual ND are altered from WT. We separately determined significantly upregulated and downregulated secreted proteins and genes for each disorder, as well as the overlap between protein and gene expression changes for each category (Supplemental Tables 3-5).

Fragile X Syndrome (FXS)

In FXS, levels of *Fmr1* gene expression were down, as expected. We found that 125 proteins showed increased secretion in FXS ACM compared to WT, while 524 genes showed increased mRNA expression. 4.6% of upregulated protein also showed altered mRNA levels in FXS, with six targets overlapping (*Gas6, Sema3e, Bmp6, Pltp, Fmod, Igfbp5*) (Figure 3.2A,B). 104 proteins showed decreased secretion in FXS ACM compared to WT, and 219 genes showed a decrease in mRNA levels, with 4 targets overlapping (*Arhgdib, Atp1a2, Vtn, Mcam*) for a 3.7% rate of overlap in downregulated proteins also showing alterations at the mRNA level in FXS (Figure 3.2G,H). Our results did not replicate previous work demonstrating increased secretion of NT3 from FXS astrocytes (Yang et al., 2012), which may be due to the difference in astrocyte isolation methods used, as Yang et. al. used the more traditional MD method. Furthermore, while others have reported decreased levels of synaptogenic factors in FXS in vitro (Blanco-Suarez et al., 2018; Cheng et al., 2016; Wallingford et al., 2017), we did not see changes in the levels of synaptogenic proteins such as GPC4, GPC6, and SPARC.

PANTHER pathway analysis of secreted proteins found upregulation in proteins related to the Alzheimer disease-amyloid secretase pathway and the blood coagulation pathway, while Reactome pathway analysis found increases in proteins relating to post-translational protein phosphorylation, regulation of IGF transport and uptake by IGFBPs, glycosaminoglycan metabolism, plasma lipoprotein remodeling, and degradation of the extracellular matrix. PANTHER protein class analysis found increases in extracellular matrix protein, serine protease

inhibitor, and complement component (Figure 3.2M). These results support a role for astrocyte secreted proteins in supporting neuronal metabolism, regulating gene expression, and regulating neurotrophic protein factors, along with having effects on the extracellular environment.

Rett Syndrome (RTT)

In RTT, *Mecp2* mRNA expression was significantly decreased. 187 proteins showed increased secretion in RTT ACM compared to WT, while only 25 genes showed an increase in mRNA expression. Interestingly, there was no overlap between the mRNA and protein level increases; 0% of upregulated protein was also altered at the mRNA level in RTT (Figure 3.2C,D). Conversely, 199 proteins showed a decrease in secretion in RTT compared to WT, while 17 genes had a decrease in mRNA expression, with an overlap of 1 target (*Ktcd12*), with 0.5% of downregulated protein also showing a decrease in mRNA levels (Figure 3.2I,J). Several proteins showing significant increases in secretion in RTT overlapped with candidates previously identified by transcriptomic analysis in RTT (Sanfeliu et al., 2019), including EFEMP1 and C1QTFN5, but these did not show concurrent increases in gene expression. One hypothesis regarding the pathology of RTT is that a deficiency in IGF signaling contributes to the pathology of the condition; as will be discussed in chapter 4, we saw a significant decrease in secretion of IGF2 and a slight decrease in IGF1 in RTT ACM, while there was increased secretion of several IGFBPs, including IGFBP2, IGFBP3, IGFBP4, and IGFBP5. However, we did not see a significant decrease in the mRNA levels for IGF1 or IGF2, or a significant increase in mRNA levels for the IGFBPs (Figure 4.2B).

PANTHER protein pathway analysis found an increased in secretion of proteins associated with the Alzheimer disease-amyloid secretase pathway and the integrin signaling pathway, while Reactome pathway analysis found increased release of proteins in several pathways, including post-translational protein phosphorylation, regulation of IGF transport and uptake by IGFBPs, glycosaminoglycan metabolism, regulation of the complement cascade,

plasma lipoprotein remodeling, degradation of the extracellular matrix, and NCAM1 interactions. PANTHER protein class analysis found increases in extracellular matrix protein, serine protease inhibitor, and complement component (Figure 3.2M). This similarly highlights the importance of astrocyte secreted proteins for maintaining a proper extracellular environment and in regulation of the expression and activity of downstream proteins.

Down Syndrome (DS)

In DS, several genes associated with this disorder were found to show increased mRNA expression, including *App, Istn1*, and *Adamts1* (Hunter et al., 2011; Lana-Elola et al., 2011; Miguel et al., 2005; Trazzi et al., 2013). Additionally, APP showed increased protein secretion, which is associated with high rates of Alzheimer's Disease in DS patients. In total, there were 235 proteins that showed increased levels in DS ACM compared to WT, while 352 genes showed increased mRNA expression. There was an overlap of 37 targets (*Scg5, Ecrg4, Ifnar2, Omd, Sema3e, Efemp1, C1ra, Fbln7, Gas6, Npvf*: see Supplemental Table 5 for full list) for a 13.6% overlap of upregulated proteins showing increased mRNA levels in DS (Figure 3.2 E,F). Conversely, 490 proteins showed a decrease in secretion in DS ACM compared to WT, while 186 genes showed a decrease in gene expression, with 10 targets overlapping from both lists (*Ahcy, Angpt2, C4b, Eno1, Gnpda1, Hmga1, Ptbp2, Qpct, Rrm2, Hn1l*) with 2% of downregulated proteins also showing decreased mRNA levels in DS astrocytes (Figure 3.2K,L). Increased expression of MT3 protein in glia in DS patient brains has been previously reported (Arai et al., 1997), which showed increased secretion in our DS ACM. Additionally, we saw an increase in secretion of EFEMP1, which has been associated with DS pathology as having a significant dosage effect (Vilardell et al., 2011). We did not see the increased secretion of SPARC and other synaptogenic proteins others have reported, as described above; this may be due to the differences in the method of astrocyte isolation or in the age of the astrocytes at the time of isolation, indicating that DS astrocytes may differentially secrete synaptogenic proteins at different times.

Protein PANTHER pathway analysis of DS ACM found enrichment in a number of pathways; in particular, there was increased secretion of proteins associated with the amyloid secretase pathway in Alzheimer's disease, the integrin signaling pathway, and the CCKR signaling map. Reactome pathway analysis found increased release of proteins associated with post-translational protein phosphorylation, regulation of IGF transport and uptake by IGFBPs, glycosaminoglycan metabolism, regulation of the complement cascade, peptide hormone metabolism, degradation of the extracellular matrix, and axon guidance. PANTHER protein class analysis found changes in extracellular matrix protein, serine protease inhibitor, and growth factor (Figure 3.2M). These pathways implicate astrocyte secreted proteins in protein metabolism and neuronal outgrowth, further supporting a role for alterations in DS as contributors to the pathology of the condition.

Overlap in protein secretion differences between astrocytes from multiple NDs.

We identified a number of changes in protein secretion in each individual ND. Next, we asked whether there were proteins or genes that showed common changes in all three NDs compared to WT. We found that there were 88 proteins that showed an increase in secretion in all 3 NDs vs. WT, including IGFBP2, CPE, and APOE, while only 6 genes showed an increase in mRNA level in all 3 NDs, with none of the proteins upregulated in the NDs showing similar alterations in mRNA levels (0% overlap) (Figure 3.3A-D, Supplemental Tables 6 and 7). In contrast, only 32 proteins showed a decrease in secretion in all 3 NDs compared to WT, with only 1 gene (*Serinc2*) showing a decrease in mRNA expression, which did not match any of the targets showing decreased protein secretion (0% overlap in downregulated protein also altered at mRNA level) (Figure 3.3E-H, Supplemental Tables 6 and 7).

Protein PANTHER pathway analysis found an increase in the secretion of proteins in the Alzheimer disease-amyloid secretase pathway, while Reactome pathway analysis found

increased release of proteins involved in regulating post-translational protein phosphorylation, regulation of IGF transport and uptake by IGFBPs, glycosaminoglycan metabolism, and regulation of the complement cascade. PANTHER protein class analysis showed an increase in extracellular matrix protein and serine protease inhibitory in all three NDs compared to WT (Figure 3.3I). The overlapping pathways between all NDs provides insight into the critical roles of astrocytes in supporting proper protein activation and processing, and highlight the similarities between all three NDs compared to WT.

Identification of candidate astrocyte protein factors that may be involved in the pathology of multiple NDs.

Based on the limited overlap between the proteomic and gene expression data, we focused on the proteomics data to select candidates. Due to the nature of the mutations causing RTT, FXS, and DS, all of which are associated with increased gene expression, we decided to focus first on proteins that show increased secretion in all three NDs. While our list of 88 matching secreted proteins presented a number of interesting candidates, we chose insulin-like growth factor binding protein 2 (IGFBP2), carboxypeptidase E (CPE), and bone morphogenetic protein 6 (BMP6) based on their increased secretion, relative abundance, and known roles in the brain. All 3 show upregulated protein secretions in ND, which may indicate that overexpression of one or more of these proteins by astrocytes is inhibiting normal neuronal development.

IGFBP2 is highly abundant in ACM, at 2.7% of all spectra counted in WT ACM, and shows an increased secretion of >50% in all 3 NDs (4.6% in FXS, 5.0% in RTT, 6.2% in DS). IGFBP2 is highly expressed by P7 astrocytes in the developing mouse cortex, and expression is enriched in astrocytes compared to other cell types (Zhang et al., 2014). IGF signaling is altered in multiple models of ASD (de Souza et al., 2017; Deacon et al., 2015; Vanhala et al., 2007; Williams et al., 2014), indicating a potential role for IGF signaling pathways in the pathology of the disorder.

IGFBP2 binds and inhibits insulin-like growth factor 1 (IGF1), as well as having IGF-independent functions (Kawai et al., 2011). IGF1 has been studied extensively for its role in RTT and its potential for treating the condition. Research has demonstrated that application of IGF1 or GPE (the first three amino acids of IGF1) can significantly ameliorate the neuronal deficits induced by RTT ACM in iPSCs (Williams et al., 2014), while treating *Mecp2-/y* mice with IGF1 can improve behavioral and physiological symptoms of RTT (Castro et al., 2014). In FXS mice, administration of NNZ-2566, a synthetic analog of GPE improves the behavioral phenotype and normalizes the alterations in dendritic spine density (Deacon et al., 2015). IGF1 is currently in Phase 2 clinical trials for treating RTT and FXS in human patients (Erickson et al., 2017; Khwaja et al., 2014). Due to the high levels of IGFBP2 seen in ACM, and the dramatic increase in ND ACM, we asked if a change in IGFBP2 protein levels might contribute to the phenotypes of these disorders by acting directly on the neurons to have an inhibitory effect on their development. These results are discussed in chapter 4.

At roughly 1% of WT protein, CPE is another protein that is highly abundant in ACM, and its level is increased by >50% in ACM from all 3 NDs (1.7% in FXS, 1.8% in RTT, 2.3% in DS). Similarly to IGFBP2, CPE is highly expressed by astrocytes in the developing cortex at P7, and shows enrichment in astrocytes compared to other brain cell types (Zhang et al., 2014). CPE is a secretory sorting molecule involved in regulated secretion and peptide maturation, including activating BDNF, and overexpression of CPE is neuroprotective (Woronowicz et al., 2010). Mice that lack CPE show more complex dendritic arbors compared to WT in adult neurons, suggesting that it could inhibit process outgrowth (Woronowicz et al., 2010). However, preliminary testing did not show an effect of CPE on neuronal outgrowth when adding the recombinant protein to WT ACM; in fact, when added to WT ACM at roughly 4x the concentration in WT ACM/2x the ND concentration (160ng/ml), CPE appeared to have a beneficial effect on neuronal outgrowth

(Figure 4.5A,B). For this reason, and due to the results we saw with IGFBP2 and BMP6, we have not pursued CPE any further at this time.

BMP6, while present at extremely low levels in WT ACM (0.005%), showed a significant increase in secretion in all three NDs (0.012% in FXS, 0.011% in RTT, 0.019% in DS). Prior work has demonstrated a role for BMPs in the functional maturation and morphology of astrocytes in vitro, inducing process elaboration, regulating GFAP expression, and inhibiting proliferation (Scholze et al., 2014). We found that BMP target genes, including *Id3, Id4*, and *Smad9* were significantly upregulated in FXS and DS astrocytes but not RTT, so we opted to focus on those two NDs. Astrocytes are not known to express BMP6, indicating an aberrant expression of the protein in these NDs. Due to the known role for BMPs in astrocyte morphology and function, we focused our attention on the cell autonomous effects of BMP6 in astrocytes and its effects on astrocytes' ability to support neuronal outgrowth in vitro. These results are discussed in chapter 5.

Discussion

Through the use of our unique immunopanning assay, we were able to isolate astrocytes from WT and three different ND models, maintain them in vitro, and conduct quantitative analysis of their protein secretome through mass spectrometry. Thus for the first time, we have been able to profile the protein secretion of astrocytes at a time point when they are known to be involved in neuronal outgrowth and synapse formation. We identified over 1200 unique proteins secreted by WT and ND astrocytes in vitro, and concurrently conducted gene expression analysis on the same astrocyte cultures to generate matched databases of the properties of P7 WT and ND murine astrocytes in vitro. Our results demonstrated that astrocytes secrete a multitude of astrocyte-associated proteins, and their gene expression profiles resemble those of acutely isolated astrocytes, providing support for our approach to this work.

Our approach identified a number of differences between each individual ND and WT, including a number of changes that have been previously described in individual disorders in vivo, further validating our approach. Furthermore, we found 88 proteins that are upregulated in their secretion from all 3 ND models compared to WT. We were also able to identify 32 proteins that showed decreased secretion in all 3 NDs compared to WT. We collected the astrocytes themselves from the same cultures for RNASeq gene expression analysis, and similarly identified a number of unique changes in each individual ND, as well as 6 genes that all show similar increases in gene expression and 1 gene that shows a common decrease in expression across all 3 NDs.

Due to the nature of these genetic mutations, it was not unexpected that we detected more increases in protein secretion and gene expression in ND compared to WT, rather than the reverse. The key protein in FXS, FMRP, is an RNA-binding protein believed to act as a negative regulator of translation. In RTT, the MECP2 protein is believed to act as a gene silencer. Their loss in FXS and RTT are predicted to lead to an increase in protein expression. DS is caused by chromosomal trisomy, which is also likely to lead to an increase in protein expression. Thus, we selected three protein candidates that showed significantly increased secretion in all 3 NDs compared to WT. In chapter 4, we will discuss the potential role of IGFBP2 in the pathology of RTT, and in chapter 5 we will discuss the impact of BMP6 protein on astrocyte function and its possible impact in FXS.

We also identified CPE as a potential candidate protein, but did not pursue it at this time due to the fact that purified recombinant protein did not have an inhibitory effect on neuronal outgrowth in vitro. Given the known roles for CPE in secretory pathways and peptide maturation, it may be that our approach simply did not highlight the functional effects of CPE. An alternative approach that should be tested in the future would be to overexpress CPE in WT astrocytes in

vitro, to determine if the internal actions of CPE in astrocytes contributes to alterations in protein secretion and neuronal function.

There are a number of other proteins altered in ND ACM that may regulate different aspects of neuronal development and will be the focus of future study. Secreted semaphorins (class 3) are upregulated in ACM from all NDs, and these are inhibitory to neurite outgrowth, so may be contributing to the inhibitory effect of ND ACM (Degano et al., 2009; Duan et al., 2014; Menon and Mihailescu, 2007; Molofsky et al., 2014). APOE is another protein upregulated in NDs that is important for the packaging and transportation of cholesterol (Vance et al., 2000) and its E4 isoform has been linked to Alzheimer's disease in humans (Strittmatter et al., 1993) and decreased grey matter in infants (Dean et al., 2014). Some work has implicated an APOE deficiency in the reduced complexity of dendritic arbors of adult newborn neurons in the hippocampus (Tensaouti et al., 2018); it may be that its overexpression in NDs plays a role in the altered dendritic arborization associated with these disorders.

It is interesting to note that alterations in the Alzheimer's disease-amyloid secretase pathway, and in particular the increased secretion of APP and APOE, are found in all 3 NDs. While DS has previously been associated with early onset Alzheimer's Disease (AD), this has not been seen in RTT or FXS. In the case of RTT, this may be due to a shorter life expectancy in patients (likely around 40-50 years, (Coppus, 2013)). In FXS, it is possible that symptoms of Alzheimer's Disease are masked by other symptoms of the disorder, or complicated by the specific nature of the FXS mutation; in adulthood, many patients with FXS are affected by Fragile-X associated Tremor/Ataxia Syndrome (FXTAS), which in addition to manifesting with intention tremors and difficulty with movement and balance, leads to cognitive deficits such as short term memory loss and loss of executive function, on par with the cognitive deficits as those seen in AD, though not an exact match (Seritan et al., 2008). The increased secretion of APP in FXS, however, is supported by research demonstrating that FMRP binds to and inhibits the translation

of *App* mRNA; its loss in FXS is therefore predicted to lead to an increase in APP protein levels (Malter et al., 2010). Additional research has found other similarities in the molecular profiles of these two diseases, including overlapping changes in synaptojanin (SYNJ1), involved in synaptogenesis, and T-cell lymphoma invasion and metastasis-inducing protein 1 (TIAM1) and Tetratricopeptide repeat protein 3 (TTC3), involved in neurogenesis, in addition to increased APP. In future work, it will be interesting to examine the similarities and differences in the profiles of DS and FXS astrocytes in particular.

Beyond the proteins showing increased secretion, there are a number of proteins that show decreased secretion in NDs compared to WT that will be worth examining. Two proteins in particular - SULF2 and HDGFRP3 - are secreted by ND astrocytes at less than half the level seen in WT astrocytes, and a lack of sufficient expression of these proteins may prevent normal neuronal development. Sulfatase 2 (SULF2) influences the activity of heparan sulfate proteoglycans (HSPGs) by selectively removing 6-O-sulfate groups from heparan sulfate (Kalus et al., 2015, 2009). Research out of our lab has previously identified HSPG family members glypicans 4 and 6 (GPC4/6) as critical for the formation of active excitatory synapses (Allen et al., 2012) and the possible interactions between SULF2 and GPC4/6 make it a good candidate for further examination. Hepatoma-derived growth factor-related protein-3 (HDGFRP3) is the only member of its family expressed in the CNS and has been implicated as a neurotrophic factor and supports neurite-outgrowth (Abouzied et al., 2010). Its decreased secretion in ND astrocytes merits further examination. The nature of the database we have generated is such that it can be explored almost endlessly to ask questions about the functional roles of astrocytes during development.

Acknowledgements

This chapter is, in part, a reprint of the material as it appears in Blanco-Suaréz E, Caldwell ALM, and Allen NJ, Role of astrocyte–synapse interactions in CNS disorders. Journal of Physiology. 2017 Mar 15;595(6):1903-1916. The dissertation author was the co-first author of this review and was the primary author of the portions used in this chapter. Additional portions of this chapter are in preparation for submission for publication. The dissertation author will be the first author of this publication, with Dr. Jolene Diedrich as second author and Dr. Nicola Allen as the senior author and principle investigator.

Figure 3.1: Characterization of the protein secretion and RNA profiles of immunopanned WT and ND astrocytes. A,B. WT and ND immunopanned astrocytes express many known astrocyte markers at high levels. **A.** Astrocytes (green) express cell-specific markers that determine their cellular identity (top left astrocyte), contact blood vessels and neuronal synapses to engage in metabolism and homeostatic functions (center astrocyte), and bind and respond to neurotransmitters released by neurons (lower right astrocyte). **B.** The corresponding heatmap shows few differences between ND and WT expression of astrocyte identity and function markers. **C.** Heatmap of most abundant proteins detected in WT ACM with corresponding ND values. **D.** Heatmap of most abundant mRNA detected in WT astrocytes with corresponding ND values. **E.** Schematic of the tripartite synapse displaying astrocyte-secreted proteins important for regulating synapse formation and function. **F-I.** Corresponding heatmaps of the abundance of secreted synaptogenic proteins in ACM (F) and expression of synaptogenic genes (G), as well as the abundance of synapse eliminating proteins in ACM (H) and corresponding expression of synapse elimination genes (I). **J.** Reactive astrocyte markers from pan reactive, A1 reactive (inflammatory) and A2 reactive (supportive) astrocytes are not consistently altered in IP astrocyte cultures from ND compared to WT, demonstrating cultures are not reactive. Data taken from RNA sequencing. For proteomics, N=6 cultures per genotype, *$p<0.05$, abundance >0.01%, fold change between WT and ND ≥1.5. For RNASeq, N=6 cultures WT, RTT, FXS; 4 cultures DS. Significance for differential expression defined as adjusted $p<0.05$, calculated using Benjamini-Hochberg's procedure for multiple comparisons, FPKM>1 and fold change between ND and WT >1.5, comparing each ND and WT after adjustment for multiple testing.

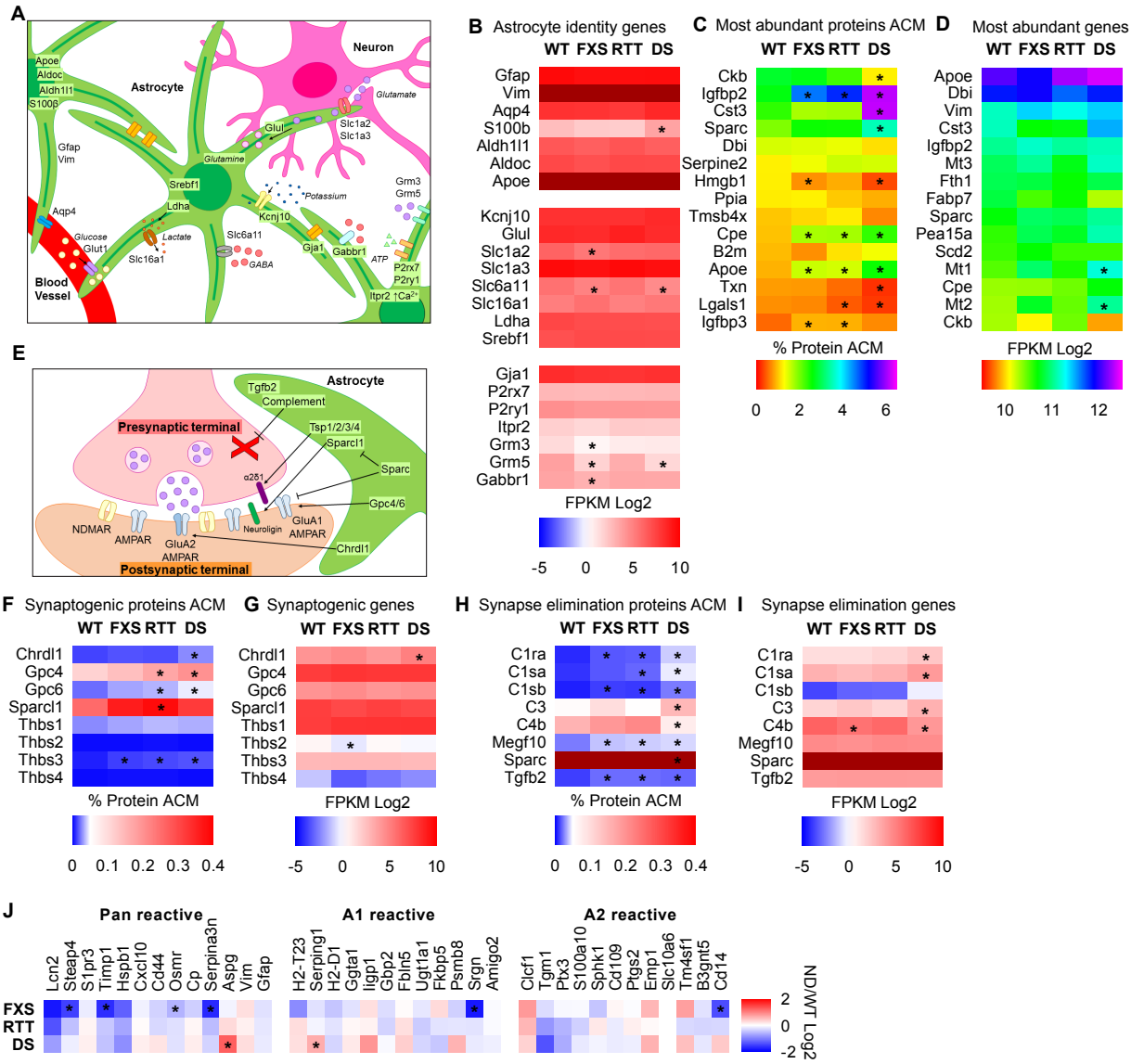
A
Neuron
Astrocyte
Apoe
Aldoc
Aldh1l1
S100β
Gfap
Vim
Aqp4
Glucose
Glut1
Blood Vessel
Lactate
Slc16a1
Srebf1
Ldha
Glutamine
Glul
Glutamate
Slc1a2
Slc1a3
Potassium
Kcnj10
Slc6a11
GABA
Gja1
Gabbr1
ATP
P2rx7
P2ry1
Itpr2 ↑Ca2+
Grm3
Grm5
B Astrocyte identity genes
WT FXS RTT DS
Gfap
Vim
Aqp4
S100b
Aldh1l1
Aldoc
Apoe
Kcnj10
Glul
Slc1a2
Slc1a3
Slc6a11
Slc16a1
Ldha
Srebf1
Gja1
P2rx7
P2ry1
Itpr2
Grm3
Grm5
Gabbr1
FPKM Log2
-5 0 5 10
C Most abundant proteins ACM
WT FXS RTT DS
Ckb
Igfbp2
Cst3
Sparc
Dbi
Serpine2
Hmgb1
Ppia
Tmsb4x
Cpe
B2m
Apoe
Txn
Lgals1
Igfbp3
% Protein ACM
0 2 4 6
D Most abundant genes
WT FXS RTT DS
Apoe
Dbi
Vim
Cst3
Igfbp2
Mt3
Fth1
Fabp7
Sparc
Pea15a
Scd2
Mt1
Cpe
Mt2
Ckb
FPKM Log2
10 11 12
E
Astrocyte
Tgfb2
Complement
Presynaptic terminal
Tsp1/2/3/4
Sparcl1
Sparc
α2δ1
Gpc4/6
NDMAR
AMPAR
GluA2 AMPAR
Neuroligin
GluA1 AMPAR
Chrdl1
Postsynaptic terminal
F Synaptogenic proteins ACM
WT FXS RTT DS
Chrdl1
Gpc4
Gpc6
Sparcl1
Thbs1
Thbs2
Thbs3
Thbs4
% Protein ACM
0 0.1 0.2 0.3 0.4
G Synaptogenic genes
WT FXS RTT DS
Chrdl1
Gpc4
Gpc6
Sparcl1
Thbs1
Thbs2
Thbs3
Thbs4
FPKM Log2
-5 0 5 10
H Synapse elimination proteins ACM
WT FXS RTT DS
C1ra
C1sa
C1sb
C3
C4b
Megf10
Sparc
Tgfb2
% Protein ACM
0 0.1 0.2 0.3 0.4
I Synapse elimination genes
WT FXS RTT DS
C1ra
C1sa
C1sb
C3
C4b
Megf10
Sparc
Tgfb2
FPKM Log2
-5 0 5 10
J
Pan reactive
Lcn2
Steap4
S1pr3
Timp1
Hspb1
Cxcl10
Cd44
Osmr
Cp
Serpina3n
Aspg
Vim
Gfap
A1 reactive
H2-T23
Serping1
H2-D1
Ggta1
Igtp1
Gbp2
Fbln5
Ugt1a1
Fkbp5
Psmb8
Srgn
Amigo2
A2 reactive
Clcf1
Tgm1
Ptx3
S100a10
Sphk1
Cd109
Ptgs2
Emp1
Slc10a6
Tm4sf1
B3gnt5
Cd14
FXS
RTT
DS
NDMT Log2
2
0
-2

Figure 3.2: Characterization of the protein secretion and gene expression profiles of each ND compared to WT. **A, G**. Heatmap of top proteins and mRNA increased (**A**) or decreased (**G)** between WT and FXS ACM and astrocytes. **B, H**. Venn diagrams showing the overlap between proteins and genes showing increased expression (**B**) or decreased expression (**H**) in FXS ACM and astrocytes. **C, I**. Heatmap of top proteins and mRNA increased (**C**) or decreased (**I**) between WT and RTT ACM and astrocytes. **D, J**. Venn diagrams showing the overlap between proteins and genes showing increased expression (**D**) or decreased expression (**J**) in RTT ACM and astrocytes. **E, K**. Heatmap of top proteins and mRNA increased (**E**) or decreased (**K**) between WT and DS ACM and astrocytes. **F, L**. Venn diagrams showing the overlap between proteins and genes showing increased expression (**F**) or decreased expression (**L**) in DS ACM and astrocytes. For proteomics, N=6 cultures per genotype, $p<0.05$, abundance >0.01%, fold change between WT and ND ≥1.5. For RNASeq, N=6 cultures WT, RTT, FXS; 4 cultures DS. Significance for differential expression defined as adjusted $p<0.05$, calculated using Benjamini-Hochberg's procedure for multiple comparisons, FPKM>1 and fold change between ND and WT >1.5, comparing each ND and WT after adjustment for multiple testing. **M.** Pathway analysis of proteins identified in ACM demonstrates unique alterations in astrocyte function in each ND compared to WT.

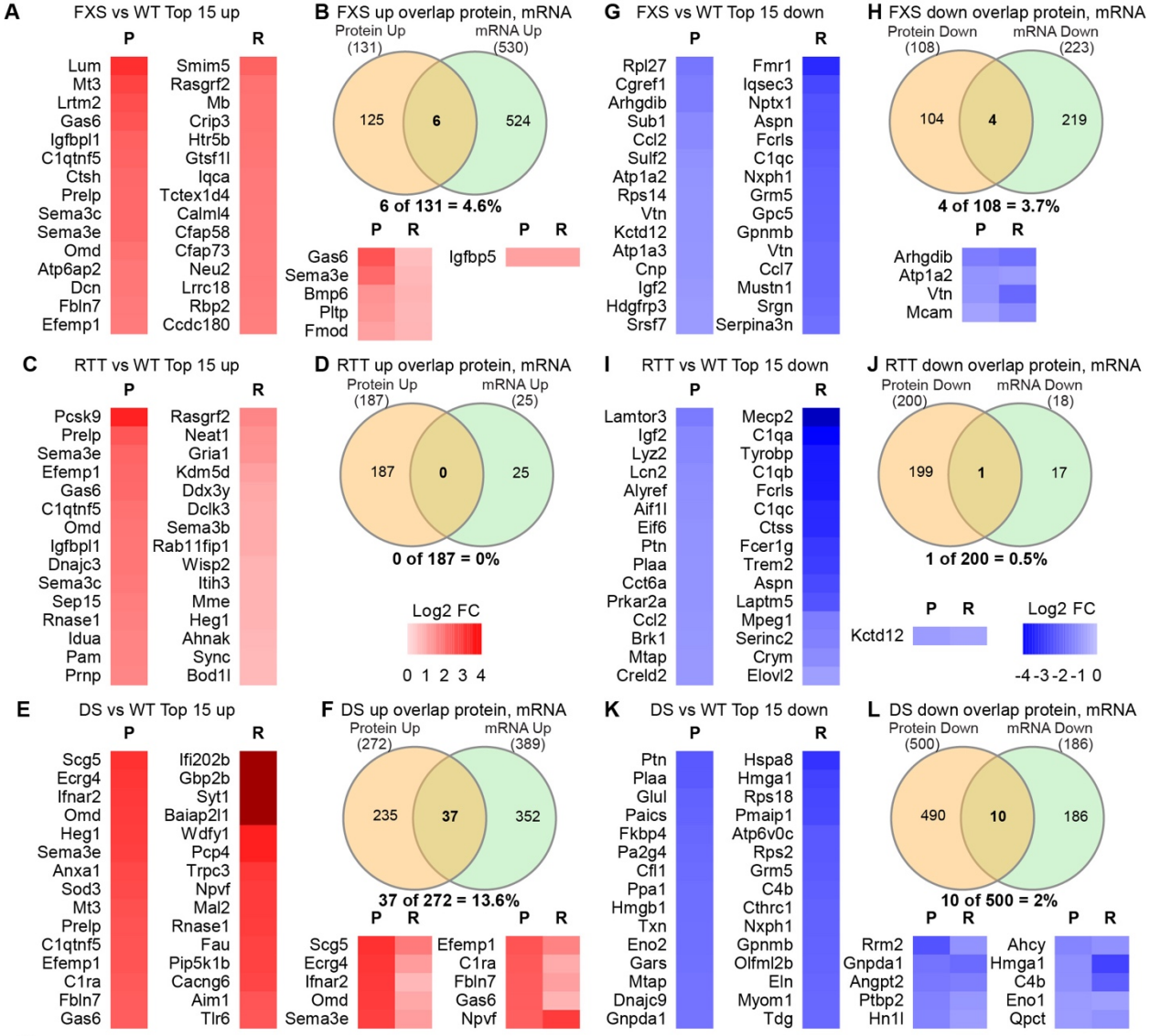

M

PANTHER Pathways	FXS (FDR)	RTT (FDR)	DS (FDR)
Alzheimer disease-amyloid secretase pathway (P00003)	1.11E-05	1.41E-04	2.43E-03
Integrin signalling pathway (P00034)	n/a	3.54E-03	6.26E-02
Blood coagulation (P00011)	1.04E-02	n/a	n/a
CCKR signaling map (P06959)	n/a	n/a	4.38E-02

Reactome pathways	FXS (FDR)	RTT (FDR)	DS (FDR)
Post-translational protein phosphorylation (R-MMU-8957275)	1.18E-07	2.16E-17	8.37E-17
Regulation of IGF transport and uptake by IGFBPs (R-MMU-381426)	1.60E-08	5.31E-17	9.27E-18
Glycosaminoglycan metabolism (R-MMU-1630316)	1.18E-05	7.59E-11	1.15E-14
Regulation of Complement cascade (R-MMU-977606)	n/a	3.56E-02	2.81E-02
Plasma lipoprotein remodeling (R-MMU-8963899)	3.86E-02	4.74E-02	n/a
Peptide hormone metabolism (R-MMU-2980736)	n/a	n/a	1.01E-02
Degradation of the extracellular matrix (R-MMU-1474228)	2.50E-03	3.47E-05	2.00E-05
Axon guidance (R-MMU-422475)	n/a	n/a	2.07E-03
NCAM1 interactions (R-MMU-419037)	n/a	3.33E-02	n/a

PANTHER Protein Class	FXS (FDR)	RTT (FDR)	DS (FDR)
extracellular matrix protein (PC00102)	4.48E-03	1.77E-04	1.20E-05
serine protease inhibitor (PC00204)	3.90E-03	2.98E-03	8.84E-04
growth factor (PC00112)	n/a	n/a	2.07E-02
complement component (PC00078)	4.20E-02	n/a	n/a

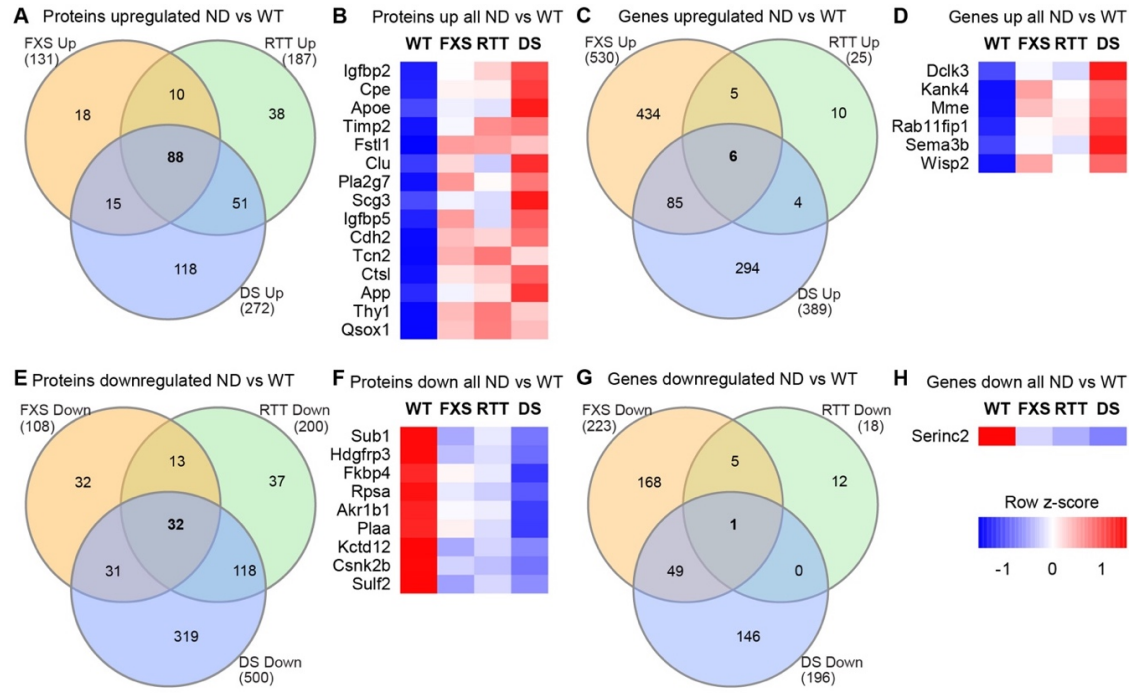

I

PANTHER Pathways	ASD (FDR)
Alzheimer disease-amyloid secretase pathway (P00003)	4.39E-07

Reactome pathways	ASD (FDR)
Post-translational protein phosphorylation (R-MMU-8957275)	1.72E-06
Regulation of IGF transport and uptake by IGFBPs (R-MMU-381426)	1.43E-06
Glycosaminoglycan metabolism (R-MMU-1630316)	9.96E-05
Regulation of Complement cascade (R-MMU-977606)	4.29E-02

PANTHER Protein Class	ASD (FDR)
extracellular matrix protein (PC00102)	1.96E-02
serine protease inhibitor (PC00204)	3.58E-02

Figure 3.3: **Astrocytes from NDs show overlapping altered protein secretion compared to WT astrocytes. A,B.** 88 proteins show increased secretion in all 3 NDs compared to WT. Venn diagrams showing number of proteins increased (**A**) and corresponding heatmap of most abundant proteins detected (**B**) in ND ACM by mass spectrometry analysis, for WT and each ND ACM, as ranked by expression in FXS, represented as row z-score (red upregulated, blue downregulated). **C,D.** Venn diagrams showing number of genes showing increased expression (**C**) and corresponding heatmap of most abundant mRNA in ND astrocytes, as ranked by expression in FXS, represented as row z-score (red upregulated, blue downregulated**) E,F.** Venn diagrams showing number of proteins decreased (**E**) and corresponding heatmap of least abundant proteins detected (**F**) in ND ACM by mass spectrometry analysis, for WT and each ND ACM, as ranked by expression in WT, represented as row z-score (red upregulated, blue downregulated). **G,H.** Venn diagrams showing number of genes showing decreased expression (**C**) and corresponding heatmap of least abundant mRNA in ND astrocytes, as ranked by expression in WT, represented as row z-score (red upregulated, blue downregulated). For proteomics, N=6 cultures per genotype, $p<0.05$, abundance >0.01%, fold change between WT and ND ≥1.5. For RNASeq, N=6 cultures WT, RTT, FXS; 4 cultures DS. Significance for differential expression defined as adjusted $p<0.05$, calculated using Benjamini-Hochberg's procedure for multiple comparisons, FPKM>1 and fold change between ND and WT >1.5, comparing each ND and WT after adjustment for multiple testing. **I.** Pathway analysis of proteins identified in ACM demonstrates overlapping alterations in ND astrocyte function compared to WT.

References

Abouzied, M.M., El-Tahir, H.M., Gieselmann, V., Franken, S., 2010. Hepatoma-derived growth factor-related protein-3: A new neurotrophic and neurite outgrowth-promoting factor for cortical neurons. J. Neurosci. Res. 88, 3610–3620. https://doi.org/10.1002/jnr.22507

Allen, N.J., Bennett, M.L., Foo, L.C., Wang, G.X., Chakraborty, C., Smith, S.J., Barres, B. a., 2012. Astrocyte glypicans 4 and 6 promote formation of excitatory synapses via GluA1 AMPA receptors. Nature 486, 410–414. https://doi.org/10.1038/nature11059

Arai, Y., Uchida, Y., Takashima, S., 1997. Developmental immunohistochemistry of growth inhibitory factor in normal brains and brains of patients with Down syndrome. Pediatr. Neurol. 17, 134–138.

Bialas, A.R., Stevens, B., 2013. TGF-β signaling regulates neuronal C1q expression and developmental synaptic refinement. Nat. Neurosci. 16, 1773–1782. https://doi.org/10.1038/nn.3560

Blanco-suárez, E., Caldwell, A.L.M., Allen, N.J., 2016. Role of astrocyte-synapse interactions in CNS disorders. J. Physiol. 00, 1–14. https://doi.org/10.1113/JP270988.This

Blanco-Suarez, E., Liu, T.F., Kopelevich, A., Allen, N.J., 2018. Astrocyte-Secreted Chordin-like 1 Drives Synapse Maturation and Limits Plasticity by Increasing Synaptic GluA2 AMPA Receptors. Neuron 1–17. https://doi.org/10.1016/j.neuron.2018.09.043

Broek, J.A., Guest, P.C., Rahmoune, H., Bahn, S., 2014. Proteomic analysis of post mortem brain tissue from autism patients: evidence for opposite changes in prefrontal cortex and cerebellum in synaptic connectivity-related proteins. Mol. Autism 5, 41. https://doi.org/10.1186/2040-2392-5-41

Cahoy, J.D., Emery, B., Kaushal, A., Foo, L.C., Zamanian, J.L., Christopherson, K.S., Xing, Y., Lubischer, J.L., Krieg, P. a, Krupenko, S. a, Thompson, W.J., Barres, B. a, 2008. A transcriptome database for astrocytes, neurons, and oligodendrocytes: a new resource for understanding brain development and function. J. Neurosci. 28, 264–278. https://doi.org/10.1523/JNEUROSCI.4178-07.2008

Castro, J., Garcia, R.I., Kwok, S., Banerjee, A., Petravicz, J., Woodson, J., Mellios, N., Tropea, D., Sur, M., 2014. Functional recovery with recombinant human IGF1 treatment in a mouse model of Rett Syndrome. Proc. Natl. Acad. Sci. U. S. A. 111, 9941–6. https://doi.org/10.1073/pnas.1311685111

Chen, C., Jiang, P., Xue, H., Peterson, S.E., Tran, H.T., McCann, A.E., Parast, M.M., Li, S., Pleasure, D.E., Laurent, L.C., Loring, J.F., Liu, Y., Deng, W., 2014. Role of astroglia in Down's syndrome revealed by patient-derived human-induced pluripotent stem cells. Nat. Commun. 5, 4430. https://doi.org/10.1038/ncomms5430

Cheng, C., Lau, S.K.M., Doering, L.C., 2016. Astrocyte-secreted thrombospondin-1 modulates synapse and spine defects in the fragile X mouse model. Mol. Brain 9, 74. https://doi.org/10.1186/s13041-016-0256-9

Christopherson, K.S., Ullian, E.M., Stokes, C.C. a, Mullowney, C.E., Hell, J.W., Agah, A., Lawler, J., Mosher, D.F., Bornstein, P., Barres, B. a., 2005. Thrombospondins are astrocyte-secreted proteins that promote CNS synaptogenesis. Cell 120, 421–433. https://doi.org/10.1016/j.cell.2004.12.020

Coppus, A.M.W., 2013. People with intellectual disability: What do we know about adulthood and life expectancy? Dev. Disabil. Res. Rev. 18, 6–16. https://doi.org/10.1002/ddrr.1123

Cortelazzo, A., De Felice, C., Guerranti, R., Signorini, C., Leoncini, S., Zollo, G., Leoncini, R., Timperio, A.M., Zolla, L., Ciccoli, L., Hayek, J., 2016. Expression and oxidative modifications of plasma proteins in autism spectrum disorders: Interplay between inflammatory response and lipid peroxidation. PROTEOMICS - Clin. Appl. 10, 1103–1112. https://doi.org/10.1002/prca.201500076

de Souza, J.S., Carromeu, C., Torres, L.B., Bruno, B.H., Cugola, F.R., Maciel, R.M.B., Muotri, A.R., Giannocco, G., 2017. IGF1 neuronal response in the absence of MECP2 is dependent on TRalpha 3. Hum. Mol. Genet. 26, 270–281. https://doi.org/10.1093/hmg/ddw384

Deacon, R.M.J., Glass, L., Snape, M., Hurley, M.J., Altimiras, F.J., Biekofsky, R.R., Cogram, P., 2015. NNZ-2566, a Novel Analog of (1–3) IGF-1, as a Potential Therapeutic Agent for Fragile X Syndrome. NeuroMolecular Med. 17, 71–82. https://doi.org/10.1007/s12017-015-8341-2

Dean, D.C., Jerskey, B.A., Chen, K., Protas, H., Thiyyagura, P., Roontiva, A., O'Muircheartaigh, J., Dirks, H., Waskiewicz, N., Lehman, K., Siniard, A.L., Turk, M.N., Hua, X., Madsen, S.K., Thompson, P.M., Fleisher, A.S., Huentelman, M.J., Deoni, S.C.L., Reiman, E.M., Reiman, E.M., 2014. Brain differences in infants at differential genetic risk for late-onset Alzheimer disease: a cross-sectional imaging study. JAMA Neurol. 71, 11–22. https://doi.org/10.1001/jamaneurol.2013.4544

Degano, A.L., Pasterkamp, J., Ronnett, G. V., 2009. MeCP2 deficiency disrupts axonal guidance, fasciculation, and targeting by altering Semaphorin 3F function Alicia. Mol. Cell. Neurosci. 42, 243–254. https://doi.org/10.1038/mp.2011.182.doi

Dowell, J.A., Johnson, J.A., Li, L., 2009. Identification of Astrocyte Secreted Proteins with a Combination of Shotgun Proteomics and Bioinformatics. J. Proteome Res. 8, 4135–4143. https://doi.org/10.1038/mp.2011.182.doi

Duan, Y., Wang, S.-H., Song, J., Mironova, Y., Ming, G., Kolodkin, A.L., Giger, R.J., 2014. Semaphorin 5A inhibits synaptogenesis in early postnatal- and adult-born hippocampal dentate granule cells. Elife 3, 1–24. https://doi.org/10.7554/elife.04390

Erickson, C.A., Davenport, M.H., Schaefer, T.L., Wink, L.K., Pedapati, E. V., Sweeney, J.A., Fitzpatrick, S.E., Brown, W.T., Budimirovic, D., Hagerman, R.J., Hessl, D., Kaufmann, W.E., Berry-Kravis, E., 2017. Fragile X targeted pharmacotherapy: Lessons learned and future directions. J. Neurodev. Disord. 9, 1–14. https://doi.org/10.1186/s11689-017-9186-9

Farhy-Tselnicker, I., Allen, N.J., 2018. Astrocytes, neurons, synapses: a tripartite view on cortical circuit development. Neural Dev. 13, 7. https://doi.org/10.1186/s13064-018-0104-y

Foo, L.C., Allen, N.J., Bushong, E.A., Ventura, P.B., Chung, W.S., Zhou, L., Cahoy, J.D., Daneman, R., Zong, H., Ellisman, M.H., Barres, B.A., 2011. Development of a method for the purification and culture of rodent astrocytes. Neuron 71, 799–811. https://doi.org/10.1016/j.neuron.2011.07.022

Garcia, O., Torres, M., Helguera, P., Coskun, P., Busciglio, J., 2010. A role for thrombospondin-1 deficits in astrocyte-mediated spine and synaptic pathology in down's syndrome. PLoS One 5. https://doi.org/10.1371/journal.pone.0014200

Garg, S., Brooks, A., Burns, A., Burkitt-Wright, E., Kerr, B., Huson, S., Emsley, R., Green, J., 2017. Autism spectrum disorder and other neurobehavioural comorbidities in rare disorders of the Ras/MAPK pathway. Dev. Med. Child Neurol. 59, 544–549. https://doi.org/10.1111/dmcn.13394

Greco, T.M., Seeholzer, S.H., Mak, A., Spruce, L., Ischiropoulos, H., 2010. Quantitative Mass Spectrometry-based Proteomics Reveals the Dynamic Range of Primary Mouse Astrocyte Protein Secretion. J. Proteome Res. 9, 2764–2774. https://doi.org/10.1021/pr100134n

Guest, P.C., Martins-de-Souza, D., 2017. What Have Proteomic Studies Taught Us About Novel Drug Targets in Autism? Springer, Cham, pp. 49–67. https://doi.org/10.1007/978-3-319-52479-5_3

Higashimori, H., Morel, L., Huth, J., Lindemann, L., Dulla, C., Taylor, A., Freeman, M., Yang, Y., 2013. Astroglial FMRP-dependent translational down-regulation of mGluR5 underlies

glutamate transporter GLT1 dysregulation in the fragile X mouse. Hum. Mol. Genet. 22, 2041–54. https://doi.org/10.1093/hmg/ddt055

Higashimori, H., Schin, C.S., Chiang, M.S.R., Morel, L., Shoneye, T.A., Nelson, D.L., Yang, Y., 2016. Selective Deletion of Astroglial FMRP Dysregulates Glutamate Transporter GLT1 and Contributes to Fragile X Syndrome Phenotypes In Vivo. J. Neurosci. 36, 7079–94. https://doi.org/10.1523/JNEUROSCI.1069-16.2016

Hunter, M.P., Nelson, M., Kurzer, M., Wang, X., Kryscio, R.J., Head, E., Pinna, G., O'Bryan, J.P., 2011. Intersectin 1 contributes to phenotypes in vivo: implications for Down's syndrome. Neuroreport 22, 767–72. https://doi.org/10.1097/WNR.0b013e32834ae348

Kalus, I., Rohn, S., Puvirajesinghe, T.M., Guimond, S.E., Eyckerman-Kölln, P.J., Ten Dam, G., Van Kuppevelt, T.H., Turnbull, J.E., Dierks, T., 2015. Sulf1 and Sulf2 differentially modulate heparan sulfate proteoglycan sulfation during postnatal cerebellum development: Evidence for neuroprotective and neurite outgrowth promoting functions. PLoS One 10, 1–19. https://doi.org/10.1371/journal.pone.0139853

Kalus, I., Salmen, B., Viebahn, C., Figura, K. von, Schmitz, D., D'Hooge, R., Dierks, T., 2009. Differential involvement of the extracellular 6-O-endosulfatases Sulf1 and Sulf2 in brain development and neuronal and behavioural plasticity. J. Cell. Mol. Med. 13, 4505–4521. https://doi.org/10.1111/j.1582-4934.2008.00558.x

Kawai, M., Breggia, A.C., Demambro, V.E., Shen, X., Canalis, E., Bouxsein, M.L., Beamer, W.G., Clemmons, D.R., Rosen, C.J., 2011. The heparin-binding domain of IGFBP-2 has insulin-like growth factor binding-independent biologic activity in the growing skeleton. J. Biol. Chem. 286, 14670–14680. https://doi.org/10.1074/jbc.M110.193334

Keene, S.D., Greco, T.M., Parastatidis, I., Lee, S.-H., Hughes, E.G., Balice-Gordon, R.J., Speicher, D.W., Ischiropoulos, H., Dimitrova, N., Zamudio, J.R., Jong, R.M., Soukup, D., Resnick, R., Sarma, K., Ward, A.J., Raj, A., Lee, J., Sharp, P.A., Jacks, T., 2009. Mass spectrometric and computational analysis of cytokineinduced alterations in the astrocyte secretome. Proteomics 9, 768–782. https://doi.org/10.1371/journal.pone.0178059

Khwaja, O.S., Ho, E., Barnes, K. V., O'Leary, H.M., Pereira, L.M., Finkelstein, Y., Nelson, C.A., Vogel-Farley, V., DeGregorio, G., Holm, I.A., Khatwa, U., Kapur, K., Alexander, M.E., Finnegan, D.M., Cantwell, N.G., Walco, A.C., Rappaport, L., Gregas, M., Fichorova, R.N., Shannon, M.W., Sur, M., Kaufmann, W.E., 2014. Safety, pharmacokinetics, and preliminary assessment of efficacy of mecasermin (recombinant human IGF-1) for the treatment of Rett syndrome. Proc. Natl. Acad. Sci. 111, 4596–4601. https://doi.org/10.1073/pnas.1311141111

Kim, J.J., Savas, J.N., Miller, M.T., Hu, X., Carromeu, C., Lavallée-Adam, M., Freitas, B.C.G.,

Muotri, A.R., Yates, J.R., Ghosh, A., 2019. Proteomic analyses reveal misregulation of LIN28 expression and delayed timing of glial differentiation in human iPS cells with MECP2 loss-of-function. PLoS One 14, e0212553. https://doi.org/10.1371/journal.pone.0212553

Krencik, R., Hokanson, K.C., Narayan, A.R., Dvornik, J., Rooney, G.E., Rauen, K. a, Weiss, L. a, Rowitch, D.H., Ullian, E.M., 2015. Dysregulation of astrocyte extracellular signaling in Costello syndrome. Sci. Transl. Med. 7, 286ra66. https://doi.org/10.1126/scitranslmed.aaa5645

Kucukdereli, H., Allen, N.J., Lee, A.T., Feng, A., Ozlu, M.I., Conatser, L.M., Chakraborty, C., Workman, G., Weaver, M., Sage, E.H., Barres, B.A., Eroglu, C., 2011. Control of excitatory CNS synaptogenesis by astrocyte-secreted proteins Hevin and SPARC. Proc. Natl. Acad. Sci. U. S. A. 108, E440-9. https://doi.org/10.1073/pnas.1104977108

Lana-Elola, E., Watson-Scales, S.D., Fisher, E.M.C., Tybulewicz, V.L.J., 2011. Down syndrome: searching for the genetic culprits. Dis. Model. Mech. 4, 586–95. https://doi.org/10.1242/dmm.008078

Liddelow, S.A., Guttenplan, K.A., Clarke, L.E., Bennett, F.C., Bohlen, C.J., Schirmer, L., Bennett, M.L., Münch, A.E., Chung, W.-S., Peterson, T.C., Wilton, D.K., Frouin, A., Napier, B.A., Panicker, N., Kumar, M., Buckwalter, M.S., Rowitch, D.H., Dawson, V.L., Dawson, T.M., Stevens, B., Barres, B.A., 2017. Neurotoxic reactive astrocytes are induced by activated microglia. Nature 541, 481–487. https://doi.org/10.1038/nature21029

Liu, Y., Borel, C., Li, L., Müller, T., Williams, E.G., Germain, P.-L., Buljan, M., Sajic, T., Boersema, P.J., Shao, W., Faini, M., Testa, G., Beyer, A., Antonarakis, S.E., Aebersold, R., 2017. Systematic proteome and proteostasis profiling in human Trisomy 21 fibroblast cells. Nat. Commun. 8, 1212. https://doi.org/10.1038/s41467-017-01422-6

Malter, J.S., Ray, B.C., Westmark, P.R., Westmark, C.J., 2010. Fragile X Syndrome and Alzheimer's Disease: Another story about APP and beta-amyloid. Curr. Alzheimer Res. 7, 200–6.

McCarthy, K.D., De Vellis, J., 1980. PREPARATION OF SEPARATE ASTROGLIAL AND OLIGODENDROGLIAL CELL CULTURES FROM RAT CEREBRAL TISSUE A novel method has been developed for the preparation of nearly pure separate cultures of astrocytes and oligodendrocytes . The method is based on (a) the abs. J. Cell Biol. 85, 890–902.

Menon, L., Mihailescu, M.R., 2007. Interactions of the G quartet forming semaphorin 3F RNA with the RGG box domain of the fragile X protein family. Nucleic Acids Res. 35, 5379–

5392. https://doi.org/10.1093/nar/gkm581

Miguel, R.F., Pollak, A., Lubec, G., 2005. Metalloproteinase ADAMTS-1 but not ADAMTS-5 is manifold overexpressed in neurodegenerative disorders as Down syndrome, Alzheimer's and Pick's disease. Mol. Brain Res. 133, 1–5. https://doi.org/10.1016/j.molbrainres.2004.09.008

Molofsky, A. V, Kelley, K.W., Tsai, H.-H., Redmond, S.A., Chang, S.M., Madireddy, L., Chan, J.R., Baranzini, S.E., Ullian, E.M., Rowitch, D.H., 2014. Astrocyte-encoded positional cues maintain sensorimotor circuit integrity. Nature 509, 189–94. https://doi.org/10.1038/nature13161

Pacheco, N.L., Heaven, M.R., Holt, L.M., Crossman, D.K., Boggio, K.J., Shaffer, S.A., Flint, D.L., Olsen, M.L., 2017. RNA sequencing and proteomics approaches reveal novel deficits in the cortex of Mecp2-deficient mice, a model for Rett syndrome. Mol. Autism 8, 56. https://doi.org/10.1186/s13229-017-0174-4

Russo, F.B., Freitas, B.C., Pignatari, G.C., Fernandes, I.R., Sebat, J., Muotri, A.R., Beltrão-Braga, P.C.B., 2018. Modeling the Interplay Between Neurons and Astrocytes in Autism Using Human Induced Pluripotent Stem Cells. Biol. Psychiatry 83, 569–578. https://doi.org/10.1016/J.BIOPSYCH.2017.09.021

Sanfeliu, A., Kaufmann, W.E., Gill, M., Guasoni, P., Tropea, D., 2019. Transcriptomic Studies in Mouse Models of Rett Syndrome: A Review. Neuroscience. https://doi.org/10.1016/j.neuroscience.2019.06.013

Schwartz, D.D., Katzenstein, J.M., Highley, E.J., Stabley, D.L., Sol-Church, K., Gripp, K.W., Axelrad, M.E., 2017. Age-related differences in prevalence of autism spectrum disorder symptoms in children and adolescents with Costello syndrome. Am. J. Med. Genet. A 173, 1294–1300. https://doi.org/10.1002/ajmg.a.38174

Sekar, A., Bialas, A.R., de Rivera, H., Davis, A., Hammond, T.R., Kamitaki, N., Tooley, K., Presumey, J., Baum, M., Van Doren, V., Genovese, G., Rose, S.A., Handsaker, R.E., Daly, M.J., Carroll, M.C., Stevens, B., McCarroll, S.A., McCarroll, S.A., 2016. Schizophrenia risk from complex variation of complement component 4. Nature 530, 177–183. https://doi.org/10.1038/nature16549

Seritan, A.L., Nguyen, D. V, Farias, S.T., Hinton, L., Grigsby, J., Bourgeois, J.A., Hagerman, R.J., 2008. Dementia in fragile X-associated tremor/ataxia syndrome (FXTAS): comparison with Alzheimer's disease. Am. J. Med. Genet. B. Neuropsychiatr. Genet. 147B, 1138–44. https://doi.org/10.1002/ajmg.b.30732

Shankar, S.L., O'Guin, K., Cammer, M., McMorris, F.A., Stitt, T.N., Basch, R.S., Varnum, B.,

Shafit-Zagardo, B., 2003. The growth arrest-specific gene product Gas6 promotes the survival of human oligodendrocytes via a phosphatidylinositol 3-kinase-dependent pathway. J. Neurosci. 23, 4208–18. https://doi.org/10.1523/jneurosci.5063-05.2006

Steeb, H., Ramsey, J.M., Guest, P.C., Stocki, P., Cooper, J.D., Rahmoune, H., Ingudomnukul, E., Auyeung, B., Ruta, L., Baron-Cohen, S., Bahn, S., 2014. Serum proteomic analysis identifies sex-specific differences in lipid metabolism and inflammation profiles in adults diagnosed with Asperger syndrome. Mol. Autism 5, 4. https://doi.org/10.1186/2040-2392-5-4

Stevens, B., Allen, N.J., Vazquez, L.E., Howell, G.R., Christopherson, K.S., Nouri, N., Micheva, K.D., Mehalow, A.K., Huberman, A.D., Stafford, B., Sher, A., Litke, A.M., Lambris, J.D., Smith, S.J., John, S.W.M., Barres, B. a., 2007. The Classical Complement Cascade Mediates CNS Synapse Elimination. Cell 131, 1164–1178. https://doi.org/10.1016/j.cell.2007.10.036

Strittmatter, W.J., Saunders, A.M., Schmechel, D., Pericak-Vance, M., Enghild, J., Salvesen, G.S., Roses, A.D., 1993. Apolipoprotein E: high-avidity binding to beta-amyloid and increased frequency of type 4 allele in late-onset familial Alzheimer disease. Proc. Natl. Acad. Sci. U. S. A. 90, 1977–81. https://doi.org/10.1073/pnas.90.5.1977

Tensaouti, Y., Stephanz, E.P., Yu, T.-S., Kernie, S.G., 2018. ApoE Regulates the Development of Adult Newborn Hippocampal Neurons. eNeuro 5. https://doi.org/10.1523/ENEURO.0155-18.2018

Torres, M.D., Garcia, O., Tang, C., Busciglio, J., 2018. Dendritic spine pathology and thrombospondin-1 deficits in Down syndrome. Free Radic. Biol. Med. 114, 10–14. https://doi.org/10.1016/j.freeradbiomed.2017.09.025

Trazzi, S., Fuchs, C., Valli, E., Perini, G., Bartesaghi, R., Ciani, E., 2013. The amyloid precursor protein (APP) triplicated gene impairs neuronal precursor differentiation and neurite development through two different domains in the Ts65Dn mouse model for Down syndrome. J. Biol. Chem. 288, 20817–29. https://doi.org/10.1074/jbc.M113.451088

Vance, J.E., Campenot, R.B., Vance, D.E., 2000. The synthesis and transport of lipids for axonal growth and nerve regeneration. Biochim. Biophys. Acta 1486, 84–96. https://doi.org/10.1016/s1388-1981(00)00050-0

Vanhala, R., Turpeinen, U., Riikonen, R., 2007. Low levels of insulin-like growth factor-I in cerebrospinal fluid in children with autism. Dev. Med. Child Neurol. 43, 614–616. https://doi.org/10.1111/j.1469-8749.2001.tb00244.x

Vilardell, M., Rasche, A., Thormann, A., Maschke-Dutz, E., Pérez-Jurado, L.A., Lehrach, H.,

Herwig, R., 2011. Meta-analysis of heterogeneous Down Syndrome data reveals consistent genome-wide dosage effects related to neurological processes. BMC Genomics 12, 229. https://doi.org/10.1186/1471-2164-12-229

Wallingford, J., Scott, A.L., Rodrigues, K., Doering, L.C., 2017. Altered Developmental Expression of the Astrocyte-Secreted Factors Hevin and SPARC in the Fragile X Mouse Model. Front. Mol. Neurosci. 10, 1–12. https://doi.org/10.3389/fnmol.2017.00268

Williams, E.C., Zhong, X., Mohamed, A., Li, R., Liu, Y., Dong, Q., Ananiev, G.E., Choongmok, J.C., Lin, B.R., Lu, J., Chiao, C., Cherney, R., Li, H., Zhang, S.-C.C., Chang, Q., Mok, J.C.C., Lin, B.R., Lu, J., Chiao, C., Cherney, R., Li, H., Zhang, S.-C.C., Chang, Q., 2014. Mutant astrocytes differentiated from Rett syndrome patients-specific iPSCs have adverse effects on wildtype neurons. Hum. Mol. Genet. 23, 2968–2980. https://doi.org/10.1093/hmg/ddu008

Woronowicz, A., Cawley, N.X., Chang, S.-Y., Koshimizu, H., Phillips, A., Xiong, Z.-G., Loh, Y.P., 2010. Carboxypeptidase E knock-out mice exhibit abnormal dendritic arborization and spine morphology in CNS neurons. J Neurosci Res 88, 64–72. https://doi.org/10.1016/j.drugalcdep.2008.02.002.A

Yagami, T., Ueda, K., Asakura, K., Sakaeda, T., Nakazato, H., Kuroda, T., Hata, S., Sakaguchi, G., Itoh, N., Nakano, T., Kambayashi, Y., Tsuzuki, H., 2002. Gas6 rescues cortical neurons from amyloid β protein-induced apoptosis. Neuropharmacology 43, 1289–1296. https://doi.org/10.1016/S0028-3908(02)00333-7

Yang, Q., Feng, B., Zhang, K., Guo, Y., Liu, S., Wu, Y., Li, X., Zhao, M., 2012. Excessive Astrocyte-Derived Neurotrophin-3 Contributes to the Abnormal Neuronal Dendritic Development in a Mouse Model of Fragile X Syndrome. PLoS Genet. 8, e1003172. https://doi.org/10.1371/journal.pgen.1003172

Young, O., Perati, S., Weiss, L.A., Rauen, K.A., 2018. Age and ASD symptoms in Costello syndrome. Am. J. Med. Genet. A 176, 1027–1028. https://doi.org/10.1002/ajmg.a.38641

Yuskaitis, C.J., Beurel, E., Jope, R.S., 2010. Evidence of reactive astrocytes but not peripheral immune system activation in a mouse model of Fragile X syndrome. Biochim. Biophys. Acta - Mol. Basis Dis. 1802, 1006–1012. https://doi.org/10.1016/J.BBADIS.2010.06.015

Zhang, Y., Chen, K., Sloan, S.A., Bennett, M.L., Scholze, A.R., O'Keeffe, S., Phatnani, H.P., Guarnieri, P., Caneda, C., Ruderisch, N., Deng, S., Liddelow, S.A., Zhang, C., Daneman, R., Maniatis, T., Barres, B.A., Wu, J.Q., 2014. An RNA-sequencing transcriptome and splicing database of glia, neurons, and vascular cells of the cerebral cortex. J. Neurosci. 34, 11929–11947. https://doi.org/10.1523/JNEUROSCI.1860-14.2014

Zhang, Z., Trautmann, K., Artelt, M., Burnet, M., Schluesener, H.J., 2006. Bone morphogenetic protein-6 is expressed early by activated astrocytes in lesions of rat traumatic brain injury. Neuroscience 138, 47–53. https://doi.org/10.1016/j.neuroscience.2005.11.036

Chapter 4: Increased secretion of IGFBP2 from *Mecp2* KO astrocytes induces deficits in neuronal outgrowth in vitro, which can be rescued with the application of an IGFBP2 neutralizing antibody

Formatting note: every chapter in this dissertation has its own, self-contained introduction and discussion. The introduction and conclusion chapters are intended to broadly frame and contextualize the dissertation. All methods are confined to a single methods chapter at the end of the dissertation.

Introduction

Using immunopanning, we successfully isolated and cultured astrocytes from three different models of genetic neurodevelopmental disorders (NDs), as well as wild-type astrocytes (WT) at postnatal day 7 (P7), a time point when astrocytes are known to be involved in neuronal development and synapse formation. With this approach, we conducted an unbiased analysis of the astrocyte protein secretome in vitro, and identified over 80 proteins that showed significantly increased protein secretion in all three NDs compared to WT. One of the proteins identified by the analysis was insulin-like growth factor binding protein 2 (IGFBP2), which is one of the most abundant proteins in astrocyte conditioned media (ACM) (roughly 2% of total peptide spectra detected) and shows at least a 0.5-fold increase in all three NDs. IGFBP2 is one of six IGF binding proteins which act as carrier proteins for IGF1 and modulate its activity. IGFBPs can have either inhibitory effects on IGF1 signaling by sequestering IGF1 away from the IGF receptor or they may enhance IGF1 activity by interacting with matrix components to concentrate IGF1 near its receptor (Siwanowicz et al., 2005). IGFBPs can also have IGF-independent effects due to their ability to interact with extracellular matrix (ECM) proteins and other binding partners, as well as their ability to locate to the nucleus (Forbes et al., 2012). IGFBP2 is one of the most abundant IGFBPs in the central nervous system (Dyer et al., 2016; Hwa et al., 1999; Ocrant et al., 1990), is highly expressed by astrocytes in vivo (Zhang et al., 2014), and shows coordinated expression with neuronal IGF1 expression during development (Lee et al., 1992), thus making IGFBP2 an intriguing candidate for better understanding astrocyte effects on neuronal development.

As discussed in chapter 3, insulin-like growth factor 1 (IGF1) is a promising candidate in the search for therapeutic treatments for autism spectrum disorder (ASD) (Vahdatpour et al., 2016). IGF1 is a member of a superfamily of related hormones, including insulin, IGF1, and IGF2. IGF1 is a potent growth factor that plays a number of critical roles in early brain development (Wrigley et al., 2017). IGF1 is synthesized primarily by the liver, but is also produced in the brain

and is found in circulation throughout the body. Binding of IGF1 to IGF receptors (IGFRs) leads to autophosphorylation of the receptor, which subsequently leads to the phosphorylation of insulin receptor substrate 1 (IRS1). This reaction is the start of a complex cascade of downstream signaling, including activation of the canonical PI3K-AKT pathway. The phosphoinositide 3-kinase-protein kinase B (PI3K-AKT) pathway is highly conserved across species, and is important for many developmental processes. When PI3K is activated via IRS phosphorylation, its catalytic domain converts phosphatidylinositol (3,4)-bis- phosphate (PIP2) lipids to phosphatidylinositol (3,4,5)-tris- phosphate (PIP3). This in turn allows for activation of PKD/AKT; once activated, AKT can further phosphorylate proteins in both the cytoplasm and nucleus, leading to many downstream effects including cell survival, protein synthesis, glucose metabolism, and neuroprotection (Hemmings and Restuccia, 2012) (Figure 4.1).

During development, IGF1 is expressed by all major central nervous system (CNS) cell types throughout the brain, with regional expression in areas where cell proliferation, differentiation, and synaptogenesis are taking place (Costales and Kolevzon, 2016). CNS expression of IGF1 drops off across the lifetime and the protein is primarily expressed by the liver in adulthood (Jones and Clemmons, 1995). Mice lacking IGF1 and IGF1R demonstrate severe growth deficiencies and die at birth due to respiratory failure (Liu et al., 1993). Low levels of IGF1 in children have been associated with slowed childhood growth and low IQ (Gunnell et al., 2005). Alterations in IGF signaling contributing to neuronal dysfunction have been found in multiple genetic disorders known to cause autism (de Souza et al., 2017; Deacon et al., 2015; Williams et al., 2014). Small studies have found that children with autism have lower levels of IGF1 in their cerebrospinal fluid (CSF) (Riikonen et al., 2006; Vanhala et al., 2007) and reduced IGF1 urinary secretion (Anlar et al., 2007) compared to controls, but other studies are conflicting, showing increased levels of IGF1 in ASD (Reim and Schmeisser, 2017). Additional work has found that the brains of autistic children have decreased expression of phosphorylated AKT compared to

controls (Russo, 2015; Sheikh et al., 2010). There is evidence for decreased PI3K/mTOR and ERK pathway activation in RTT brains, contributing to a reduction in protein synthesis initiation which precedes neurological signs of the disorder (Ricciardi et al., 2011). In contrast, in FXS, overactive PI3K/AKT signaling has been implicated in the impaired trafficking of GluA1-containing AMPA receptors to the synapse, leading to a loss of GluA1-dependent long term potentiation (LTP) (Hu et al., 2008). Phosphatase and tensin homolog (PTEN) is a negative regulator of PI3K/AKT. Mutations in PTEN in mice leads to an autism-like phenotype, including changes in social behavior and brain overgrowth (Kwon et al., 2006) and PTEN mutations have been found in autistic individuals with macrocephaly (Butler et al., 2005; Goffin et al., 2001; Ueno et al., 2019).

For these reasons, and for its potent neurotrophic activity, IGF1 makes an appealing candidate for treating conditions associated with alterations in neuronal development and synapse formation. Treating RTT mice with the active peptide fragment of IGF1, (1-3)IGF1 (also called GPE), can significantly improve the behavioral and physiological effects of MECP2 deficiency in vivo (Tropea et al., 2009) and adding GPE to RTT ACM can rescue the neuronal deficits induced by *MECP2* KO astrocytes generated from RTT patient induced pluripotent stem cells (iPSCs) (Williams et al., 2014). Its effectiveness in treating RTT has led many scientists to explore the potential for IGF1 in other genetic NDs. In a mouse model of Phelan-McDermid (PD) Syndrome (*SHANK3* KO), daily injections of IGF1 similarly rescued deficits in neuronal and synaptic function as well as behavioral symptoms (Bozdagi et al., 2013). Treating FXS mice with NNZ-2566, a synthetic analog of IGF1, corrected learning and memory deficits, rescued abnormal dendritic spine density, and reduced overactive ERK and AKT signaling in vivo (Deacon et al., 2015). Early clinical trials have found that IGF1 treatment in children with RTT, FXS, and PD (Berry-Kravis et al., 2014; Khwaja et al., 2014; Kolevzon et al., 2014; Pini et al., 2014, 2012) have demonstrated that recombinant IGF1 and the GPE peptide are well tolerated, and patients have

shown improvement in both behavioral and respiratory symptoms in RTT and in social impairment in PD (Khwaja et al., 2014; Kolevzon et al., 2014; Pini et al., 2014, 2012).

While IGF1/PI3K/AKT signaling has been implicated in ASD, little work has been done to determine whether or not alterations in IGFBPs may be affecting IGF1 signaling in these disorders. However, there is evidence that MECP2 binds to the IGFBP3 promotor and increased IGFBP3 (the most abundant IGFBP in serum) has been seen in the brains of *Mecp2* KO mice and RTT humans (Itoh et al., 2007). Transcriptomic analysis has found that astrocytes show dysregulation of IGFBP4 in RTT (Yasui et al., 2013), while RTT microglia show increased expression of IGFBP3 (Cronk et al., 2015). Overexpression of IGFBP2 in transgenic mice leads to a significant decrease in body weight and a modest decrease in brain weight, suggesting it is inhibiting IGF1 signaling (Hoeflich, 1999).

While there is little evidence of IGFBP2 dysfunction in ASD thus far, the mass spectrometry results and the relationship between IGF1 and IGFBP2 led us to examine whether or not the increased secretion of IGFBP2 might be playing a role in the pathology of these NDs. We conducted Western blot analysis of IGFBP2 levels in both whole brain tissue and cerebrospinal fluid from RTT mice and their WT littermates, but found the results to be variable. Next, we determined via immunohistochemical analysis that there are increased levels of extracellular IGFBP2 in the cortex of P7 RTT mice compared to WT littermates. These results led us to examine the effects of excess recombinant IGFBP2 on neuronal growth in vitro, where we determined that the addition of IGFBP2 induces deficits in neuronal outgrowth compared to WT ACM alone, and those deficits can be prevented by the application of an IGFBP2-neutralizing antibody. Furthermore, we determined that the addition of an IGFBP2-neutralizing antibody to RTT ACM, but not to FXS or DS ACM, is sufficient to partially rescue the neuronal outgrowth deficits seen in RTT in vitro. These results indicate that increased IGFBP2 secretion may play a

role in the pathology of RTT, and may represent a unique therapeutic avenue for treating the condition.

Results

IGFBP2 protein is enriched in ND ACM compared to WT

Mass spectrometry analysis identified IGFBP2 as a highly-abundant protein in ACM showing significantly enriched protein secretion in all 3 NDs compared to WT (2.7% of all spectra counted in WT ACM, 4.6% in FXS, 5.0% in RTT, 6.2% in DS) (Figure 4.2A). Interestingly, several other IGFBPs showed increased secretion in ND ACM; IGFBP5 showed significantly increased secretion in all 3 NDs, while IGFBP3 was increased in FXS and RTT, and IGFBP4 was increased in RTT. Concurrently, there was a reduction in IGF1 secretion in FXS and IGF2 secretion in both FXS and RTT, while IGF1 actually showed increased secretion in DS (Figure 4.2A). This provide support for our hypothesis that there is an overall dysregulation in IGF signaling in astrocytes in these NDs. Importantly, when we examined gene expression changes in ND astrocytes, we determined that while there was a slight increase in *Igfbp2* expression by RNASeq analysis, it was not significant (Figure 4.2B); only *Igfbp5* showed a significant increase in expression and only in FXS. Surprisingly, *Igfbp4* actually showed significant downregulation in FXS and DS, and *Igfbp7* was significantly downregulated in FXS. Similarly, while we saw trends in decreased expression of IGF1 and IGF2 in FXS and RTT, and increased expression in DS, the changes did not reach significance (Figure 4.2B). These results highlight the importance of examining both protein and gene expression of secreted factors when identifying functional changes in astrocyte behavior.

We chose to focus more closely on IGFBP2 as a potentially inhibitory factor in ND ACM because IGFBP2 is very highly expressed in astrocytes compared to other brain cell types (Figure 4.2D), while other IGFBPs show high expression in a variety of cell types, including neurons.

While *Igfbp2* is highly enriched in astrocytes, *Igf1* shows high levels of expression in neurons compared to other cell types (Figure 4.2D); given the known interactions between IGFBPs and IGFs in the extracellular space, this further supports IGFBP2 as an intriguing astrocyte-secreted protein factor that may be involved in alterations in IGF signaling in ASD. These results led us to further examine the role of IGFBP2 in neuronal development in vivo and in vitro.

IGFBP2 is detectable in whole brain lysate and CSF by Western blot in RTT and WT littermate mice.

We first attempted to validate the mass spectrometry data showing that IGFBP2 is present in increased levels in ND ACM compared to WT by Western blotting ACM with an antibody against IGFBP2 (R&D AF797), along with increasing doses of purified IGFBP2 protein (Figure 4.3A,D). Our results were inconsistent, however. This was likely due to the challenges of performing a quantitative Western blot analysis on secreted proteins. While we determined the concentration of ACM by Bradford Assay and loaded 2 ug total protein in each lane, each individual ACM sample had a very low concentration (typically <1 mg/mL), and it was difficult to ensure that an equal amount of protein was loaded in each lane. Furthermore, assessing an internal loading control proved to be challenging, as there were few secreted proteins that showed no changes in secretion in ND vs. WT that also met other criteria for acting as a control (i.e. present at a high concentration in ACM, a size of >50 kDa to ensure adequate separation from IGFBP2, the existence of a specific antibody).

We next examined IGFBP2 levels in vivo by performing a Western blot analysis on whole cortical tissue lysate isolated from P7 RTT and WT littermate mice (Figure 4.3B,E). Again, we found our results to be inconsistent. This may be due to the large amounts of total protein load required to detect IGFBP2. Another possibility is that the total level of IGFBP2 does not change

in RTT, but that there is an alteration in protein localization, with more present in the extracellular space, which we next investigated.

Finally, because IGFBP2 is a secreted protein, we decided to examine levels of IGFBP2 in cerebrospinal fluid (CSF). IGFBP2 is found circulating at high levels throughout the body, in addition to being one of the most abundant IGFBPs in the CNS (Dyer et al., 2016; Ocrant et al., 1990). IGFBP2 is abundant in CSF (Ocrant et al., 1990), and astrocyte-secreted proteins are known to contribute to CSF content (Lafon-Cazal et al., 2003). We collected CSF from the cisterna magna of P7 RTT and WT littermate mice post-mortem and conducted Western blot analysis on IGFBP2 levels. Again, results were inconclusive (Figure 4.3C,F). Due to the age and size of the mice, we were unable to obtain large volumes of CSF, and had difficulty obtaining clean samples without any contamination from blood. We were thus only able to load 5 ug of protein for each sample; this made it challenging to use total protein load as a loading control, as most methods for detecting total protein load in a membrane require larger amounts of protein for accurate detection (Aldridge et al., 2008; Thacker et al., 2016).

IGFBP2 protein is increased in the extracellular space of RTT mice.

Due to the inconsistent results obtained with Western blotting, we next took an immunohistochemical approach to ask if the intra or extracellular localization of IGFBP2 is altered in RTT mice. We asked if IGFBP2 protein is increased in the cortex in vivo in ND compared to WT mice at P7, both in astrocytes and in the extracellular space. To do this, we crossed our RTT mouse line with an Aldh1L1-eGFP expressing transgenic line, which expresses GFP protein exclusively in astrocytes. This approach enabled us to easily identify and image astrocytes in vivo and examine IGFBP2 localization both within and surrounding astrocytes in the cortex. Fixed tissue was isolated from P7 RTT and WT littermate male mice, sectioned and mounted coronally, and stained for IGFBP2 using a polyclonal goat anti-IGFBP2 antibody (R&D AF797) and a donkey

anti-goat Alexafluor 594 secondary antibody. We performed this staining with only a low concentration of BSA and no goat serum in the buffers, to prevent cross interactions between our antibodies and serum proteins. Sections were imaged using Zeiss LSM 880 Rear Port Laser Scanning Confocal Microscope and layer 2/3 astrocytes of the visual cortex were targeted, with images obtained at 63X magnification across a total thickness of 3.85 um. These images were analyzed in Bitplane IMARIS software to create surfaces of astrocytes within the region of interest (ROI) and the IGFBP2 puncta both within the astrocyte surface (intracellular IGFBP2) and outside the astrocyte surface (extracellular IGFBP2). All work was performed while the investigator was blinded to the genotypes of the animals. This analysis revealed an increase in the overall intensity of extracellular IGFBP2 expression per ROI in RTT KO cortex versus WT at P7 (Figure 4.4C), with no change in the average intensity per puncta (Figure 4.4B). We also saw an increase in the size of individual IGFBP2 puncta in the extracellular space of layer 2/3 astrocytes in RTT mice compared to WT, and found a trend toward an increase in the overall volume of extracellular IGFBP2 signal in each ROI (Figure 4.4D,E). There was no significant change in the volume of internal IGFBP2 in astrocytes in RTT versus WT P7 cortex (Figure 4F,G).

Excess IGFBP2 inhibits neurite outgrowth when added to WT ACM.

Having determined that extracellular IGFBP2 is increased in the extracellular space of RTT mice, we next asked if increased levels of IGFBP2 in ND ACM are responsible for the inhibitory effect of ND ACM on WT neuron outgrowth. To test this we added excess recombinant IGFBP2 protein to WT ACM, and determined if this ACM now inhibited neuronal outgrowth. We used our mass spectrometry data to estimate the relative abundance of IGFBP2 in ND vs. WT ACM to determine how much IGFBP2 should be added to WT ACM to bring it up to the ND level. As IGFBP2 is present at 2.2% of total protein in WT ACM, we chose to add IGFBP2 at 4x the WT level, or 2x the ND level, to amplify any potential effect seen in vitro. Additional testing at a higher

concentration of IGFBP2 (10x) did not show an enhanced effect. IGFBP2 (R&D 797-B2) was added to WT ACM at 240ng/ml, cortical neurons were treated with WT ACM +/- protein factor, and total neurite outgrowth measured 48 hours later. Treating neurons with IGFBP2 in the absence of ACM had no effect on outgrowth, whereas adding IGFBP2 to WT ACM blocked the neurite-outgrowth promoting effect of WT ACM (N=3 experiments, 3 coverslips per condition per experiment, at least 10 cells imaged per coverslip). This shows that increasing the level of IGFBP2 in WT ACM is sufficient to inhibit neuronal outgrowth (Figure 4.5A,B).

IGF1 overcomes the inhibitory effects of RTT ACM on neurite outgrowth (Williams et al., 2014b), and it is possible that IGF1 does this by binding to IGFBP2 and enabling endogenous IGF1 to signal to neurons. To test this we treated WT neurons with WT ACM+IGFBP2+IGF1 (100ng/ml). The addition of IGF1 was sufficient to overcome the inhibitory effect of adding excess IGFBP2 to WT ACM, suggesting that IGFBP2 is inhibiting neuronal outgrowth by blocking ongoing IGF signaling (Figure 4.5A,B). The positive effect of IGF1 on neurite outgrowth may be unrelated to IGFBP2, however, and due to IGF1 directly signaling to neurons to enhance neurite outgrowth. To specifically target IGFBP2 we used an anti-IGFBP2 blocking antibody (IGFBP2 Ab, R&D MAB797) that overcomes the inhibitory effect of IGFBP2 on IGF signaling. We first validated that the IGFBP2 Ab could block the inhibitory effect of excess IGFBP2 protein in WT ACM by adding it at 7mg/ml (2x the ND50) (N=3 experiments, 3 coverslips per condition per experiment, at least 20 cells imaged per coverslip). WT ACM+IGFBP2+IGFBP2 Ab no longer inhibited neurite outgrowth, demonstrating the functionality of the IGFBP2 Ab (Figure 4.5C-F). Igfbp2 Ab alone had no effect (Figure 4.5G).

Blocking IGFBP2 activity is sufficient to rescue the inhibitory effect of RTT ACM on WT neurite outgrowth

FXS, RTT and DS neurons have decreased dendritic complexity and altered spine morphology, with an increase in the number of filopodia-like (immature) spines and a decrease in the number of mushroom (mature) spines (Jawaid et al., 2017; Torres et al., 2018; Tropea et al., 2009). We next asked if adding the IGFBP2 Ab to ND ACM would be sufficient to overcome the inhibitory effect of ND ACM on WT neurite outgrowth. RTT ACM did not significantly increase neurite outgrowth compared to neurons alone, whereas the addition of IGFBP2 Ab to RTT ACM induced a significant increase in neurite outgrowth (Figure 4.6A-D) (N=3 experiments, 3 coverslips per condition per experiment, at least 20 cells imaged per coverslip). In contrast, while FXS ACM had a similarly inhibitory effect on WT neurite outgrowth, adding the IGFBP2 Ab to FXS ACM did not rescue the effect (Figure 4.6E-H) (N=3 experiments, 3 coverslips per condition per experiment, at least 20 cells imaged per coverslip). Finally, we determined that DS ACM does not have an inhibitory effect on neuronal outgrowth compared to WT ACM, and addition of the IGFBP2 Ab also had no effect on outgrowth (Figure 4.6I-L) (N=3 experiments, 3 coverslips per condition per experiment, at least 20 cells imaged per coverslip).

Discussion

Our mass spectrometry data identified IGFBP2 as a protein that showed dramatically increased secretion in all 3 NDs compared to WT, and our in vitro experiments suggest increased astrocytic IGFBP2 is contributing to aberrant neuronal development in RTT but not FXS or DS. IGFBPs inhibit secreted IGF1 by binding it and preventing it reaching the IGF receptor, or alternatively protect it from degradation by acting as a carrier protein (O'Kushky and Ye, 2012). IGF signaling is also altered in ASD, however depending on the study, increased, decreased or unchanged levels of IGF1 have been detected in patients (Reim and Schmeisser, 2017). Despite the discrepancies regarding IGF1 level, treatment with IGF1 or the shorter 3 amino acid form (GPE) rescues dendritic spine defects in RTT mice, and is in clinical trials for RTT (Vahdatpour

et al., 2016) and FXS (Wise, 2017). As IGF signaling is altered in ASD (Deacon et al., 2015; Khwaja et al., 2014) and IGFBP2 regulates IGF signaling (O'Kushky and Ye, 2012) we hypothesize that ND astrocytes negatively impact neurons by inhibiting IGF signaling. Interestingly studies have shown that IGF signaling is overactive in DS neurons, rather than deficient (Araujo et al., 2018).

Although IGFBP2 was present at increased levels in ACM from all three NDs, blocking IGFBP2 was only capable of rescuing the neuronal outgrowth deficits induced by the application of RTT ACM, and not FXS ACM. This indicates that while IGFBP2 is likely to play a role in the pathology of RTT, there must be other signals contributing to the outgrowth inhibition in FXS. In contrast to the other two NDs, DS ACM did not have an inhibitory effect on neuronal outgrowth, and blocking IGFBP2 had no effect. While there is evidence for abnormal dendritic arborization in DS, the observed effect may be inhibition or overgrowth, depending on the age of the patient (Becker et al., 1991, 1986). While research in human iPSCs indicates that DS ACM may stunt neurite outgrowth compared to WT ACM, the effect observed was small, with a reduction in neurite length of around 20% (Chen et al., 2014). We found that DS astrocytes have a significant increase in secretion of IGF1 compared to WT, whereas FXS and RTT astrocytes show decreased secretion of IGF1, so it is possible that the increase in IGF1 in the DS ACM counteracts the effects of increased IGFBP2. However, most studies on the roles of astrocytes in DS have focused on spine and synapse defects, where a wide variety of protein signals are at play during development. The spine morphology and synaptic deficits observed in DS appear to represent a more robust phenotype, and it may be that altered secretion of IGFBP2 has an effect on synapse and spine formation in DS, but that is outside the scope of this dissertation. Alternately, it may be that other proteins that show differential secretion in DS ACM, for example APP, which shows dramatically increased secretion in DS and has been implicated in synaptic plasticity (Montagna et al., 2017), play a role in the filopodia-type spines and decreased synapse density seen in DS.

Future studies will examine the effects of DS ACM, and our candidate proteins, on spine and synapse development and morphology.

Our in vitro experiments suggest increased astrocytic IGFBP2 is contributing to aberrant neuronal development in RTT, but it remains to be determined if this is also occurring in vivo. We are currently working to determine if IGFBP2 has a similar role in the developing cortex in RTT mouse models, by testing if the IGFBP2 blocking Ab can reverse the dendritic deficits in RTT mice. We are injecting the IGFBP2 Ab into the cortex of RTT and WT littermate mice at P2, and collecting at P7, to analyze dendritic arbor size at an early time point that matches the in vitro data; 1ug of antibody at 1mg/ml will be injected into the upper layers of the visual cortex, following similar procedures to (Singh et al., 2016). For each time point and ND model there will be 4 conditions, each within one litter of mice: WT + rat isotype control Ab (R&D 6-0001-A); WT + IGFBP2 Ab (R&D MAB797); RTT + control Ab; RTT + IGFBP2 Ab. To test this approach, IGFBP2-neutralizing antibody (R&D MAB797) or its control IgG antibody (R&D 6-001-F) were labeled with Alexa Fluor 594 Succinimidyl Ester (Thermo Fisher Scientific A20004) according to protocol and 1ug of antibody was injected into the cortex of P2 RTT and WT littermate pups at -250 and -150 um at roughly 3.4mm posterior to Bregma. We have determined that we are capable of injecting the antibody at the correct coordinates, and that the spread of the antibody encompasses our region of interest (Figure 4.7). Brains will thus be collected at P7 and processed for Golgi staining using the RD Rapid GolgiStain™ kit (FD Neurotechnologies PK401) and imaged at 20X using a brightfield microscope to capture entire layer 2/3 neurons for analysis. With the assistance of the Waitts Advanced Biophotonics Core Facilities at The Salk Institute, we are using Bitplane IMARIS software to perform pre-processing and automatic tracing analysis of individual cells. With this approach, we will measure both dendritic arbor branching and dendrite length, to examine the effects of IGFBP2 Ab on dendritic arbor morphology. Additionally, the Bitplane IMARIS software is capable of spine morphology analysis and counting, which will allow us to examine spine

density and morphology in RTT vs WT brains at P7, and to determine whether or not IGFBP2 Ab has an effect on spines in vivo. The results of these experiments will clarify whether or not increased IGFBP2 plays a role in the pathology of RTT, and whether the deficits associated with RTT can be rescued by blocking IGFBP2 activity directly. This will further elucidate the molecular mechanisms underlying RTT pathology and potentially provide a new direct therapeutic target for treating the condition.

Acknowledgements

This chapter is, in part, in preparation for submission for publication. The dissertation author will be the first author of this publication, with Dr. Jolene Diedrich as second author and Dr. Nicola Allen as the senior author and principle investigator.

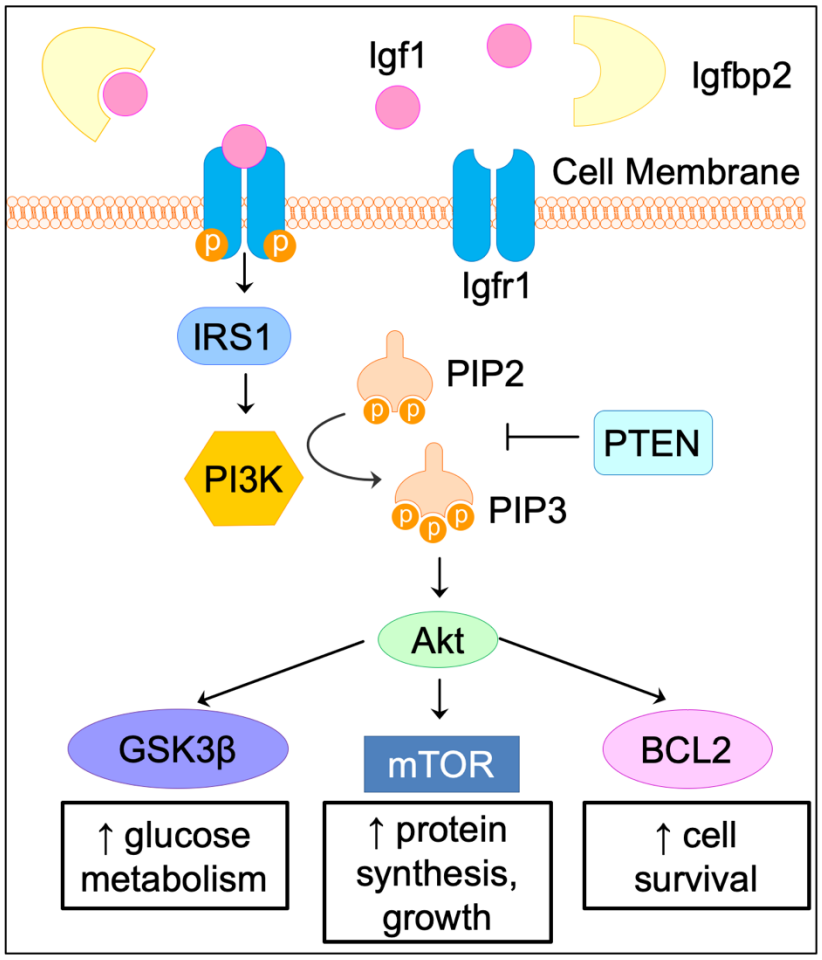

Figure 4.1: Schematic of IGF signaling via the PI3K/Akt pathway. IGF1 binds to IGF1R, leading to its phosphorylation, which in turn activates IRS1, which activates PI3K and leads to the conversion of PIP2 to PIP3. This leads to the activation of AKT, which has many effects on cell metabolism, growth, and development.

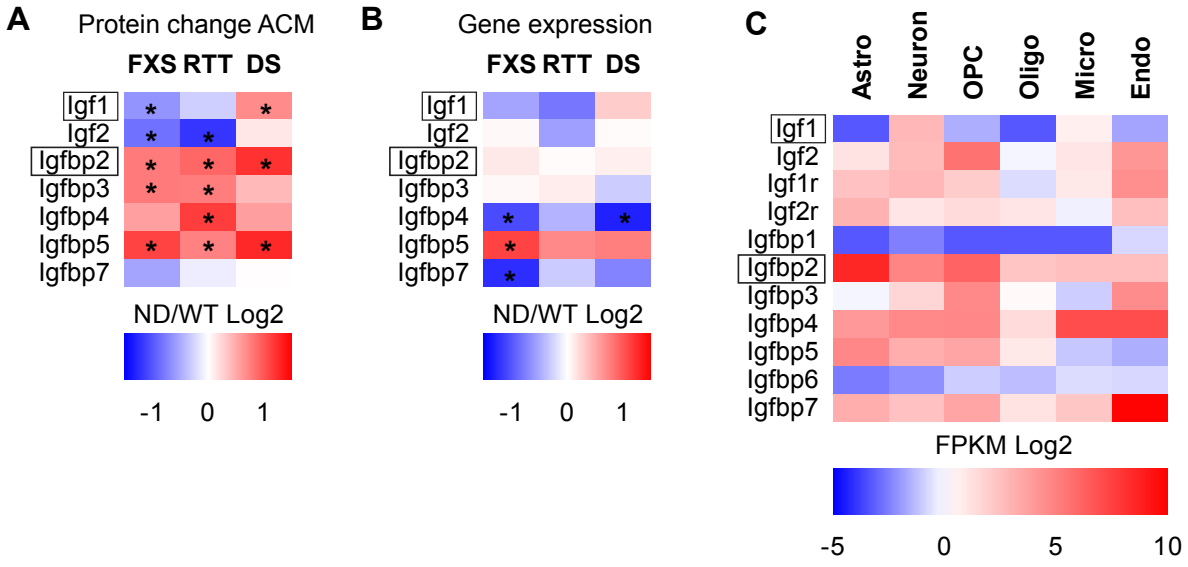

Figure 4.2: Protein secretion and gene expression profiles of IGFBP2 in WT and ND astrocytes. A. Fold change in protein for IGFBP family members in ND ACM compared to WT (log2), red upregulated and blue downregulated in ND**. B.** Fold change in gene expression for *Igfbp* family members in ND astrocytes compared to WT (log2). For proteomics, N=6 cultures per genotype, *p<0.05, abundance >0.01%, fold change between WT and ND ≥1.5. For RNASeq, N=6 cultures WT, RTT, FXS; 4 cultures DS. Significance for differential expression defined as adjusted p<0.05, calculated using Benjamini-Hochberg's procedure for multiple comparisons, FPKM>1 and fold change between ND and WT >1.5, comparing each ND and WT after adjustment for multiple testing. **C.** Relative expression of *Igfbp* family members in purified cell types in the cortex, shows enrichment for *Igfbp2* in astrocytes (Zhang et al., 2014).

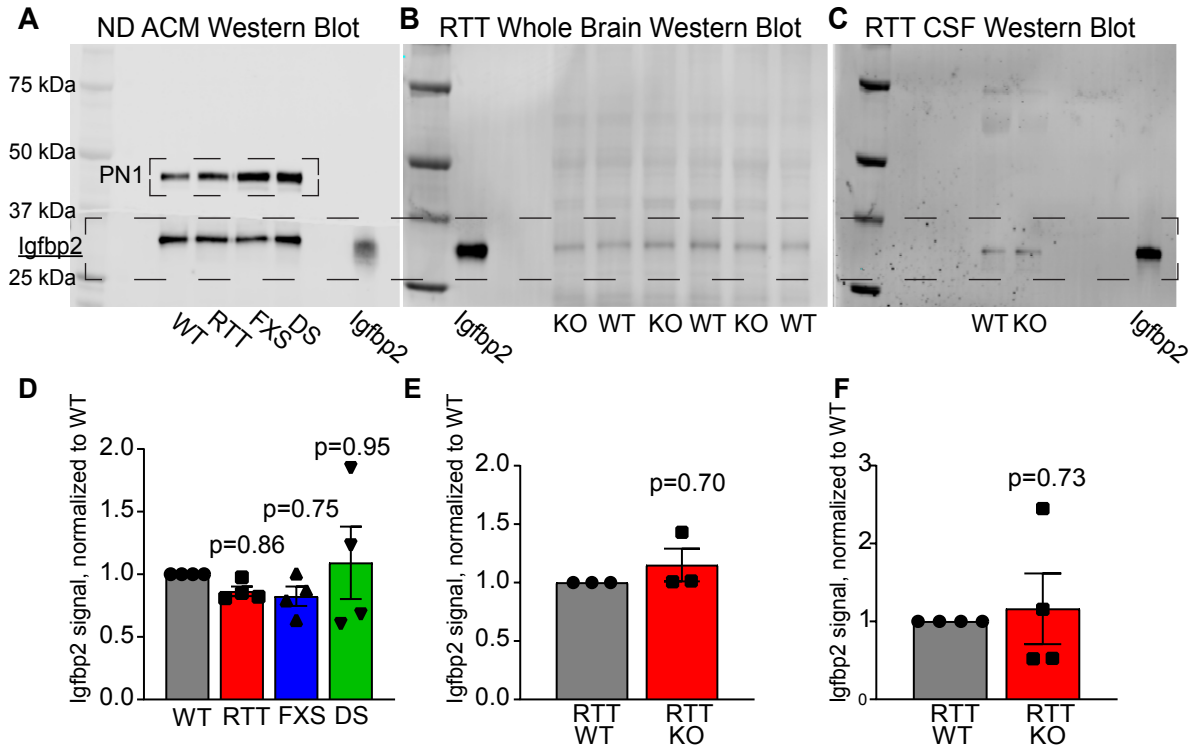

Figure 4.3: Western blotting of IGFBP2 in ND ACM, whole cortex, and cerebrospinal fluid. A,D. Western blotting for IGFBP2 in WT and ND ACM does not show an increase in IGFBP2 levels in ND ACM. N=4 blots, 1 culture per genotype per blot, 5 ug protein loaded per lane, normalized to PN1 expression. **B,E.** Western blotting for IGFBP2 in RTT and WT littermate whole cortical lysate does not show an increase in overall IGFBP2 level in RTT cortex. N=3 blots, 3 mice per genotype per blot, 20 ug protein loaded per lane, normalized to β-tublin expression run on a separate blot (not shown). **C,F.** Western blotting for IGFBP2 in RTT and WT littermate cerebrospinal fluid (CSF) does not show an increased in secreted IGFBP2 in RTT CSF. N=4 blots, 1 mouse per genotype per blot, 5 ug protein loaded per lane, normalized to total protein load via Ponceau S staining.

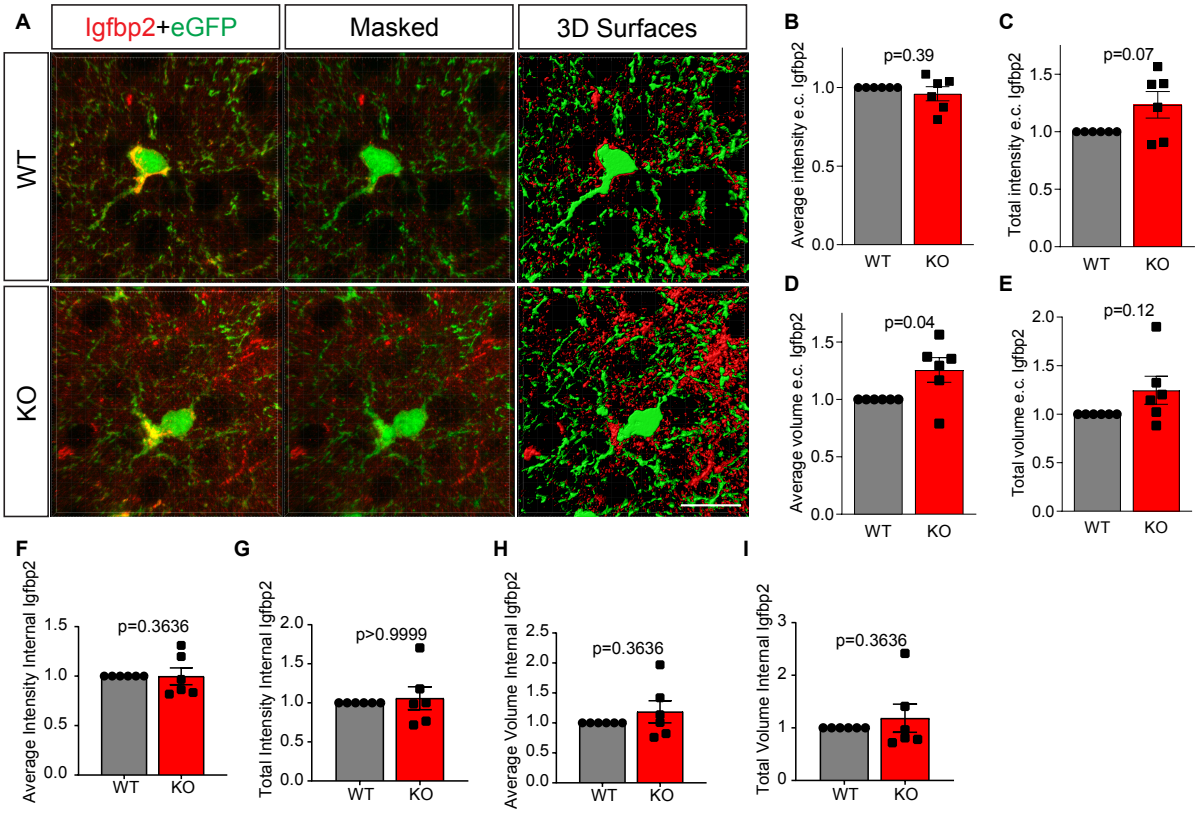

Figure 4.4: Staining for IGFBP2 in RTT and WT littermate cortex reveals an increase in extracellular IGFBP2. A. Example images of layer 2/3 WT and RTT KO astrocytes (green) with IGFBP2 expression (red). Bitplane IMARIS software was used to generate 3D surfaces of astrocytes and IGFBP2 puncta and images were masked to analyze intracellular (within the astrocyte surface) or extracellular (outside the astrocyte surface) IGFBP2 levels separately. **B.** There is no change in the average intensity of extracellular IGFBP2 puncta in RTT KO compared to WT. **C.** There is a trend toward an increase in the overall intensity of extracellular IGFBP2 staining in RTT KO cortex compared to WT. **D,E.** There is an increase in the volume of the individual puncta of extracellular IGFBP2 in RTT KO cortex compared to WT (**D**), and a trend toward an increase in the overall volume of IGFBP2 staining (**E**). **F-I.** There are no significant changes in the volume of intracellular IGFBP2 in RTT compared to WT.

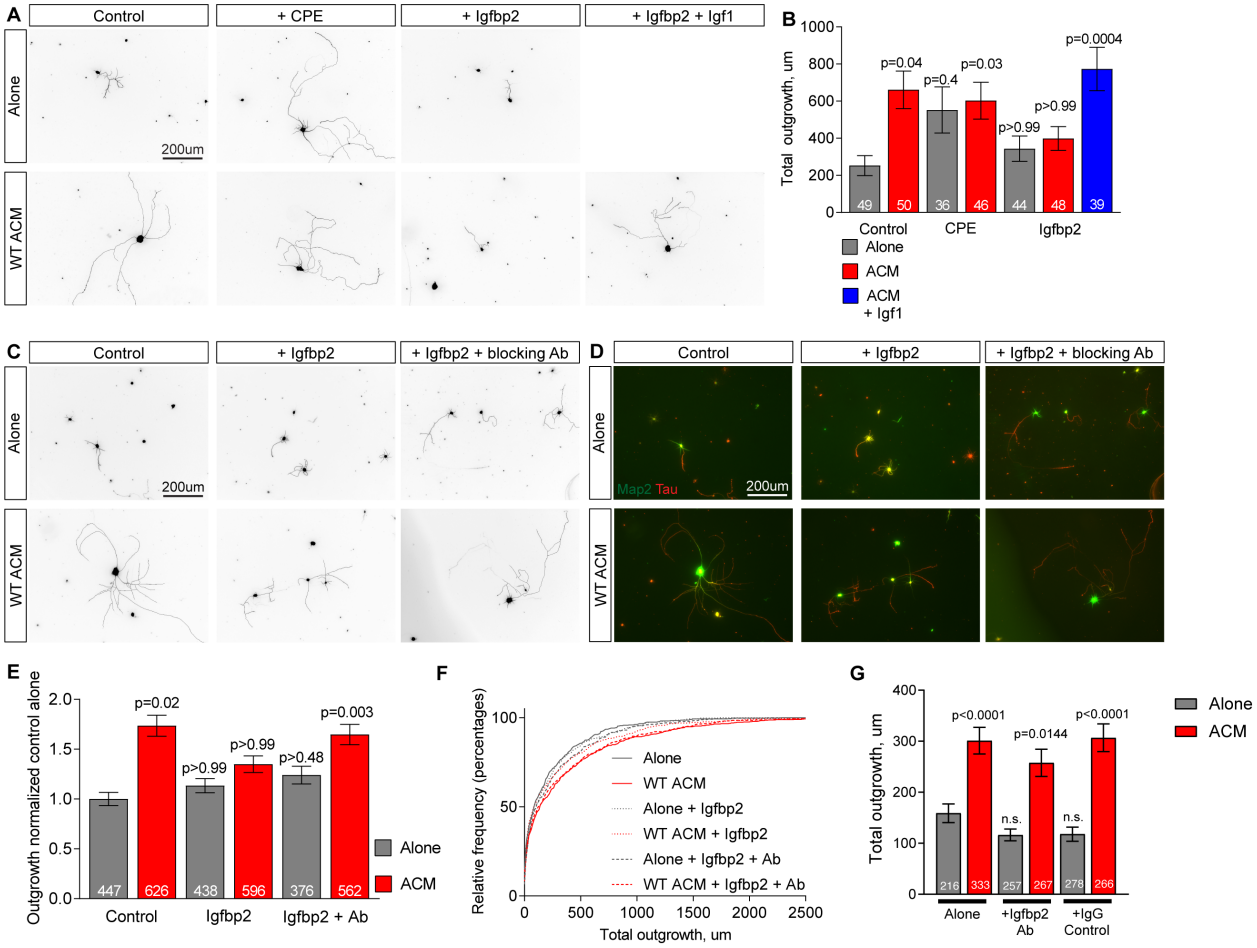

Figure 4.5: IGFBP2 protein inhibits neurite outgrowth in vitro, which can be rescued with the application of an IGFBP2-neutralizing antibody. A,B. Addition of IGFBP2 protein to WT ACM inhibits WT neurite outgrowth, which is reversed by adding IGF1. Addition of CPE protein to WT ACM does not inhibit WT neurite outgrowth and may support neurite outgrowth in the absence of WT ACM. **A.** Example images after processing with MetaMorph Neurite Outgrowth module, neurons immunostained with Map2 + Tau. **B.** Quantification of total neurite outgrowth (MAP2 + tau). Example experiment shown, experiment repeated 2 times with same result. **C-F.** An IGFBP2 blocking antibody overcomes the inhibitory effect of adding excess IGFBP2 protein to WT ACM. Example images after processing with MetaMorph Neurite Outgrowth module (**C**), neurons immunostained with Map2 + Tau before processing (**D**). **E,F.** Quantification of total neurite outgrowth normalized to a control alone condition. **G.** Igfbp2 neutralizing antibody or a control IgG antibody alone do not induce changes in neurite outgrowth. Example experiment shown, experiment repeated 2 times with same result. Bar graphs represent mean ± s.e.m. Number inside bar = number of neurons analyzed. Statistics by one-way ANOVA, p values compared to Alone condition.

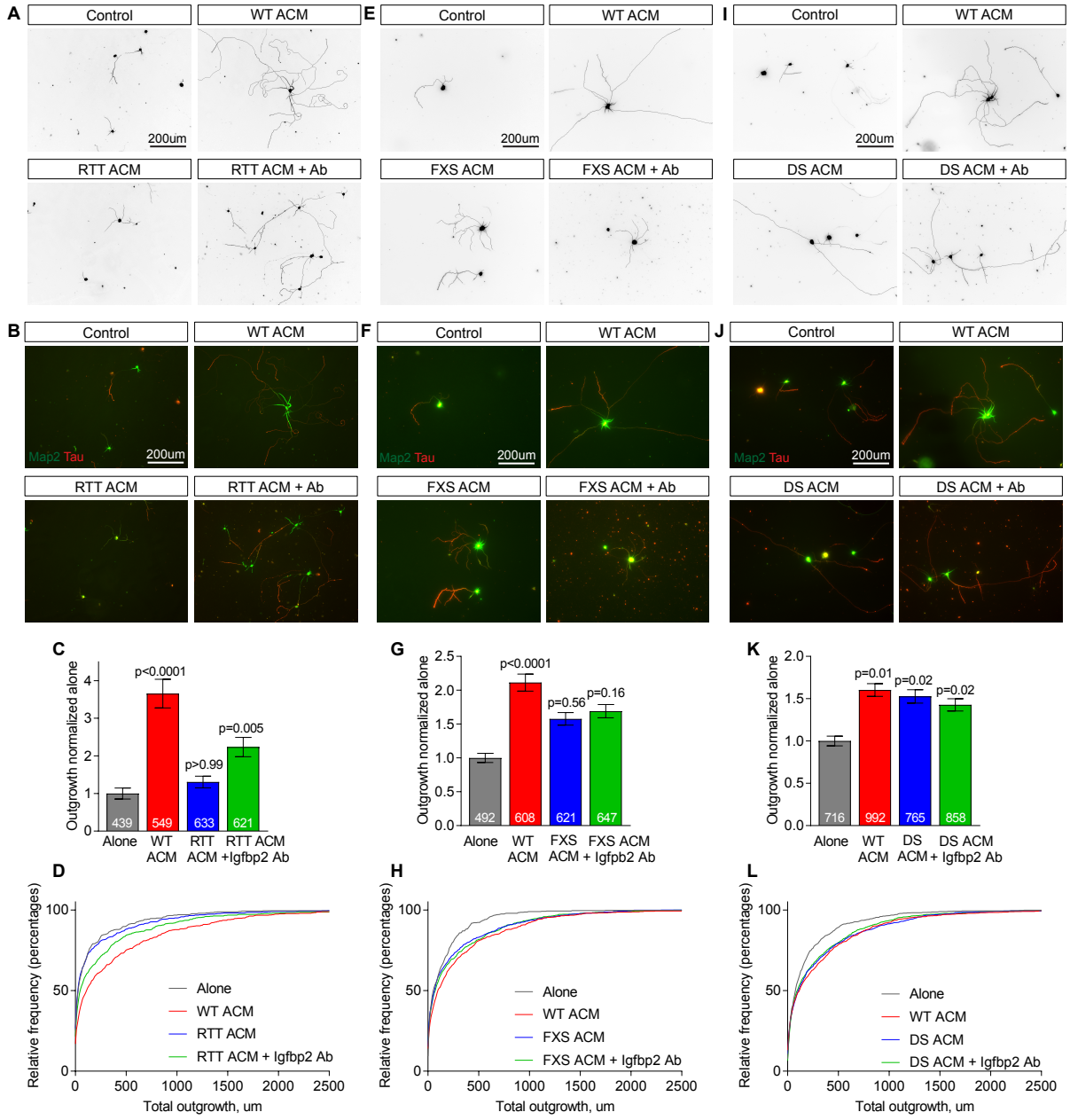

Figure 4.6: Application of IGFBP2-neutralizing antibody can prevent neurite outgrowth inhibition in RTT but not FXS ACM. **A-D.** The IGFBP2 blocking antibody partially overcomes the inhibitory effect of RTT ACM on WT neuron outgrowth. Neurons were stained for Map2 + Tau (**B**) and analyzed with MetaMorph Neurite Outgrowth module; example images in (**A**) are after processing. Bar graphs represent mean ± s.e.m. Number inside bar = number of neurons analyzed. Statistics by one-way ANOVA, p value compared to Alone condition. **E-H**. The addition of IGFBP2 neutralizing antibody to FXS ACM does not rescue neurite outgrowth. **I-L**. DS ACM does not inhibit neurite outgrowth in vitro and the addition of IGFBP2 neutralizing antibody has no effect. E-L data presented and analyzed in same manner as A-D.

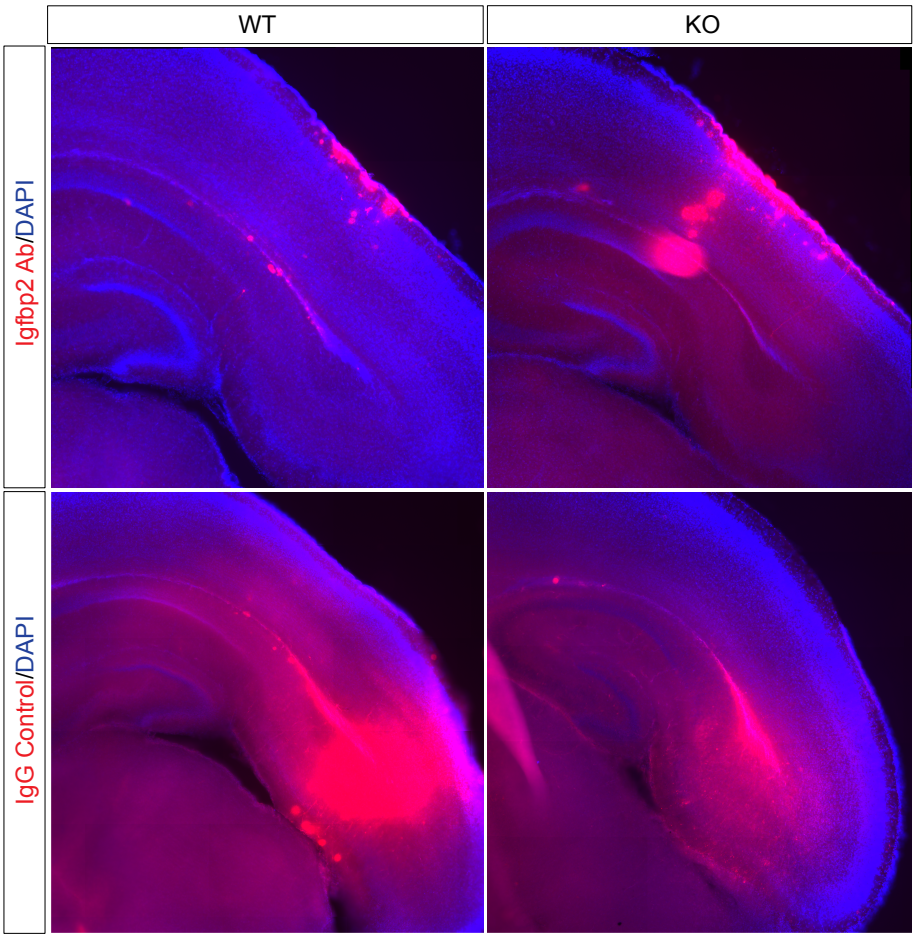

Figure 4.7: Demonstration of the spread of IGFBP2-neutralizing antibody in P7 cortex. 1 ug of labeled IGFBP2-neutralizing antibody or an IgG control antibody injected into the cortex at P2 roughly 3.4mm posterior to Bregma at -250 and -150 um spreads throughout the region and is still present at P7, five days after injection. This technique will be used to assess the potential for the use of IGFBP2-neutralizing antibody to rescue neuronal outgrowth defects in RTT in vivo.

References

Aldridge, G.M., Podrebarac, D.M., Greenough, W.T., Weiler, I.J., 2008. The use of total protein stains as loading controls: An alternative to high-abundance single-protein controls in semi-quantitative immunoblotting. J. Neurosci. Methods 172, 250–254. https://doi.org/10.1016/J.JNEUMETH.2008.05.003

Anlar, B., Oktem, F., Bakkaloglu, B., Haliloglu, M., Oguz, H., Unal, F., Pehlivanturk, B., Gokler, B., Ozbesler, C., Yordam, N., 2007. Urinary Epidermal and Insulin-Like Growth Factor Excretion in Autistic Children. Neuropediatrics 38, 151–153. https://doi.org/10.1055/s-2007-990282

Araujo, B.H.S., Kaid, C., De Souza, J.S., Gomes da Silva, S., Goulart, E., Caires, L.C.J., Musso, C.M., Torres, L.B., Ferrasa, A., Herai, R., Zatz, M., Okamoto, O.K., Cavalheiro, E.A., 2018. Down Syndrome iPSC-Derived Astrocytes Impair Neuronal Synaptogenesis and the mTOR Pathway In Vitro. Mol. Neurobiol. 55, 5962–5975. https://doi.org/10.1007/s12035-017-0818-6

Becker, L., Mito, T., Takashima, S., Onodera, K., 1991. Growth and development of the brain in Down syndrome. Prog. Clin. Biol. Res. 373, 133–52.

Becker, L.E., Armstrong, D.L., Chan, F., 1986. Dendritic atrophy in children with Down's syndrome. Ann. Neurol. 20, 520–526. https://doi.org/10.1002/ana.410200413

Berry-Kravis, E.M., Cubells, J., Kolevzon, A., Tartaglia, N., Frazier, J., Hatti, S., Erickson, C., Challman, T., Sanders, K., Treatwell-Deering, D., Innis, J., Needleman, H., Skinner, S., King, B., Hagerman, R., Findling, R., 2014. A Safety Study of NNZ-2566 in Patients With Fragile X Syndrome - Full Text View - ClinicalTrials.gov [WWW Document]. ClinicalTrials.gov. URL https://clinicaltrials.gov/ct2/show/NCT01894958 (accessed 7.6.19).

Bozdagi, O., Tavassoli, T., Buxbaum, J.D., 2013. Insulin-like growth factor-1 rescues synaptic and motor deficits in a mouse model of autism and developmental delay. Mol. Autism 4, 9. https://doi.org/10.1186/2040-2392-4-9

Butler, M.G., Dasouki, M.J., Zhou, X.-P., Talebizadeh, Z., Brown, M., Takahashi, T.N., Miles, J.H., Wang, C.H., Stratton, R., Pilarski, R., Eng, C., 2005. Subset of individuals with autism spectrum disorders and extreme macrocephaly associated with germline PTEN tumour suppressor gene mutations. J. Med. Genet. 42, 318–321. https://doi.org/10.1136/JMG.2004.024646

Chen, C., Jiang, P., Xue, H., Peterson, S.E., Tran, H.T., McCann, A.E., Parast, M.M., Li, S., Pleasure, D.E., Laurent, L.C., Loring, J.F., Liu, Y., Deng, W., 2014. Role of astroglia in

Down's syndrome revealed by patient-derived human-induced pluripotent stem cells. Nat. Commun. 5, 4430. https://doi.org/10.1038/ncomms5430

Costales, J., Kolevzon, A., 2016. The therapeutic potential of insulin-like growth factor-1 in central nervous system disorders. Neurosci. Biobehav. Rev. 63, 207–222. https://doi.org/10.1016/j.neubiorev.2016.01.001

Cronk, J.C.C., Derecki, N.C.C., Ji, E., Xu, Y., Lampano, A.E.E., Smirnov, I., Baker, W., Norris, G.T.T., Marin, I., Coddington, N., Wolf, Y., Turner, S.D.D., Aderem, A., Klibanov, A.L.L., Harris, T.H.H., Jung, S., Litvak, V., Kipnis, J., 2015. Methyl-CpG Binding Protein 2 Regulates Microglia and Macrophage Gene Expression in Response to Inflammatory Stimuli. Immunity 42, 679–691. https://doi.org/10.1016/j.immuni.2015.03.013

de Souza, J.S., Carromeu, C., Torres, L.B., Bruno, B.H., Cugola, F.R., Maciel, R.M.B., Muotri, A.R., Giannocco, G., 2017. IGF1 neuronal response in the absence of MECP2 is dependent on TRalpha 3. Hum. Mol. Genet. 26, 270–281. https://doi.org/10.1093/hmg/ddw384

Deacon, R.M.J., Glass, L., Snape, M., Hurley, M.J., Altimiras, F.J., Biekofsky, R.R., Cogram, P., 2015. NNZ-2566, a Novel Analog of (1–3) IGF-1, as a Potential Therapeutic Agent for Fragile X Syndrome. NeuroMolecular Med. 17, 71–82. https://doi.org/10.1007/s12017-015-8341-2

Dyer, A.H., Vahdatpour, C., Sanfeliu, A., Tropea, D., 2016. The role of Insulin-Like Growth Factor 1 (IGF-1) in brain development, maturation and neuroplasticity. Neuroscience 325, 89–99. https://doi.org/10.1016/j.neuroscience.2016.03.056

Forbes, B.E., McCarthy, P., Norton, R.S., 2012. Insulin-like growth factor binding proteins: A structural perspective. Front. Endocrinol. (Lausanne). 3, 1–13. https://doi.org/10.3389/fendo.2012.00038

Goffin, A., Hoefsloot, L.H., Bosgoed, E., Swillen, A., Fryns, J.-P., 2001. PTEN mutation in a family with Cowden syndrome and autism. Am. J. Med. Genet. 105, 521–524. https://doi.org/10.1002/ajmg.1477

Gunnell, D., Miller, L.L., Rogers, I., Holly, J.M.P., ALSPAC Study Team, 2005. Association of Insulin-like Growth Factor I and Insulin-like Growth Factor-Binding Protein-3 With Intelligence Quotient Among 8- to 9-Year-Old Children in the Avon Longitudinal Study of Parents and Children. Pediatrics 116, e681–e686. https://doi.org/10.1542/peds.2004-2390

Hemmings, B.A., Restuccia, D.F., 2012. PI3K-PKB/Akt pathway. Cold Spring Harb. Perspect. Biol. 4, a011189. https://doi.org/10.1101/cshperspect.a011189

Hoeflich, A., 1999. Overexpression of Insulin-Like Growth Factor-Binding Protein-2 in Transgenic Mice Reduces Postnatal Body Weight Gain. Endocrinology 140, 5488–5496. https://doi.org/10.1210/en.140.12.5488

Hu, H., Qin, Y., Bochorishvili, G., Zhu, Y., van Aelst, L., Zhu, J.J., 2008. Ras signaling mechanisms underlying impaired GluR1-dependent plasticity associated with fragile X syndrome. J. Neurosci. 28, 7847–7862. https://doi.org/10.1523/JNEUROSCI.1496-08.2008

Hwa, V., Oh, Y., Rosenfeld, R.G., 1999. The Insulin-Like Growth Factor-Binding Protein (IGFBP) Superfamily [1]. Endocr. Rev. 20, 761–787. https://doi.org/10.1210/edrv.20.6.0382

Itoh, M., Ide, S., Takashima, S., Kudo, S., Nomura, Y., Segawa, M., Kubota, T., Mori, H., Tanaka, S., Horie, H., Tanabe, Y., Goto, Y., 2007. Methyl CpG-binding protein 2 (a mutation of which causes Rett syndrome) directly regulates insulin-like growth factor binding protein 3 in mouse and human brains. J. Neuropathol. Exp. Neurol. 66, 117–123. https://doi.org/10.1097/nen.0b013e3180302078

Jones, J.I., Clemmons, D.R., 1995. Insulin-like growth factors and their binding proteins: biological actions. Endocr. Rev. 16, 3–34. https://doi.org/10.1210/er.16.1.3

Khwaja, O.S., Ho, E., Barnes, K. V., O'Leary, H.M., Pereira, L.M., Finkelstein, Y., Nelson, C.A., Vogel-Farley, V., DeGregorio, G., Holm, I.A., Khatwa, U., Kapur, K., Alexander, M.E., Finnegan, D.M., Cantwell, N.G., Walco, A.C., Rappaport, L., Gregas, M., Fichorova, R.N., Shannon, M.W., Sur, M., Kaufmann, W.E., 2014. Safety, pharmacokinetics, and preliminary assessment of efficacy of mecasermin (recombinant human IGF-1) for the treatment of Rett syndrome. Proc. Natl. Acad. Sci. 111, 4596–4601. https://doi.org/10.1073/pnas.1311141111

Kolevzon, A., Bush, L., Wang, A., Halpern, D., Frank, Y., Grodberg, D., Rapaport, R., Tavassoli, T., Chaplin, W., Soorya, L., Buxbaum, J.D., 2014. A pilot controlled trial of insulin-like growth factor-1 in children with Phelan-McDermid syndrome. Mol. Autism 5, 54. https://doi.org/10.1186/2040-2392-5-54

Kwon, C.H., Luikart, B.W., Powell, C.M., Zhou, J., Matheny, S.A., Zhang, W., Li, Y., Baker, S.J., Parada, L.F., 2006. Pten Regulates Neuronal Arborization and Social Interaction in Mice. Neuron 50, 377–388. https://doi.org/10.1016/j.neuron.2006.03.023

Lafon-Cazal, M., Adjali, O., Galéotti, N., Poncet, J., Jouin, P., Homburger, V., Bockaert, J., Marin, P., 2003. Proteomic analysis of astrocytic secretion in the mouse. Comparison with the cerebrospinal fluid proteome. J. Biol. Chem. 278, 24438–48. https://doi.org/10.1074/jbc.M211980200

Lee, W.H., Javedan, S., Bondy, C. a, 1992. Coordinate expression of insulin-like growth factor system components by neurons and neuroglia during retinal and cerebellar development. J. Neurosci. 12, 4737–44.

Liu, J.-P., Baker, J., Perkins, A.S., Robertson, E.J., Efstratiadis, A., 1993. Mice carrying null mutations of the genes encoding insulin-like growth factor I (Igf-1) and type 1 IGF receptor (Igf1r). Cell 75, 59–72.

Montagna, E., Dorostkar, M.M., Herms, J., 2017. The Role of APP in Structural Spine Plasticity. Front. Mol. Neurosci. 10, 136. https://doi.org/10.3389/fnmol.2017.00136

O'Kushky, J., Ye, P., 2012. Neurodevelopmental effects of insulin-like growth factor signaling. Front Neuroendocrinol. 33, 230–251. https://doi.org/10.1016/j.yfrne.2012.06.002.Neurodevelopmental

Ocrant, I., Fay, C.T., Parmelee, J.T., 1990. Characterization of Insulin-Like Growth Factor Binding Proteins Produced in the Rat Central Nervous System*. Endocrinology 127, 1260–1267. https://doi.org/10.1210/endo-127-3-1260

Pini, G., Scusa, M.F., Benincasa, A., Bottiglioni, I., Congiu, L., Vadhatpour, C., Romanelli, A.M., Gemo, I., Puccetti, C., McNamara, R., O'Leary, S., Corvin, A., Gill, M., Tropea, D., 2014. Repeated insulin-like growth factor 1 treatment in a patient with rett syndrome: a single case study. Front. Pediatr. 2, 52. https://doi.org/10.3389/fped.2014.00052

Pini, G., Scusa, M.F., Congiu, L., Benincasa, A., Morescalchi, P., Bottiglioni, I., Di Marco, P., Borelli, P., Bonuccelli, U., Della-Chiesa, A., Prina-Mello, A., Tropea, D., 2012. IGF1 as a Potential Treatment for Rett Syndrome: Safety Assessment in Six Rett Patients. Autism Res. Treat. 2012, 679801. https://doi.org/10.1155/2012/679801

Reim, D., Schmeisser, M.J., 2017. Neurotrophic Factors in Mouse Models of Autism Spectrum Disorder: Focus on BDNF and IGF-1, in: Advances in Anatomy, Embryology, and Cell Biology. pp. 121–134. https://doi.org/10.1007/978-3-319-52498-6_7

Ricciardi, S., Boggio, E.M., Grosso, S., Lonetti, G., Forlani, G., Stefanelli, G., Calcagno, E., Morello, N., Landsberger, N., Biffo, S., Pizzorusso, T., Giustetto, M., Broccoli, V., 2011. Reduced AKT/mTOR signaling and protein synthesis dysregulation in a Rett syndrome animal model. Hum. Mol. Genet. 20, 1182–1196. https://doi.org/10.1093/hmg/ddq563

Riikonen, R., Makkonen, I., Vanhala, R., Turpeinen, U., Kuikka, J., Kokki, H., 2006. Cerebrospinal fluid insulin-like growth factors IGF-1 and IGF-2 in infantile autism. Dev. Med. Child Neurol. 48, 751. https://doi.org/10.1017/S0012162206001605

Russo, A.J., 2015. Decreased Phosphorylated Protein Kinase B (Akt) in Individuals with Autism

Associated with High Epidermal Growth Factor Receptor (EGFR) and Low Gamma-Aminobutyric Acid (GABA). Biomark. Insights 10, BMI.S21946. https://doi.org/10.4137/BMI.S21946

Sheikh, A.M., Malik, M., Wen, G., Chauhan, A., Chauhan, V., Gong, C.X., Liu, F., Brown, W.T., Li, X., 2010. BDNF-Akt-Bcl2 antiapoptotic signaling pathway is compromised in the brain of autistic subjects. J. Neurosci. Res. 88, 2641–2647. https://doi.org/10.1002/jnr.22416

Singh, S.K., Stogsdill, J.A., Pulimood, N.S., Dingsdale, H., Kim, Y.H., Pilaz, L.-J., Kim, I.H., Manhaes, A.C., Rodrigues, W.S., Pamukcu, A., Enustun, E., Ertuz, Z., Scheiffele, P., Soderling, S.H., Silver, D.L., Ji, R.-R., Medina, A.E., Eroglu, C., 2016. Astrocytes Assemble Thalamocortical Synapses by Bridging NRX1α and NL1 via Hevin. Cell 164, 183–196. https://doi.org/10.1016/J.CELL.2015.11.034

Siwanowicz, I., Popowicz, G.M., Wisniewska, M., Huber, R., Kuenkele, K.P., Lang, K., Engh, R.A., Holak, T.A., 2005. Structural basis for the regulation of insulin-like growth factors by IGF binding proteins. Structure 13, 155–167. https://doi.org/10.1016/j.str.2004.11.009

Thacker, J.S., Yeung, D.H., Staines, W.R., Mielke, J.G., 2016. Total protein or high-abundance protein: Which offers the best loading control for Western blotting? Anal. Biochem. 496, 76–78. https://doi.org/10.1016/j.ab.2015.11.022

Tropea, D., Giacometti, E., Wilson, N.R., Beard, C., McCurry, C., Fu, D.D., Flannery, R., Jaenisch, R., Sur, M., Holm, I.A., Khatwa, U., Kapur, K., Alexander, M.E., Finnegan, D.M., Cantwell, N.G., Walco, A.C., Rappaport, L., Gregas, M., Fichorova, R.N., Shannon, M.W., Sur, M., Kaufmann, W.E., 2009. Partial reversal of Rett Syndrome-like symptoms in MeCP2 mutant mice. Proc. Natl. Acad. Sci. U. S. A. 106, 2029–2034. https://doi.org/10.1073/pnas.0812394106

Ueno, Y., Enokizono, T., Fukushima, H., Ohto, T., Imagawa, K., Tanaka, M., Sakai, A., Suzuki, H., Uehara, T., Takenouchi, T., Kosaki, K., Takada, H., 2019. A novel missense PTEN mutation identified in a patient with macrocephaly and developmental delay. Hum. Genome Var. 6, 25. https://doi.org/10.1038/s41439-019-0056-8

Vahdatpour, C., Dyer, A.H., Tropea, D., 2016. Insulin-Like Growth Factor 1 and Related Compounds in the Treatment of Childhood-Onset Neurodevelopmental Disorders. Front. Neurosci. 10, 450. https://doi.org/10.3389/fnins.2016.00450

Vanhala, R., Turpeinen, U., Riikonen, R., 2007. Low levels of insulin-like growth factor-I in cerebrospinal fluid in children with autism. Dev. Med. Child Neurol. 43, 614–616. https://doi.org/10.1111/j.1469-8749.2001.tb00244.x

Williams, E.C., Zhong, X., Mohamed, A., Li, R., Liu, Y., Dong, Q., Ananiev, G.E., Choongmok,

J.C., Lin, B.R., Lu, J., Chiao, C., Cherney, R., Li, H., Zhang, S.-C.C., Chang, Q., Mok, J.C.C., Lin, B.R., Lu, J., Chiao, C., Cherney, R., Li, H., Zhang, S.-C.C., Chang, Q., 2014. Mutant astrocytes differentiated from Rett syndrome patients-specific iPSCs have adverse effects on wildtype neurons. Hum. Mol. Genet. 23, 2968–2980. https://doi.org/10.1093/hmg/ddu008

Wise, T.L., 2017. Changes in insulin-like growth factor signaling alter phenotypes in Fragile X Mice. Genes, Brain Behav. 16, 241–249. https://doi.org/10.1111/gbb.12340

Wrigley, S., Arafa, D., Tropea, D., 2017. Insulin-Like Growth Factor 1: At the Crossroads of Brain Development and Aging. Front. Cell. Neurosci. 11, 1–15. https://doi.org/10.3389/fncel.2017.00014

Yasui, D.H., Xu, H., Dunaway, K.W., LaSalle, J.M., Jin, L.-W., Maezawa, I., 2013. MeCP2 modulates gene expression pathways in astrocytes. Mol. Autism 4, 3. https://doi.org/10.1186/2040-2392-4-3

Zhang, Y., Chen, K., Sloan, S.A., Bennett, M.L., Scholze, A.R., O'Keeffe, S., Phatnani, H.P., Guarnieri, P., Caneda, C., Ruderisch, N., Deng, S., Liddelow, S.A., Zhang, C., Daneman, R., Maniatis, T., Barres, B.A., Wu, J.Q., 2014. An RNA-sequencing transcriptome and splicing database of glia, neurons, and vascular cells of the cerebral cortex. J. Neurosci. 34, 11929–11947. https://doi.org/10.1523/JNEUROSCI.1860-14.2014

Chapter 5: Increased secretion of BMP6 leads to functional deficits in *Fmr1* KO astrocytes which can be rescued by treating *Fmr1* KO astrocytes with the BMP antagonist noggin

Formatting note: every chapter in this dissertation has its own, self-contained introduction and discussion. The introduction and conclusion chapters are intended to broadly frame and contextualize the dissertation. All methods are confined to a single methods chapter at the end of the dissertation.

Introduction

The successful isolation and culturing of P7 cortical astrocytes from wild-type (WT) and neurodevelopmental disordered (ND) brains has allowed us to identify a number of protein factors that show differential secretion in Rett Syndrome (RTT), Fragile X Syndrome (FXS), and Down Syndrome (DS) astrocytes compared to WT. This allowed us to identify insulin-like growth factor binding protein 2 (IGFBP2) as a protein that plays a role in the pathology of RTT in vitro, discussed in chapter 4. We have also identified bone morphogenetic protein 6 (BMP6) as a protein that shows dramatically increased secretion in all 3 NDs compared to WT astrocyte conditioned media (ACM). Unlike IGFBP2, BMP6 is extremely low abundance in astrocyte conditioned media, present at only about 0.005% of total spectra counted in WT ACM (Supplemental Table 1). However, as other research and the mass spectrometry analysis described in this dissertation demonstrate, potent growth factors do not need to be expressed at high levels to have significant effects on neuronal development (Allen et al., 2012); (Figure 3.1). Furthermore, BMP6 is not known to be highly expressed by astrocytes; instead it shows high levels of expression in neurons and oligodendrocyte precursor cells (OPCs) at postnatal day 7 (P7) in vivo (Zhang et al., 2014). Thus, the increased secretion of BMP6 in NDs (0.011% of all spectra counted in RTT ACM; 0.012% in FXS ACM; 0.019% in DS ACM) represents an aberrant phenotype of these astrocytes in vitro.

BMPs are members of the transforming growth factor β superfamily (TGFβ), made up of a number of cell regulatory proteins including BMPs, TGFβ, growth differentiation factors (GDFs), and glial cell-derived neurotrophic factor (GDNF) (Attisano and Wrana, 2002; Kingsley, 1994). BMPs act by binding to heterotetrameric complexes of serine/threonine kinase receptors, known as BMP receptor type I (BMPR1) and BMP receptor type 2 (BMPR2). BMP binding to the receptor complex activates BMPR1, which then phosphorylates SMAD1, SMAD5, and SMAD8. Once

activated, these SMADs form a complex with SMAD4 and translocate to the nucleus (Blanco Calvo et al., 2009; Miyazono et al., 2010), leading to gene expression changes that include an increase in the expression of *Id* genes (Hollnagel et al., 1999) and a reduction in the expression of epidermal growth factor receptor (EGFR) (Lillien and Raphael, 2000). This pathway influences a number of important cellular activities, including mitogenesis, cell differentiation, and cell survival (Figure 5.1).

BMP6 presents an intriguing candidate due to the evidence that BMPs play important roles in the brain during development, including in synaptogenesis, and in particular, in the maturity and function of astrocytes. Spatial and temporal expression patterns of TGFβ family members, including BMPs, implicate these proteins in a number of developmental processes, including neuronal and astroglial differentiation and neuronal growth and survival (Ebendal et al., 1998). BMP7, also known as osteogenic protein-1 or OP-1, enhances dendritic growth in neurons in vitro (Guo et al., 1998; Le Roux et al., 1999; Lein et al., 1995; Withers et al., 2000). There is also evidence that glial-derived BMPs and BMP antagonists such as noggin and follistatin regulate dendritic outgrowth (Lein et al., 2002).

BMP signaling has been found to influence synapse formation and function in *Drosophila* as well as in mammals. In particular, work in *Drosophilia* has found that the BMP ortholog Glass bottom boat (Gbb) and Wishful thinking (Wit), an ortholog for human BMPR2, are required in motor neurons for normal synapse formation and transmission (Aberle et al., 2002; Marqués et al., 2002; McCabe et al., 2003). BMPs are believed to exert their effect in a retrograde fashion to enhance synapse size at active synapses by acting on the microtubule system in fly larvae to enhance synaptic strength (Ball et al., 2015; Berke et al., 2013). Dnlg4, the *Drosophila* ortholog of neuroligin 4, regulates synaptic growth through the upregulation of BMP signaling (Zhang et al., 2017). BMPs have also been found to support the development of large, fast synapses at the

calyx of Held in mice (Xiao et al., 2013) and to modify synaptic function by regulating the localization of ionotropic glutamate receptors in the human retina (Shen et al., 2004).

Perhaps more relevant to this dissertation, however, is that BMPs are implicated in the morphology and function of astrocytes. Like neurons, during development, astrocytes depend on critical signals from other brain cells to support their survival and growth in vivo (Barres et al., 1992; Foo et al., 2011; Krueger, 1996) but at this time, little is known about the identities of these proteins and the mechanisms by which they act. To begin answering this question, Scholze et. al. used immunopanning to isolate rat astrocytes, maintained them in vitro, and identified a number of trophic factors that support astrocyte survival (Scholze et al., 2014). BMPs were targeted specifically because BMP5 is a cytokine that is strongly expressed in pericytes, which had previously been found to support astrocyte survival (Daneman et al., 2010; Zhang et al., 2014). Their research determined that BMP5 is a robust trophic factor for astrocytes in vitro, similar to HB-EGF, which is used in our cultures to sustain astrocyte survival in a minimal media. Similarly, other members of the TGFβ family, including BMP6, were found to support astrocyte survival, and like BMP5, BMP6 is highly expressed in CNS pericytes. These pericytes are associated with the blood vessels of the brain, and most astrocytes contact blood vessels with endfeet by about P14 (Foo et al., 2011), thus placing these cells and their signals in the correct time and location for their interactions to support astrocyte development.

Additional examination determined that BMP5, BMP4, BMP6, or BMP10 treatment of P7 rat astrocytes promoted a more process-bearing phenotype with smaller, rounded cell bodies and shorter, highly-branched processes compared to untreated astrocytes (Scholze et al., 2014). BMP treatment also stimulated GFAP expression in cultured astrocytes and increased expression of astrocyte markers such as AQP4 and S100β, while Nestin expression was decreased, indicating that BMPs promote astrocyte maturation. BMP-treated astrocytes also cease to proliferate, and

have a downregulation of EGFR expression (Scholze et al., 2014). EGFR is important for numerous aspects of astrocyte development and displays high levels of expression early in development, with a dramatic reduction in expression as the brain ages (Cahoy et al., 2008; Doyle et al., 2008; Foo et al., 2011).

Interestingly, the transition from neurogenesis to astrogenesis is mediated by soluble factors including interleukin-6 (IL-6) and BMP4 (Miller and Gauthier, 2007). When working with human induced pluripotent stem cells (iPSCs), BMP4, along with ciliary neurotrophic factor (CNTF), is used to promote astrocyte differentiation in vitro (Chandrasekaran et al., 2016; Liu et al., 2018). All of this evidence supports a role for BMPs in regulating the maturation of astrocytes during development, which is likely to lead to functional effects.

Interestingly, little work has been done on the roles of BMPs in the three NDs we are studying, but there is some evidence that BMPs may play a role in autism spectrum disorder (ASD). BTBR T+Itpr3tf/J (BTBR) mice, a model of ASD, have been found to have lower levels of TGFβ expression in brain compared to C57Bl/6J counterparts (Ansari et al., 2017). A small study found an increase in BMP6 in the serum of adult male patients with Asperger's Syndrome but not females, compared to non-ASD counterparts (Steeb et al., 2014), while other work found an increase in EGFR levels in the plasma of children with ASD compared to non-ASD children (Russo, 2014).

There is additional evidence that BMP dysregulation may play a role in the pathology of FXS in particular. Kashima et. al. determined that BMPR2 is a target of fragile x mental retardation protein (FMRP). Loss of FMRP due to mutations in fragile x mental retardation 1 (*Fmr1*) enhances BMPR2 abundance, which acts via a noncanonical pathway to bind and activate LIM domain kinase 1 (LIMK1) to stimulate actin reorganization and subsequent neurite outgrowth and synapse formation in mice, and additional examination found increased levels of BMPR2 and LIMK1 activation in the prefrontal cortex of deceased FXS patients compared to control (Kashima et al.,

2016a). Reduction of BMPR2 levels in heterozygous *Bmpr2* mice (lacking one copy of *Bmpr2*) can partially ameliorate the spine deficits seen in FXS (Kashima et al., 2016a).

Another study determined that BMPs may play a role in RTT through their role in silencing *Mecp2* on the inactive X chromosome, by regulating the expression of X-inactive specific transcript (Xist). By targeting BMP modulation of Xist, it is possible to reactivate *Mecp2* on the inactive chromosome and restore MECP2 expression in cells (Sripathy et al., 2017). As there is evidence that restoration of MECP2 to individual cell types in the central nervous system can have profound effects on the physiological and behavioral phenotypes of the condition (Garg et al., 2017; Lioy et al., 2011; Ure et al., 2016), this makes an appealing therapeutic avenue. Additionally, secreted amyloid precursor protein α (sAPPα) has been associated with gliogenesis; treatment of human embryonic teratocarcinoma cells (NT-2/D1) with sAPPα induces an astrocyte-like phenotype, including expression of glial fibrillary acidic protein (GFAP), and an upregulation of BMP4 mRNA expression and increased pSMAD 1/5/8 (Kwak et al., 2014). As our ND astrocytes also showed increased secretion of APP, it is possible that the interactions between these proteins and their expression patterns may be playing a role in the downstream effects of altered protein secretion.

With some evidence that BMPs are dysregulated in NDs and work demonstrating that BMPs can have dramatic effects on astrocyte morphology and function, we examined the mass spectrometry and RNA sequencing data and found that in addition to increased BMP6 secretion in ND ACM compared to WT, FXS and DS mice also have increased expression of BMP target genes. Furthermore, FXS mice show an increase in the proportion of astrocytes expression pSMAD in the visual cortex at P7 compared to their WT littermates. We hypothesized that altered BMP signaling in NDs may be having a downstream effect on protein secretion and gene expression. To study this, we treated WT astrocytes with BMP6 in vitro and examined protein

changes in ACM using mass spectrometry and gene expression changes with RNA sequencing. Our results demonstrate that BMP6-treated astrocytes show altered morphology compared to untreated counterparts and partially resemble ND astrocytes in their protein and gene expression profiles, with nearly half of the proteins showing increased secretion in all NDs also showing increased secretion in BMP6-treated WT astrocytes. While FXS ACM leads to deficits of neuronal outgrowth compared to WT ACM in vitro, we also found that treating FXS astrocytes with noggin, a BMP antagonist, during their conditioning phase was sufficient to prevent these deficits, restoring outgrowth levels to those seen in WT ACM. These results indicate that altered BMP signaling in FXS astrocytes may be contributing to alterations in protein secretion that play a role in the pathology of the disorder.

Results

BMP signaling is upregulated in FXS and DS astrocytes in vitro.

Mismatched maturation of neurons and astrocytes has been proposed to contribute to NDs (Sloan and Barres, 2014). The addition of purified recombinant BMPs is sufficient to induce morphological maturation of astrocytes in vitro (Scholze et al., 2014) and BMP6 is increased in ACM from all 3 NDs vs WT (Figure 5.2A). We detected an increase in expression of BMP target genes, including *Id3*, *Id4*, and *Smad9*, in astrocytes isolated and cultured from FXS and DS mice compared to WT (Figure 5.2B), evidence that BMP signaling is enhanced. In the WT brain, pericytes and neurons are the predominant source of BMP6 (Figure 5.2C) (Zhang et al., 2014) suggesting increased BMP6 in ND astrocytes reflects an aberrant feature of these cells.

An increased proportion of astrocytes express pSMAD in the visual cortex of FXS KO mice compared to WT

To determine if the increased expression of BMP6 and BMP target genes in FXS astrocytes might play a role in vivo, we next examined expression of phosphorylated SMAD 1/5/8 (pSMAD) in the visual cortex of FXS and WT littermates at P7. pSMAD is a downstream target of BMPs and an increase in canonical BMP signaling would be reflected by an increase in pSMAD activation and translocation to the nucleus. To accomplish this, we crossed the FXS mouse line with the same Aldh1L1-eGFP expressing transgenic mouse line described in chapter 4, generating WT and FXS KO mice expressing GFP exclusively in astrocytes. Immunostaining for pSMAD in P7 cortex demonstrated an increase in the proportion of astrocytes positive for pSMAD expression, as determined by counting pSMAD labeled cells colocalized with Aldh1L1-GFP, normalized to the total number of astrocytes (n=3 mice per group, 3 ROIs across 3 sections per brain) (Figure 5.3 A,B). These results indicate an increase in BMP signaling in astrocytes in the visual cortex of FXS KO mice at P7 compared to WT counterparts, supporting the hypothesis that aberrant BMP signaling may be involved in the disorder.

WT astrocytes treated with BMP6 partially resemble ND astrocytes.

Given the increase in BMP6 protein present in ND ACM, and activation of BMP target genes in FXS astrocytes in vitro and in vivo, we asked whether increased BMP6 is acting on astrocytes to change their properties, and is upstream of the secretion differences in ND. WT astrocytes were treated with BMP6 at 10ng/ml (a level sufficient to induce changes in morphology, (Scholze et al., 2014)) during the conditioning period, and compared to untreated astrocytes from the same culture (N=6 cultures). Immunopanned astrocytes treated with BMP6 showed distinct changes in morphology, exhibiting thinner processes and appearing darker and more rounded than their untreated counterparts. BMP6 treated astrocytes expressed higher levels of AQP4 and GFAP compared to untreated astrocytes, supporting the evidence from Scholze et. al. that BMP signaling can alter the expression of astrocytic markers associated with maturation (Figure 5.4).

Using mass spectrometry and RNA sequencing, we determined that BMP6-treated astrocytes express all of the same astrocyte marker genes as their untreated counterparts; some genes were expressed at higher levels, including *Apoe, Aldoc,* and members of the *Slc* superfamily. Other genes were downregulated following BMP6 treatment, including *Grm3* and *Grm5*, showing a change in expression similar to that seen in FXS astrocytes. (Figure 5.5A). BMP6-treated and untreated astrocytes also showed similar secretion patterns and gene expression of synaptogenic factors, with a significant increase in the secretion of SPARCL1, and significant increases in the expression of GPC6 and SPARCL1 seen in BMP6-treated astrocytes (Figure 5.5B,C). Interestingly, BMP6-treated astrocytes secreted significantly more of complement component proteins associated with synapse elimination compared to untreated astrocytes, including C1sa, C1sb, C3, and C4b; except for C1sb, these increases in protein secretion were mirrored by corresponding increases in gene expression (Figure 5.5D,E). These results indicate that BMP6-treated astrocytes may have an inhibitory effect on synapse formation and stability.

Next, we examined the changes in protein secretion in BMP6 treated astrocytes compared to WT. BMP6 treatment induced a >50% increase in secretion of 128 proteins, and a significant increase in expression of 725 genes, with 45 of the proteins showing increased secretion also showing increased gene expression (Supplemental Tables 3-5) for a total overlap of 35.2% (Figure 5.4F,G). We also saw a >50% decrease in secretion of 272 proteins and a decrease in 538 genes, with only 18 of the proteins showing decreased secretion also showing decreased expression (Supplemental Tables 3-5), for an overlap of 6.6% (Figure 5.5H,I).

We then compared the proteins altered in secretion in all 3 NDs with those altered by BMP6 treatment, and remarkably found that 43.1% of the 88 proteins that are increased in ND ACM were also increased in BMP6-ACM (38 of 88), and 43.8% of the 14 downregulated proteins were also downregulated by BMP6 (14 of 32) (Supplemental Table 6, Figure 5.6A). Furthermore,

of the 6 genes that showed increased expression in all NDs compared to WT, 2 of the genes were also increased in BMP6-treated astrocytes, and the gene showing decreased expression in all NDs, *Serinc2,* also showed decreased expression following BMP6 treatment. This shows a strong overlap in the protein secretion and gene expression profiles of ND astrocytes and WT astrocytes treated with BMP6, indicating that BMP6 treatment induces similar changes in astrocytes as ND pathology. Interestingly, IGFBP2 and IGFBP5 both showed similar increases in secretion in BMP6-treated astrocytes and in NDs (Figure 5.6B), providing support for the possibility that BMP6 induces upstream changes in astrocyte function contributing to aberrant IGF signaling in NDs.

ACM from BMP6-treated WT astrocytes inhibits neuronal outgrowth, mimicking ND ACM.

Given the overlap in altered protein secretion induced in WT astrocytes by BMP6 treatment with ND ACM, we next asked if ACM from BMP6-treated WT astrocytes would be sufficient to inhibit outgrowth of WT cortical neurons. As in the IGFBP2 and ND experiments described in chapter 4, neurons were cultured for 48 hours alone, with WT ACM or BMP6-ACM, and process outgrowth analyzed. This demonstrated that BMP6-ACM is not able to enhance neurite outgrowth compared to neurons grown alone, whereas WT ACM can (Figure 5.7A-C; N=3 experiments, 3 coverslips per condition per experiment, at least 20 cells imaged per coverslip), strongly suggesting that aberrant BMP signaling in ND astrocytes is upstream of secretion alterations that lead to changes in astrocyte support of neuronal development.

Blocking BMP6 signaling in FXS astrocytes reverses the neuron-inhibitory effect of ACM.

We determined that ND astrocytes show increased activation of BMP target genes compared to WT astrocytes, that BMP6-ACM inhibits neurite outgrowth, and that there is strong overlap between secretion differences induced by BMP6 and ND. We therefore predicted that inhibiting BMP signaling in ND astrocytes would rescue the inhibitory effects of ND ACM on WT

neuron development. We chose to focus on FXS for these experiments, as BMP target genes showed increased expression in FXS and DS astrocytes, and by our analysis, DS ACM does not induce an inhibition of neurite outgrowth compared to WT. We treated FXS astrocytes during the conditioning period with the secreted BMP inhibitor noggin at 1 ug/ml as previously described (Blanco-Suarez et al., 2018) to bind BMP6 and prevent BMP-receptor interaction.

Intriguingly, blocking BMP signaling in FXS astrocytes during conditioning by treating with noggin allows FXS ACM to support neuronal outgrowth at a level similar to that of WT ACM (Figure 5.7D-F). We tested adding purified recombinant noggin to WT and FXS ACM at the time of plating cortical neurons and determined that noggin alone does not enhance neurite outgrowth, indicating that it is the effects of noggin on FXS astrocytes during conditioning that allows noggin-treated FXS ACM to support neuronal outgrowth compared to untreated FXS ACM (Figure 5.7G-I). These results support a critical role for BMP signaling in the pathology of FXS and provide a new target for the treatment of the condition.

Discussion

While BMPs are less studied in the context of ASD than IGF/PI3K/AKT signaling, our results present evidence for altered BMP signaling in NDs associated with autism. We determined that ND astrocytes secrete BMP6 at a much higher level than their WT counterparts, and hypothesized that this abnormal expression of BMP6 protein could be influencing astrocyte function and causing downstream effects on neuronal outgrowth. Treatment of WT astrocytes with BMP6 during their conditioning phase alters their morphology and leads to changes in protein secretion and gene expression that resemble those seen in ND astrocytes, providing support for the hypothesis that altered BMP signaling in ND astrocytes contributes to changes in protein secretion. BMP6-treated WT ACM is less sufficient for supporting neuronal outgrowth than untreated WT ACM, indicating that these alterations in protein secretion have functional effects.

Importantly, both IGFBP2 and IGFBP5 showed similar increases in secretion in BMP6-treated WT ACM and in ND ACM, indicating that these changes in BMP signaling may be upstream of the altered IGF signaling in NDs.

BMPs and their subsequent phosphorylation and activation of the SMAD complex can have a multitude of effects on cell differentiation and growth (Wang et al., 2014). There is evidence that BMPs can act via noncanonical pathways to influence synapse formation in FXS (Kashima et al., 2016b), but given that we saw an increase in the proportion of pSMAD-positive astrocytes in the cortex of FXS KO mice compared to their WT littermates, it is likely that enhanced BMP activity in FXS is leading to activation of the canonical pathway, possibly in addition to its noncanonical actions. Thus it may be that the increased levels of BMP6 in FXS lead to a cascade of changes in astrocytes that alter protein secretion and lead to deficits in neurite outgrowth. It is important to note that while BMP6 treatment of WT astrocytes led to increased secretion of IGFBP2 and 5, blocking IGFBP2 was capable of rescuing neurite outgrowth deficits only in RTT ACM in vitro, and not in FXS ACM. This indicates that while enhanced IGFBP2 may have an inhibitory effect on neurite outgrowth, in FXS, there are additional mechanisms at play. It may be that there are other protein secretion changes induced by BMP activity in FXS that cannot be overcome by blocking IGFBP2. It is also interesting to note that while DS astrocytes also showed increased secretion of BMP6 (and at very high levels indeed, nearly 4x that seen in WT ACM), by our measure, DS ACM does not induce a deficit in neurite outgrowth. This is particularly intriguing in light of evidence that there are many similarities in the pathology and underlying molecular mechanisms in FXS and DS, with dysregulation of amyloid precursor protein (APP) being central to both (De Toma et al., 2016; Faundez et al., 2018). As discussed in chapter 4, DS astrocytes also display increased secretion of IGF1, which may prevent the inhibitory effects of IGFBP2 in vitro, or it may enhance neurite outgrowth by signaling directly to neurons to overcome the inhibition of IGFBP2. However, DS astrocytes display many unique changes in protein secretion;

it is also possible that other alterations in DS astrocytes enable them to support neurite outgrowth despite the presence of inhibitory factors like IGFBP2 and BMP6, and additional research should explore which protein factors make DS astrocytes uniquely capable of supporting neurite outgrowth compared to RTT and FXS.

Whether or not increased BMP signaling in astrocytes in FXS has functional effects in vivo remains unknown. While we saw evidence for increased pSMAD activation in astrocytes in FXS KO cortex compared to WT, the scope of this dissertation did not address whether or not there were changes in BMP6 expression itself in the cortex, or whether such a change might have consequences for neurite outgrowth. It would be interesting to examine the effects of blocking BMP activity in FXS in vivo, to determine if it is capable of preventing the abnormalities in dendritic arborization associated with the disease. While application of the BMP antagonist noggin may be sufficient in vitro, noggin has a wide variety of effects in the developing brain; thus it would be best to use a BMP selective inhibitor, such as K02288 (Sigma Aldrich SML1307), to test this question. Importantly, K02288 targets BMPR1 to inhibit pSMAD activation and not BMPR2. If BMP6 is acting to influence dendritic outgrowth directly in neurons via the noncanonical BMPR2/LIMK1 pathway (Kashima et al., 2016b), blocking BMPR1 is not likely to have an effect; if BMP6 is acting via the canonical BMP signaling pathway, then blocking pSMAD activity with K02288 is likely to lead to an improvement in the dendritic arborization phenotype. However, K02288 is a non-selective BMP inhibitor, and would block all BMPs, not just BMP6; thus it would be difficult to determine if the actions of BMP6 are responsible for any changes seen in vivo without additional tools.

Additional research should also examine the role of BMPs in synapse formation in these NDs. There is evidence that BMP signaling is key for normal synapse formation (Xiao et al., 2013) and that deficits in BMP/BMPR2 activation contribute to abnormal synapse formation in FXS

(Kashima et al., 2016b). It may be that abnormal BMP activation in ND astrocytes contributes to the known deficits in spine morphology and synapse formation in these three disorders.

Acknowledgements

This chapter is, in part, in preparation for submission for publication. The dissertation author will be the first author of this publication, with Dr. Jolene Diedrich as second author and Dr. Nicola Allen as the senior author and principle investigator.

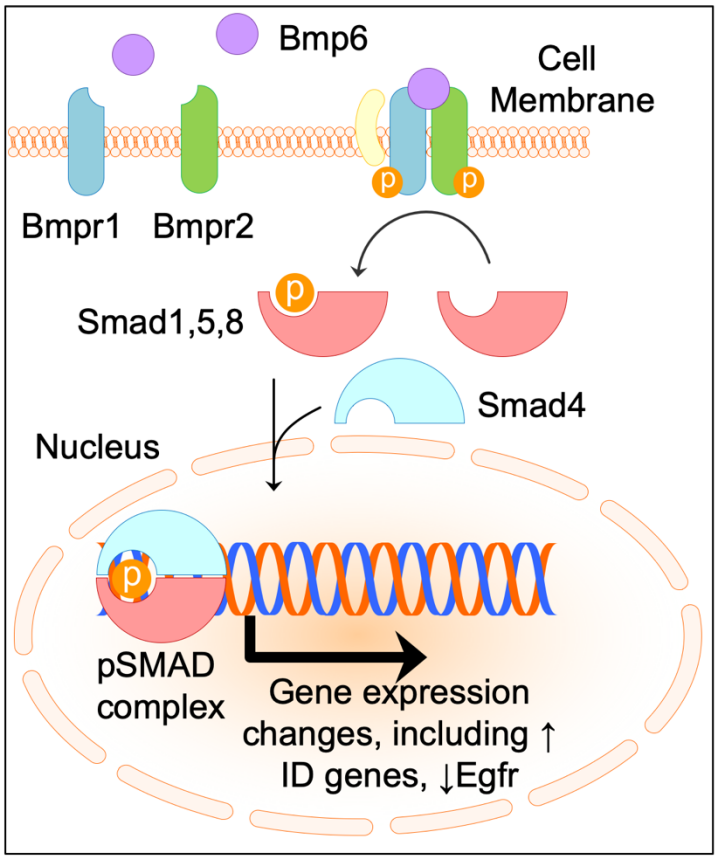

Figure 5.1: Schematic of canonical BMP signaling pathway. BMP6 binds to BMPR1 and BMPR2, which form a heteroterameric complex and activate to phosphorylate SMAD1/5/8. SMAD1/5/8 forms a complex with SMAD4 and translocates to the nucleus, leading to a cascade of gene expression changes that influence a variety of cellular activities, including mitogenesis, cell survival, and cell differentiation.

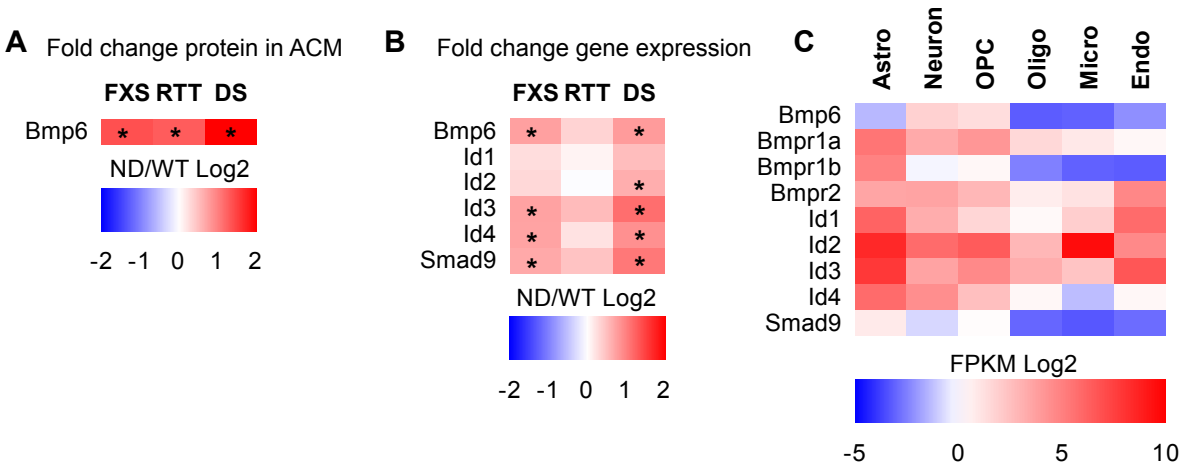

Figure 5.2: BMP6 is increased in ND ACM. A. Fold change in BMP6 protein in ND ACM compared to WT (log2); red upregulated and blue downregulated in ND**. B.** Fold change in gene expression for BMP family members in ND astrocytes compared to WT (log2). For proteomics, N=6 cultures per genotype, *p<0.05, abundance >0.01%, fold change between WT and ND ≥1.5. For RNASeq, N=6 cultures WT, RTT, FXS; 4 cultures DS. Significance for differential expression defined as adjusted p<0.05, calculated using Benjamini-Hochberg's procedure for multiple comparisons, FPKM>1 and fold change between ND and WT >1.5, comparing each ND and WT after adjustment for multiple testing. **C.** Relative expression of BMP family members in purified cell types in the cortex, shows enrichment for BMP target genes in astrocytes (Zhang et al., 2014).

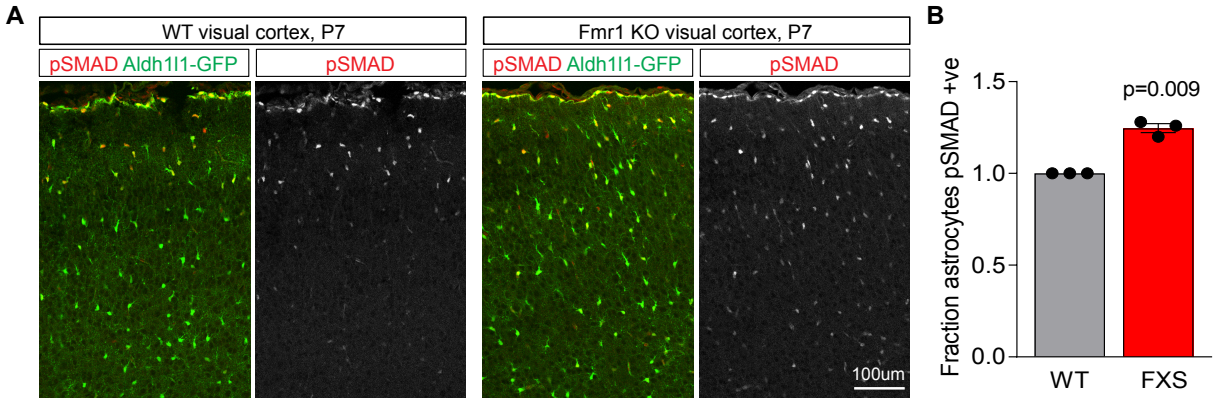

Figure 5.3: There is an increase in the proportion of pSMAD+ astrocytes in FXS KO visual cortex. A. Example images of astrocytes (green) and pSMAD expression (red) by immunohistochemical staining. **B**. Quantification of the proportion of astrocytes that are positive for pSMAD in the visual cortex in FXS and WT littermates. Images analyzed using the ImageJ Cell Counter plugin, N=3 animals per condition, 3 ROIs counted per animal, normalized to WT.

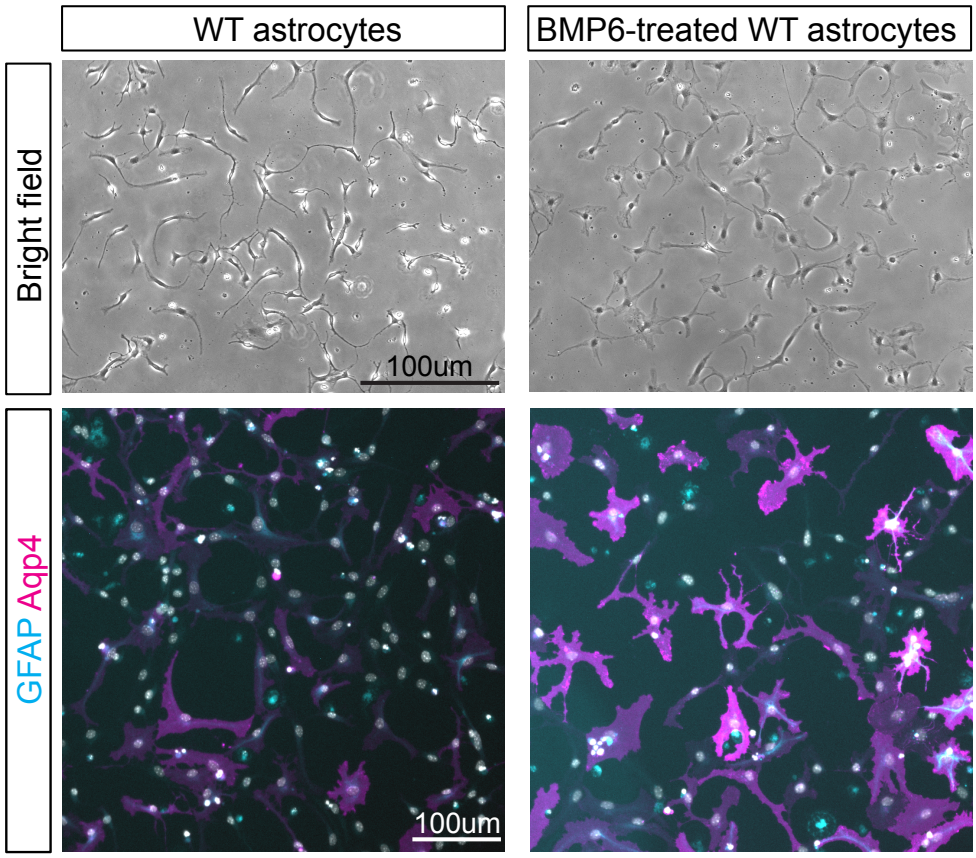

Figure 5.4: BMP6-treated astrocytes show changes in morphology and expression of astrocyte markers. Under brightfield, BMP6-treated astrocytes appear darker and rounder than their untreated counterparts, with thinner, more branched processes. By immunohistochemical staining, BMP6-treated astrocytes show increased expression of both GFAP (cyan) and AQP4 (magenta). Example images shown, experiment repeated 3 times with same effect.

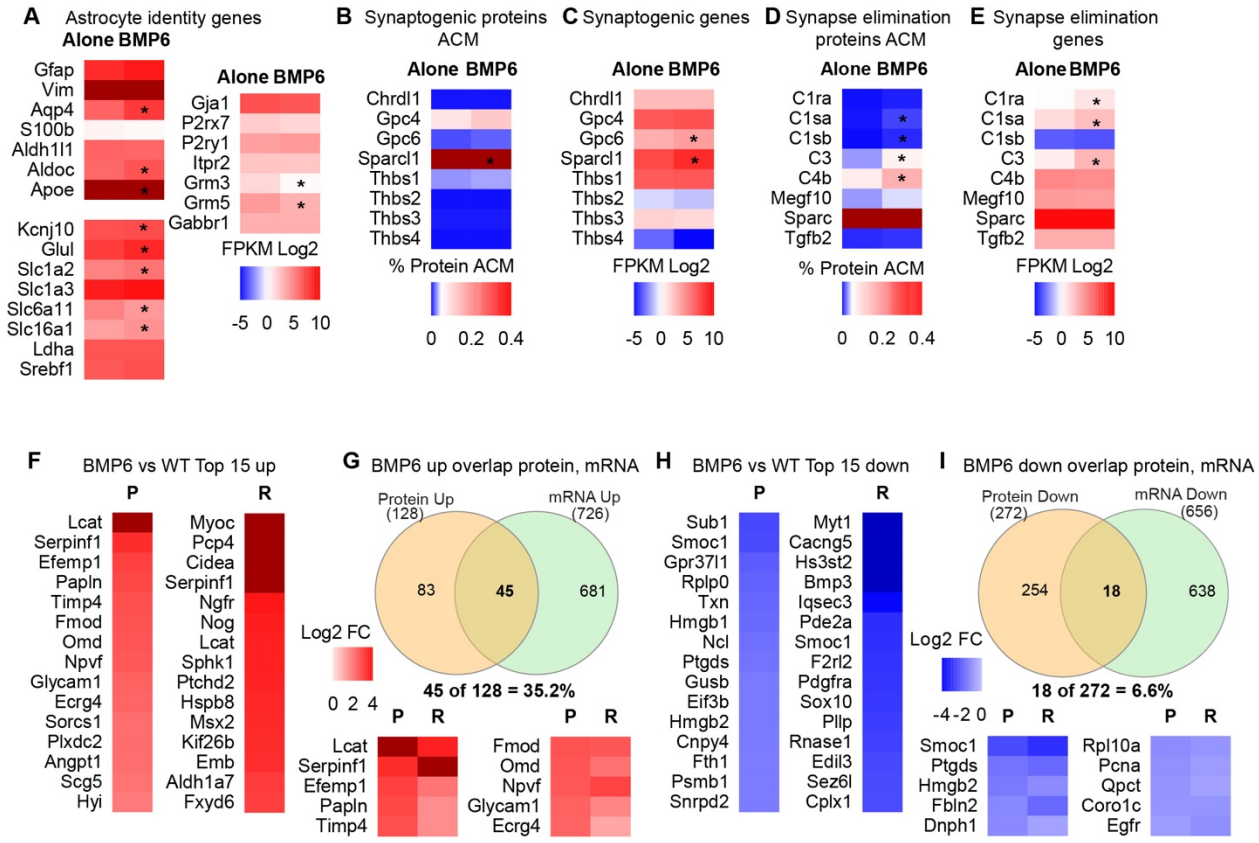

Figure 5.5: Characterization of the protein secretion and gene expression profiles of BMP6-treated astrocytes compared to WT. A. Heatmap showing differences between BMP6-treated and untreated astrocytes expression of astrocyte identity and function markers. **B-E.** Heatmap of the abundance of secreted synaptogenic proteins in BMP6-treated and untreated ACM (**B**) and expression of synaptogenic genes (**C**), as well as the abundance of synapse eliminating proteins in ACM (**D**) and corresponding expression of synapse elimination genes (**E**). **F, H.** Heatmaps of top proteins and mRNA increased (**F**) or decreased (**H)** between BMP6-treated and untreated WT ACM and astrocytes. **G, I**. Venn diagrams showing the overlap between proteins and genes showing increased expression (**G**) or decreased expression (**I**) in BMP6-treated and untreated WT ACM and astrocytes. N=6 cultures, with half of each culture being treated with BMP6 and the other half left untreated, for both mass spectrometry and RNA Sequencing. For proteomics, *p<0.05, abundance >0.01%, fold change between WT and BMP6 ≥1.5. For RNASeq, significance for differential expression defined as adjusted p<0.05, calculated using Benjamini-Hochberg's procedure for multiple comparisons, FPKM>1 and fold change between BMP6 and WT >1.5, comparing BMP6 and WT after adjustment for multiple testing.

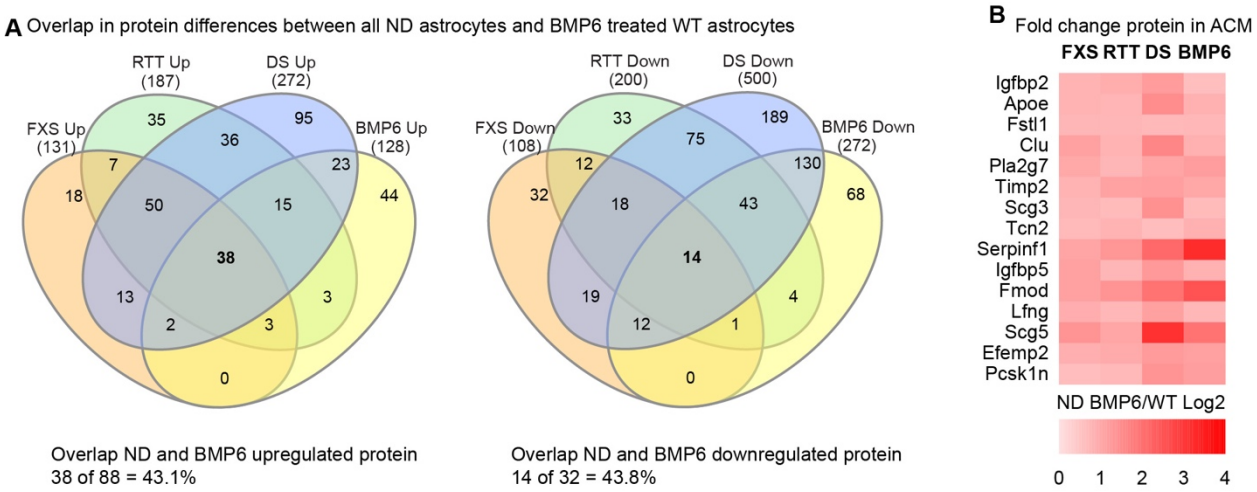

Figure 5.6: **BMP6-treated astrocytes show altered protein secretion compared to untreated WT astrocytes and partially resemble ND astrocytes**. **A,B.** Overlap in protein secretion differences vs WT for all ND astrocytes and BMP6-treated astrocytes, shows nearly half the proteins are increased in secretion in all conditions (38 proteins total), while roughly half are also decreased in secretion in all conditions (14 proteins total). Venn diagrams showing number of proteins increased and decreased between WT, all ND, and BMP6-treated astrocytes (**A**) and corresponding heatmap of proteins increased between all ND and BMP6-treated astrocytes vs. WT (**B**), ranked by abundance in FXS ACM, shown as fold-change vs WT (log2). N=6 cultures each WT, FXS, RTT, DS, plus 6 cultures +/-BMP6.

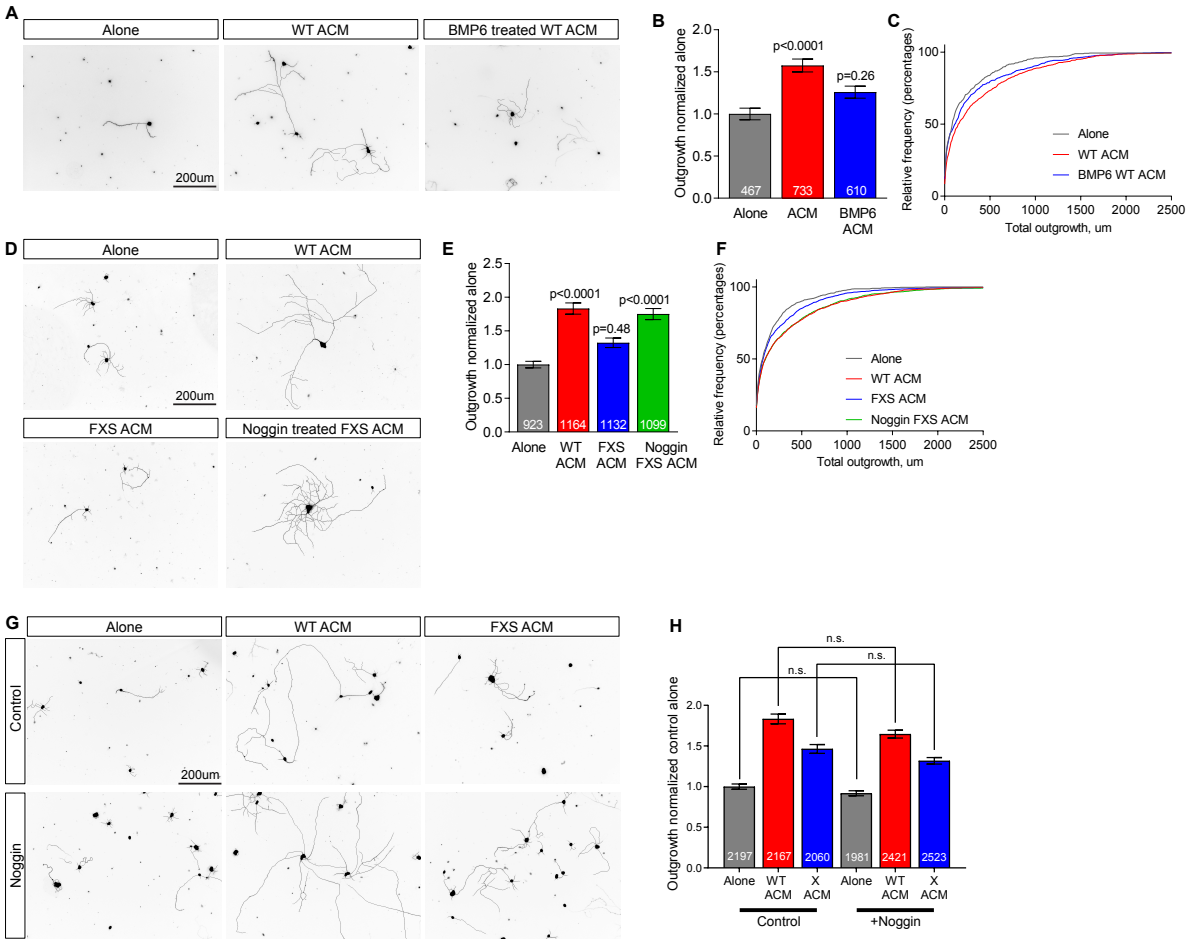

Figure 5.7: ACM from astrocytes treated with BMP6 inhibits WT neurite outgrowth, while blocking BMP6 in FXS ACM rescues deficits in neurite outgrowth. **A.** Example images of neurons alone, with WT ACM, and with BMP6-treated ACM, immunostained with Map2 and Tau, as processed by the MetaMorph Neurite Outgrowth module. **B, C**. Quantification of total neurite outgrowth (MAP2 + tau) demonstrates that astrocytes treated with BMP6 are less capable of supporting neurite outgrowth than their untreated counterparts. **D.** Example images of neurons alone, with WT ACM, with FXS ACM, and with noggin-treated FXS ACM, immunostained with Map2 and Tau, as processed by the MetaMorph Neurite Outgrowth module. **E, F**. Quantification of total neurite outgrowth (MAP2 + tau) demonstrates that application of noggin is sufficient to rescue the outgrowth deficits induced by FXS ACM in vitro. **G.** Example images of neurons alone, with WT ACM, and with FXS ACM, +/- noggin at the time of plating, immunostained with Map2 and Tau, as processed by the MetaMorph Neurite Outgrowth module. **H**. Quantification of total neurite outgrowth (MAP2 + tau) demonstrates that noggin alone does not rescue FXS-induced outgrowth deficits. N=3 experiments, bar graph represents mean ± s.e.m. Number inside bar = number of neurons analyzed. Statistics by one-way ANOVA, p value marked compared to Alone condition.

References

Aberle, H., Haghighi, A.P., Fetter, R.D., McCabe, B.D., Magalhães, T.R., Goodman, C.S., 2002. Wishful thinking encodes a BMP type II receptor that regulates synaptic growth in Drosophila. Neuron 33, 545–558. https://doi.org/10.1016/S0896-6273(02)00589-5

Allen, N.J., Bennett, M.L., Foo, L.C., Wang, G.X., Chakraborty, C., Smith, S.J., Barres, B. a., 2012. Astrocyte glypicans 4 and 6 promote formation of excitatory synapses via GluA1 AMPA receptors. Nature 486, 410–414. https://doi.org/10.1038/nature11059

Ansari, M.A., Attia, S.M., Nadeem, A., Bakheet, S.A., Raish, M., Khan, T.H., Al-Shabanah, O.A., Ahmad, S.F., 2017. Activation of adenosine A2A receptor signaling regulates the expression of cytokines associated with immunologic dysfunction in BTBR T+ Itpr3tf/J mice, Molecular and Cellular Neuroscience. Elsevier Inc. https://doi.org/10.1016/j.mcn.2017.04.012

Attisano, L., Wrana, J.L., 2002. Signal transduction by the TGF-β superfamily. Science (80-.). 296, 1646–1647. https://doi.org/10.1126/science.1071809

Ball, R.W., Peled, E., Guerrero, G., Isacoff, E.Y., 2015. BMP signaling and microtubule organization regulate synaptic strength. Neuroscience 291, 155–166. https://doi.org/10.1016/j.neuroscience.2015.01.069. BMP

Barres, B.A., Hart, I.K., Coles, H.S.R., Burne, J.F., Voyvodic, J.T., Richardson, W.D., Raff, M.C., 1992. Cell death and control of cell survival in the oligodendrocyte lineage. Cell 70, 31–46. https://doi.org/10.1016/0092-8674(92)90531-G

Berke, B., Wittnam, J., McNeill, E., Van Vactor, D.L., Keshishian, H., 2013. Retrograde BMP Signaling at the Synapse: A Permissive Signal for Synapse Maturation and Activity-Dependent Plasticity. J. Neurosci. 33, 17937–17950. https://doi.org/10.1523/jneurosci.6075-11.2013

Blanco-Suarez, E., Liu, T.F., Kopelevich, A., Allen, N.J., 2018. Astrocyte-Secreted Chordin-like 1 Drives Synapse Maturation and Limits Plasticity by Increasing Synaptic GluA2 AMPA Receptors. Neuron 1–17. https://doi.org/10.1016/j.neuron.2018.09.043

Blanco Calvo, M., Bolós Fernández, V., Medina Villaamil, V., Aparicio Gallego, G., Díaz Prado, S., Grande Pulido, E., 2009. Biology of BMP signalling and cancer. Clin. Transl. Oncol. 11, 126–37.

Cahoy, J.D., Emery, B., Kaushal, A., Foo, L.C., Zamanian, J.L., Christopherson, K.S., Xing, Y., Lubischer, J.L., Krieg, P. a, Krupenko, S. a, Thompson, W.J., Barres, B. a, 2008. A transcriptome database for astrocytes, neurons, and oligodendrocytes: a new resource for understanding brain development and function. J. Neurosci. 28, 264–278.

https://doi.org/10.1523/JNEUROSCI.4178-07.2008

Chandrasekaran, A., Avci, H.X., Leist, M., Kobolák, J., Dinnyés, A., 2016. Astrocyte Differentiation of Human Pluripotent Stem Cells: New Tools for Neurological Disorder Research. Front. Cell. Neurosci. 10, 215. https://doi.org/10.3389/fncel.2016.00215

Daneman, R., Zhou, L., Agalliu, D., Cahoy, J.D., Kaushal, A., Barres, B.A., 2010. The Mouse Blood-Brain Barrier Transcriptome: A New Resource for Understanding the Development and Function of Brain Endothelial Cells. PLoS One 5, e13741. https://doi.org/10.1371/journal.pone.0013741

De Toma, I., Manubens-Gil, L., Ossowski, S., Dierssen, M., 2016. Where Environment Meets Cognition: A Focus on Two Developmental Intellectual Disability Disorders. Neural Plast. 2016, 4235898. https://doi.org/10.1155/2016/4235898

Doyle, J.P., Dougherty, J.D., Heiman, M., Schmidt, E.F., Stevens, T.R., Ma, G., Bupp, S., Shrestha, P., Shah, R.D., Doughty, M.L., Gong, S., Greengard, P., Heintz, N., 2008. Application of a Translational Profiling Approach for the Comparative Analysis of CNS Cell Types. Cell 135, 749–762. https://doi.org/10.1016/J.CELL.2008.10.029

Ebendal, T., Bengtsson, H., Soderstrom, S., 1998. Bone morphogenetic proteins and their receptors: potential functions in the brain. [Review] [54 refs]. J. Neurosci. Res. 51, 139–146.

Faundez, V., De Toma, I., Bardoni, B., Bartesaghi, R., Nizetic, D., de la Torre, R., Cohen Kadosh, R., Herault, Y., Dierssen, M., Potier, M.-C., Antonarakis, S., Bartesaghi, R., Contestabile, A., Coppus, T., De Deyn, P., Dekker, A., Delabar, J.-M., Dierssen, M., Fisher, E., Hérault, Y., Martinez-Cué, C., Potier, M.-C., Strydom, A., 2018. Translating molecular advances in Down syndrome and Fragile X syndrome into therapies. Eur. Neuropsychopharmacol. 28, 675–690. https://doi.org/10.1016/J.EURONEURO.2018.03.006

Foo, L.C., Allen, N.J., Bushong, E.A., Ventura, P.B., Chung, W.S., Zhou, L., Cahoy, J.D., Daneman, R., Zong, H., Ellisman, M.H., Barres, B.A., 2011. Development of a method for the purification and culture of rodent astrocytes. Neuron 71, 799–811. https://doi.org/10.1016/j.neuron.2011.07.022

Garg, S., Brooks, A., Burns, A., Burkitt-Wright, E., Kerr, B., Huson, S., Emsley, R., Green, J., 2017. Autism spectrum disorder and other neurobehavioural comorbidities in rare disorders of the Ras/MAPK pathway. Dev. Med. Child Neurol. 59, 544–549. https://doi.org/10.1111/dmcn.13394

Guo, X., Rueger, D., Higgins, D., 1998. Osteogenic protein-1 and related bone morphogenetic proteins regulate dendritic growth and the expression of microtubule-associated protein-

2 in rat sympathetic neurons. Neurosci. Lett. 245, 131–134. https://doi.org/10.1016/S0304-3940(98)00192-X

Hollnagel, A., Oehlmann, V., Heymer, J., Rüther, U., Nordheim, A., 1999. Id Genes Are Direct Targets of Bone Morphogenetic Protein Induction in Embryonic Stem Cells. J. Biol. Chem. 274, 19838–19845. https://doi.org/10.1074/jbc.274.28.19838

Kashima, R., Roy, S., Ascano, M., Martinez-cerdeno, V., Ariza-torres, J., Kim, S., Louie, J., Lu, Y., Leyton, P., Bloch, K.D., Kornberg, T.B., Hagerman, P.J., Hagerman, R., Lagna, G., Hata, A., 2016a. Augmented noncanonical BMP type II receptor signaling mediates the synaptic abnormality of fragile X syndrome 9, 1–13.

Kashima, R., Roy, S., Ascano, M., Martinez-Cerdeno, V., Ariza-Torres, J., Kim, S., Louie, J., Lu, Y., Leyton, P., Bloch, K.D., Kornberg, T.B., Hagerman, P.J., Hagerman, R., Lagna, G., Hata, A., 2016b. Augmented noncanonical BMP type II receptor signaling mediates the synaptic abnormality of fragile X syndrome. Sci. Signal. 9. https://doi.org/10.1126/scisignal.aaf6060

Kingsley, D.M., 1994. The TGF-β superfamily: New members, new receptors, and new genetic tests of function in different organisms. Genes Dev. 8, 133–146. https://doi.org/10.1101/gad.8.2.133

Krueger, B.R.M., 1996. Large-Scale Death in Developing Cerebellum. J Neurosci 75, 9.

Kwak, Y.D., Hendrix, B.J., Sugaya, K., 2014. Secreted type of amyloid precursor protein induces glial differentiation by stimulating the BMP/Smad signaling pathway. Biochem. Biophys. Res. Commun. 447, 394–399. https://doi.org/10.1016/j.bbrc.2014.03.139

Le Roux, P., Behar, S., Higgins, D., Charette, M., 1999. OP-1 enhances dendritic growth from cerebral cortical neurons in vitro. Exp. Neurol. 160, 151–163. https://doi.org/10.1006/exnr.1999.7194

Lein, P., Johnson, M., Guo, X., Rueger, D., Higgins, D., 1995. Osteogenic protein-1 induces dendritic growth in rat sympathetic neurons. Neuron 15, 597–605. https://doi.org/10.1016/0896-6273(95)90148-5

Lein, P.J., Beck, H.N., Chandrasekaran, V., Gallagher, P.J., Chen, H.-L., Lin, Y., Guo, X., Kaplan, P.L., Tiedge, H., Higgins, D., 2002. Glia induce dendritic growth in cultured sympathetic neurons by modulating the balance between bone morphogenetic proteins (BMPs) and BMP antagonists. J. Neurosci. 22, 10377–10387.

Lillien, L., Raphael, H., 2000. BMP and FGF regulate the development of EGF-responsive neural progenitor cells. Development 127, 4993–5005.

Lioy, D.T., Garg, S.K., Monaghan, C.E., Raber, J., Foust, K.D., Kaspar, B.K., Hirrlinger, P.G.,

Kirchhoff, F., Bissonnette, J.M., Ballas, N., Mandel, G., 2011. A role for glia in the progression of Rett's syndrome. Nature 475, 497–500. https://doi.org/10.1038/nature10214

Liu, Y., Zhang, S., Chen, Y., Shi, K., Zou, B., Liu, J., Yang, Q., Jiang, H., Wei, L., Li, C., Zhao, M., Gabrilovich, D.I., Zhang, H., 2018. Fast Generation of Functional Subtype Astrocytes from Human Pluripotent Stem Cells. Stem Cell Reports 11, 1–16. https://doi.org/10.1016/j.stemcr.2018.05.016

Marqués, G., Bao, H., Haerry, T.E., Shimell, M.J., Duchek, P., Zhang, B., O'Connor, M.B., 2002. The Drosophila BMP type II receptor Wishful Thinking regulates neuromuscular synapse morphology and function. Neuron 33, 529–43. https://doi.org/10.1016/S0896-6273(02)00595-0

McCabe, B.D., Marqués, G., Haghighi, A.P., Fetter, R.D., Crotty, M.L., Haerry, T.E., Goodman, C.S., O'Connor, M.B., 2003. The BMP homolog Gbb provides a retrograde signal that regulates synaptic growth at the Drosophila neuromuscular junction. Neuron 39, 241–54. https://doi.org/10.1016/S0896-6273(03)00426-4

Miller, F.D., Gauthier, A.S., 2007. Timing Is Everything: Making Neurons versus Glia in the Developing Cortex. Neuron 54, 357–369. https://doi.org/10.1016/J.NEURON.2007.04.019

Miyazono, K., Kamiya, Y., Morikawa, M., 2010. Bone morphogenetic protein receptors and signal transduction. J. Biochem. 147, 35–51. https://doi.org/10.1093/jb/mvp148

Russo, A.J., 2014. Increased Epidermal Growth Factor Receptor (EGFR) Associated with Hepatocyte Growth Factor (HGF) and Symptom Severity in Children with Autism Spectrum Disorders (ASDs). J. Cent. Nerv. Syst. Dis. 6, 79–83. https://doi.org/10.4137/JCNSD.S13767

Scholze, A.R., Foo, L.C., Mulinyawe, S., Barres, B. a., 2014. BMP Signaling in Astrocytes Downregulates EGFR to Modulate Survival and Maturation. PLoS One 9, e110668. https://doi.org/10.1371/journal.pone.0110668

Shen, W., Finnegan, S., Lein, P., Sullivan, S., Slaughter, M., Higgins, D., 2004. Bone morphogenetic proteins regulate ionotropic glutamate receptors in human retina. Eur. J. Neurosci. 20, 2031–2037. https://doi.org/10.1111/j.1460-9568.2004.03681.x

Sloan, S. a, Barres, B. a, 2014. Mechanisms of astrocyte development and their contributions to neurodevelopmental disorders. Curr. Opin. Neurobiol. 27, 75–81. https://doi.org/10.1016/j.conb.2014.03.005

Sripathy, S., Leko, V., Adrianse, R.L., Loe, T., Foss, E.J., Dalrymple, E., Lao, U., Gatbonton-

Schwager, T., Carter, K.T., Payer, B., Paddison, P.J., Grady, W.M., Lee, J.T., Bartolomei, M.S., Bedalov, A., 2017. Screen for reactivation of MeCP2 on the inactive X chromosome identifies the BMP/TGF-β superfamily as a regulator of XIST expression. Proc. Natl. Acad. Sci. 114, 1619–1624. https://doi.org/10.1073/pnas.1621356114

Steeb, H., Ramsey, J.M., Guest, P.C., Stocki, P., Cooper, J.D., Rahmoune, H., Ingudomnukul, E., Auyeung, B., Ruta, L., Baron-Cohen, S., Bahn, S., 2014. Serum proteomic analysis identifies sex-specific differences in lipid metabolism and inflammation profiles in adults diagnosed with Asperger syndrome. Mol. Autism 5, 4. https://doi.org/10.1186/2040-2392-5-4

Ure, K., Lu, H., Wang, W., Ito-Ishida, A., Wu, Z., He, L.-J., Sztainberg, Y., Chen, W., Tang, J., Zoghbi, H.Y., 2016. Restoration of Mecp2 expression in GABAergic neurons is sufficient to rescue multiple disease features in a mouse model of Rett Syndrome. Elife 5, 1–21. https://doi.org/10.7554/eLife.14198

Wang, R.N., Green, J., Wang, Z., Deng, Y., Qiao, M., Peabody, M., Zhang, Q., Ye, J., Yan, Z., Denduluri, S., Idowu, O., Li, M., Shen, C., Hu, A., Haydon, R.C., Kang, R., Mok, J., Lee, M.J., Luu, H.L., Shi, L.L., 2014. Bone Morphogenetic Protein (BMP) signaling in development and human diseases. Genes Dis. 1, 87–105. https://doi.org/10.1016/j.gendis.2014.07.005

Withers, G.S., Higgins, D., Charette, M., Banker, G., 2000. Bone morphogenetic protein-7 enhances dendritic growth and receptivity to innervation in cultured hippocampal neurons. Eur. J. Neurosci. 12, 106–116. https://doi.org/10.1046/j.1460-9568.2000.00889.x

Xiao, L., Michalski, N., Kronander, E., Gjoni, E., Genoud, C., Knott, G., Schneggenburger, R., 2013. BMP signaling specifies the development of a large and fast CNS synapse. Nat. Neurosci. 16, 856–864. https://doi.org/10.1038/nn.3414

Zhang, X., Rui, M., Gan, G., Huang, C., Yi, J., Lv, H., Xie, W., Colbran, R.J., 2017. Neuroligin 4 regulates synaptic growth via the bone morphogenetic protein (BMP) signaling pathway at the Drosophila neuromuscular junction. J. Biol. Chem. 292, 17991–18005. https://doi.org/10.1074/jbc.M117.810242

Zhang, Y., Chen, K., Sloan, S.A., Bennett, M.L., Scholze, A.R., O'Keeffe, S., Phatnani, H.P., Guarnieri, P., Caneda, C., Ruderisch, N., Deng, S., Liddelow, S.A., Zhang, C., Daneman, R., Maniatis, T., Barres, B.A., Wu, J.Q., 2014. An RNA-sequencing transcriptome and splicing database of glia, neurons, and vascular cells of the cerebral cortex. J. Neurosci. 34, 11929–11947. https://doi.org/10.1523/JNEUROSCI.1860-14.2014

Chapter 6: Conclusions and Future Directions

In this dissertation, I have adapted an existing protocol for the isolation of murine astrocytes at a time point when astrocytes are known to be actively involved in neuron growth and synapse formation, and cultured them under serum-free culture conditions to examine the astrocyte protein secretome and transcriptome in vitro using mass spectrometry and RNA sequencing. Using this approach, I isolated astrocytes from the cortices of wild-type (WT), Rett Syndrome (RTT), Fragile X Syndrome (FXS), and Down Syndrome (DS) mouse models and identified key alterations in protein secretion and gene expression between WT and neurodevelopmental disordered (ND) astrocytes. I determined that there are a variety of individual changes in protein secretion and gene expression between WT astrocytes and each individual ND, as well as 88 proteins that show increased secretion in all three NDs compared to WT, and 32 proteins that showed decreased secretion in all NDs. Importantly, these changes in protein secretion are not generally reflected by changes in gene expression, highlighting the importance of examining protein expression alongside mRNA levels when searching for functional changes in astrocytes. Furthermore, I found evidence that two proteins that show increased secretion in all three NDs, insulin-like growth factor binding protein 2 (IGFBP2) and bone morphogenetic protein 6 (BMP6), are implicated in the pathological differences observed in NDs compared to WT.

IGFBP2 plays a role in the pathology of RTT in vitro

IGFBP2, one of the most abundant proteins in WT astrocyte conditioned media (ACM), is dramatically increased in secretion in all 3 NDs, and the addition of purified recombinant IGFBP2 protein to WT ACM renders it incapable of supporting normal neurite outgrowth, inducing outgrowth deficits similar to those seen in RTT and FXS ACM. Blocking IGFBP2 activity in vitro through the addition of a neutralizing antibody rescues this effect in WT ACM supplemented with IGFBP2, but intriguingly, blocking IGFBP2 in ND ACM only leads to an improvement in outgrowth

in RTT ACM and not FXS ACM. There is an increase in the volume of individual IGFBP2 protein puncta and a trend toward an increase in overall volume of IGFBP2 in the extracellular space surrounding astrocytes in RTT KO cortex at postnatal day 7 (P7) compared to WT littermates, indicating a role for secreted IGFBP2 in RTT in vivo. Taken together, these results implicate IGFBP2 as a contributor to RTT pathology, a role which is supported by numerous studies indicating that alterations in IGF signaling may have an effect in autism spectrum disorder (ASD). Because blocking IGFBP2 in RTT ACM rescues the neuronal outgrowth deficits in vitro, I am working to determine if blocking IGFBP2 in vivo has a similar effect. To accomplish this, we are injecting the IGFBP2-neutralizing antibody into the cortex of RTT KO mice and their WT littermates at P2 (Figure 4.7), and collecting the brains for Golgi analysis at P7. I will analyze dendritic arborization via Sholl analysis and examine spine morphology to determine if neutralizing IGFBP2 in vivo can rescue the pathology of RTT. These results will further clarify the role of IGFBP2 and IGF signaling in RTT.

IGFBP2 makes an appealing candidate in the study of these NDs due to the known alterations in IGF signaling in ASD (Ricciardi et al., 2011; Riikonen et al., 2006; Williams et al., 2014) and the ongoing clinical trials examining IGF1 as a potential treatment for RTT (Khwaja et al., 2014; Pini et al., 2014, 2012). Our preliminary results studying the effects of IGFBP2 in vitro determined that the addition of IGF1 to IGFBP2-containing WT ACM was sufficient to rescue the outgrowth deficit induced by IGFBP2, indicating that the inhibitory effects of IGFBP2 are likely to act via the canonical IGF signaling pathway. However, it is still unclear how, exactly, IGF1 acts to ameliorate the symptoms of RTT and other conditions in human patients. IGF signaling, while traditionally thought of as activating the PI3K/AKT pathway, can also activate the mitogen-activated protein kinase (MAPK) pathway. The MAPK pathway is activated when the signaling molecule growth factor receptor-bound protein 2 (GRB2) binds to IRS and son of sevenless (SOS) (Rauen, 2013). This leads to the activation of Ras and the subsequent MAPK cascade. Like the

PI3K-AKT pathway, the MAPK pathway controls many downstream processes, including apoptosis, cell differentiation, cell growth, and metabolism. Thus while evidence currently supports a role for altered PI3K/AKT signaling in ASD, it is possible that alterations in MAPK signaling contribute to the pathology of the condition. In addition to their canonical roles as IGF carrier proteins, IGFBPs can act via IGF-independent pathways, such as via binding to α-5-β integrin (Hwa et al., 1999; Jones et al., 1993; Schütt et al., 2004). In cancer cells, this IGFBP2-integrin binding interaction can lead to reduced proliferation and cell deadhesion in vitro (Schütt et al., 2004). It is possible that IGFBP2 may be acting via a noncanonical interaction to inhibit neuronal growth in RTT, and that IGF1 treatment of NDs in patients is effective simply due to the potency of the factor. Thus further research should examine the precise mechanism by which IGFBP2 acts to inhibit neuronal outgrowth, to better clarify its role in RTT and aid in the development of targeted therapies.

BMP6 plays a role in FXS pathology in vitro

BMP6 is secreted only at very low levels by WT astrocytes. Treating WT astrocytes with BMP6 induces changes in astrocyte morphology in vitro, and leads to alterations in protein secretion and gene expression that partially resemble ND astrocytes. ACM from BMP6-treated WT astrocytes is less capable of supporting neuronal outgrowth compared to untreated WT ACM, further enhancing the resemblance to ND astrocytes. While FXS ACM is less capable of supporting neuronal outgrowth than WT ACM, blocking BMP activity in FXS astrocytes by treating them with the BMP antagonist noggin during conditioning rescues this phenotype, returning outgrowth levels to those seen in WT ACM. Furthermore, there is an increase in the proportion of phosphoSMAD (pSMAD)-positive astrocytes in the visual cortex of FXS KO mice at P7 compared to WT littermates, indicating that there is an increase in BMP signaling in FXS KO cortex over baseline at that time. These results indicate that BMP signaling is altered in FXS astrocytes during

development and identify BMP6 as a novel target for therapeutic interventions in ASD. It would be interesting to examine the effects of blocking BMP activity in FXS in vivo, to determine if it leads to a reduction of pSMAD expression in astrocytes and rescues the dendritic arborization defects seen in FXS.

Work out of the Barres lab demonstrated that BMP signaling influences astrocyte maturity and function in vitro (Scholze et al., 2014). One of the hypotheses regarding NDs affecting neuronal development is the possibility of a “mismatch” in the maturity of the astrocytes versus the maturity of the neurons themselves (Sloan and Barres, 2014) and there is evidence that neural precursor cells are more disposed toward astroglial fates in some NDs such as Costello Syndrome and DS (Chen et al., 2014; Krencik et al., 2015). If the astrocytes themselves are “more mature” than their neuronal counterparts, this may lead to aberrant signaling between cell types in the brain and result in a failure of normal neuronal development. Increased secretion of BMP6 may reflect an abnormal phenotype in ND astrocytes that leads to downstream effects on protein secretion and gene expression having functional effects. This hypothesis is supported by the mass spectrometry results demonstrating that there is a great deal of overlap between the protein secretion profiles of BMP6-treated WT astrocytes and ND astrocytes, including an increase in IGFBP2, which I have determined has an inhibitory effect on neuronal outgrowth and plays a role in RTT pathology. Thus it is likely that altered BMP signaling further exacerbates the functional changes seen in ND astrocytes and contributes to their failure to support normal neuronal development.

Little work has been done on the roles of BMPs in NDs associated with ASD, but there is some evidence that there may be increased levels of BMP6 in male patients with a mild form of ASD (Steeb et al., 2014) and changes in the expression of a number of genes affecting BMP signaling such as neuroligins and fragile x mental retardation protein (FMRP) have been associated with ASD (Kashima et al., 2016). Furthermore, FMRP has been found to downregulate

bone morphogenetic protein receptor type 2 (BMPR2), and the absence of FMRP in FXS leads to increased levels of BMPR2 that subsequently cause an increase in LIM domain kinase 1 (LIMK1), a protein associated with neurite outgrowth and synapse formation (Kashima et al., 2016; Kashima and Hata, 2018), via a noncanonical BMP pathway. My analysis found an increase in the expression of canonical BMP signaling genes in FXS and DS astrocytes, indicating that BMPs may be influencing neuronal development via multiple pathways. Further study should examine whether or not BMP6 is also leading to changes in noncanonical BMP signaling pathways in ND astrocytes. Additionally, while I saw an increase in the proportion of pSMAD expressing astrocytes in FXS cortex compared to WT, I did not examine possible alterations in pSMAD activation in DS or RTT, nor did we attempt an in vivo rescue of this phenotype; future experiments may help determine if BMP6 represents a viable target for therapeutic interventions.

Future directions

There are many questions that remain to be explored regarding these experiments. These mass spectrometry results identified over 1200 unique proteins secreted by P7 WT astrocytes in vitro, providing a long list of candidates to be examined for potential roles in astrocyte function, neuronal development, neurite outgrowth, axonal guidance, spine development, and synapse formation and function. This assay is the first of its kind, using astrocytes isolated at a key timepoint in development and maintained in serum-free media, and this data is sure to support many future studies on the roles of astrocytes in the developing brain. In addition, I have identified nearly 100 proteins that show differential secretion patterns in 3 different genetic neurodevelopmental disorders associated with ASD, in addition to numerous proteins that show changes in protein secretion and gene expression in each individual ND. While the scope of this dissertation has only focused on 2 of those proteins, these other proteins represent new potential avenues of study for better understanding these NDs and for identifying new therapeutic targets

for treating ASD. Indeed, I feel that one could complete several additional PhDs in the exploration of this dataset!

Each of these NDs has been associated with deficits in neuronal development, including alterations in dendritic arborization, immature spine morphology, and impaired synapse formation and plasticity; examining the alterations in astrocyte protein secretion in these NDs may provide additional insight into the mechanisms of these conditions. This dissertation focused only on the effects of two candidate proteins on neurite outgrowth; it does not address whether or not IGFBP2 or BMP6 also affect spine morphology and/or synapse formation and function. Future experiments may include culturing cortical neurons in WT and ND ACM for longer periods of time and staining for synaptic markers, or conducting electrophysiological analysis of synaptic function in vitro, and determining if blocking IGFBP2 or BMP6 leads to an improvement in the spine and synapse deficits seen in NDs. Additional experiments could examine similar questions in vivo, through immunohistochemical approaches to examine synaptic markers and conducting electrophysiological analyses on acutely isolated cortical slices.

It is important to note that this dissertation focused on the study of astrocyte function at postnatal day 7 (P7), an early developmental timepoint when synaptogenesis is just beginning; therefore it may be difficult to identify key changes in synapse formation and function with this approach. Additional work in our lab is aimed at better understanding the relationship between astrocytes and synapses in adult RTT and FXS mice. Electron microscopy studies have found that there is a decrease in the number of synapses with an associated astrocyte process wrapped around them in FXS (Jawaid et al., 2018). There are also known alterations in the levels of astrocyte proteins that influence synaptic function such as glutamate transporter 1 (GLT1) and the Kir4.1 potassium channel in ASD (Sicca et al., 2011). We are examining the relationship between astrocytic processes and synapses in RTT and FXS using an electron microscopy approach, to search for alterations in astrocyte morphology at the synapse, as well as examining

the expression of GLT1 in RTT and FXS KO cortex by immunohistochemistry. Preliminary results suggest a reduction in the overall number of GLT1 puncta and a reduction in the colocalization between GLT1 and VGLUT1 (a presynaptic marker for intracortical synapses) at P35 in RTT KO cortex compared to their WT littermates (Figure 6.1), which may contribute to synaptic deficits in this condition by leading to incomplete clearance of glutamate from the synapse following synaptic transmission. Further analysis will examine the expression of Kir4.1 to determine if altered astrocyte expression of this potassium channel further contribute to synaptic deficits due to improper ion buffering. Ultimately, the lab plans to examine overall changes in astrocyte morphology in NDs using a cell dye filling approach; it is possible that a lack of proper astrocyte ensheathment of synapses in the central nervous system contributes to the altered spine morphology and synapse formation seen in these NDs. Examination of adult mice may elucidate lifelong alterations in astrocyte function that contribute to the ongoing neurological deficits associated with these disorders.

If in vivo results continue to support roles for IGFBP2 and BMP6 in RTT and FXS, future studies could examine whether or not blocking these proteins in vivo is capable of rescuing some of the behavioral deficits associated with these conditions; this would provide support for these proteins being important mediators of ND pathology and further emphasize their potential as therapeutic targets. We have also begun a collaboration with the Gage Lab at The Salk Institute for Biological Studies, who are currently in the process of differentiating astroglial cells from iPSCs from RTT patient fibroblasts. Once these cells are successfully differentiated, we will examine their protein secretome and determine if human astroglial cells show similar protein secretion changes as those seen in mouse astrocytes, which may provide more insight into the roles of these proteins in ASD.

It is my hope that, in addition to the experiments already in progress, the results described in this dissertation will help inform studies on the functional roles of astrocytes in the developing cortex for years to come.

Acknowledgements

This chapter is, in part, in preparation for submission for publication. The dissertation author will be the first author of this publication, with Dr. Jolene Diedrich as second author and Dr. Nicola Allen as the senior author and principle investigator.

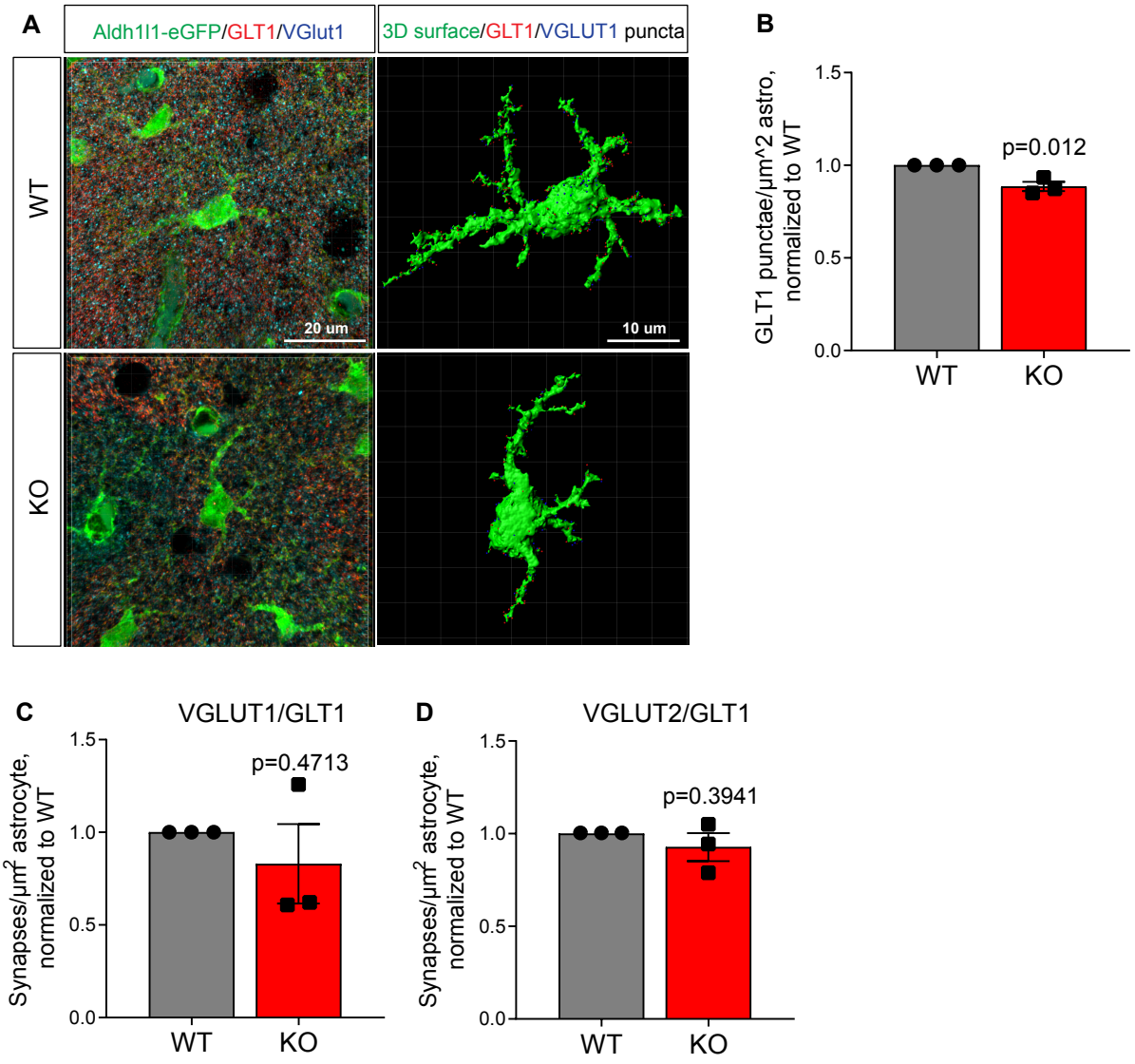

Figure 6.1: Immunohistochemical analysis reveals a decrease in GLT1 puncta on astrocytes in RTT cortex. **A.** Example images of astrocytes (green) from P35 WT and RTT KO cortices, stained for GLT1 (red) and VGLUT1 (blue), alongside their 3D renderings and puncta from Bitplane IMARIS analysis. **B-D.** Quantification of colocalized puncta reveals a decrease in the overall density of GLT1 puncta on RTT KO astrocytes (**B**), with no significant change in the colocalization of VGLUT1/GLT1 (**C**) or VGLUT2/GLT1 (**D**), though there may be a trend toward a decrease in VGLUT1/GLT1 colocalization. N=3 mice per condition, 3 (VGLUT1/2+GLT1) or 6 (GLT1 alone) astrocytes analyzed per mouse.

References

Chen, C., Jiang, P., Xue, H., Peterson, S.E., Tran, H.T., McCann, A.E., Parast, M.M., Li, S., Pleasure, D.E., Laurent, L.C., Loring, J.F., Liu, Y., Deng, W., 2014. Role of astroglia in Down's syndrome revealed by patient-derived human-induced pluripotent stem cells. Nat. Commun. 5, 4430. https://doi.org/10.1038/ncomms5430

Hwa, V., Oh, Y., Rosenfeld, R.G., 1999. The Insulin-Like Growth Factor-Binding Protein (IGFBP) Superfamily [1]. Endocr. Rev. 20, 761–787. https://doi.org/10.1210/edrv.20.6.0382

Jawaid, S., Grahame, l, Kidd, J., Wang, J., Swetlik, C., Dutta, R., Trapp, B.D., Kidd, G.J., Wang, J., Swetlik, C., Dutta, R., Trapp, B.D., 2018. Alterations in CA1 hippocampal synapses in a mouse model of fragile X syndrome. Glia 66, 789–800. https://doi.org/10.1002/glia.23284

Jones, J.I., Gockerman, A., Busby, W.H., Wright, G., Clemmons, D.R., 1993. Insulin-like growth factor binding protein 1 stimulates cell migration and binds to the alpha 5 beta 1 integrin by means of its Arg-Gly-Asp sequence. Proc. Natl. Acad. Sci. U. S. A. 90, 10553–7. https://doi.org/10.1073/pnas.90.22.10553

Kashima, R., Hata, A., 2018. The role of TGF-β superfamily signaling in neurological disorders. Acta Biochim. Biophys. Sin. (Shanghai). 50, 106–120. https://doi.org/10.1093/abbs/gmx124

Kashima, R., Roy, S., Ascano, M., Martinez-cerdeno, V., Ariza-torres, J., Kim, S., Louie, J., Lu, Y., Leyton, P., Bloch, K.D., Kornberg, T.B., Hagerman, P.J., Hagerman, R., Lagna, G., Hata, A., 2016. Augmented noncanonical BMP type II receptor signaling mediates the synaptic abnormality of fragile X syndrome 9, 1–13.

Khwaja, O.S., Ho, E., Barnes, K. V., O'Leary, H.M., Pereira, L.M., Finkelstein, Y., Nelson, C.A., Vogel-Farley, V., DeGregorio, G., Holm, I.A., Khatwa, U., Kapur, K., Alexander, M.E., Finnegan, D.M., Cantwell, N.G., Walco, A.C., Rappaport, L., Gregas, M., Fichorova, R.N., Shannon, M.W., Sur, M., Kaufmann, W.E., 2014. Safety, pharmacokinetics, and preliminary assessment of efficacy of mecasermin (recombinant human IGF-1) for the treatment of Rett syndrome. Proc. Natl. Acad. Sci. 111, 4596–4601. https://doi.org/10.1073/pnas.1311141111

Krencik, R., Hokanson, K.C., Narayan, A.R., Dvornik, J., Rooney, G.E., Rauen, K. a, Weiss, L. a, Rowitch, D.H., Ullian, E.M., 2015. Dysregulation of astrocyte extracellular signaling in Costello syndrome. Sci. Transl. Med. 7, 286ra66. https://doi.org/10.1126/scitranslmed.aaa5645

Pini, G., Scusa, M.F., Benincasa, A., Bottiglioni, I., Congiu, L., Vadhatpour, C., Romanelli, A.M.,

Gemo, I., Puccetti, C., McNamara, R., O'Leary, S., Corvin, A., Gill, M., Tropea, D., 2014. Repeated insulin-like growth factor 1 treatment in a patient with rett syndrome: a single case study. Front. Pediatr. 2, 52. https://doi.org/10.3389/fped.2014.00052

Pini, G., Scusa, M.F., Congiu, L., Benincasa, A., Morescalchi, P., Bottiglioni, I., Di Marco, P., Borelli, P., Bonuccelli, U., Della-Chiesa, A., Prina-Mello, A., Tropea, D., 2012. IGF1 as a Potential Treatment for Rett Syndrome: Safety Assessment in Six Rett Patients. Autism Res. Treat. 2012, 679801. https://doi.org/10.1155/2012/679801

Rauen, K. a, 2013. The RASopathies. Annu. Rev. Genomics Hum. Genet. 14, 355–69. https://doi.org/10.1146/annurev-genom-091212-153523

Ricciardi, S., Boggio, E.M., Grosso, S., Lonetti, G., Forlani, G., Stefanelli, G., Calcagno, E., Morello, N., Landsberger, N., Biffo, S., Pizzorusso, T., Giustetto, M., Broccoli, V., 2011. Reduced AKT/mTOR signaling and protein synthesis dysregulation in a Rett syndrome animal model. Hum. Mol. Genet. 20, 1182–1196. https://doi.org/10.1093/hmg/ddq563

Riikonen, R., Makkonen, I., Vanhala, R., Turpeinen, U., Kuikka, J., Kokki, H., 2006. Cerebrospinal fluid insulin-like growth factors IGF-1 and IGF-2 in infantile autism. Dev. Med. Child Neurol. 48, 751. https://doi.org/10.1017/S0012162206001605

Scholze, A.R., Foo, L.C., Mulinyawe, S., Barres, B. a., 2014. BMP Signaling in Astrocytes Downregulates EGFR to Modulate Survival and Maturation. PLoS One 9, e110668. https://doi.org/10.1371/journal.pone.0110668

Schütt, B.S., Langkamp, M., Rauschnabel, U., Ranke, M.B., Elmlinger, M.W., 2004. Integrin-mediated action of insulin-like factor binding protein-2 in tumor cells. J. Mol. Endocrinol. 32, 859–868. https://doi.org/10.1677/jme.0.0320859

Sicca, F., Imbrici, P., D'Adamo, M.C., Moro, F., Bonatti, F., Brovedani, P., Grottesi, A., Guerrini, R., Masi, G., Santorelli, F.M., Pessia, M., 2011. Autism with seizures and intellectual disability: possible causative role of gain-of-function of the inwardly-rectifying K+ channel Kir4.1. Neurobiol. Dis. 43, 239–47. https://doi.org/10.1016/j.nbd.2011.03.016

Sloan, S. a, Barres, B. a, 2014. Mechanisms of astrocyte development and their contributions to neurodevelopmental disorders. Curr. Opin. Neurobiol. 27, 75–81. https://doi.org/10.1016/j.conb.2014.03.005

Steeb, H., Ramsey, J.M., Guest, P.C., Stocki, P., Cooper, J.D., Rahmoune, H., Ingudomnukul, E., Auyeung, B., Ruta, L., Baron-Cohen, S., Bahn, S., 2014. Serum proteomic analysis identifies sex-specific differences in lipid metabolism and inflammation profiles in adults diagnosed with Asperger syndrome. Mol. Autism 5, 4. https://doi.org/10.1186/2040-2392-5-4

Williams, E.C., Zhong, X., Mohamed, A., Li, R., Liu, Y., Dong, Q., Ananiev, G.E., Choongmok, J.C., Lin, B.R., Lu, J., Chiao, C., Cherney, R., Li, H., Zhang, S.-C.C., Chang, Q., Mok, J.C.C., Lin, B.R., Lu, J., Chiao, C., Cherney, R., Li, H., Zhang, S.-C.C., Chang, Q., 2014. Mutant astrocytes differentiated from Rett syndrome patients-specific iPSCs have adverse effects on wildtype neurons. Hum. Mol. Genet. 23, 2968–2980. https://doi.org/10.1093/hmg/ddu008

Chapter 7: Methods

Animals

All animal work was approved by the Institutional Animal Care and Use Committee (IACUC) of the Salk Institute for Biological Studies.

Mice

Mice were housed in the Salk Institute animal facility at a light cycle of 12 hr light: 12 hr dark, with access to water and food ad libitum.

Wild-type (WT) mice

WT C57BL/6J (Jax stock number 000664) mice were used to generate WT astrocytes in vitro, to generate neurons for all cortical neuronal assays, and to breed *Mecp2* and *Fmr1* mice. Mice of both genders were used.

Mecp2 knockout (KO) mice

Mecp2 KO (Jax 003890) mice were used to generate RTT astrocytes in vitro, to breed *Mecp2* mice, and to breed Aldh1L1-eGFPxMecp2 mice. *Mecp2* is found on the X chromosome and the hemizygous condition is fatal to males by 6 weeks of age, so experimental mice were generated by breeding heterozygous (+/-) *Mecp2* females to WT (+/y) C57BL/6J males. Astrocytes were isolated from male *Mecp2* (-/y) mice.

Fmr1 KO mice

Fmr1 KO (Jax 003025) mice were used to generate FXS astrocytes in vitro, to breed *Fmr1* mice, and to breed Aldh1L1-eGFPxFmr1. *Fmr1* is found on the X chromosome and KO males are fertile, so experimental mice were generated by breeding heterozygous (+/-) *Fmr1* females to KO (-/y) males. Astrocytes prepared from both male and female KO mice.

Down syndrome transgenic mice

Ts65Dn (Jax 005252) mice were used to generate DS astrocytes in vitro, and to breed *Ts65Dn* mice. *Ts65Dn* mice are trisomic for about two-thirds of the genes orthologous to human

chromosome 21 and only one copy of the mutation is required for the condition, so experimental mice were generated by breeding *Ts65Dn+* female mice to WT males. Astrocytes were prepared from both male and female *Ts65Dn+* mice.

Aldh1l1-EGFP x *Mecp2* KO or *Fmr1* KO mice

Tg(Aldh1l1-EGFP)OFC789Gsat/Mmucd mice express Aldh1l1-eGFP in astrocytes (011015-UCD). Male Aldh1l1-eGFP mice were bred to *Mecp2* or *Fmr1* heterozygous (+/-) females. *Mecp2* and *Fmr1* KO mice and their WT littermates expressing eGFP in astrocytes were used for experiments.

Cell culture

Cortical astrocyte cultures

Cortical mouse astrocytes were isolated by immunopanning, using an adapted version of a protocol previously described (Foo, 2013; Foo et al., 2011), from P5-P7 WT, RTT, FXS, and DS mice. The full version of this protocol is available on in Appendix 1 on page 188. The cortices of 2-4 mouse pups (P5-P7) were dissected out and the meninges removed before tissue was digested in a papain enzymatic solution to generate a single cell suspension. This was then passed over a series of five plates to deplete unwanted cell types (lectin [Vector Labs Inc, #L-1100], 10 minutes, to deplete endothelia; cd11b [Ebioscience, #14-01112-86], 10 minutes, to deplete microglia, cd45 [BD Pharmingen, #550539], 20 minutes, to deplete macrophages, and O4 hybridoma [see (Bansal and Pfeiffer, 1989) for recipe], 15 minutes, x2, to deplete oligodendrocyte precursor cells) before positive selection for astrocytes using the astrocyte cell surface antigen 2 (ACSA2, Miltenyi Biotech #130-099-138). Astrocytes were plated on glass coverslips (12mm diameter, Carolina Biological Supply 633029) coated with poly-D-lysine (Sigma P6407) in 24 well plates (Falcon 353047) at a density of 50,000-80,000 cells/well or in six well plates (Falcon 353046) coated with poly-D-lysine at a density of 280,000 - 350,000 cells/well in a

growth medium containing: 50% DMEM (Thermo Fisher Scientific 11960044), 50% Neurobasal (Thermo Fisher Scientific 21103049), Penicillin-Streptomycin (LifeTech 15140-122), GlutaMax (Thermo Fisher Scientific 35050-061), sodium pyruvate (Thermo Fisher Scientific 11360-070), N-acetyl-L-cysteine (Sigma A8199), SATO (containing: transferrin (Sigma T-1147), BSA (Sigma A-4161), progesterone (Sigma P6149), putrescine (Sigma P5780), sodium selenite (Sigma S9133)), and heparin binding EGF like growth factor (HbEGF, R&D Systems 259-HE/CF). Astrocyte cultures were maintained in a humidified incubator at 37°C and 10% CO2 and grown to confluence (5-7 days).

Generation of astrocyte conditioned media (ACM)

Astrocytes grown in 6 well plates were washed 3 times with warm DPBS (HyClone SH30264) to remove any minor traces of added protein from growth media, and the growth media was replaced by minimal low protein conditioning media (50% DMEM, 50% Neurobasal, penicillin-streptomycin, glutamax and sodium pyruvate, N-acetyl-Lcysteine (Sigma A8199), and carrier-free HbEGF (R&D Systems, 259-HE/CF, resuspended in dPBS only at 10 ug/ml, with no BSA). Astrocytes were conditioned in low protein media for 5 days in a tissue culture incubator at 37°C, 10% CO2. The astrocyte conditioned media (ACM) was collected and concentrated 30-fold using Vivaspin 20 or 6 centrifugal concentrators with a MW cut-off of 3 kDa (Sartorius VS2052 or VS0652). Protein concentration of the ACM was assessed by Bradford protein assay (Bio-Rad 500-0006). ACM for mass spectrometry and Western blotting was flash-frozen with liquid nitrogen and stored at -80°C until analysis. ACM for cortical assays was stored at 4°C until use, for no more than 2 weeks.

Cortical neuron cultures

Cortical neurons were isolated from P5-P7 C57Bl6J WT mice (Jax stock number 000664) as previously described (Risher et al., 2014; Steinmetz et al., 2006). The full version of this protocol is available on in Appendix 2 on page 201. The single cell suspension was passed over two plates to deplete unwanted cell types (lectin, IgG H+L [Jackson Immunoresearch #115-005-167] only) before positive selection for cortical neurons using the neuronal marker NCAM-L1 (Millipore MAB5272). Cortical neurons were plated on glass coverslips (12mm diameter, Carolina Biological Supply 633029) coated with poly-D-lysine (Sigma P6407) and laminin (R&D 340001001) at a density of 50,000-80,000 cells/well in a minimal medium, with the addition of astrocyte conditioned media and/or protein factors and antibodies as described in the text. Cortical neuron minimal media contained: 50% DMEM (Thermo Fisher Scientific 11960044), 50% Neurobasal (Thermo Fisher Scientific 21103049), Penicillin-Streptomycin (LifeTech 15140-122), glutamax (Thermo Fisher Scientific 35050-061), sodium pyruvate (Thermo Fisher Scientific 11360-070), N-acetyl-Lcysteine (Sigma A8199), insulin (Sigma I1882), triiodo-thyronine (Sigma T6397), SATO (containing: transferrin (Sigma T-1147), BSA (Sigma A-4161), progesterone (Sigma P6149), putrescine (Sigma P5780), sodium selenite (Sigma S9133)), B27 (see (Winzeler and Wang, 2013) for recipe), and forskolin (Sigma F6886). Cortical neuron cultures were maintained in a humidified incubator at 37°C and 10% CO2.

Additions of factors (concentrations, etc)

Unless stated otherwise in the text, all treatments were applied for 48 hours before cortical neurons were analyzed. In each experiment there was a negative control condition, cortical neurons in minimal media (alone condition; treated with buffer), and a positive control condition, cortical neurons treated with WT astrocyte conditioned media (ACM) at 3 ug/mL (ACM condition). The candidate proteins identified by mass spectrometry were insulin growth factor binding protein 2 (IGFBP2) (R&D 797-B2 at 100 ug/mL in sterile PBS), carboxypeptidase E (CPE) (Abcam

#ab169054 at 100 ug/mL in sterile deionized water), and BMP6 (R&D 507-BP/CF at 10 ug/mL in sterile dPBS). IGFBP2 and CPE were tested at a concentration determined by their overall levels in WT and ND ACM, at a level of roughly 4X the concentration expected in WT ACM (2X the concentration expected in ND ACM). IGFBP2 was added directly to the neuronal minimal medium, with or without WT ACM, immediately before plating at a concentration of 240 ng/mL, while CPE was applied at a concentration of 160 ng/mL. For BMP6 treatments, BMP6 was added to half of the wells of WT astrocytes during the conditioning phase, for a total of 5 days, at a concentration determined by previously published research (Scholze et al., 2014), 10 ng/mL, before being collected as normal and applied to cortical neurons at the same concentration of 3 ug/mL. IGFBP2-neutralizing antibody (R&D MAB797 at 0.5 mg/mL in sterile PBS) and its control IgG (R&D 6-001-F at 0.5 mg/mL in sterile PBS) were tested at 7 mg/mL directly in neuronal minimal media, a concentration determined to be twice the ND50 for the level of IGFBP2 in solution. For noggin treatments, noggin (R&D 1967-NG/CF at 200 ug/mL in sterile PBS) was added to half of the wells of FXS astrocytes during the conditioning phase, for a total of 5 days, at 1 ug/mL, before being collected as normal. Due to the high levels of residual noggin in the treated ACM, FXS untreated and FXS+noggin ACM was concentrated to the same volume and a protein concentration of 3 ug/mL determined in the untreated ACM; equal volumes of FXS untreated and FXS+noggin ACM were applied to cortical neurons. To test the effects of noggin alone, noggin was added at a concentration of 1 ug/mL directly to the minimal medium, with or without WT or FXS ACM, immediately before plating cortical neurons.

Mass spectrometry details & analysis

Protein concentration was determined by Bradford Assay and ACM was distributed into aliquots of 15 ug before being flash-frozen with liquid nitrogen and stored at -80°C until analysis. Samples were thawed and split into 3 equal parts of 5 ug each to produce technical triplicates for

each biological replicate. Samples were precipitated by methanol/chloroform. Dried pellets were dissolved in 8 M urea/100 mM TEAB, pH 8.5. Proteins were reduced with 5 mM tris(2-carboxyethyl)phosphine hydrochloride (TCEP, Sigma-Aldrich) and alkylated with 10 mM chloroacetamide (Sigma-Aldrich). Proteins were digested overnight at 37°C in 2 M urea/100 mM TEAB, pH 8.5, with trypsin (Promega). Digestion was quenched with formic acid, 5% final concentration. The digested samples were analyzed on a Fusion Lumos Orbitrap tribrid mass spectrometer (Thermo). The digest was injected directly onto a 30 cm, 75 um ID column packed with BEH 1.7um C18 resin (Waters). Samples were separated at a flow rate of 300 nl/min on a nLC 1000 (Thermo). Buffer A and B were 0.1% formic acid in water and 0.1% formic acid in 90% acetonitrile, respectively. A gradient of 1-25% B over 160 min, an increase to 35% B over 60 min, an increase to 90% B over 10 min and held at 100%B for a final 10 min was used for 240 min total run time. Column was re-equilibrated with 20 ul of buffer A prior to the injection of sample. Peptides were eluted directly from the tip of the column and nanosprayed directly into the mass spectrometer by application of 2.5 kV voltage at the back of the column. The Orbitrap Fusion was operated in a data dependent mode. Full MS scans were collected in the Orbitrap at 120K resolution with a mass range of 400 to 1500 m/z and an AGC target of 4e5. The cycle time was set to 3 sec, and within this 3 sec the most abundant ions per scan were selected for CID MS/MS in the iontrap with an AGC target of 1e4 and minimum intensity of 5000. Maximum fill times were set to 50 ms and 200 ms for MS and MS/MS scans respectively. Quadrupole isolation at 1.6 m/z was used, monoisotopic precursor selection was enabled and dynamic exclusion was used with exclusion duration of 5 sec. Protein and peptide identification were done with Integrated Proteomics Pipeline – IP2 (Integrated Proteomics Applications). Tandem mass spectra were extracted from raw files using RawConverter (He et al., 2015) and searched with ProLuCID (Xu et al., 2015) against Uniprot mouse database. The search space included all fully-tryptic and half-

tryptic peptide candidates, carbamidomethylation on cysteine was considered as a static modification.

The validity of the peptide spectrum matches (PSMs) generated by ProLuCID was assessed using Search Engine Processor (SEPro) module from PatternLab for Proteomics platform (Carvalho et al., 2016). XCorr, DeltaCN, DeltaMass, ZScore, number of peaks matched, and secondary rank values were used to generate a Bayesian discriminating function. A cutoff score was established to accept a false discovery rate (FDR) of 1% based on the number of decoys. A minimum sequence length of six residues per peptide was required and results were post-processed to only accept PSMs with < 10ppm precursor mass error.

Volcano plots were generated by a pairwise comparison of each individual ND versus WT using the PatternLab's TFold module. The following parameters were used to select differentially expressed proteins: spectral count data were normalized using NSAF values (Boris Zybailov et al., 2006), and two nonzero replicate values were required for each condition (at least two out of three technical replicates). A BH q-value was set at 0.05 (5 % FDR). A variable fold-change cutoff for each individual protein was calculated according to the t-test p-value using an F-Stringency value automatically optimized using the TFold software.

qPCR & RNAseq details & analysis

Immediately following ACM collection, ACM was replaced with warmed dPBS and RNA was collected using the RNEasy Micro Plus kit (Qiagen 74034). Small aliquots (0.1 - 0.5 ug) of RNA was used for cDNA synthesis by RT-PCR using Superscript VILO master mix (Thermo Fisher Scientific 11755050) according to manufacturer's instructions. For each sample, an equal amount of whole brain RNA from an animal with a matching genotype (WT, MeCP2 KO, Fmr1

KO, or Ts65Dn Mut) was used to generate control cDNA. 1 uL of the obtained cDNA was used for qPCR reaction using SYBR green PCR mastermix (Life Supply 4309155). All samples were run in triplicates (technical replicates). Primer pairs were as follows, all by Integrated DNA Technologies: GAPDH (Control; forward TGCCACTCAGAAGACTGTGG, and reverse GCATGTCAGATCCACAATGG); Syt1 (neurons; forward CTGCATCACAACACTACTAGC, reverse CCAACATTTCTACGAGACACAG); GFAP (astrocytes; forward AGAAAACCGCATCACCATTC, reverse TTGAGAGGTCTTGTGACTTTT); CSPG4 (oligodendrocyte precursor cells; forward CTCAGAACCCTATCTTCACG, reverse TACATGGTAGTGGACCTCAT); CD68 (microglia; forward ATACAATGTGTCCTTCCCAC, reverse CTATGCTTGCATTTCCACAG); and FGFr4 (fibroblasts; forward AGAGTGACGTGTGGTCTTT, reverse ACTCCCTCATTAGCCCATAC). Only samples that had GFAP expression of ≥3x whole brain and CSPG4 expression of ≤2x whole brain were used for mass spec and RNASeq analysis.

RNA libraries were prepared with TrueSeq Stranded mRNA Library Prep Kit (Illumina). Poly(A) mRNA was isolated from total RNA samples, followed by mRNA fragmentation, first strand cDNA synthesis, second cDNA synthesis and adaptor ligation, and isolation and amplification of cDNA fragments. Illumina HiSeq 2500 instrument was used for sequencing. For the analysis, sequenced reads were quality-tested using FASTQC and aligned to the mm10 mouse genome using the STAR aligner version 2.4.0k. Mapping was carried out using default parameters (up to 10 mismatches per read, and up to 9 multi- mapping locations per read). The genome index was constructed using the gene annotation supplied with the mm10 or rn6 Illumina iGenomes collection and sjdbOverhang value of 100. Normalized gene expression (Fragments per kilobase per million mapped reads, FPKM) was quantified with HOMER v4.8.3 across all gene

exons using the top-expressed isoform as proxy for gene expression. Quality of samples was assessed with the assistance of the Bioinformatics Core at the Salk Institute (Tables 7.1&2)

Immunocytochemistry staining, imaging & analysis

Staining astrocytes for cell-specific markers

After 7 days (for astrocytes that were not treated with additional protein factors) or 12 days (for astrocytes treated with either BMP6 or noggin in minimal growth medium), astrocytes were fixed with fresh warm (37°C) 4% paraformaldehyde (EMS 50980487) for 20 minutes at room temperature (RT). Coverslips were washed three times with RT PBS and blocked and permeabilized for 30 minutes in 50% goat serum/50% antibody buffer (150 mM NaCl; 50 mM Tris; 100 mM L-lysine; 1% BSA; pH 7.4) and 0.5% Triton X-100 (Sigma T9284). Coverslips were washed once with PBS and incubated overnight at 4°C with primary antibodies against GFAP (1:1000, Millipore, MAB360), Aqp4 (1:1000, Sigma, A5971), GLAST (1:100, Miltenyi 130-095-822), NeuN (1:1000, Millipore, MAB377), Iba1 (1:1000, Wako, 016-20001), or NG2 (1:1000, Millipore, AB5320) in a solution of antibody buffer + 10% goat serum. The following day, cells were washed three times with PBS and incubated for 1-2 hours with appropriate secondary antibodies (goat anti-rabbit Alexafluor 594 (1:1000, Thermo Fisher Scientific A-11037), goat anti-mouse Alexafluor 488 (1:1000, Thermo Fisher Scientific A-11029), goat anti-mouse Alexafluor 594 (1:1000, Thermo Fisher Scientific A-11032)) in a solution of antibody buffer + 10% goat serum before being washed a final three times and mounted with SlowFade + DAPI (Life Technologies s36939) on glass slides (Fisherfinest 12-244-2) and sealed with clear nail polish. Astrocytes were imaged using a Zeiss AXIO Imager Z2 motorized microscope (430000-9902) at 20X magnification. Images were analyzed using ImageJ by counting the % of cells that were positive for the cell marker and statistics performed in Microsoft Excel.

Neurite staining in cortical neurons

After 48 hours in culture, cortical neurons were fixed with fresh 4% paraformaldehyde in PBS warmed to 37°C for 10 minutes at RT. Coverslips were washed three times with RT PBS and blocked and permebilized for 30 minutes in 50% antibody buffer/50% goat serum and 0.5% Triton X-100. Coverslips were washed once with PBS and incubated overnight at 4°C with primary antibodies against MAP2 (to mark dendrites) (1:5000, EnCor Biotechnologies CPCA-MAP2) and Tau (to mark axons) (1:500, Millipore Sigma MAB3420) in a solution of antibody buffer + 10% goat serum. The following day, cells were washed three times with PBS and incubated for 1-2 hours with secondary antibodies (goat anti-chicken Alexafluor 488 (1:1000, Thermo Fisher Scientific A11039), goat anti-mouse Alexafluor 594 (1:1000)) in a solution of antibody buffer + 10% goat serum before being washed a final three times and mounted with SlowFade + DAPI on glass slides, sealed with nail polish, and stored at -20°C until imaging. Cortical neurons were imaged at 10X on a Zeiss AXIO Imager Z2 motorized microscope (430000-9902). For each assay, there were 3 coverslips per condition, and 20 images were taken per coverslip (except for the IGF1/CPE assays, where 10 images were taken per coverslip), for a total of 60 images per condition per assay with at least 1 neuron per image, for a total of at least 60 neurons imaged per condition per assay. Images were exported as TIFFs. Images were processed in ImageJ to merge all channels, convert the images to 16-bit, and apply a normalization of 0.1. Images were analyzed using MetaMorph software (Molecular Devices), using the Neurite Outgrowth Module to measure total, mean, max, and median neurite outgrowth length, number of processes per cell, and number of process branches per cell, and data were analyzed using Microsoft Excel and GraphPad Prism. Experiments were completed in triplicate, for a total of at least 180 neurons imaged and analyzed per condition.

Immunohistochemistry staining, imaging & analysis

Tissue collection and preparation

P7 or P35 mice (Aldh1L1-eGFP x *Mecp2* KO, *Fmr1* KO and their WT littermates) were anesthetized with intraperitoneal injection of 100 mg/kg Ketamine (Victor Medical Company) and 20 mg/kg Xylazine (Anased) mix and transcardially perfused with PBS followed by 4% PFA. Brains were dissected out and postfixed in 4% PFA at 4°C overnight. Brains were washed three times in PBS and cryoprotected in 30% sucrose at 4°C. After at least 48 hours in sucrose, brains were frozen in TFM (General data healthcare TFM-5) in a dry ice/ethanol mix and stored at -80°C until use. Fixed tissue was used for immunohistochemistry.

Immunohistochemical staining for IGFBP2 and pSMAD in P7 mouse brains

Littermate male mice (Aldh1l1-EGFP x *Fmr1* or *Mecp2* KO or WT) were used for these experiments. Fixed coronal sections were collected on Superfrost Plus micro slides (VWR 48311-703) at 14 um thickness (3.4 mm posterior to Bregma) on a cryostat (Hacker Industries OTF5000). Sections were blocked and permeabilized for 1 hr at room temperature in a humidified chamber in antibody buffer + 0.3% Triton X-100 in PBS. Primary antibodies goat anti-IGFBP2 (1:500, R&D AF797), rabbit anti-pSMAD (1:800, Cell Signaling 9516), rabbit anti-GLT1 (1:300, Novus Biologicals NBP1-20136), guinea pig anti-VGlut1 (1:1000, Millipore AB5905) or guinea pig anti-VGlut2 (1:1000, Millipore AB2251) were incubated in antibody buffer + 0.3% Triton X-100 in the humidified chamber overnight at 4°C. Slices were washed three times with PBS and incubated for 1-2 hr at room temperature with secondary antibody donkey anti-goat Alexa 594 (1:500, Thermo Fisher Scientific A-11058), goat anti-rabbit Alexa 594 (1:500, Thermo Fisher Scientific A-11037), and goat anti-guinea pig Alexa 647 (1:500, Thermo Fisher Scientific A-21450) in antibody buffer + 0.3% Triton X-100. Sections were washed with PBS three times and mounted with SlowFade gold antifade mountant with DAPI. Coverslips (22 mm x 50 mm 1.5 thickness (Fisher

Scientific 12-544-D)) were placed on top of the sections and sealed with nail polish (Electron Microscopy Sciences 72180). Negative controls included sections where IGFBP2 or pSMAD antibody was omitted.

For IGFBP2 analysis, layer 2/3 of the visual cortex was imaged using the Zeiss LSM 880 Rear Port Laser Scanning Confocal and Airyscan FAST Microscope, using confocal imaging. Images were taken at 63X magnification, as 16 bit images, as z stacks of 10 steps with a total thickness of 3.85um. The investigator was blinded to the genotypes of the mice during sectioning, staining, imaging, and analysis. Exposure acquisition was consistent across WT and KO samples from the same experiment. Imaging was performed on 3 sections (technical replicates) from 3 mice (biological replicates) per genotype. Analysis was performed using IMARIS software (Bitplane). Astrocytes (eGFP) were defined as surfaces with background subtraction (largest sphere contained within the surface set to 5um) and smoothed to 0.110um. IGFBP2 (channel 594) was masked within and without these surfaces to allow separate analysis of internal and external IGFBP2, which was also defined as surfaces. Representative images are snapshots of the full 3D z-stack image, the z-stack with internal IGFBP2 masked, and 3D surfaces of astrocytes and IGFBP2.

For pSMAD analysis, all layers of the visual cortex were imaged using the Zeiss LSM 880 Rear Port Laser Scanning Confocal and Airyscan FAST Microscope, using confocal imaging. Images were taken at 20X magnification, as 16 bit images of 4-6 tiles with 10% overlap, z stacks of 3 steps with a total thickness of 2.27 um. The investigator was blinded to the genotypes of the mice during sectioning, staining, imaging, and analysis. Images were used to generate maximum intensity projections and exported as TIFF images for analysis. Using ImageJ software (NIH), ROIs of 1800 x 1200 pixels were drawn in each image, capturing layers I-IV of the cortex.

Expression of pSMAD in the nucleus was measured using the particle analysis tool in ImageJ and counted using the Cell Counter plugin (Kurt de Vos). DAPI was used to create a mask. pSMAD expression was measured as mean intensity within the area of the ROI, and number of pSMAD positive cells was determined by counting the number of colocalized DAPI + pSMAD cells and the number of pSMAD + eGFP+ cells and normalizing to the total number of astrocytes per ROI.

For GLT1 analysis, littermate Aldh1l1-EGFP x *Mecp2* KO and WT P35 male mice were used. The investigator was blinded to the genotypes of the mice during sectioning, staining, imaging, and analysis. Upper layers of the visual cortex were imaged on a Zeiss LSM 880 Airyscan FAST super-resolution microscope using the 63X oil-immersion objective as a Z-stack of 10 slices with a total thickness of 3.51 um. Aldh1l1-EGFP was imaged along with GLT1 and VGlut1 and 2. The z stacks of each condition (Aldh1l1-EGFP x *Mecp2* KO or WT) were presented as 3D images, using IMARIS software (Bitplane). Gaussian filter of 0.0725 mm was applied to all channels in order to smooth the images and reduce noise. Astrocytes (Aldh1l1-EGFP) were defined in channel 488 as surface objects with a surface detail of 0.085 mm, and GLT1 and VGlut1 or 2 were defined as spheres of 0.5 mm of diameter. GLT1 spheres that were in proximity to the surface of the astrocyte (distance of GLT1 sphere to surface object defined as 0.5 mm) were considered for co-localization to VGlut 1 or 2 analysis, using the spots closest to surface function. The co-localization spots function defined a distance from center to center of spots of 0.7 mm. Spots from different channels that were within 0.7 mm from each other's center were quantified as co-localized. Total GLT1 and total VGlut1 or 2 puncta referred to the total number of spots detected by the spot detection function in the entire Z-stack.

In Vivo Protein Levels

Collecting whole cortical lysate from P7 mice

P7 mice (*Mecp2* KO, *Fmr1* KO, *Ts65Dn* Mutants, or WT littermates) were anesthetized with intraperitoneal injection of 100 mg/kg Ketamine (Victor Medical Company) and 20 mg/kg Xylazine (Anased) mix and transcardially perfused with PBS. Brains were quickly dissected out, and cortices removed and placed in Eppendorf tubes, and frozen on liquid nitrogen before being stored at -80°C until further use. To prepare protein lysate, protease inhibitors (Thermo Fisher Scientific 78430) and phosphatase inhibitors (Thermo Fisher Scientific 78420) were added at a ratio of 1:100 to RIPA buffer (Thermo Fisher Scientific 89901) and added to frozen cortical tissue at a ratio of approximately 100 ul per 10 mg tissue. Tissue was then lysed with an electric homogenizer in the Eppendorf tube and placed on a rotator at 4°C for 1 hour to fully lyse the tissue. Lysate was then spun down at 14000 rpm at 4°C for 15 minutes to pellet out the unsolubilized tissue and the supernatant was collected and placed in fresh Eppendorf tubes. The protein concentration of each sample was obtained using a Bradford Assay and samples were snap frozen on liquid nitrogen and stored at -80°C until use in a Western blot.

Collecting CSF from P7 pups

CSF was collected from post-mortem neonatal mice. P7 mice (Aldh1L1-eGFP x Mecp2 KO and their WT littermates) were anesthetized with intraperitoneal injection of 100 mg/kg Ketamine (Victor Medical Company) and 20 mg/kg Xylazine (Anased) mix. Death was determined by a lack of toe pinch reflex and cessation of respiration. After death, pups were affixed with their heads at a downward angle underneath a dissecting microscope and the back of the neck was dissected to reveal the cisterna magna. Glass micropipettes were pulled on a Model P-1000 Flaming/Browning Micropipette puller (Sutter Instruments) and the tips cut to an inner diameter of about 10 um. The tip of the pipette was then manually inserted into the cisterna magna and CSF

was drawn into the pipette by capillary action. CSF was stored in low adhesion Eppendorf tubes at 4°C until use and concentration was determined by Bradford Assay prior to Western blotting.

Western Blotting

Western blot samples were thawed on ice or kept at 4°C until use. Samples were mixed with reducing sample buffer (Thermo Fisher Scientific 39000) and denatured for 45 minutes at 55°C. Protein samples were separated on Bolt 12% Bis-Tris Plus gel (NW00120BOX) for 1.5 hours at constant voltage of 120V. Proteins were transferred onto Immobilion-FL PVDF membranes (Millipore IPFL00010), for 2.5 hr at constant current of 0.4A on ice. For CSF experiments, membranes were stained using Ponceau S for 30 minutes at RT and washed at least 3x10 minutes in water before imaging on the Odyssey Infrared Imager (Li-Cor) and Image Studio software (Li-Cor) system to examine total protein load. Membranes were then washed until the Ponceau stain was completely gone and were blocked for 1 hr at room temperature on a rocker with blocking buffer (10% 10X TBS, 80% H2O, 10% Casein stock (Bio-Rad 1610782). Membranes were incubated overnight at 4°C on a shaker with the primary antibodies in blocking buffer, goat anti-IGFBP2 (R&D AF797) at 1:500, rat anti-B-tubulin (ThermoFisher Scientific MA5-16308) at 1:10,000, or rat anti-PN1 (R&D Systems MAB2175) at 1:500. Membranes were washed three times with TBS+0.1% Tween and incubated on a rocker at room temperature for one hour with the appropriate secondary antibody (donkey anti-goat Alexa 680 (Thermo Fisher Scientific A21058) or goat anti-rat Alexa 680 (Thermo Fisher Scientific A21096)). Membranes were washed three times with TBS+0.1% Tween before imaging on Odyssey Infrared Imager (Li-Cor) and Image Studio software (Li-Cor). Semi-quantitative analysis was performed using the Image Studio software and Microsoft Excel. Bands were selected with the Image Studio Rectangle tool and raw intensities were measured. The intensities were then normalized to either the control band (B-tubulin or PN1) or total protein load (for CSF) and further normalized to the WT values.

Cortical Injections and Morphological Analysis

Neonatal Cortical Injections of IGFBP2-neutralizing antibody

P2 mice (male MeCP2 and their male WT littermates) were cryo-anesthetized (Phifer and Terry, 1986) for 10 minutes on ice, taking care to avoid directly contacting the pups with ice. Anesthesia depth was determined by lack of movement and lack of response to toe pinch. Pups were secured dorsal side up on an ice pack to maintain anesthesia and injection site was marked using a surgical pen (McKesson 19-0752), at roughly 3.4mm posterior to Bregma, to inject directly into the visual cortex of the right hemisphere. Pulled glass micropipettes with a 5-10um-diameter beveled tip were prepared using a Model P-1000 Flaming/Browning Micropipette puller (Sutter Instruments) and beveled to a 15 degree angle. Injections were performed using a Digital Small Animal Stereotaxic “U” frame (Kopf, Model 940) to hold a Nanoject III Programmable Nanoliter Injector (Drummond, 3-000-207) to ensure accurate injection targeting and amount. The IGFBP2-neutralizing antibody (R&D MAB797) or its control IgG antibody (R&D 6-001-F) were labeled with Alexa Fluor 594 Succinimidyl Ester (Thermo Fisher Scientific A20004) according to the product manual and excess dye was removed by running the samples through a Zeba™ Spin Desalting Column (40 kDa MWCO, Thermo Fisher Scientific, 87768) and eluting at a final concentration of 1 ug/uL. Each mouse was injected twice with a volume of 500 nL, at a depth of 150 um and 50 um, at a rate of 50 nL/s, for a total volume of 1 uL of antibody (1 ug total). After each injection, there was a wait of at least 2 minutes prior to moving the needle to allow antibody spread and to prevent backflow. Pups were kept on the ice pack for no more than 15 minutes and recovered on a heat pad and were returned to their home cage once awake and re-warmed.

Tissue collection and fixation

Five days after injection, P7 mice (male MeCP2 KO & WT littermates, with either IGFBP2 neutralizing antibody or IgG control) were anesthetized with intraperitoneal injection of 100 mg/kg Ketamine (Victor Medical Company) and 20 mg/kg Xylazine (Anased) mix and transcardially perfused with PBS followed by 4% PFA before brains were dissected out and postfixed in 4% PFA at 4°C overnight. Brains were washed three times in PBS and cryoprotected in 30% sucrose at 4°C. After at least 48 hours in sucrose, brains were frozen in TFM (General data healthcare TFM-5) in a dry ice/ethanol mix and stored at -80°C until use.

Imaging injected antibody spread in P7 mice

Fixed tissue was used for imaging antibody spread. Fixed coronal sections were collected on Superfrost Plus micro slides (VWR 48311-703) at 50 um thickness (3.4 mm posterior to Bregma) on a cryostat (Hacker Industries OTF5000) and mounted sequentially. Slides were washed for 10 minutes in 1X PBS to remove excess mounting media and coverslips (22 mm x 50 mm 1.5 thickness (Fisher Scientific 12-544-D)) were placed on top of the sections and sealed with nail polish (Electron Microscopy Sciences 72180). Sections were imaged at 10X using a tile scan mode on a Zeiss AXIO Imager Z2 motorized microscope (430000-9902) to capture the full region of antibody spread.

Statistical Analysis

Statistical tests and graphs were designed using Prism 7 and Sigmaplot. All tests are two-tailed. To compare more than two groups, one-way ANOVA with Dunnett's post hoc test for multiple comparisons was used. Student's t test was used to compare two groups. When data did not pass normal distribution test, multiple comparisons were done by Kruskal-Wallis ANOVA on ranks and pairwise comparisons were done with Mann-Whitney Rank Sum test. Exact p values reported on graphs or in the figure captions.

Table 7.1: Quality control analysis of WT and ND samples submitted for RNA sequencing analysis to the Salk Institute for Biological Studies Next Generation Sequencing Core.

Sample	NAAC 17 FXS	NAAC 18 RTT	NAAC 19 DS	NAAC 20 RTT	NAAC 21 DS	NAAC 22 WT	NAAC 24 FXS	NAAC 26 WT	NAAC 27 RTT	NAAC 28 FXS	NAAC 29 FXS
Unique%	85.99	85.27	86.82	85.62	85.37	85.75	86.78	84.91	85.88	85.47	85.91
Multiple%	12.48	13.21	11.82	12.77	13.02	12.59	11.73	13.72	12.67	13.14	12.67
Unmapped %	0.8	0.74	0.69	0.8	0.76	0.77	0.73	0.48	0.62	0.53	0.62
Total Reads	5.27E +07	3.97E +07	4.36E +07	4.62E +07	4.16E +07	2.23E +07	1.92E +07	2.06E +07	3.77E +07	6.54E +07	5.18E +07
PosToMinusRatio	8.83	9.34	9.79	9.62	10.06	10.32	9.99	10.05	10.17	10.05	9.26

Sample	NAAC 30 WT	NAAC 31 FXS	NAAC 32 DS	NAAC 33 WT	NAAC 34 WT	NAAC 35 WT	NAAC 38 FXS	NAAC 39 DS	NAAC 40 RTT	NAAC 43 RTT	NAAC 44 RTT
Unique%	83.48	82.15	80.45	85.11	84.06	84.87	85.99	87.13	86.45	86.53	85.45
Multiple%	14.72	16.07	17.74	13.54	14.23	13.52	12.39	11.42	12.04	11.92	13.03
Unmapped %	0.88	0.89	0.91	0.5	0.82	0.71	0.81	0.67	0.71	0.68	0.63
Total Reads	3.12E +07	5.51E +07	3.36E +07	1.24E +07	4.36E +07	2.07E +07	3.15E +07	2.98E +07	3.63E +07	5.45E +07	4.52E +07
PosToMinusRatio	8.46	8.44	7.71	9.19	9.65	9.47	8.69	9.74	8.79	9.74	9.31

Table 7.2: Quality control analysis of BMP6-treated and untreated samples submitted for RNA sequencing analysis to the Salk Institute for Biological Studies Next Generation Sequencing Core.

Sample	**NAAC76 BMP6**	**NAAC76 noBMP6**	**NAAC79 BMP6**	**NAAC79 noBMP6**	**NAAC81 BMP6**	**NAAC81 noBMP6**	**NAAC120 BMP6**	**NAAC120 no BMP6**	**NAAC122 BMP6**	**NAAC122 no BMP6**	**NAAC124 BMP6**	**NAAC124 no BMP6**
Unique %	88.33	86.35	85.79	85.37	86.63	86.43	85.54	84.14	85.71	82.96	86.23	85.81
Multiple %	10.49	12.35	12.96	13.31	11.84	12.09	12.78	14.16	12.57	15.36	12.47	12.83
Unmapped%	0.34	0.39	0.4	0.4	0.62	0.53	0.76	0.7	0.73	0.46	0.46	0.49
Total Reads	3.74E+07	4.19E+07	2.51E+07	3.83E+07	3.39E+07	3.40E+07	3.32E+07	3.17E+07	1.81E+07	3.14E+07	3.32E+07	3.09E+07
PosToMinus Ratio	9.49	8.82	9.52	8.86	10.39	10.66	8.04	8.35	8.35	7.58	6.72	6.71

References

Bansal, R., Pfeiffer, S.E., 1989. Reversible Inhibition of Oligodendrocyte Progenitor Differentiation by a Monoclonal Antibody against Surface Galactolipids. Proc. Natl. Acad. Sci. U. S. A. https://doi.org/10.2307/34290

Boris Zybailov, Amber L. Mosley, Mihaela E. Sardiu, Michael K. Coleman, Laurence Florens, and, Washburn*, M.P., 2006. Statistical Analysis of Membrane Proteome Expression Changes in Saccharomyces cerevisiae. https://doi.org/10.1021/PR060161N

Carvalho, P.C., Lima, D.B., Leprevost, F. V, Santos, M.D.M., Fischer, J.S.G., Aquino, P.F., Moresco, J.J., Yates, J.R., Barbosa, V.C., 2016. Integrated analysis of shotgun proteomic data with PatternLab for proteomics 4.0. Nat. Protoc. 11, 102–117. https://doi.org/10.1038/nprot.2015.133

Foo, L.C., 2013. Purification of rat and mouse astrocytes by immunopanning. Cold Spring Harb. Protoc. 8, 421–432. https://doi.org/10.1101/pdb.prot074211

Foo, L.C., Allen, N.J., Bushong, E.A., Ventura, P.B., Chung, W.S., Zhou, L., Cahoy, J.D., Daneman, R., Zong, H., Ellisman, M.H., Barres, B.A., 2011. Development of a method for the purification and culture of rodent astrocytes. Neuron 71, 799–811. https://doi.org/10.1016/j.neuron.2011.07.022

He, L., Diedrich, J., Chu, Y.-Y., Yates, J.R., 2015. Extracting Accurate Precursor Information for Tandem Mass Spectra by RawConverter. Anal. Chem. 87, 11361–11367. https://doi.org/10.1021/acs.analchem.5b02721

Phifer, C.B., Terry, L.M., 1986. Use of hypothermia for general anesthesia in preweanling rodents. Physiol. Behav. 38, 887–890. https://doi.org/10.1016/0031-9384(86)90058-2

Risher, W.C., Patel, S., Kim, I.H. wan, Uezu, A., Bhagat, S., Wilton, D.K., Pilaz, L.-J.J., Singh Alvarado, J., Calhan, O.Y., Silver, D.L., Stevens, B., Calakos, N., Soderling, S.H., Eroglu, C., 2014. Astrocytes refine cortical connectivity at dendritic spines. Elife 3, 1–24. https://doi.org/10.7554/eLife.04047

Scholze, A.R., Foo, L.C., Mulinyawe, S., Barres, B. a., 2014. BMP Signaling in Astrocytes Downregulates EGFR to Modulate Survival and Maturation. PLoS One 9, e110668. https://doi.org/10.1371/journal.pone.0110668

Steinmetz, C.C., Buard, I., Claudepierre, T., Nägler, K., Pfrieger, F.W., 2006. Regional variations in the glial influence on synapse development in the mouse CNS. J. Physiol. 577, 249–61. https://doi.org/10.1113/jphysiol.2006.117358

Winzeler, A., Wang, J.T., 2013. Purification and Culture of Retinal Ganglion Cells from Rodents.

Cold Spring Harb. Protoc. 8, 643–652. https://doi.org/10.1101/pdb.prot074906

Xu, T., Park, S.K., Venable, J.D., Wohlschlegel, J.A., Diedrich, J.K., Cociorva, D., Lu, B., Liao, L., Hewel, J., Han, X., Wong, C.C.L., Fonslow, B., Delahunty, C., Gao, Y., Shah, H., Yates, J.R., 2015. ProLuCID: An improved SEQUEST-like algorithm with enhanced sensitivity and specificity. J. Proteomics 129, 16–24. https://doi.org/10.1016/J.JPROT.2015.07.001

Appendix 1: Immunopanning purification of cortical astrocytes (mouse), ACSA2

This protocol is for isolating astrocytes from P5 – P7 mouse cortex, 2-4 pups per prep. It is adapted from (Foo, 2013).

Day Before

Prepare coverslips/plates with PDL for astrocytes

- Coat coverslips with PDL (Sigma P6407)
    - Coverslips (Carolina Biological Supply 633029 – 12mm, Thickness 0.13-0.17) are stored in 70% EtOH after extensive washing.
    - Place coverslips in large 150mm Petri Dish (BD 351058) and wash 3X times with sterile H2O.
    - Add 100ul of PDL (dilute 100X in H2O: 100ul aliquot + 10mL H2O) to each coverslip.
    - Let sit at RT 30 minutes. **Do not exceed incubation time**
- Wash 3X with sterile H2O and place in 24 well plate in individual wells, PDL side up
- Dry overnight in incubator
    - NB: Can skip the coverslips if doing some kind of live imaging (i.e. calcein AM) but need to fix and stain for cell markers on coverslips
- For 6 well plate: 1 mL PDL per well, incubate for 30 minutes, wash 3X with sterile H2O, vacuum final wash and dry overnight in the incubator.

Prepare panning dishes:

- Set up panning dishes in 10 and 15cm petri dishes (non-TCT, Falcon are best).
- Each dish receives 12.5 ml of Tris-HCl (pH 9.5) per dish, plus 2^{o} antibodies:
    1. 1 x isolectinB4 – 10ul lectin
    2. 1 x cd11b - 30μl anti-rat IgG (H+L)
    3. 1 x cd45 - 30μl anti-rat IgG (H+L)
    4. 2 x O4 - 60μl anti-mouse IgM (μ-chain specific)
    5. 1 x ACSA2 - 30μl anti-rat IgG (H+L)
- Leave plates at 4^{o}C overnight on level flat surface; make sure the bottom of the plate is fully covered by Tris solution.

Day of Immunopanning

- Set a heatblock to 37^{o}C. Add a damp paper towel so the plastic won't be in direct contact with the heater.
- Set waterbath to 34^{o}C

Solutions to prepare:

1. Bubble CO2 through solution of enzyme stock (11 mL aliquot – see recipe at end of protocol)
    a. Use a pasteur pipette, attach filter to top with parafilm, bubble CO_2 through until solution turns from red to orange, then place in 34^{o}C water bath

2. Bubble CO2 through solutions of inhibitor stock (42 mL and 10 mL aliquots – see recipe at end of protocol)
    a. (NB. can re-use pipette and filter)
3. Once colour change occurs, finish making papain, low and high ovo solutions – keep at 34°C until needed (NB. leave all solutions at 34°C while you dissect, this seems to work better for postnatal mouse preps.). This should be done before dissection.
4. Equilibrate 20ml 30% FCS in incubator at 37°C (6mls FCS + 14mls EBSS, filtered)
5. Equilibrate 4ml EBSS aliquot in incubator at 37°C

Then add following to pre-equilibrated media:

1. Low ovo: 1 x 42ml inhibitor stock + 3ml Low Ovo + 200μl DNase (see end of protocol for recipe)
2. High ovo: 1 x 10ml inhibitor stock + 2ml High Ovo + 20μl DNase
3. BSA: 2x40ml 0.2% BSA (38ml dPBS + 2ml 4% BSA)
4. Panning buffer: 1 x 20ml 0.02% BSA (17ml dPBS + 2ml 0.2% BSA (from step 3) + 1ml 30% glucose + 20μl DNase)
5. Papain: 1 x 11ml enzyme stock + 65 units Papain (Worthington LS003126) + 0.0032-0.0040g L-cysteine (Sigma C7880) and place in water bath at 34°C to warm.

Dissect brains in dPBS:

6. Pipette 2 x 10ml dPBS into 2 x 6cm petri dishes
    i. remove all hindbrain, olfactory bulb, hippocampus etc. – leaving ONLY the cortex
    i. peel off meninges, take no longer than 20mins for dissection total
7. Transfer cortices into a new, empty 6cm dish and use a No. 10 scalpel blade to dice brains into approximately 1mm^3 cubes
    a. Place no more than 4 brains (8 hemispheres) in each dish
8. Suck up 11 ml of papain solution in syringe (warmed to 34°C), attach 0.22μm filter, squirt out excess so you have 10ml remaining.
9. Filter 10ml of solution into petri dish (containing diced brains)
10. Add <u>50μl DNase to each 6cm petri dish</u>, and swirl gently to mix
11. Place dishes on heat block at 37°C with damp paper towel to prevent overheating
12. Allow CO_2 to pass over brains (attach a filter to tubes before gas enters petri dishes), for approximately 45 minutes (shake gently every 10-15 minutes)
    a. NB. the CO_2 should only flow over the TOP of the solution, NOT through it. Check routinely to make sure the brains in solution are not bubbling over

Finish plate prep:

13. Finish making panning dishes using BSA solutions
    a. wash each panning dish with PBS (x3) then add the following 1° antibodies and incubate at room temperature:
        i. lectin plate – leave as is
        ii. Cd11b – 10ul cd11b into 15mls 0.2% BSA (microglia) 0.5ug/ul
        iii. Cd45 – 10μl cd45 into 15 ml 0.2% BSA (macrophages) (0.62ug/ul)
        iv. 2 x O4 – 8ml O4 hybridoma + 7ml 0.2% BSA (OPCs)

v. ACSA2 plate – 25ul **ACSA2** into 15mls 0.2% BSA (to collect astrocytes) (0.1ug/ul)

b. NB. these antibodies need to be on the plates for AT LEAST two hours prior to immunopanning

Dissociation of tissue:

14. After digestion (and CO_2 bubbling), put brains and solution into a 50mL Falcon tube (swirl then pour)
    a. wait for tissue to settle, then aspirate excess liquid – ~2 min, using glass pipette attached to vacuum tube
    b. add 4.5ml Low Ovo solution to cells to wash – use slow setting
    c. wait for tissue to settle for 1 minute, then aspirate excess liquid
    d. REPEAT STEPS (b-c) a total of 4 times

    (NB. remember to leave behind 4ml Low Ovo in a new Falcon tube – this is the Low Ovo that the single cells will be added to, see below)
15. Triturate
    a. add 4ml Low Ovo into the same 50mL Falcon tube for trituration
    b. Suck up brain chunks + Low Ovo solution with a 5ml serological pipette slowly on the lowest setting, tip at angle against bottom of tube. Do 3-5x up and down per round.
        ii. NB. be CAREFUL NOT to introduce bubbles
        iii. NB. DON'T lift 5ml pipette out of solution during trituration to minimise introduction of CO_2 into solution
    c. The solution will become cloudy (this is due to single cells in suspension), let larger chunks of brain settle for 1-2 minutes and collect single cells with a 1ml BLUE pipette (cloudy solution on top) and add to 4mls of Low Ovo that was put aside in a new tube – check each transfer carefully for chunks; if chunks are visible, stop transferring and repeat trituration as above.
        i. When repeating trituration, only add the amount of low ovo that was already removed (not necessarily 4mL as in step 15f)
        ii. NB use 1 mL pipette tips without filter as the opening is wider and less damaging to cells
    d. Repeat until 95% of chunks are gone
    e. Add remaining Low Ovo to bring to volume (~12 mL)
16. CAREFULLY (and SLOWLY) use a 10ml pipette placed to the bottom of the Falcon tube to layer 12ml High Ovo under the single cell suspension. This should lead to a clear layer of liquid beneath a cloudy cell suspension
    a. NB. this layering means that when you centrifuge the solution the cells will pass through a High Ovo concentration and denature any residual enzyme
    b. NB. Put tip at the bottom of the tube. Do NOT create bubbles.
17. Spin cells – 800rpm, 6 minutes
18. Aspirate liquid – you should see a large pellet of cells still in the tube
    a. NB. not all cells will have spun down, but the majority of cells will have

b. NB. spinning at higher speeds affects the viability of the cells

19. Resuspend cell pellet in 3ml of panning buffer and gently pipette up and down with 1ml BLUE pipette
    a. add 7 mL additional panning buffer to make up to 10ml total (final volume will be ~14mL)
20. Filter cell solution
    a. spray forceps with 70% ethanol (to sterilize)
    b. fold Nitex into filter cone over 50ml falcon tube and hold in place with sterilised forceps – use 1 mL panning buffer to wet filter to help it "stick" to the sides of the Falcon tube.
    c. filter 1ml at a time
    d. once complete, wash tube and filter with 3ml panning buffer
21. Leave cells at 34^{o}C for 45 minutes of recovery (use a water bath)
    a. NB. this step is necessary to allow antigens to return to the cell surface

Prep for Plating Cells

22. Make solution of 20mL AGM (see recipe at the end of protocol) + 20 uL HBEGF
23. Pipet 500uL of AGM on coverslips in 24-well plate and 2mL in each well of 6-well plate
24. Place plates in incubator at 37^{o}C

Panning:

25. Wash each panning dish with dPBS (3x) just before use – at RT, just pour but be gentle
26. Add filtered cell suspension to lectin plate – 10 minutes, shake after 5
27. Wash, then add cells to Cd11b plate – 10 minutes, shake after 5
28. Wash, then add cells to CD45 plate – 20 minutes, shake after 10
29. Wash, then add cells to O4 dish 1 – 15 minutes, shake after 7.5
30. Wash, then add cells to O4 dish 2 – 15 minutes, shake after 7.5
31. Wash, then add cells to ACSA2 dish – 40 minutes, shake after 20

Astrocyte harvest:

32. At end of panning incubation wash the ACSA2 panning dish with dPBS (8x), check after couple of washes – make sure cells are sticking
    a. NB. be VERY gentle while washing positive plate – mouse astrocytes are weakly adhered to plate and can easily slough off
33. Add 100 units of trypsin (Sigma T9935) to 4 mL equilibrated EBSS and add to cells.
34. Put in incubator (37^{o}C) for 3 mins, the cells may come off easily with tapping and may not need to be incubated
35. If the cells come off easily with tapping, start removing
    a. Apply 5 ml 30% FCS to plate and systematically go around the plate and squirt the cells with a 10ml serological pipette (or 1mL blue pipette tip) to dislodge the cells – no bubbles, don't drag on plate
    b. NB. some contaminating cells (eg. OPCs) will remain stuck to the plate – these are blue under phase microscope. These cells should be left stuck to the plate to ensure purity
36. Remove dislodged cells and add to a new 50ml Falcon tube

37. Check under inverted microscope for where cells are still stuck to positive plate, then use another 10ml 30% FCS to squirt off and collect into Falcon tube
38. Count cells – yield should be approximately 1 million cells per P7 pup
39. Add 100μl of DNase per 10ml of solution
40. Spin cells down, 1200rpm for 11 minutes
41. Aspirate supernatant
42. Resuspend cell pellet in AGM
43. Plate cells at required density
    a. for coverslips, plate in 500 uL AGM+HBEGF (usually 60-80K per well)
    b. for 6-well plate, plate in 2 mL AGM+HBEGF (250-330K, usually around 300K per well)
44. After plating, spin plates at 300 rpm (lowest speed setting) for 1 min to bring cells to the bottom of the plate before placing plates in the incubator.

To Plate Cells

- To grow cells, take 20ml Astrocyte Growth Media with 20μl HBEGF
- Resuspend cells in GM
- Half change media every 7 days

Antibody catalogue numbers:

- Lectin:
    - Primary: Unconjugated Griffonia (Bandeiraea) Simplicifolia Lectin I (GSL I, BSL I), Vector Labs Inc, #L-1100 https://vectorlabs.com/unconjugated-griffonia-bandeiraea-simplicifolia-lectin-i-gsl-i-bsl-i.html
    - Secondary: none
- CD11b:
    - Primary: Anti-Mouse CD11b Purified, Ebioscience, #14-01112-86 http://www.ebioscience.com/mouse-cd11b-antibody-purified-m1-70.htm
    - Secondary: AffiniPure Goat Anti-Rat IgG (H+L), Jackson Immunoresearch #115-005-167 https://www.jacksonimmuno.com/catalog/products/112-005-167
- CD45:
    - Primary: Purified Rat Anti-Mouse CD45, BD Pharmingen, #550539 http://www.bdbiosciences.com/us/applications/research/stem-cell-research/cancer- research/human/purified-rat-anti-mouse-cd45-30-f11/p/550539
    - Secondary: AffiniPure Goat Anti-Rat IgG (H+L) (see above)
- O4 hybridoma:
    - Primary: We make our own O4 hybridoma supernatant (mouse IgM), based on Bansal et al. (1989).
    - Secondary: AffiniPure Goat Anti-Mouse IgM, μ Chain Specific, Jackson Immunoresearch, #115-005-020 https://www.jacksonimmuno.com/catalog/products/115-005-020
- ACSA2:
    - Primary: Anti-ACSA-2, Miltenyl Biotech #130-099-138 http://www.miltenyibiotec.com/en/products-and-services/macs-flow-cytometry/reagents/antibodies-and-dyes/anti-acsa-2-antibodies-mouse.aspx
    - Secondary: AffiniPure Goat Anti-Rat IgG (H+L) (see above)
- NCAM L1:
    - Primary: Neural Cell Adhesion Molecule L1 clone 324 (NCAM), Millipore, #MAB5272 http://www.emdmillipore.com/US/en/product/Anti-Neural-Cell-Adhesion-Molecule-L1-Antibody,-clone-324,MM_NF-MAB5272
    - Secondary: AffiniPure Goat Anti-Rat IgG (H+L) (see above)

Reagents used for Immunopanning

	Supplier	Catalogue Code
1x Earle's balanced salt solution (EBSS)	Sigma	E6267
10x EBBS	Sigma	E7510
Bovine serum albumin	Sigma	A4161
Bovine serum albumin	Sigma	A8806
Dubelcco's modified eagle medium (DMEM)	Invitrogen	11960-044
Dubelcco's PBS (dPBS)	Gibco	
0.4% DNase, 12500units/ml	Worthington	LS002007
Fetal calf serum (FCS)	Gibco (Invitrogen)	10437-028
Griffonia Simplicifolia Lectin (BSL1)	Vector Labs	L-1100
Goat anti-rat IgG (H+L chain)	Jackson ImmunoResearch	112-005-167
Goat anti-mouse IgM (μ-chain)	Jackson ImmunoResearch	115-005-020
Heparin-binding epidermal growth factor	Sigma	E4643
L-cysteine hydrochloride monochloride	Sigma	C7880
L-glutamate	Invitrogen	25030-081
N-acetyl-L-cysteine (NAC)	Sigma	A8199
Neurobasal medium (NB)	Gibco (Invitrogen)	21103-049
Nitex Mesh	Tetko Inc. 525 Monterey Passage Road Monterey Park, CA 91754	HC3-20
O4 hybridoma supernatant (mouse IgM)	(Bansal and Pfeiffer, 1989)	
Papain	Worthington	LS003126
Penicillin / streptomycin	Invitrogen	15140-122
Poly-D-lysine	Sigma	P6407
Progesterone	Sigma	P8783
Putrescine	Sigma	P5780
Rat anti-mouse ACSA2	Milteny Biotec	130-099-138
Rat anti-mouse CD11b	Ebioscience	14-01112-86
Rat anti-mouse CD45	BD Pharmingen	550539
SATO	(see below)	
Sodium pyruvate	Invitrogen	11360-070
Sodium selenite	Sigma	S5261
3,3',5-triiodo-L-thronine sodium salt (T3)	Sigma	T6397

Transferrin	Sigma	T-1147
Trypsin, 30000 units/ml stock	Sigma	T9935
Trypsin inhibitor	Worthington	LS003086

Solutions Required for Immunopanning

1. Enzyme Stock Solution

- Mix all, bring to 200ml with ddH_2O and filter through 0.22μm vacuum filter bottle.

Component	Volume	(final concentration)
10x EBSS	20ml	
30% D(+)-glucose	2.4ml	0.46%
1M $NaHCO_3$	5.2ml	26mM
50mM EDTA	2ml	0.5mM
ddH_2O	170.4ml	
FINAL VOLUME:	**200ml**	

2. Inhibitor Stock Solution

- Mix all, bring to 500ml with ddH_2O and filter through 0.22μm vacuum filter bottle.

Component	Volume	(final concentration)
10x EBSS	50ml	
30% D(+)-glucose	6ml	0.46%
1M $NaHCO_3$	13ml	26mM
ddH_2O	431ml	
FINAL VOLUME:	**500ml**	

3. Low Ovo (ovomucoid)

1. To 150ml dPBS, add 3g BSA (Sigma, A8806).
2. Mix well.
3. Add 3g trypsin inhibitor and mix to dissolve.
4. Adjust pH to 7.4 (requires the addition of at least 1.5mL 1N NaOH)
5. Bring to 200ml with dPBS.
6. When completely dissolved, filter through 0.22μm vacuum filter bottle.
7. Make 1.0ml aliquots and store at -20^{o}C.

4. High Ovo (ovomucoid)

8. To 150ml dPBS, add 6g BSA (Sigma, A8806).
9. Mix well.
10. Add 6g trypsin inhibitor and mix to dissolve.
11. Adjust pH to 7.4 (requires the addition of at least 1.5mL 1N NaOH)
12. Bring to 200ml with dPBS.
13. When completely dissolved, filter through 0.22μm vacuum filter bottle.
14. Make 1.0ml aliquots and store at -20^{o}C.

5. SATO (100x)

- Mix all, filter through pre-rinsed 0.22μm vacuum filter.
- Make 200μl or 800μl aliquots and store at -20^{o}C

Component	Volume	(final concentration)
Neurobasal medium	80ml	
transferrin	800mg	100μg/ml
BSA	800mg	100μg/ml
Putrescine	128mg	16μg/ml
Progesterone (from stock: 2.5mg in 100μl EtOH)	20μl	60ng/ml (0.2μM)
Sodium selenite (4.0mg + 10μl NaOH in 10ml NB)	800μl	40ng/ml
FINAL VOLUME:	**~80ml**	

6. IP-Astrocyte Base Media

- Mix all, filter through pre-rinsed 0.22μm vacuum filter, then add HbEGF at a final concentration of 5 ng/ml

Component	Volume	(final concentration)	(for 150ml)
Neurobasal medium	50%		62.5ml
DMEM	50%		62.5ml
Penicillin	100 units		1.25ml
Streptomycin		100μg/ml	
Sodium pyruvate		1mM	1.25ml
L-glutamine		292μg/ml	1.25ml
1 x SATO			1.25ml
NAC		5μg/ml	125µl
FINAL VOLUME:			**150ml**

Conditioning of IP astrocytes to make ACM

Adapted from (Foo et al., 2011), supplemental methods:

- Culture IP-astrocytes P7 for 7 days in 5 ng/mL HBEGF
    - Replace IP-Astro growth media with astro conditioning media (50% neurobasal, 50% DMEM without phenol red, glutamine, pyruvate, NAC and pen-strep), also with HBEGF (see below)

IP-Astrocyte Conditioning Media

Mix all except for HbEGF, filter through 0.22 um vacuum filter, and then add HbEGF at a final concentration of 5 ng/ml

Component	Volume	Final Conc.	For 20 mLs, from stock:
Neurobasal, no phenol red	50%		10 mL
DMEM, no phenol red	50%		10 mL
Pen/Strep		100 ug/mL	0.2 mL
Sodium Pyruvate		1 mM	0.2 mL
L-glutamine		292 ug/mL	0.2 mL
NAC		5 ug/mL	20 uL
HBEGF, carrier free		5 ng/mL	20 uL

- Wash astrocytes 3x with warm dPBS (no phenol red) in order to remove excess protein and phenol red from the wells. Use the vacuum and a pipettman to wash the cells.
    - Use a volume of dPBS appropriate for the plate size, e.g. 2.5 mLs for a 6-well, 10 mLs for a 10 cm plate, 20 mLs for a 15 cm plate.
- Add conditioning media to the well, again appropriate volume for the size e.g. 2 mLs for a 6-well, 10 mLs for a 10 cm plate, 20 mLs for a 15 cm plate.
- Check cells for viability. Collect after 5 days.

Collection protocol:

ACM is concentrated using spin concentrators with a MW cut-off filter of 3kDa (Vivaspin, 6 mls volume).

- Collect the conditioned medium into 15 ml falcon tubes using a 10ml pipette (can combine multiple wells)

- Add a few mLs of sterile water to the top of each concentrator to wash it. You need two 6 mL concentrators or one 20 mL concentrator for one six-well plate.
- Spin the media and the concentrators at 3400rpm for 15 minutes at 4C. This acts to pellet any dead cells/debris present in the media and to wash the concentrators.
- Remove the water from the top and bottom half of the concentrator using a glass pasteur pipette attached to the vacuum.
- Add 6 mls of conditioned medium to the top of the concentrator using a 5 ml pipette, making sure not to disturb the pellet of dead cells.
- Spin the concentrators at 3400rpm in the centrifuge in the cold room for aprox 75 minutes to reduce the volume to 400ul. Spin for longer if 400ul is not reached after this time. (may take up to 2.5 hours given the small MW filter)
- Store the concentrated ACM in low protein binding Eppendorf tubes – transfer it from the top of the concentrator to the eppendorf tube using a P200. ACM can be stored at 4 degrees C for a week or so if it is not being used for analysis. For protein analysis, snap-freeze the ACM in liquid nitrogen immediately after collection and store at -80 degrees C until further analysis.

References

Bansal, R., Pfeiffer, S.E., 1989. Reversible Inhibition of Oligodendrocyte Progenitor Differentiation by a Monoclonal Antibody against Surface Galactolipids. Proc. Natl. Acad. Sci. U. S. A. https://doi.org/10.2307/34290

Foo, L.C., 2013. Purification of rat and mouse astrocytes by immunopanning. Cold Spring Harb. Protoc. 8, 421–432. https://doi.org/10.1101/pdb.prot074211

Foo, L.C., Allen, N.J., Bushong, E.A., Ventura, P.B., Chung, W.S., Zhou, L., Cahoy, J.D., Daneman, R., Zong, H., Ellisman, M.H., Barres, B.A., 2011. Development of a method for the purification and culture of rodent astrocytes. Neuron 71, 799–811. https://doi.org/10.1016/j.neuron.2011.07.022

Appendix 2: Immunopanning purification of cortical neurons (mouse), NCAM-L1

This protocol is for isolating cortical neurons from P5 – P7 mouse cortex, 2-4 pups per prep. It is adapted from (Foo et al., 2011; Risher et al., 2014; Steinmetz et al., 2006).

Day Before

Prepare panning dishes:

- Set up panning dishes in 15cm petri dishes (Falcon are best)
- Each dish receives 25ml of Tris-HCl (pH 9.5) per dish, plus additional antibodies:
    6. 1 x isolectinB4 – 10ul lectin/plate
    7. 1 x secondary only plate - 60μl goat anti-rat IgG (H+L)
    8. 1 x L1 - 60μl goat anti-rat IgG (H+L)
- Leave plates at 4^{o}C overnight.

Prepare coverslips/plates with PDL + laminin for neurons

- Coat coverslips with PDL (Sigma P6407)
    - Coverslips (Carolina Biological Supply 633029 – 12mm, Thickness 0.13-0.17) are stored in 70% EtOH after extensive washing.
    - Place coverslips in large 150mm Petri Dish (BD 351058) and wash 3X times with sterile H2O.
    - Add 100ul of PDL (dilute 100X in H2O: 100ul aliquot + 10mL H2O) to each coverslip.
    - Let sit at RT 30 minutes. **Do not exceed incubation time** Wash 3X with sterile H2O.
- Laminin (Cultrex Trevigen 3400-010-01).
    - Add 100ul Laminin (dilute 500X in Neurobasal: 5ml Neurobasal + 10 ul aliquot) to each coverslip
    - Incubate at 37 degrees for at least 2 hours. Overnight is preferred.
        - **Thaw laminin just prior to use, do not let it stay in room temp**.

Day of Immunopanning

- Set a heat block inside TC hood close to carbogen line to 37^{o}C. Add a damp paper towel so the plastic won't be in direct contact with the heater.
- Set waterbath to 34^{o}C

Solutions to prepare:

6. Aliquot 22ml of enzyme stock into 50ml Falcon tube, bubble CO_2 through solution
    a. Use a pasteur pipette, attach filter to top with parafilm, bubble CO_2 through until solution turns from red to orange, then place in 34^{o}C water bath
7. Aliquot and bubble 1 x 42ml and 1 x 10ml inhibitor stock
    a. as in 1(a) (NB. can re-use pasteur pipette and filter)

8. Once colour change occurs, finish making papain, low and high ovo solutions – keep at 34^{o}C until needed (NB. leave all solutions at 34^{o}C while you dissect, this seems to work better for postnatal mouse preps.). This should be done before dissection.

Then add following to pre-equilibrated media:

9. Papain: 1 x 22ml enzyme stock (see recipe at end of protocol) + 130units Papain (Worthington LS003126) + 0.0032-0.0040g L-cysteine (3.2 – 4.0 mg, Sigma C7880). Warm to 34^{o}C in waterbath.
10. Low ovo: 1 x 42ml inhibitor stock (see recipe at end of protocol) + 3ml Low Ovo (see recipe at end of protocol) + 200μl DNase
11. High ovo: 1 x 10ml inhibitor stock + 2ml High Ovo (see recipe at end of protocol) + 20μl DNase
12. BSA: 2 x 40ml 0.2% BSA (38ml dPBS + 2ml 4% BSA (Sigma A4161)
13. Panning buffer: 1 x 50ml 0.02% BSA (43ml dPBS + 5ml 0.2% BSA + 2ml 30% glucose + 50μl DNase)

Dissect brains in dPBS:

14. 2 x 10ml dPBS into 2 x 6cm petri dishes (for dissection)
    a. remove all hindbrain, olfactory bulb, hippocampus etc. – leaving ONLY the cortex
    b. peel off meninges
        iv. (NB. for older postnatal and adult mice, take NO longer than 20 minutes for dissections, leave excess meninges. Taking too long for dissection decreases viability of cells drastically)
15. Add a small drop of dPBS into 2 x 6cm petri dishes (new), split brains evenly into the two dishes and use a No. 10 scalpel blade to dice brains into approximately 1mm^3 cubes (NB. no more than 4 neonate brains per dish)
16. Suck up 22ml of enzyme stock (warmed to 34^{o}C, with papain and L-cysteine), attach 0.22μm filter, squirt out excess so you have 20ml remaining.
    Filter 10ml of solution into each petri dish (containing diced brains)
17. Add 50μl DNase to each petri dish, and swirl gently to mix
18. Bubble CO_2 over brains (attach a filter to tubes before gas enters petri dishes), for approximately **30 minutes** (shake gently every 10-15 minutes) on a heat block set to 34C.
    (NB. the CO_2 should only bubble over the TOP of the solution, NOT through it. Check routinely to make sure the brains in solution are not bubbling over)

Finish plate prep during digestion:

19. Finish making panning dishes using BSA solutions
    c. wash each panning dish with PBS (x3) then add the following antibodies:
        i. lectin plates – leave as is
        ii. secondary only plate – 15mls 0.2% BSA to block
        iii. L1 - 5μl L1 (Millipore MAB5272) into 15ml 0.2% BSA (to collect neurons)

(NB. these antibodies need to be on the plates for AT LEAST two hours)

Dissociation of tissue:

20. After digestion (and CO_2 bubbling), put brains and enzyme solution into a 50 mL Falcon tube
    b) wait for tissue to settle, then aspirate excess liquid
    c) add 4.5ml Low Ovo solution to cells to wash
    d) wait for tissue to settle, then aspirate excess liquid
    e) REPEAT STEPS (b-c) 4 times

    (NB. remember to leave behind 4ml Low Ovo in a new Falcon tube – this is the Low Ovo that the single cells will be added to, see below)
21. Triturate
    f) add 4ml Low Ovo into the Falcon tube for trituration
    g) suck up brain chunks + Low Ovo solution with a 5ml serological pipette slowly. Do 3-5x up and down per round.
        i. (NB. be CAREFUL NOT to introduce bubbles)
        ii. (NB. DON'T lift 5ml pipette out of solution during trituration to minimise introduction of CO_2 into solution)
    h) the solution will become cloudy (this is due to single cells in suspension), let larger chunks of brain settle and collect single cells with a 1ml pipette (cloudy solution on top) and add to 4mls of Low Ovo that was put aside in a new tube
    i) Repeat until 95% of chunks are gone
22. Use a 5ml pipette to remove any additional chunks that settled at the bottom of the Falcon tube
23. CAREFULLY (and SLOWLY) use a 10ml pipette at the bottom of the Falcon tube to layer 12ml High Ovo under the single cell suspension. This should lead to a clear layer of liquid beneath a cloudy cell suspension
    a. (NB. this layering means that when you centrifuge the solution the cells will pass through a High Ovo concentration and denature any residual enzyme)
24. Spin cells – 800rpm, 5 minutes
25. Aspirate liquid – you should see a large pellet of cells still in the tube

    (NB. not all cells will have spun down, but the majority of cells will have)

    (NB. spinning at higher speeds affects the viability of the cells)
26. Resuspend cell pellet in 3ml of panning buffer and gently pipette up and down with 1ml pipette
    j) add additional panning buffer to make up to 12ml
27. Filter cell solution
    k) spray forceps with 70% ethanol (to sterilize)
    l) fold Nitex into filter cone over 50ml falcon tube and hold in place with sterilised forceps
    m) filter 1ml at a time
    n) once complete, wash tube and filter with 3ml panning buffer
28. Count cells
    o) 20µl cells + 80µl 0.2% BSA, then add 100µl Trypan blue (so 1:10 dilution)
    p) there should be about 8-10 million cells per p7 pup

29. Leave cells at 37°C for 30-45 minutes of recovery (use a water bath)
    NB: In theory this step is not necessary for cortical neurons; however, the author (ALMC) did a couple preps without any incubation/recovery step and none of the cells survived, so I have done a standard 30 minute incubation since then and it seems to work just fine

Panning:

30. Wash panning dishes with dPBS (3x) just before use
31. Add cells to lectin plate – 5 minutes, shake after 2.5
32. Add cells to 2° plate – 10 minutes, shake after 5
33. Add cells to L1 dish – 30 minutes, shake after 15

Neuron harvest:

34. Wash the L1 panning dish with dPBS (8x), check after couple of washes
    a. (NB. be VERY gentle while washing positive plate – mouse neurons are weakly adhered to plate and can easily slough off)
35. Add 12mls of panning buffer to the plate and squirt off the neurons. Try a 10ml pipette, then a P1000 if doesn't work. Neurons should come off without trypsin.
36. Suck off dislodged cells and add to a new 50ml Falcon tube
37. Check under inverted microscope for where cells are still stuck to positive plate, then use another 12ml panning buffer to squirt off and collect into Falcon tube.
38. Count cells
39. Add 100μl of DNase per 10ml of solution
40. Spin cells down, 1000rpm for 11 minutes
41. Aspirate supernatant
42. Resuspend cell pellet in NB-SATO + forskolin media
43. Plate on coverslip that has been PDL/laminin coated, grow in RGC GM. The author (ALMC) plated at 60-80K per well for neuronal outgrowth experiments.

Reagents used for Immunopanning

	Supplier	Catalogue Code
1x Earle's balanced salt solution (EBSS)	Sigma	E6267
10x EBBS	Sigma	E7510
Bovine serum albumin	Sigma	A4161
Bovine serum albumin	Sigma	A8806
Dubelcco's modified eagle medium (DMEM)	Invitrogen	11960-044
Dubelcco's PBS (dPBS)	Gibco	
0.4% DNase, 12500units/ml	Worthington	LS002007
Fetal calf serum (FCS)	Gibco (Invitrogen)	10437-028
Griffonia Simplicifolia Lectin (BSL1)	Vector Labs	L-1100
Goat anti-rat IgG (H+L chain)	Jackson ImmunoResearch	112-005-167
Neuronal Adhesion Molecule L1	Millipore	MAB5272
L-cysteine hydrochloride monochloride	Sigma	C7880
L-glutamate	Invitrogen	25030-081
N-acetyl-L-cysteine (NAC)	Sigma	A8199
Neurobasal medium (NB)	Gibco (Invitrogen)	21103-049
Nitex Mesh	Tetko Inc. 525 Monterey Passage Road Monterey Park, CA 91754	HC3-20
Papain	Worthington	LS003126
Penicillin / streptomycin	Invitrogen	15140-122
Poly-D-lysine	Sigma	P6407
Progesterone	Sigma	P8783
Putrescine	Sigma	P5780
SATO	(see below)	
Sodium pyruvate	Invitrogen	11360-070
Sodium selenite	Sigma	S5261
3,3',5-triiodo-L-thronine sodium salt (T3)	Sigma	T6397
Transferrin	Sigma	T-1147
Trypsin, 30000 units/ml stock	Sigma	T9935
Trypsin inhibitor	Worthington	LS003086

Solutions Required for Immunopanning

7. Enzyme Stock Solution

- Mix all, bring to 200ml with ddH_2O and filter through 0.22μm vacuum filter bottle.

Component	Volume	(final concentration)
10x EBSS	20ml	
30% D(+)-glucose	2.4ml	0.46%
1M $NaHCO_3$	5.2ml	26mM
50mM EDTA	2ml	0.5mM
ddH_2O	170.4ml	
FINAL VOLUME:	**200ml**	

8. Inhibitor Stock Solution

- Mix all, bring to 500ml with ddH_2O and filter through 0.22μm vacuum filter bottle.

Component	Volume	(final concentration)
10x EBSS	50ml	
30% D(+)-glucose	6ml	0.46%
1M $NaHCO_3$	13ml	26mM
ddH_2O	431ml	
FINAL VOLUME:	**500ml**	

9. Low Ovo (ovomucoid)

15. To 150ml dPBS, add 3g BSA (Sigma, A8806).
16. Mix well.
17. Add 3g trypsin inhibitor and mix to dissolve.
18. Adjust pH to 7.4 (requires the addition of at least 1.5mL 1N NaOH)
19. Bring to 200ml with dPBS.
20. When completely dissolved, filter through 0.22μm vacuum filter bottle.
21. Make 1.0ml aliquots and store at -20^{o}C.

10. High Ovo (ovomucoid)

22. To 150ml dPBS, add 6g BSA (Sigma, A8806).
23. Mix well.
24. Add 6g trypsin inhibitor and mix to dissolve.
25. Adjust pH to 7.4 (requires the addition of at least 1.5mL 1N NaOH)
26. Bring to 200ml with dPBS.

27. When completely dissolved, filter through 0.22μm vacuum filter bottle.
28. Make 1.0ml aliquots and store at -20^{o}C.

11. SATO (100x)

- Mix all, filter through pre-rinsed 0.22μm vacuum filter.
- Make 200μl or 800μl aliquots and store at -20^{o}C

Component	Volume	(final concentration)
Neurobasal medium	80ml	
transferrin	800mg	100μg/ml
BSA	800mg	100μg/ml
Putrescine	128mg	16μg/ml
Progesterone (from stock: 2.5mg in 100μl EtOH)	20μl	60ng/ml (0.2μM)
Sodium selenite (4.0mg + 10μl NaOH in 10ml NB)	800μl	40ng/ml
FINAL VOLUME:	**~80ml**	

RGM:

NB/SATO	**Minimal Growth Media**
For 20 ml: • 9.5 mL Neurobasal (Life Tech 21103049) • 9.5 mL DMEM (Life Tech 11960-044) • 400 ul B27 (see protocol) • 200 ul 100X Pen/Strep (P/S) (Life Tech 15140122) • 200 ul 100X Na Pyruvate (Life Tech 11360070) • 200 ul 100X Insulin • 200 ul 100X L-Glutamine or Glutamax (Life Tech) • 200 ul 100X Sato Stock • 200 ul T3 • 20 ul 1000X NAC • Filter 0.22um • Store in 4^{0} for up to a week (without factors)	**For 20 ml:** Add the factors just prior to use Each stock is at 1000X • 20 ul Forskolin (5 μg/ml) • Thawed aliquots can be stored at 4˚C for up to three days. • Once factor is added, do not use after 3 days. Store at 4^{0} when not in use.

References:

Foo, L.C., Allen, N.J., Bushong, E.A., Ventura, P.B., Chung, W.S., Zhou, L., Cahoy, J.D., Daneman, R., Zong, H., Ellisman, M.H., Barres, B.A., 2011. Development of a method for the purification and culture of rodent astrocytes. Neuron 71, 799–811. https://doi.org/10.1016/j.neuron.2011.07.022

Risher, W.C., Patel, S., Kim, I.H. wan, Uezu, A., Bhagat, S., Wilton, D.K., Pilaz, L.-J.J., Singh Alvarado, J., Calhan, O.Y., Silver, D.L., Stevens, B., Calakos, N., Soderling, S.H., Eroglu, C., 2014. Astrocytes refine cortical connectivity at dendritic spines. Elife 3, 1–24. https://doi.org/10.7554/eLife.04047

Steinmetz, C.C., Buard, I., Claudepierre, T., Nägler, K., Pfrieger, F.W., 2006. Regional variations in the glial influence on synapse development in the mouse CNS. J. Physiol. 577, 249–61. https://doi.org/10.1113/jphysiol.2006.117358